

**STUDY OF DETERIORATION MECHANISMS AND
PROTECTIVE TREATMENTS
FOR THE EGYPTIAN LIMESTONE OF THE AYYUBID CITY
WALL OF CAIRO**

Elsa Sophie Odile BOURGUIGNON

A THESIS

in

Historic Preservation

Presented to the Faculties of the University of Pennsylvania in
Partial Fulfillment of the Requirements for the Degree of

MASTER OF SCIENCE

2000

Supervisor
Dr. A. Elena Charola
Lecturer in Historic Preservation

Reader
Dr. Silvia Centeno
Research Fellow
The Metropolitan Museum of Art

Graduate Group Chair
Frank G. Matero
Associate Professor of Architecture

TO MY MOTHER

ACKNOWLEDGMENTS

I would like to thank my advisor, Dr. A. Elena Charola, for her constant support and her down-to-earth approach to scientific problems. Her vast experience on numerous conservation topics proved to be invaluable. I am also grateful to her for never saying a word about getting called on weekends.

I also want to thank my reader, Dr. S. Centeno, for her assistance and sound advice.

I would like to thank Prof. Frank G. Matero for giving me the opportunity to be involved in such an interesting project. His competence and his passion for the field of historic preservation made my graduate studies both enjoyable and challenging.

My thanks also go to Rynta Fourier, the manager of the Architectural Conservation Laboratory at the University of Pennsylvania, for her constant support and friendship. She was always ready to help me find the supplies I needed in record time. She has created the most organized lab I ever worked in and made my life so much easier.

I am also in debt to the project team members in Cairo, Thomas Roby and Catherine Dewey. Thomas Roby used all his Egyptian diplomatic skills to get me the recently quarried cubes of Egyptian limestone I relied on for my experiments. After much drama, they safely arrived in Philadelphia. Thanks again, Tom.

The help of Doug Yates at the Laboratory for Research on the Structure of Matter at the University of Pennsylvania was also greatly appreciated. He patiently worked with me on Scanning Electron Microscopy to obtain great photos of growing salt crystals.

I must thank H el ene Bourguignon, my sister, which kindly helped me translate German literature articles despite her personal heavy workload and the couple of thousands miles which kept us apart.

Finally, I would like to thank my mother who gave me the best gift any parent can offer to their children, an incredible education. I am forever grateful.

TABLE OF CONTENTS

	Page
Acknowledgements	iii
Table of Contents	iv
List of Figures	viii
List of Tables	xi
Abstract	xiii
Chapter I Introduction	1
I.1 - The al-Azhar Park project	1
I.2 - The Ayyubid city wall of Cairo	3
I.2.1 - Brief history of the fortifications of the city of Cairo	3
<i>I.2.1.a - Construction periods</i>	3
<i>I.2.1.b - Subsequent history of the eastern section of the city wall</i>	6
I.2.2 - The eastern section of the city wall	11
<i>I.2.2.a - Description</i>	11
<i>I.2.2.b - Current State</i>	13
I.3 - General aims of the project	14
Chapter II Deterioration of Egyptian limestone	17
II.1 - Egyptian limestone	17
II.1.1 - Geology	17
II.1.2 - Composition	19
II.1.3 - Egyptian limestone deterioration	21
<i>II.1.3.a - Museum setting</i>	21
<i>II.1.3.b - Outdoor environment</i>	25
II.2 - Salt deterioration of porous materials	26
II.2.1 - A poorly understood phenomena	26
II.2.2 - Origin of salts	27
II.2.3 - Salt movement	28
II.2.4 - Deterioration mechanisms	29
<i>II.2.4.a - Crystallization / dissolution cycling</i>	29
<i>II.2.4.b - Hydration / dehydration cycling</i>	33
II.2.5 - Salt mixtures	33
II.2.6 - Salt behavior in arid climates	34
II.3 - Clay minerals and stone deterioration	36
II.3.1 - Clay content and stone deterioration	36
II.3.2 - Swelling of clays	39
<i>II.3.2.a - Inner-crystalline swelling</i>	39
<i>II.3.2.b - Osmotic swelling</i>	40
II.4 - Synergy between salts and clay minerals in stone deterioration	41

Chapter III Treatments for Egyptian limestone	46
III.1 - Treating Egyptian limestone	46
III.1.1 - Consolidation treatments	47
<i>III.1.1.a - Consolidating deteriorated stone</i>	47
<i>III.1.1.b - Salt encapsulation</i>	50
III.1.2 - Salt removal methods	52
III.1.2.a - Mechanical removal	52
III.1.2.b - Water immersion	52
III.1.2.c - Poulticing	55
III.1.2.d - Electro-osmosis	57
III.1.3 - Environmental control	57
III.1.4 - Protective treatments	61
<i>III.1.4.a - Ion-exchange resins</i>	61
<i>III.1.4.b - Application of surfactant</i>	62
III.2 - Surfactant impregnation as a conservation treatment	63
III.2.1 - Chemical characteristics of surfactants	63
<i>III.2.1.a - Definition</i>	63
<i>III.2.1.b - Principal structural requirements for surface activity</i>	64
<i>III.2.1.c - Main classes of surfactants</i>	64
III.2.2 - Surfactant behavior	66
<i>III.2.2.a - Concentration at interfaces</i>	66
<i>III.2.2.b - Spatial orientation of surfactant at interfaces</i>	66
<i>III.2.2.c - Surface tension</i>	67
<i>III.2.2.d - Presence of electrolytes</i>	69
<i>III.2.2.e - Effect of surfactant adsorption on solid surface</i>	70
III.2.3 - Action of surfactant on stone-water-clay-salt systems	71
<i>III.2.3.a - Potential effects of surfactants upon salt deterioration</i>	71
<i>III.2.3.b - Potential effects of surfactants upon clays deterioration</i>	73
<i>III.2.3.c - Salt extraction by surfactants</i>	75
<i>III.2.3.d - Sulphatation reaction of calcareous stone</i>	76
III.2.4 - Surfactant treatment of the Ayyubid city wall of Cairo	77
Chapter IV Limestone from the Ayyubid city wall of Cairo	79
IV.1 - Mineralogical and petrographic analysis	79
IV.1.1 - Texture	79
IV.1.2 - Acid-insoluble residue	80
IV.2 - Physical properties	82
IV.2.1 - Density	82
IV.2.2 - Porosity	82
IV.2.3 - Micro-cracking and surface condition	85
IV.3 - Mechanical Properties	87
IV.4 - Salt characterization	89
IV.4.1 - Salt deterioration pattern distribution	89
IV.4.2 - Salt crystal growth	92
IV.4.3 - Scanning Electron Microscopy	96

IV.4.4 - Qualitative chemical analysis	99
IV.5 - Salt distribution in the wall	101
IV.5.1 - Methodology	101
IV.5.2 - Results	103
<i>IV.5.2.a - Salt content</i>	103
<i>IV.5.2.b - Acid-insoluble residue</i>	109
<i>IV.5.2.c - X-Ray Diffraction analysis</i>	109
IV.5.3 - Discussion	110
Chapter V Conservation treatment of Egyptian limestone	114
V.1 - Materials	114
V.1.1 - Overview of the experiment	114
V.1.2 - Stone samples	114
<i>V.1.2.a - Replacement stone characteristics</i>	115
<i>V.1.2.b - Experimental samples</i>	116
V.1.3 - Salt	117
V.1.4 - Surfactant	117
V.2 - Methodology	118
V.2.1 - Treatment procedures	118
V.2.2 - Capillary absorption	119
<i>V.2.2.a - Parameters</i>	119
<i>V.2.2.b - Sample preparation</i>	119
<i>V.2.2.c - Experimental procedure</i>	121
V.2.3 - Total immersion	122
V.2.4 - Drying	122
<i>V.2.4.a - Parameters</i>	122
<i>V.2.4.b - Experimental procedure</i>	123
V.2.5 - Application of surfactant by brushing	124
V.2.6 - Application of surfactant to salt impregnated samples	125
<i>V.2.6.a - Capillary absorption and total immersion</i>	125
<i>V.2.6.b - Application by brushing</i>	125
V.2.7 - Cycling	126
<i>V.2.7.a - Environmental conditions</i>	126
<i>V.2.7.b - Measurements</i>	127
V.3 - Results	130
V.3.1 - Capillary rise	130
<i>V.3.1.a - Capillary Absorption Rate</i>	130
<i>V.3.1.b - Capillary Absorption Coefficient</i>	131
<i>V.3.1.c - Total immersion</i>	132
V.3.2 - Drying	133
<i>V.3.2.a - Residual Water Content</i>	133
<i>V.3.2.b - Drying Index</i>	136
V.3.3 - Cycling	137
V.4 - Discussion	143
V.4.1 - Sample preparation	143

V.4.2 - Capillary rise	146
V.4.3 - Drying	149
V.4.4 - Cycling	150
<i>V.4.4.a - Weight changes during cycling</i>	150
<i>V.4.4.b - Length changes during cycling</i>	153
Conclusion	156
Appendices	160
Appendix A: Description of the samples from the Ayyubid city wall	160
Appendix B: Core samples analyses	164
Appendix C: Sample weight changes during preparation	167
Appendix D: Initial drying results	170
Appendix E: Capillary absorption and total immersion results	171
Appendix F: Drying results	180
Appendix G: Wet-dry cycling results	191
Appendix H: Statistical analysis of the wet-dry cycling results	197
Bibliography	202
Index	214

LIST OF FIGURES

		Pages
Figure I.1	General view of the eastern section of the city wall of Cairo in 1924, showing the Darassa hills in the foreground, towers 1, 2, and 3 of the wall and the Blue Mosque in the background.	2
Figure I.2	Same general view than Figure I.1 in 1998.	2
Figure I.3	The three fortifications of the city of Cairo. From Creswell 1952-59, <i>The Muslim Architecture of Egypt</i> .	5
Figure I.4	View of the eastern portion of the Ayyubid city wall of Cairo from the Darassa hills with the former Darb Shoughlan School noticeable in the center of the photo. Note the extensive loss of veneer stone in certain areas of the wall.	7
Figure I.5	Similar view of city wall of Cairo in 1998 with the former Darb Shoughlan School in the center of the photo. Note the higher grade level, the reconstruction of one tower and crenellation by the Comité.	7
Figure I.6	Tower 4 before reconstruction, 1950.	10
Figure I.7	Tower 4 after Comité reconstruction, 1951.	10
Figure I.8	Site plan showing the eastern portion of the Ayyubid city wall of Cairo separating the landscaped al-Azhar park on the east side and the al-Darb al-Ahmar district on the west side. From an unpublished Egypt Ministry of Culture / Aga Khan Trust for Culture map.	11
Figure I.9	Segment of the city wall showing construction technique, running and Flemish bonds.	12
Figure I.10	Typical Flemish and running bond patterns.	13
Figure I.11	Differential weathering of the veneer stones of the city wall.	14
Figure II.1	Map of Egypt showing locations of ancient limestone quarries and formation contacts (heavy dashed lines). From Harrell 1992.	18
Figure II.2	Limestone relief panel of the scribe Iahmose and family (E.A. 1314), seventeenth dynasty (c. 1600 BC) from Thebes or Abydos. Left photography between 1900 and 1920, right photography in 1983. From Hanna, 1984.	22
Figure II.3	Block Statute of "Hati" with two squatting figures of Anuris and Mehyt (EA 1726) attributed to Abydos or Thinis. Left photography around 1920, middle around 1940, right 1983. From Bradley and Middleton, 1988.	23
Figure II.4	Royal head of Amenophis III (E.A. 69054) from the Temple of Merneptah, Thebes. Left Photography after excavation in 1896, right photography in 1983. From Hanna, 1984.	24
Figure II.5	Innecrystalline swelling of sodium montmorillonite. Given are the layer distances and the maximum number of water molecules per sodium ion. From Madsen and Müller-Vonmoos 1989.	39
Figure II.6	Two negatively charged clay layers with ion cloud. From Madsen and Müller-Vonmoos 1989.	41
Figure II.7	Expansion and contraction of clays in presence of salts. From Snethlage and Wendler 1996.	45
Figure III.1	Schematic representation of the basic structure of a surfactant.	64
Figure III.2	Adsorption and concentration of surfactant. From Porter 1994, 30.	67
Figure III.3	Surface tension (left), and interfacial tension (right) <i>versus</i> surfactant concentration. From Porter 1994, 33.	69
Figure III.4	Model of the ionic exchange of cations against bifunctional cationic surfactants on clay basal planes. From Wendler, Klemm, Snethlage 1991.	74

Figure IV.1	Thin section limestone (sample 5), Comité repair stone. Homogeneous fine-grained limestone, with small, well-distributed fossil fragments and iron inclusions. (From Dewey 2000, photo 3.12).	81
Figure IV.2	Thin section limestone (sample 14), appears to be original Ayyubid stone. Fine-grained calcite matrix with abundant fossils – some micro-cracked - and iron inclusions. Magnification $\times 25$. (From Dewey 2000, photo 1.17).	81
Figure IV.3	Thin section of limestone (sample 14), appears to be original Ayyubid stone. Fine-grained calcite matrix with iron inclusions, microcracking, many small pores and some large pores are present. Magnification $\times 25$. (From Dewey 2000, photo 1.16).	84
Figure IV.4	Thin section of limestone (sample 15), appears to be original Ayyubid stone. Tightly packed foraminifera and fossil fragments – some have collapsed internal structure - cemented by calcite matrix creating abundant small voids between the fossils as well as large voids inside them. Magnification $\times 25$. (From Dewey 2000, photo 1.12).	84
Figure IV.5	Thin section of limestone (sample 6), possibly original Ayyubid stone. High porosity fine-grained limestone with an abundance of broken bioclasts, foraminifera and microcracks. Magnification $\times 25$. (From Dewey 2000, photo 2.7).	86
Figure IV.6	Thin section of limestone (sample 14), appears to be original Ayyubid stone. Fine-grained stone with many small pores, microcracks and salt crystals. Magnification $\times 25$. (From Dewey 2000, photo 1.25).	86
Figure IV.7	Thin section of limestone (sample 5), Comité repair stone. Fine-grained stone with microcracks and apparent densification of the outer surface. (From Dewey 2000, photo 3.19).	87
Figure IV.8	Detail of the survey of salt deterioration patterns between tower 4 and 5 of the eastern section of the Ayyubid wall of Cairo.	90
Figure IV.9	Eastern section of the Ayyubid wall of Cairo between towers 3 and 4 looking North toward tower 4, showing the grade level before recent excavation, 2000.	91
Figure IV.10	Detail of the thin salt crusts (veil) falling off in large plaques from the surface of the stones, 2000.	91
Figure IV.11	Layered salt crust on limestone from a surface flake (U sample). Total magnification $\times 2.5$.	92
Figure IV.12	Detail of parallel columnar calcite crystals elongated perpendicularly to the layers, in previous sample (U sample). Total magnification $\times 6.25$.	93
Figure IV.13	Detail of parallel columnar calcite crystals view from above. (U sample). Total mag. $\times 1.875$.	93
Figure IV.14	Detail of typical layered sinter forms of parallel prisms and needle of calcite arranged in layers (U sample). Total magnification $\times 3.125$.	94
Figure IV.15	Fragment of salt crystal detached from the stone exhibiting the characteristic parallel columnar crystals separated by horizontal layers (U sample). Total magnification $\times 3.125$.	94
Figure IV.16	Flaking and delamination of the stone surface caused by salt crystallization. Sample 9, possibly Comité repair stone from a recently excavated area. Total magnification $\times 5$	95
Figure IV.17	Scanning electron microphotography of a surface flake (Towers 4/5, sector 7/8) showing well-defined salt crystal covered by loose material. Magnification $\times 2000$.	97
Figure IV.18	Scanning electron microphotography of a surface flake (Towers 4/5, sector 7/8) showing salt crystals growing from within pores and in a microcrack of the stone. Mag. $\times 2000$.	97
Figure IV.19	Scanning electron microphotography of a surface flake (Towers 4/5, sector 7/8) showing salt crystals growing out from a pore of the stone. Magnification $\times 1000$.	98
Figure IV.20	Scanning electron microphotography of a surface flake (Towers 4/5, sector 7/8) showing salt crystals growing out of a microcrack. Magnification $\times 1000$.	98

Figure IV.21	Thin section of limestone (sample 11) probably original Ayyubid stone. Coarse-grained matrix with a large amount of fossils and fossils fragments and high porosity. Salts are well distributed within the matrix voids. Magnification $\times 25$. (From Dewey 2000, photo 3.6).	99
Figure IV.22	Coring of the first core sample. From Rock Engineering Laboratory 2000a.	102
Figure IV.23	Water-soluble salt content of the three core samples in function of the depth of penetration of the coring. Dotted lines mark the end of the veneer stone.	106
Figure IV.24	Acid insoluble residue content for the three core samples in function of the depth of penetration of the coring. Dotted lines mark the end of the veneer stone.	109
Figure V.1	Identification of each cube face.	116
Figure V.2	Prepared samples before cycling. On the right, nummulitic samples, on the left non-nummulitic samples, displayed for each stone type by increasing sample number from top to bottom, left to right.	126
Figure V.3	Humboldt length comparator with dial indicator. Model H-3250.	128
Figure V.4	Two parts extension of the length comparator with a cube in measurement position.	128
Figure V.5	Graph of the average values of the Capillary Water Absorption ($\text{g}\cdot\text{cm}^{-2}$) per stone and impregnation solution type.	131
Figure V.6	Graph of the average values of the Residual Water Content (%) per stone and impregnation solution type. Standard deviations are given between brackets.	134
Figure V.7	Graph of the average values weight loss per stone and impregnation solution type. Standard deviations are given between brackets.	135
Figure V.8	Average weight difference per preparation treatment during cycling, non-nummulitic stones. Standard deviations are given between brackets.	138
Figure V.9	Average weight difference per preparation treatment during cycling, nummulitic stones. Standard deviations are given between brackets.	139
Figure V.10	Average sum of length difference per preparation treatment during cycling, non-nummulitic stones. Standard deviations are given between brackets.	141
Figure V.11	Average sum of length difference per preparation treatment during cycling, nummulitic stones. Standard deviations are given between brackets.	142
Figure V.12	Back sides of non-nummulitic samples L4, L5, and L6 (from left to right) after impregnation with saturated solution of NaCl and following drying.	145
Figure V.13	Back sides of nummulitic samples F4, F5, and F6 (from left to right) after impregnation with saturated solution of NaCl and following drying.	145
Figure V.14	Back side of non-nummulitic samples L4 after impregnation with saturated solution of NaCl and following drying showing preferential salt crystallization pattern.	146

LIST OF TABLES

	Pages
Table IV.1 Porosity and acid insoluble fraction of selected samples from the Cairo wall. See Appendix A for a complete description of each sample.	82
Table IV.2 Mechanical properties of the historic limestone blocs.	88
Table IV.3 Micro-chemical spot tests of eleven samples (see Appendix A for a complete description of each sample). +++ Presence, + Traces, Ø, Absence.	100
Table IV.4 Water-soluble salt content and acid insoluble residue content of the core samples.	105
Table IV.5 Chlorides, ammonium and sulfates content of the core samples.	107
Table IV.6 Results of the XRD analysis performed on the core samples.	110
Table V.1 Physical characteristics of the historic and replacement stones.	115
Table V.2 Mechanical characteristics of the historic and replacement stones. (Note: $1 \text{ kg.cm}^{-2} = 9.8 \text{ N.cm}^{-2}$).	115
Table V.3 Chemical analysis of the replacement stones.	116
Table V.4 Main physical properties of sodium chloride and its saturated solution. From <i>Handbook of Chemistry and Physics</i> 1995 and Rodriguez-Navarro and Doehne 1999.	117
Table V.5 Matrix of treatments for of the limestone cubes.	120
Table V.6 Average values of the capillary absorption coefficient per stone and impregnation solution type.	132
Table V.7 Average weight gain in percent of the dry weight per stone and impregnation solution type.	132
Table V.8 Average values of the Drying Index per stone and impregnation solution type.	137
Table V.9 Average differences in percent between the weights of the samples before preparation and at the difference preparation stages.	143
Table V.10 Average values of the capillary water absorption per stone and impregnation solution type.	147
Table V.11 Characteristic values of the percentual weight changes during wet-dry cycling. Standard deviation is given between brackets.	151
Table V.12 Characteristic values of the percentual sum of length changes during wet-dry cycling. Standard deviation is given between brackets.	153
Table B.1 Moisture content of sections from core sample 1, low coring point front side.	164
Table B.2 Moisture content of sections from core sample 2, middle coring point, front side.	165
Table B.3 Moisture content of sections from core sample 3, high coring point, front side.	165
Table B.4 Moisture content of sections from core sample 4, back side coring point.	166
Table C.1 Weights of the samples before preparation and at the difference preparation stages.	167
Table D.1 Variation of the sample weight during the initial drying before sample preparation.	168
Table E.1 Weight (g) over time during capillarity absorption, non-nummulitic samples (L).	170
Table E.2 Weight (g) over time during capillarity absorption, nummulitic samples (F).	171
Table E.3 Weight (g) over time during capillarity absorption, second impregnation of samples 16, 17, and 18.	172
Table E.4 Capillarity Water Absorption (g.cm^{-2}), non-nummulitic samples (L).	173
Table E.5 Capillarity Water Absorption (g.cm^{-2}), nummulitic samples (F).	174
Table E.6 Capillarity Water Absorption (g.cm^{-2}), second impregnation of samples 16, 17, and 18.	175
Table E.7 Average values of the Capillarity Absorption (g.cm^{-2}) per stone and impregnation solution type. (a) Above, first impregnation, (b) below, second impregnation of samples 16, 17 and 18 only.	176
Table E.8 Capillary absorption coefficient per stone and impregnation solution type.	177
Table F.1a Weight over time during drying, non-nummulitic samples (L). Part I.	179

Table F.1b	Weight over time during drying, non-nummulitic samples (L). Part II.	180
Table F.2a	Weight over time during drying, nummulitic samples (F). Part I.	181
Table F.2b	Weight over time during drying, nummulitic samples (L). Part II.	182
Table F.3	Weight over time during drying, after second impregnation for samples 16, 17, and 18.	183
Table F.4	Residual Water Content over time during drying, non-nummulitic samples (L).	184
Table F.5	Residual Water Content over time during drying, nummulitic samples (F).	185
Table F.6	Residual Water Content over time during drying, after second impregnation for samples 16, 17, and 18.	186
Table F.7	Average values of the Residual Water Content (%) per stone and impregnation solution type.(a) Above, first impregnation. (b) Below, second impregnation of samples 16, 17, and 18 only.	187
Table F.8	Drying Index per stone and impregnation solution type.	188
Table G.1	Weight in grams (W) and lengths in inches (TB: top-bottom, FB: front-back, RL: right-left) over time, non-nummulitic samples (L), number 1-9.	190
Table G.2	Weight in grams (W) and lengths in inches (TB: top-bottom, FB: front-back, RL: right-left) over time, non-nummulitic samples (L), number 10-18.	191
Table G.3	Weight in grams (W) and lengths in inches (TB: top-bottom, FB: front-back, RL: right-left) over time, nummulitic samples (F), number 1-9.	192
Table G.4	Weight in grams (W) and lengths in inches (TB: top-bottom, FB: front-back, RL: right-left) over time, nummulitic samples (F), number 10-18.	193
Table G.5	Average difference in percent between the sample weight at t=0 and at t= i per stone and impregnation solution type.	194
Table G.6	Average sum of the length difference in percent between the sample lengths at t=0 and at t= i per stone and impregnation solution type.	194
Table H.1	Characteristic values of the percentual weight changes during wet-dry cycling. By convention all the amplitude are positive values.	196
Table H.2	Characteristic values of the percentual sum of length changes during wet-dry cycling. By convention all the amplitude are positive values.	197
Table H.3	Values of <i>t</i> for 10 degrees of freedom for various confidence levels.	198

ABSTRACT

The al-Azhar project of the Aga Kahn Trust for Culture will create one of the largest urban parks in Cairo. This has brought attention to the eastern portion of the Ayyubid city wall which would border the western edge of the park. Partially buried during centuries, the stone wall presents different forms of deterioration, including flaking and disaggregation as well as large areas of salt crusts on the stone surface requiring a comprehensive conservation treatment.

After a brief history of the fortifications of the city of Cairo including previous interventions on the eastern section of the fortifications, this work presents a review of the literature on Egyptian limestone since this was the stone used in the wall construction. This stone contains an unusually high concentration of salts but only a relatively low concentration of clay minerals.

An overview of the literature on deterioration mechanisms shows that the daily variations in relative humidity and temperature, particularly important in the arid climate of Cairo, cause both cyclic swelling of the clays and crystallization the salts. Furthermore several examples highlight that a synergy exists between the deterioration caused by the salts and that due to the clay minerals, the presence of one exacerbating the deterioration caused by the other. These processes contribute to the deterioration of this moderately resistant limestone, and are ultimately detrimental to integrity of the masonry.

A review of past and recent treatments of Egyptian limestone is presented. Overall, salt removal treatments of Egyptian limestone have been only moderately successful, while spectacular failures have been reported due to the high sensitivity of some Egyptian limestone to water. In addition, few desalinization methods can be applied *in situ* and on the large scale of the city wall. Furthermore, most treatments fail to address the issue of the high clay minerals content of most Egyptian limestone, even

tough it has been recognized in some cases as the single most important deterioration factor. This problem has been recently addressed by means of the protective treatment based on the application of surfactants. Basic chemical characteristics and behavior of surfactants are summarized and the possible actions of surfactant on the stone-water-clay-salt systems investigated.

In order to better assess the current deterioration of the wall, a number of analyses were performed. Chemical and instrumental analyses allowed to identify the nature and concentration of salts present. Their spatial distribution within the wall is correlated to the observed deterioration. This allowed to elucidate the probable origin of these salts and their deterioration mechanisms.

An experimental program was designed to evaluate the action of a surfactant, the butyl- α - ω -diammonium chloride (BDAC), on two types of Egyptian limestone being considered for use as replacement veneer stones. One type is a fossiliferous, nummulitic limestone, while the other one is essentially non-fossiliferous. Samples were cut from recently quarried material of both types, and were treated by different combinations of salt and surfactant impregnation. They were then subjected to wet-dry cycling for one and a half month. The changes in weight and length – in all three dimensions – of each samples was measured daily.

It was found that the surfactant reduces the weight gain of salt-impregnated samples while reducing somewhat the amplitude of the expansion-contraction suffered by the samples during cycling. However, the results obtained do not warrant as yet a recommendation of the application of this treatment to the Ayyubid city wall of Cairo.

CHAPTER I

INTRODUCTION

I.1 - The al-Azhar Park project

At the initiative of the Aga Kahn Trust for Culture, within its Historic Cities Support Program, and in collaboration with the Governorate of Cairo, a project to create a 36-hectare park, the al-Azhar park, in metropolitan Cairo was begun in 1998. The proposed park is to be situated on top of the Darassa Hills, east of the al-Darb al-Ahmar district, in the heart of Islamic Cairo and is to become its major green space. The project also includes the construction of cisterns buried under the green space to improve the supply of potable water for the city of Cairo (Aga Kahn Trust for Culture 1998, 3).

The creation of the park presents serious risks for an area socially and environmentally fragile. The awareness of potential risks prompted A.K.T.C. in cooperation with the Near East Foundation (N.E.F., a philanthropic organization) to begin parallel planning efforts in the district of al-Darb al-Ahmar - to the west of the proposed park - aimed at the preservation and appropriate development of the area. The recommended planning actions were further complemented by a series of ten targeted interventions in specific locations within al-Darb al-Ahmar.



Figure I.1 General view of the eastern section of the city wall of Cairo in 1924, showing the Darassa hills in the foreground, towers 1, 2, and 3 of the wall and the Blue Mosque in the background.



Figure I.2 Same general view than Figure I.1 in 1998.

The conservation and presentation of the historic Ayyubid city wall situated along the eastern edge of al-Azhar park was chosen as one of the pilot projects (A.K.T.C. 1998, 4). Situated just below the Darassa Hill, the Ayyubid city wall physically separates the future al-Azhar park and the densely inhabited historic district of al-Darb al-Ahmar. It is seen as an important articulation between two of the main components of the A.K.T.C. project. Work on the twelfth-century historic wall will also help to identify and test forms of intervention and specific material conservation practices that may be applied not only to this monument, but also to its immediate context, including several inhabited structures which are to be rehabilitated (A.K.T.C. 1998, 8).

The overall project is particularly remarkable by its scope. The organization at the origin of the project has taken a comprehensive approach towards the site, addressing social and environmental concerns, as well as conservation of the historic fabric.

I.2 - The Ayyubid city wall of Cairo

I.2.1 - Brief history of the fortifications of the city of Cairo

I.2.1.a - Construction periods

Like numerous walled cities, several fortification campaigns took place in Cairo to accommodate both the urban expansion of the city and the latest military fortification technology. Three main periods of construction can be distinguished.

The first enclosure was built when the city was founded in 358 H¹ (969 AD) at the beginning of the Fatimid period (Creswell 1952, 112). No traces of this fortification remain today. Through texts it is known that the walls were made of mud brick and were thick enough for two horsemen to ride side by side.

The second fortification was built by Emīr al-Guyūsh Badr al-Gamālī at the end of the eleventh century² to improve the protection of the city after the repeated attempts of the Seljūq to seize Cairo. It also served to keep up with the natural growth of the city which had spilled over the first walls. The second wall was made of mud brick with stone gates. Parts of the second fortification remain in the form of three gates, Bāb an-Nasr, Bāb al-Futūh and Bāb Zuwayla, 400 meters of the north wall with five of its towers and around 70 meters of the south wall (Creswell 1952, 112).

The third enclosure was built around 1176 AD during the reign of Salāh ad-Dīn, sultan of Egypt, founder of the Ayyubid dynasty who overthrew the Fatimid caliphate in 1171 AD. This construction campaign began to provide the city with a more adequate fortification as well as more complex defensive arrangements than the previous Fatimid walls. Unlike the previous city walls, this third fortification, a succession of gates with curtain walls and towers in between, was entirely built in stone and made use of new advances in defensive techniques such as bent entrances and arrow-slits reaching the floor.

¹ The Muslim Era is computed from the starting point of the year Muḥammad, the prophet of Islam, emigrated from Mecca to Medina in 622 AD. However, the years of the Muslim calendar are lunar and have 354 or 355 days. Thus the months do not keep to the same seasons in relation to the sun, they regress through all the seasons every 32 ¹/₂ years. Therefore, there is no easy relationship between the Muslim calendar years and Gregorian calendar years. *Encyclopedia Britannica*, s.v. "calendar".

² 480 H (1087 AD).

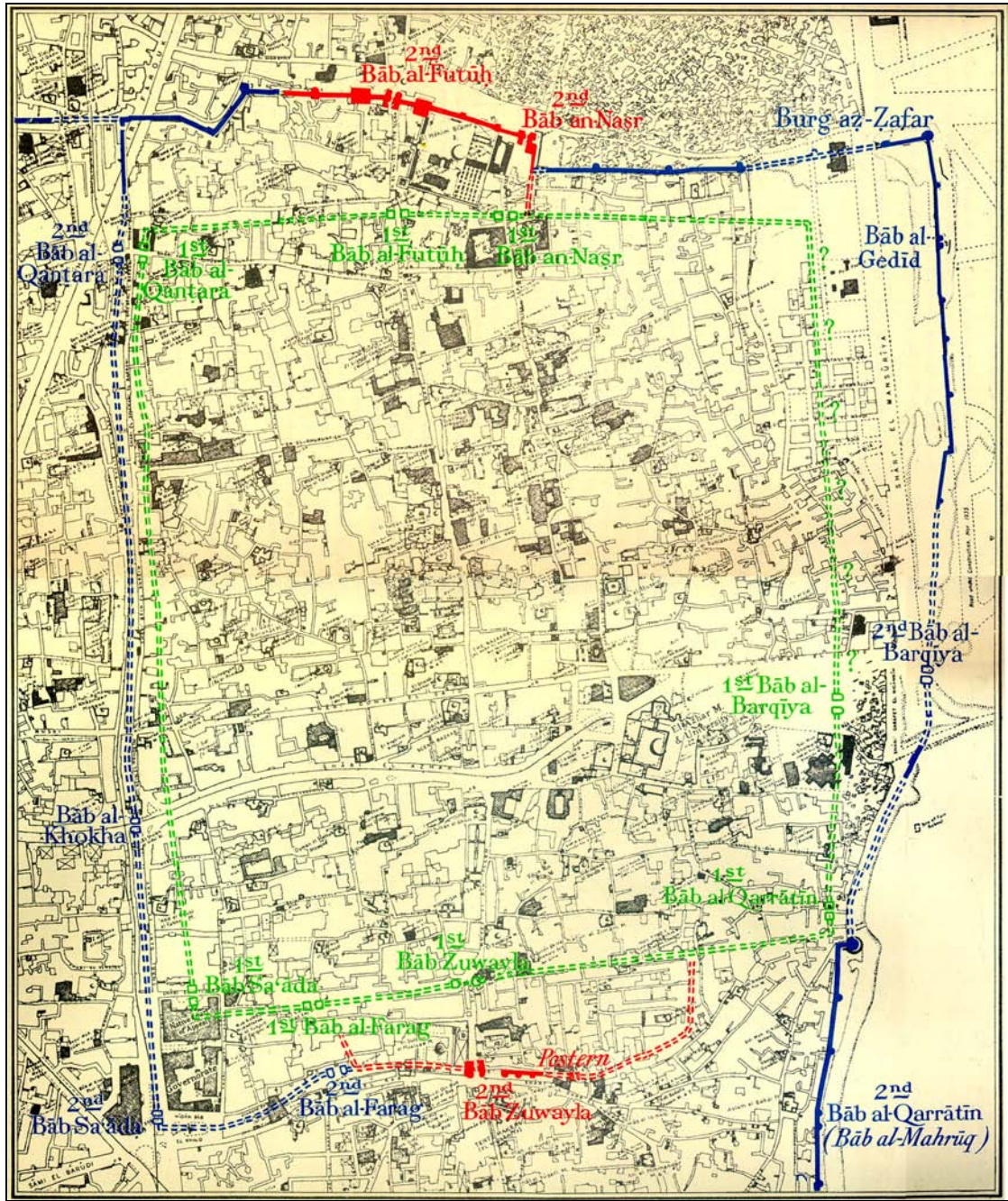


Figure I.3 The three fortifications of the city of Cairo.
 From Creswell 1952-59, *The Muslim Architecture of Egypt*.

It is the third enclosure which consequently gave to the city of Cairo the epithet “the protected” (Fong 1999, 1.3:2). In addition of being the builder of the fortifications, Salāh ad-Dīn was also the constructor of the Citadel of Cairo, which is considered his greatest military work (Creswell 1952, 121).

The eastern section of the city walls, bordering the Darassa hills and the proposed Al-Azhar park, belongs, like most of the surviving walls of Cairo, to the Salāh ad-Dīn 's fortification. This part of the walls was called Bāb-al-Quarrātin and latter Bāb al-Mahrūq from the name of the main gate in this section (see Fig. I.3).

Additional information on the history of the Cairo fortifications can be found in Creswell (1952, 1952-59) and Casanova (1894-97).

1.2.1.b - Subsequent history of the eastern section of the city wall

In the centuries following the construction of the Salāh ad-Dīn’s fortifications, the continuous expansion of Cairo gradually extended the urban fabric beyond the city wall making it obsolete as military defense. It progressively became integrated into the urban fabric through the continuous accretion of structures along it. However, unlike other parts of the walled city, urban expansion did not take place outside the eastern section of the fortifications because the area had been used as a dumping ground since very early on. This use was continued for centuries and the wall was gradually buried under debris which lead to the formations of what is now called the Darassa hills. Although resembling natural formation, these hills are man-made accumulation of organic materials and human activity debris (pottery sheds, etc).



Figure I.4 View of the eastern portion of the Ayyubid city wall of Cairo from the Darassa hills with the former Darb Shoughlan School noticeable in the center of the photo. Note the extensive loss of veneer stone in certain areas of the wall.



Figure I.5 Similar view of city wall of Cairo in 1998 with the former Darb Shoughlan School in the center of the photo. Note the higher grade level, the reconstruction of one tower and crenellation by the Comité.

By the beginning of the nineteenth century, the mounds were some thirty meters high forming a major barrier to urban expansion (A.K.T.C. 1998, 26).

During the Napoleonic campaign of 1798, the French utilized the Darassa Hills and certain sections of the Ayyubid wall as military posts. At the time of their occupation, much of the eastern section of the wall was almost completely buried under debris. Nonetheless, the French made a few interventions to the wall in concern about its structure and functionality. This was by no means a restoration intervention but merely maintenance. Additional information about the state of the city walls of Cairo at the time of the French occupation can be found in the *Description de l'Egypte* (1993).

The creation of the Comité de Conservation des Monuments de l'Art Arabe in 1882 (to become the Conseil Supérieur du Service de Conservation des Monuments Arabes after World War II), led to various interventions on the east segment of the wall. An extensive record of issues surrounding the wall and of the decisions taken by the Comité exists through the yearly compiled *Procès-Verbaux des Séances* of the Comité de Conservation des Monuments de l'Art Arabe (in French). In 1894, the Comité decided to order a comprehensive examination of the surviving portions of the wall to decide which sections were in good enough condition to be considered as monuments (Comité de Conservation des Monuments de l'Art Arabe, Exercice 1894) leading to a survey of the existing walls in 1902 (Comité, Exercice 1902).

In the first half of the twentieth century the Comité was also concerned with residents extending their houses onto or into the wall. It actively sought to reacquire portions of the wall which had been sold off to private individuals in the late nineteenth century. A number of those private purchases were recorded by the Comité's *Procès-*

Verbaux and describe individuals interested in purchasing portions of the wall for their own use as a building expansion. In general, the Comité agreed when the wall was in poor condition or the stonework was not original, and refused if the portion in question had kept its historic value.

In 1943, the Comité carried out some excavations around the east wall area, close to Al-Azhar Street, to look for the remains of the Bab al-Barqiyya gate. The excavation was unsuccessful in locating the gate and only revealed a stretch of wall between two towers (Conseil Supérieur du Service de Conservation des Monuments Arabes, Exercice 1941-1945).

In 1950 the Comité undertook a major restoration campaign of the eastern section of the wall, south of Bāb al-Mahrūq. The work included selective replacement of damaged and missing masonry as well as the complete rebuilding of two towers to restore the structural and architectural integrity of the wall as a valued historic monument (Fong 1999, 1.3:6). The majority of the Comité work concentrated in those areas suffering the most dramatic deterioration: the base and the top of the wall. The repairs were made with local limestone, relatively similar to the original stone, but using a Portland cement-based mortar rather than the lime-based medieval mortar. Today, the Comité work is visually clearly distinguishable from the historic stonework, in addition of having been occasionally documented in meeting notes, reports, histories and photographs (Fong 1999, 2.1:5.)

Little attention was given to the eastern section of the Cairo city wall after 1951, the end of the restoration project, until summer 1998 when the al-Azhar Park project was started.



Figure I.6 Tower 4 before reconstruction, 1950.



Figure I.7 Tower 4 after Comité reconstruction, 1951.

I.2.2 - The eastern section of the city wall

I.2.2.a - Description

Today, a portion of the east wall bordering with the mounds of the Darassa hills is being unburied and once again exposed to view. The grading process for the new park is being unburied and once again exposed to view. The grading process for the new park has now brought up the question of long-term preservation of the twelfth-century wall.



Figure I.8 Site plan showing the eastern portion of the Ayyubid city wall of Cairo separating the landscaped al-Azhar park on the east side and the al-Darb al-Ahmar district on the west side.
From an unpublished Egypt Ministry of Culture / Aga Khan Trust for Culture map.

The eastern segment of the historic Ayyubid wall included in the al-Azhar Pilot Initiative project is approximately 800 meters long. This segment runs in a fairly continuous north-south direction from Bāb al-Wazīr to Bāb al-Mahrūq, slightly south of al-Azhar Street, and lies between al-Darb al-Ahmar to the west and the Darassa Hills to the east (A.K.T.C. 1998, 25).

This segment of wall constitutes a uniform piece of construction. It comprises a few repeating elements, such as round-fronted towers and curtain walls, and is consistent in its use of materials. This section contains ten-round-fronted towers spaced approximately every 70-110 meters along the curtain wall. Bāb al-Mahrūq is the only gate within this section. The walls are adorned and punctuated by crenellations, arrow slits, stairwells and chambers (Fong 1999, 1.4: 1).

The wall is approximately 3-3.5 meters wide and measures up to 9 meters in height. The depth of the actual foundation is not known. The wall, built entirely of masonry, is constructed of two veneer surfaces and a mortar and



Figure 1.9 Segment of the city wall showing construction technique, running and Flemish bonds.

rubble fill core. The veneer stone is buff colored, massive, fine-grained Egyptian limestone. The 42 cm-high stones are masonry bonded and regularly coursed in Flemish and running bond patterns. The stone unit length is variable and the stone thickness ranges from 15 to 25 cm for the stretchers and 40 cm for the headers (Fong 1999, 1.4:3).

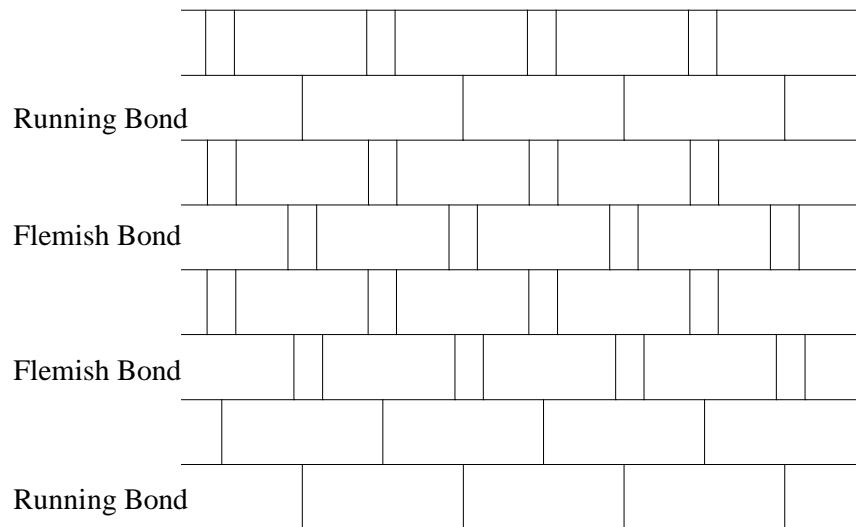


Figure I.10 Typical Flemish and running bond patterns.

I.2.2.b - Current State

In the fall of 1998, a general assessment of the wall's physical condition and its relationship to the adjoining urban fabric was carried out as the preliminary step to the conservation intervention. The survey identified the major conditions of total loss of the wall fabric, loss of the facing stone and recorded the grade of the ground at the time of the survey. A representative pilot section of about 100 meters between towers 4 and 5 was then selected to test possible conservation treatments. This section was chosen because it displays the most complete range of conditions found on the monument and it consists of an equal percentage of original and repair stones.



Figure I.11 Differential weathering of the veneer stones of the city wall.

In September 1999 scaffolding was erected between tower 4 and 5 and a detailed material condition survey was carried out to obtain a better picture of the types and extent of deterioration of the wall. The scaffolding allowed a closer examination of the wall surface and allowed additional information to be obtained. For example, the surface was covered with a thick film of silt and it was found that the stones, originally identified as flaking or delaminating, were in reality encrusted with thick crystalline deposits. In addition, material testing was carried out on selected samples in order to accurately characterize the materials and conditions of the wall.

I.3 - General aims of the project

On-site survey showed that the Ayyubid city wall of Cairo presents different forms of deterioration, including flaking and disaggregation of the stone surface (Fong

1999; Dewey 1999). The wall is made of limestone which contains an unusually high concentration of salts, mainly sodium chloride, forming columnar crystals clearly visible with the naked eye. The stone also contains clay minerals (Rock Engineering Laboratory 2000a).

Daily variations in relative humidity and temperature, which are particularly important in the arid climate of Cairo, cause both cyclic swelling of the clays and crystallization of the salts. It is furthermore suspected that a synergy exists between the deterioration caused by the salts and that due to the clay minerals, the presence of salts exacerbating the swelling of clays. These processes contribute to the deterioration of this moderately resistant limestone, and are ultimately detrimental to the integrity of the masonry.

Clay minerals are constituents of the stone so it is not possible to remove them, whereas several techniques exist to desalinate stone. However, salt removal treatments of Egyptian limestone from certain areas have been only moderately successful, while spectacular failures have been reported due to the high sensitivity of some Egyptian limestone to water. Moreover, few desalination methods can be applied *in situ* and at the large scale of the city wall. Considering the size of the wall, its natural and human environment, a desalination procedure by traditional methods, such as poulticing, is not considered feasible. Hence, a different approach is needed.

This work concentrates on the possibility of an alternative treatment based on the use of surfactants (or surface-active agents) to decrease the expansion of clays. Their use has been successfully reported in the literature (Wendler, Klemm, and Sneath 1991; Wendler, Charola and Fitzner 1996). However, surfactants alter the

properties of the water/salt/stone system and their use in salt-containing stone needs to be explored further.

The present work attempts to evaluate the action of a surfactant through laboratory testing by treating artificially salt-laden cubes of Egyptian limestone with a specific surfactant and subjecting them to wet-dry cycling. The question to be answered is whether this treatment will reduce the damaging effect that the presence of a high salt content has on the stones. The testing will also evaluate the effectiveness of the treatment and, as far as possible, its durability.

CHAPTER II

DETERIORATION OF EGYPTIAN LIMESTONE

II.1 - Egyptian limestone

II.1.1 - Geology

Egyptian limestone was formed at the floor of the sea created by the southward transgression of the Mediterranean Sea beginning some 80 million years ago. The sedimentary limestone, shale and clays form the uppermost geological layer. They are found exposed in the oases of the western desert and in the northern part of the Nile valley. A slight tilting of the land during the Eocene period (50-40 Millions years) uplifted southern Egypt, the northern end of the country was therefore submerged longer and overlaid with a thicker layer of limestone. This rock forms the surface of the desert between the apex of the Delta and the town of Es-Sebaiya in Upper Egypt, at which point the 'Nubian' sandstone definitively emerges to the surface (Tanimoto, Yoshimura, and Kondo 1993).

The Egyptian limestone, one of the major types of building stones used in ancient Egyptian structures, was quarried in geological formations dating from the Palaeocene especially the Eocene epochs of the Palaeogene period (Harrell 1992). There is, however, little consensus on the names, ages, correlation and geographic distributions of the geological formations in the Nile valley. These are primarily defined by their fossil content and the lithological differences are graded and often subtle

(Harrell 1992). Harrell, after synthesis of the literature on the Palaeogene stratigraphy of Egypt, located all the ancient limestone quarries in six formations which are highlighted in Figure II.1.

Using petrographic and geochemical parameters, studies have shown that it is possible to determine the geographic provenance of limestone used in ancient Egyptian sculptures and monuments. Middleton and Bradley (1989) studied museum objects of well-known origin to build their methodology, whereas Harrell (1992) studied of rocks coming from ancient limestone quarries to establish his criteria. Additional information about Egypt geologic formations and an important bibliography can be found in Harrell (1992). Said (1962, 1990) is also a good general reference on the lithology and palaeontology of Egyptian limestone.

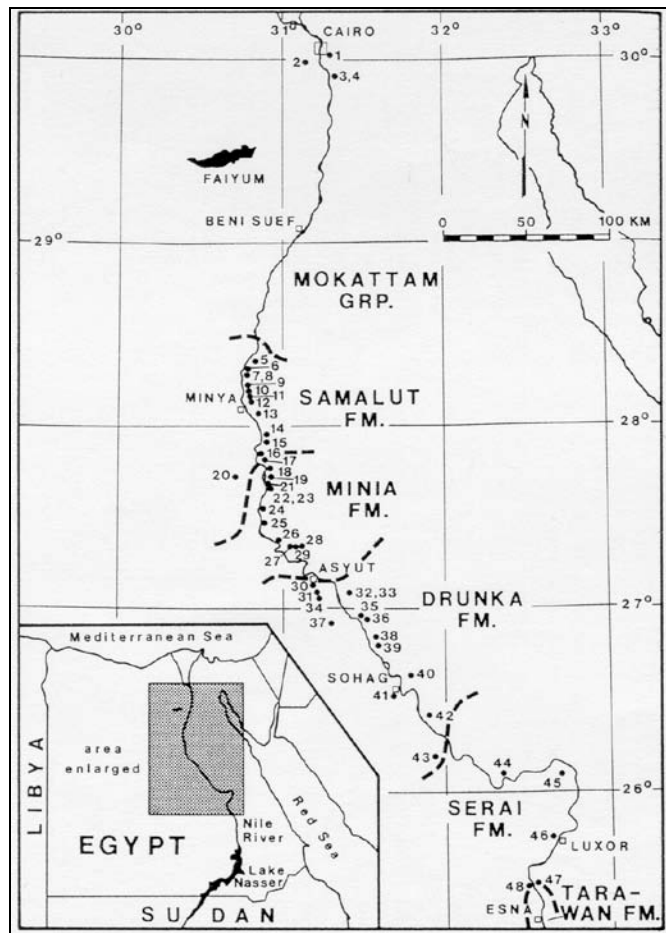


Figure II.1 Map of Egypt showing locations of ancient limestone quarries and formation contacts (heavy dashed lines). From Harrell 1992.

II.1.2 - Composition

The Egyptian limestone is mainly composed by calcite (calcium carbonate) along with secondary minerals. Of these, the clay minerals and the soluble salts are particularly relevant to the deterioration mechanisms of the stone. Jarmontowicz (1988) and Abd el-Hady (1988) carried out analysis of the limestones of three Egyptian monuments: The Cairo Citadel, Bab Zwela and Harthur temples and Zoser's pyramid. They found the main component to be calcite and also identified a range of secondary minerals, among them kaolinite, quartz, amorphous silicium dioxide, tridymite, gypsum, hydrous iron sulfate, and goethite.

Egyptian limestone was formed by precipitation of calcium carbonate from seawater, and the deposition of sand. Gypsum and halite also crystallized in the precipitation process. On their settling, these salts become incorporated in the depositing calcite and sand, which, on consolidation, constitute the limestone. Halite and gypsum are therefore natural constituents of the Egyptian limestone (Gauri 1981a; Gauri, Holdren, and Vaughan 1986; Helmi 1990; Shoeib, Roznerska, and Boryk-Jòzefowicz 1990). Gauri (1981a) affirmed that these salts were initially uniformly distributed in the rock and that they only become concentrated towards the exposed surface after use in construction and subsequent weathering in the desert climate. He also affirmed that the deterioration of Egyptian stone is primarily due to the inherent presence of water-soluble salts such as gypsum and halite through their repeated dissolution and crystallization cycles.

Almost all studies carried out on Egyptian limestone address the soluble salts content of the stone which appears to be one of the characteristics of the stone. In a very early study of deterioration of building stones in Egypt, Lucas (1915) examined 132 limestone samples from quarries located east and southeast of Cairo. He found a soluble salt content up to 4.64%, the major salt being sodium chloride. He also examined 19 soil samples from Cairo and its surroundings finding a maximum content of 20.25% with an average of 5.46%. Later Coremans (1947), reviewing the qualities and flaws of Egyptian limestone, found that while it has a fine-texture and is easily carved, it inherently contains the source of its deterioration: soluble salts. He lists sodium chloride as the most common salt, then sodium sulfate, and in a smaller quantities other salts such as sodium carbonate, sodium nitrate, and potassium nitrate. He analyzed four objects made of Egyptian limestone and found a soluble salt content ranging between 2.62% and 7.29% with sodium chloride and sodium sulfate being the most important salts present.

Egyptian limestone is also well known for its relatively high clay content which originates from the settlement of silt and clay particles onto the oceanic water becoming incorporated into the limestone (Helmi 1990).

Two examples found in the literature can illustrate the main types of Egyptian limestone. An Egyptian limestone head of Amenophis II was acquired by the Victoria and Albert Museum and then transferred to the British Museum (Hanna 1984). It contained 10.54% of acid-insoluble matter and 0.95% of chloride content (sulphate and nitrate anions were not detected). And secondly, the Abydos reliefs at the Metropolitan Museum of Art in New York City which showed a dramatic deterioration since their

arrival in a museum setting nearly a century ago. The detailed composition of this marly Egyptian limestone from the Thebes formation contains 81% of calcareous part (calcite, minor dolomite), 13% of acid-insoluble residue, clays (possibly illite and sepiolite), quartz, 4% soluble salts (predominantly calcium nitrate and sodium chloride) (Nunberg, Heywood, and Wheeler 1996) and 2% of moisture (Charola, Wheeler, and Koestler 1982). However, it will be misleading to think that all Egyptian limestone pieces have a high soluble-salt content and a high clay content. For example Bradley and Hanna (1986) analyzed a limestone figure of Ptolemy IV from the Ptolemaic period. Analysis showed an acid insoluble matter content of 0.1% and a soluble chloride content of 0.08%. The data on Egyptian limestone found in the literature generally report both high soluble-salt content and high clay minerals content because as it will be discussed, limestone exhibiting these characteristics tends to be prone to rapid deterioration.

II.1.3 - Egyptian limestone deterioration

II.1.3.a - Museum setting

Numerous Egyptian limestone sculptures stored in different museums have developed the same pattern and degree of decay, even though they were not exposed to an outdoor environment (Charola, Wheeler, and Koestler 1982; Bradley and Middleton, 1998; Rodriguez-Navarro *et al.* 1997). They generally experienced partial or complete loss of material, sometimes spectacular, in particular of the carved surface relief even though they were not subject to the relative humidity and temperature changes of an arid climate but only to those of a storage area.



Figure II.2 *Limestone relief panel of the scribe Iahmose and family (E.A. 1314), seventeenth dynasty (c. 1600 BC) from Thebes or Abydos. Left photograph between 1900 and 1920, right photograph in 1983. From Hanna, 1984.*

Barton and Blackshaw (1976) and Bradley and Middleton (1988) studied various types of Egyptian limestone sculptures that exhibited similar deterioration to try to correlate composition and mineralogy with deterioration pattern. Bradley and Middleton (1988) examined 24 Egyptian limestone sculptures of the British Museum collection, stored and displayed in different settings, which had undergone considerable deterioration since their arrival at the museum. Chemical analyses, petrographic examination and porosity measurements of both deteriorated and sound stones were carried out to investigate the factors important to the decay of Egyptian limestone in a museum environment. The percentage of chlorides found varied between 0.01% and 1.2% for undeteriorated stones, and 0.3% and 2.4% for the deteriorated stones, the percentage of nitrates reached 1.2% for both undeteriorated and deteriorated samples with a minimum of 0.2% for deteriorated stones. For several undeteriorated samples the

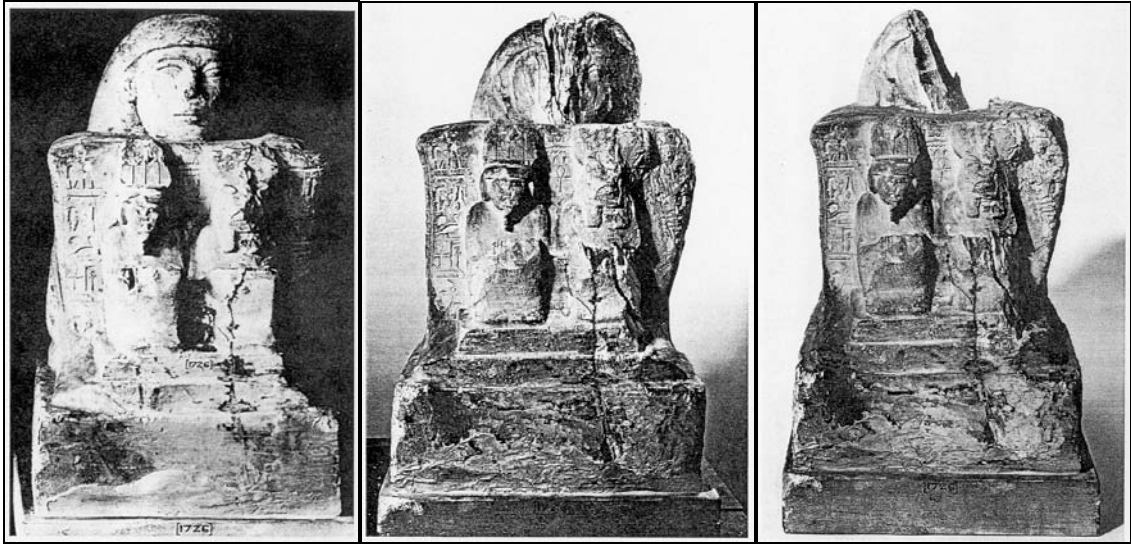


Figure II.3 Block Statute of “Hati” with two squatting figures of Anuris and Mehyt (EA 1726) attributed to Abydos or Thinis. Left photography around 1920, middle around 1940, right 1983. From Bradley and Middleton, 1988.

level of nitrates was too low to be detectable. The acid-insoluble matter (identified as clays and silica) varied between 0.6% and 12.8% for undeteriorated stones and 4.8% and 21.7% for deteriorated stones. The authors concluded that the chemical and physical properties of the various limestones used for the sculptures have exerted a strong influence upon the degree and mode of their subsequent decay in museum storage.

Three main factors are apparently significant for the decay. The first is the presence of a relatively high proportion of acid insoluble materials, predominantly clay minerals, rendering the stone liable to structural decay. The second is the presence of high levels of soluble salts, particularly when these include a high proportion of nitrates, increasing the susceptibility of the sculptures to localized powdering and pitting. The third factor is the petrographic character of the limestone, particularly porosity and number of micropores. Those from Thebes/Abydos have textures in which the calcite



Figure II.4 Royal head of Amenophis III (E.A. 69054) from the Temple of Merneptah, Thebes. Left Photography after excavation in 1896, right photography in 1983. From Hanna, 1984.

is highly fragmented, occurring as dispersed grains and aggregates separated by fine clay and open pores, providing easy access for moisture and a greater surface area for chemical reaction. In contrast, the better-preserved sculptures from Cairo and El Bersha exhibit less fragmented textures, with solid islands of calcite separated by regions of higher porosity.

Several studies tried to establish the maximum levels beyond which salt and clay become harmful to the limestone. While studying the advanced state of decay of some Egyptian limestone from the British Museum collection, Hanna (1984) found that it is particularly difficult to treat limestone objects if it contains a high concentration (>2%) of clays and consolidation is necessary before any other treatment. Furthermore, if the concentration of chloride is above 0.1%, desalination of the stone is necessary.

Miller (1992), after studying highly deteriorated limestone objects from the Thebes/Abydos region of Egypt, confirmed that a high clay (5% or above) and soluble salt content (0.1% or above), in conjunction with high microporosity of the stone, lead to serious decay. Other researches focused on the susceptibility of the Egyptian

limestone to water and a more detailed review can be found in the sections on treatment by water immersion and poulticing (Chapter III).

II.1.3.b - Outdoor environment

Most studies of Egyptian limestone deterioration concentrated on the decay of museum objects and few studies of *in-situ* Egyptian limestone structures can be found in the literature. The Great Sphinx on the Giza plateau is one of them.

The Great Sphinx rock is made of different layers: the very hard limestone constituting the base of the Sphinx, the body composed of successive layers of very soft limestone interbedded with thin layers of a comparatively hard limestone and a very hard and compact limestone forming its neck and head (Helmi 1990). As usual, the causes of deterioration of the Sphinx are multiple, such as crystallization of soluble salts, thermal cycling, erosion by wind-driven sand, surface attack by acidic pollutants, damage from occasional earthquakes, capillary rise of groundwater, and dissolution of the stone by rainfall (Maekawa and Agnew 1996).

After environmental monitoring, Maekawa and Agnew (1996) determined that salt crystallization was the most probable cause for the deterioration of the surface of the monument, which was the conclusion reached by previous studies (Camuffo 1993; Gauri *et al.* 1988, 1983; Tanimoto, Yoshimura, and Kondo 1993). The damage patterns observed depend on the distance of the stone from the soil. The lower part of the body exhibits crumbling and exfoliation occurring at the rate of 2-3 mm per year. Since it is covered by masonry (Tanimoto, Yoshimura, and Kondo 1993), wind-erosion is completely absent and the observed deterioration is due to the action of internal salts

mobilized in the rock and released in the surface layer by wetting and drying cycles. The upper part of the body and the neck are subject to the combined effect of salt crystallization and wind erosion (Camuffo 1993). The intensity of weathering of the Sphinx is also proportional to the quantity of the soluble salts, halite (sodium chloride) and gypsum (calcium sulfate dihydrate) in the layers of the bedrock as well as inversely proportional to the large-pore-to-throat ratio of the pores (Gauri, Holdren, and Vaughan 1986; Gauri *et al.* 1988).

For further information about the Great Sphinx, Selwitz (1990) prepared a review of the literature concerning the structure, whereas *First International Symposium on the great Sphinx towards Global Treatment of the Sphinx* (1992) gives a wide range of articles dealing with its conservation.

The few examples reported show that two elements are critical to the deterioration of Egyptian limestone, soluble salts and clay minerals. A short review of the decay mechanisms due to each of these two components is necessary to be able to understand successes and failures of previous treatments and to design new treatments.

II.2 – Salt deterioration of porous materials

II.2.1 - A poorly understood phenomena

It has been known for along time that the presence of salts in porous materials such as stones can lead to their deterioration and the subject has generated an important body of literature. However, the mechanisms of salt deterioration are still poorly understood (Rodriguez-Navarro and Doehne 1999). Several theories have been drafted

to try to explain the phenomena observed and some led to well-accepted models of salt damages, although they failed to explain many field observations (Arnold and Kueng 1985). For example, no satisfactory explanation has been given to the fact that certain salts are much more destructive than others (Rodriguez-Navarro and Doehne 1999).

An in-depth look at the subject of salt deterioration, a review of the current theories as well as an extensive bibliography can be found in Charola (2000) and Rodriguez-Navarro and Doehne (1999). Arnold and Zehnder (1990) also give a good summary of the issue of salt weathering.

Despite the lack of understanding of salt deterioration mechanisms, it has been clearly established that the presence of salts combined with cyclic changes in the environmental conditions can cause damage to stones.

II.2.2 - Origin of salts

The salts can have numerous origins. Some stones naturally contain salts, as it is the case for Egyptian limestone (Gauri 1981a; Gauri, Holdren, and Vaughan 1986; Helmi 1990; Shoeib, Roznerska, and Boryk-Jòzefowicz 1989). Other construction materials can also be the source of the salts found in stone. During post-pharaonic restoration of the Great Sphinx of the Giza plateau, salt-rich mortars were used to cement less-durable limestone blocks of the veneer and have damaged the earlier, well-selected, highly durable limestone blocks and mortars (Gauri, Holdren, and Vaughan 1986). In the case of the Ayyubid wall of Cairo, the Comité used Portland cement-based

mortars for the repair of the wall in 1950. The alkali sulfates in these mortars could have been released into the surrounding stones.

Other sources of salts in Cairo include salt spray (chlorides), air pollution (sulfates), soil and human activity. The eastern section of the Ayyubid city wall has been bordered for centuries on its east side by a dump and its west side by human habitations, sometimes invasive to the wall. Those activities have certainly increased the nitrate concentration in the immediate environment of the wall.

Other literature sources (Arnold 1981; Furlan and Houst 1983) can be consulted for a more detailed review of the most commonly salts found in walls and their origin.

II.2.3 - Salt movement

Except when salts are naturally intrinsic to the stone, the salts have to be brought into the porous material to produce any damage. Water is the medium of choice to bring salts into stone and move them around once inside. This is the reason why salts of very low solubility in water are not as critical in terms of stone deterioration. Water can enter into stone through two main mechanisms: capillary rise of ground water and infiltration by rainwater. Water can also enter a porous material as a vapor by condensation or hygroscopicity.

Salts have to be dissolved in liquid water to move inside the porous material. Dissolution of salt crystals can be achieved by import of liquid water or condensation of vapor water into the pores. The latter is generally achieved by changes in environmental conditions (temperature and relative humidity) causing condensation of water and thus

allowing the salts to dissolve. Afterwards, a combination of a decrease in water vapor pressure and a change in temperature in the atmosphere will cause moisture to move towards the surface of the porous material and the dissolved salts will be redeposited close to the surface (Bradley and Hanna 1986). The movement of soluble salts inside porous materials is a complex process described in depth by Schaffer (1972).

II.2.4 - Deterioration mechanisms

Although the deterioration mechanisms are poorly understood, two main decay phenomena are generally distinguished in the literature: crystallization/dissolution and hydration/dehydration cycling.

II.2.4.a - Crystallization / dissolution cycling

It has been widely observed and reported that cycles of crystallization, dissolution, and re-crystallization of salts due to changing environmental conditions cause progressive deterioration of porous materials. The extent of deterioration however varies widely from one salt to another. Field observations showed that all soluble salts may produce very strong decay (Arnold and Kueng 1985).

There are several crystal growth theories (Furlan and Houst 1983; Lewin 1982). Different equations have been developed to calculate the so-called crystallization pressure which can develop inside pores of stones when a supersaturated solution occupied less volume than the precipitate crystals plus the resultant solution, which is the case for a number of salts.

The water vapor pressure above a salt solution is a characteristic of the salt and is lower than that of pure water at a given temperature. When the salt concentration increases, the water vapor pressure decreases, the minimum vapor pressure being reached above a saturated solution of the salt. The vapor pressure above a saturated salt solution depends on the salt and the temperature and is known as the “equilibrium relative humidity” (RH_{eq}) since the vapor pressure can be expressed as a percent of the relative humidity. For example sodium chloride (NaCl) has a theoretical RH_{eq} of 76% but the experimental value is 73% (Bonnet and Perrin 1999). Several authors provide lists of equilibrium relative humidities of saturated salt solutions frequently found in walls (Arnold 1981; Zehnder and Arnold 1989; Arnold and Zehnder 1990; Price and Brimblecombe 1994; Bonnet and Perrin 1999).

When the ambient relative humidity is above the salt RH_{eq} , the environment is humid enough for the crystallized salt to dissolve. However, as soon as the ambient RH decreases below the salt RH_{eq} , water will move by capillary action towards the outside surface of the stone to evaporate and the salt will crystallize (Arnold 1981). Experiments have shown that more cycling across the RH_{eq} of the salts contained in the stone result in more deterioration.

The location of salt crystallization also plays an important role in the deterioration mechanism of porous material. Lewin (1982) showed through laboratory experiments that the site of salt crystallization is determined by the dynamic balance between the rate of escape of water from the surface and the rate of re-supply of solution to that site. The former is a function of temperature, air humidity and local air currents. The latter is controlled by surface tension, pore radii, viscosity and the path

length from the solution to the site of the evaporation. If the migration of solution to the surface is faster than the drying rate, then the solute is deposited on the external surface of the porous material. This corresponds to the formation of efflorescences. These are highly visible and are generally a sign of an important salt concentration within the stone even though they themselves may not be damaging to the material. They can often be easily brushed off the surface.

The salt decay occurs only when the solute is deposited within the pores of the solid under the superficial layer of material. This phenomenon is generally called subflorescence. This can occur when the rate at which water departs from the surface of the solid via evaporation is equal to the rate at which fresh water solution is brought to the surface via migration through the internal capillary system of the solid.

When salt crystallization occurs deep within the stone, a phenomenon referred to as cryptoflorescence, it does not manifest itself in the form of surface decay. This is the case when the migration of the solution towards the exposed surface is very slow (Lewin 1982; Furlan and Houst 1983; Hanna 1984; Rodriguez-Navarro and Doehne 1999). In addition to the location of salt crystallization, morphology and growth rate of the newly formed salt crystals are important factors to understand the decay phenomena (Rodriguez-Navarro and Doehne 1999).

Salts do not always crystallize under their equilibrium form but can show different growth forms or habits. These can differ significantly from their equilibrium forms. The same salt mineral may form different habits simultaneously at different places or subsequently at the same place depending on external conditions.

Arnold has frequently described and categorized the different habits of salts observed in the field and reproduced them in the laboratory (Arnold and Kueng 1985; Arnold and Zehnder 1985; Zehnder and Arnold 1989). He showed that all external factors, environmental conditions, type of salt and solution supply strongly control the habit of the growing crystals. However, the humidity condition of the substrate seems to be the most significant single factor influencing the crystal habit and aggregate form. Most forms and aggregates are not very stable and undergo transformation through time. The observation of the salt forms is particularly relevant to the study of salt deterioration because some forms, such as fluffy efflorescences, cause very little damage to the stone and are easily removed from the surface, while others, such as salt crusts, have proven to be more damaging and more difficult to remove.

Characteristics of the porous material itself also play a role in the deterioration mechanism, in particular pore-size distribution, surface activity, and wettability (Arnold and Zehnder 1985). It has been observed in numerous cases that stones with a higher proportion of micropores connected to large pores are more susceptible to salt weathering (Rodriguez-Navarro and Doehne 1999).

In a very thorough article about salt weathering, Rodriguez-Navarro and Doehne (1999) concluded that “salt damage due to crystallization pressure appears to be largely a function of solution supersaturation ratio and location of crystallization. These key factors are related to solution properties and evaporation rates, which are constrained by the solution compositions, environmental conditions, substrate properties, and salt crystallization growth patterns”.

II.2.4.b - Hydration / dehydration cycling

The second phenomenon which has been held responsible for the salt deterioration of porous materials is the hydration of the salts, when possible. Upon hydration, each salt crystal absorbs moisture and finds itself surrounded by a number of water molecules. It seemed a logical approach to consider that the hydration phenomenon was accompanied by the appearance of a hydration pressure due to the volume increase upon the hydration of a salt. However few experiments have attempted to calculate this pressure.

Furthermore, recent experiments showed that in the case of sodium sulfate, the hydration of the salt does not proceed through absorption of moisture by the anhydrous crystal but only through dissolution of the anhydrous crystal and recrystallization of the decahydrate crystal afterwards (Rodriguez-Navarro and Doehne 1999). Similar phenomena have been observed in the field. Arnold and Kueng (1985) observed salt efflorescence in the Grasburg ruin near Berne (Switzerland) and found that the normal process seems to be the crystallization of the hydrated phase and then its dehydration. If hydration of any salt always follows a dissolution of the anhydrate prior to recrystallization of the hydrate, the hydration phenomenon could be considered as a particular case of crystallization (Rodriguez-Navarro and Doehne 1999).

II.2.5 - Salt mixtures

Each salt can be characterized by its relative humidity equilibrium value (RH_{eq}). For common, simple salts, those values are relatively well known, however in a natural

environment it is rare to find a single salt. Stones generally contain salt mixtures. In terms of crystallization and dissolution the behavior of salt mixtures is much more complex than that of a single salt.

The simultaneous presence of salts affects their individual solubility and, in contrast to the behavior of a single salt, the mixture is not characterized by a unique equilibrium relative humidity at a given temperature but rather by a range of RH_{eq} within which fluctuations continuously cause dissolution and reprecipitation of one compound of the mixture (Price and Brimblecombe 1994; Steiger and Zeunert 1996). Furthermore, this range is not easily predictable and does not necessarily lie between the equilibrium relative humidity values of each salt. The range of RH_{eq} depends of the interactions between the salts. The lower limit of this humidity range is given by the drying-up point, below this RH, all the salts are crystallized. Above the upper limit of the RH_{eq} range, all salts are in solution.

Theoretical models have been developed to calculate RH_{eq} of salt mixtures. Price and Brimblecombe (1994) and Steiger and Zeunert (1996) provide a good overview of the issue of salt mixtures and relative humidity equilibrium values.

II.2.6 - Salt behavior in arid climates

Cairo has a typical desert climate with only two seasons: winter, lasting from November to March (average daily minimum temperature of 21°C); and summer, from May to September (average daily maximum temperature of 35°C). The annual rainfall in Cairo is about 1 inch (*Encyclopedia Britannica*, s.v. “Egypt”, “Cairo”).

Environmental monitoring has been carried out around the great Sphinx on the Giza plateau, outside Cairo, providing more detailed data on Cairo climate (Maekawa and Agnew 1996). On the Giza plateau, over the course of a year, the relative humidity varies between 9% and 100% with daily variations between 30 and 95% being common. These seasonal variations are accompanied by large daily thermal amplitudes with dry and hot days and cooler and more humid nights. Air temperature varies between 3° and 42°C, and temperature at the surface of the Great Sphinx stone can varies between 2° and 55°C (exposed), 4° and 42°C (shaded).

It has been recognized that salts are generally the major cause of masonry deterioration in arid climates (Cooke 1979; Gauri 1981a; Gauri, Holdren, and Vaughan 1986; Gauri *et al.* 1988). The high temperature during the day causes evaporation of the water at the stone surface, which consequently draws the moisture and the salts dissolved in it from relatively greater depth of the porous material. This causes a concentration of water-soluble salts closer to the surface. The evaporation of water causes the local relative humidity to drop below the RH_{eq} of the salts inducing their crystallization. At night, the temperature decreases sharply, especially at the stone surface, quite often plunging below the dew point, causing the general relative humidity to increase. Despite its scarcity, moisture is able to condense as droplets and to penetrate into the stone and dissolve the water-soluble salts present near the surface. By capillary action, the solution then enters the pores. The salts crystallize again during the heat of the following day. These daily dissolution and crystallization cycles of the salts generate large stresses and lead to the physical deterioration of the stones in arid climates.

However paradoxical it may seem, water is a serious damage factor in arid climates even though they are notably deficient of it. Precisely due to the restricted amount of water combined with high daytime temperatures, supersaturated solutions are produced from which salts can easily crystallize. In addition, the lack of water in form of precipitation prevents the washing away of salts accumulated on the surface, leaving them in place for the next cycle.

II.3 - Clay minerals and stone deterioration

II.3.1 - Clay content and stone deterioration

Clay minerals are natural components of stones and are generally present as a minor component in ornamental and building stone. They are generally considered as harmful constituent of building stones and have been recognized to be a major problem in the conservation of cultural heritage (Dunn and Hudec 1966; Delagado-Rodrigues 1977; Caner and Seeley 1978; McGreevy and Smith 1984; Wendler, Klemm, and Snethlage 1991; Rodriguez-Navarro and Doehne 1999). Caner and Seeley (1978) studied marble, dolomitic limestone, and micritic limestone samples from six monuments across Turkey. They pointed out the persistent presence of clay minerals in decay layers. The sound and decay zones coincide with the clay mineral distribution which highlights the importance of clay minerals in the decay mechanisms. In an early article, Dunn and Hudec (1966) showed that presence of expansive clays can be a major factor in the deterioration of rocks and are often the culprit of what first appears as frost deterioration.

Much of the limestone commonly used for building and sculptural purposes usually contains a small proportion of clay. However, the clay fraction in micritic and biomicritic limestones can reach values of more than 10%. It has been reported that limestone used as building stone or for sculptures is prone to rapid decay if the stone contains more than 5% clay (Rodriguez-Navarro *et al.* 1997). One of the characteristics of Egyptian limestone is its high clay content and, in several cases, the hydration of the clays minerals has been recognized to be one of the main decay agents (Hanna 1984).

The extent of the swelling can be relatively important. Rodriguez-Navarro *et al.* (1997, 1998) studied the role of clays in the decay of Egyptian limestone sculptures and measured the swelling of the stone. When immersed in distilled water at 30°C for less than an hour, the limestone swelled about 3% in the direction perpendicular to the bedding planes. After the first wetting/drying cycle was completed, a 0.3% mechanical deformation was noted. A second wetting/drying cycle produced faster and greater expansion of the sample (up to 4%), that is, the structural damage created in the first wetting/drying cycle enhances the damage produced in the following ones.

Samples of limestone partially immersed in a beaker filled with distilled water resulted in fissure development parallel to the bedding planes and complete disintegration of the stone within a few hours. Relative humidity cycling in an environmental chamber (20°C, RH 40-90% cycling) led to almost complete destruction of the stone blocks due to spalling and exfoliation of the surface skin and fracture along the bedding planes. After their experiments, Rodriguez-Navarro *et al.* concluded that the presence of clays was the main factor responsible for the damages observed in the

Egyptian limestone from the Abydos/Thebes region they studied and showed that even nonexpandable clays can promote significant damage due to swelling.

The deterioration mechanism induced by clays is due to the capacity of swelling of the clay minerals following changes in environmental conditions. Their layered structure and the cations adsorbed between layers are responsible for the swelling capacity of clay minerals. Increase in moisture tends to make clay minerals expand but the phenomenon may be fully reversible, the clays shrinking if they dry (Madsen and Muller-Vonmoos 1989). This repetitive action can cause important damage to stones with high-clay content. The swelling behavior of clay rocks depends mainly on the type and quantity of clay minerals present, their surface charge, the valence of the cations in the double layer, and on the spatial distribution of the clay minerals contained in the stone.

A high average clay content does not necessarily weaken the stone. It has been shown that the spatial distribution of clays inside the stone is the key factor determining whether or not a high clay content will lead to a rapid stone deterioration. Dunn and Hudec (1966) highlight that if clays are thinly and uniformly distributed through an impervious rock so that air and water may not reach them to an appreciable degree, they will not necessarily lead to stone decay. New Scotland formation of the Helderbergian Group in the Hudson Valley is a good example of a stone with high clay content (up to 40% and rarely below 10%) which is not problematic because clays are disseminated in the calcite matrix. Through experiments, they show that for clays to have an impact on rock soundness, they must not only be present but they must also be available to water. It is when clays are concentrated in layers between the calcite in argillaceous limestone

and forming a continuous network accessible to water that rapid disintegration is to be expected.

A brief review of the swelling behavior of the clay minerals and the deterioration mechanism it induces is presented here. For more detailed information about clay minerals Velde (1995) and Moore and Reynolds (1989) are useful sources.

II.3.2 - Swelling of clays

II.3.2.a - Inner-crystalline swelling

Two types of swelling can be distinguished. The first type, the inner-crystalline swelling, is a short-range particle interaction due to the hydration of the exchangeable cations present between the layers of the dry clay. Crystalline swelling only occurs for clay species which have exchangeable interlayer cations, such as illites and montmorillonites. Those clay minerals are generally qualified as “swelling” or “unstable” clays. They possess interlayer cations located on

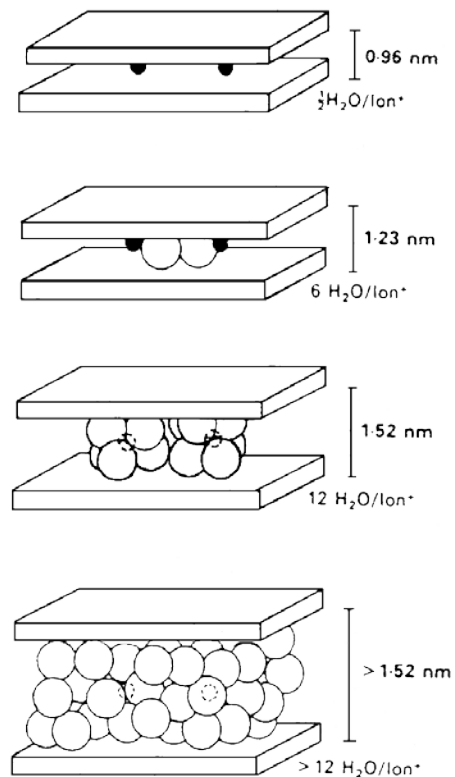


Figure II.5 Innercrystalline swelling of sodium montmorillonite. Given are the layer distances and the maximum number of water molecules per sodium ion. From Madsen and Müller-Vonmoos 1989.

the negatively charged surface of the layers holding the layers very strongly (Madsen and Müller-Vonmoos 1989).

Because water molecules are electrically neutral but polar they orient their negative poles toward the cations and their positive poles toward the negatively charged surface of the clay layers when the cations hydrate. Hydration therefore weakens the electrostatic interaction between the interlayer cations and the negatively charged layers and leads to the increase of the inter-layer distance, i.e. the swelling of the clay minerals. It has been shown that hydration of the interlayer cations occurs in several steps (Madsen and Müller-Vonmoos 1989).

The nature of the interlayer cation influences the swelling behavior of the clay minerals. For example, the swelling behavior of sodium montmorillonite is very different from that of its calcium counterpart (Madsen and Müller-Vonmoos 1989).

II.3.2.b - Osmotic swelling

The second type of swelling is the osmotic swelling. This is a long-range particle interaction due to the large difference in concentration between the ions electrically held close to the clay surface and the ions in the pore water of the rock. All types of clay minerals can undergo osmotic swelling, including the clays generally qualified as non-expandable, such as sepiolite and palygorskite. It can act over much larger distances than the inner-crystalline swelling. However, the swelling stress produced is significantly smaller than that of inner-crystalline swelling.

If the salt ion concentration between two layers of clays is significantly higher than the concentration in the pore water osmosis results. The phenomenon of

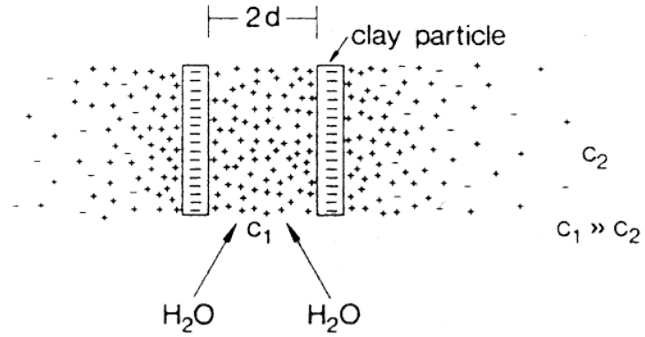


Figure II.6 Two negatively charged clay layers with ion cloud. From Madsen and Müller-Vonmoos 1989.

osmosis is the natural tendency towards equilibrium of the two concentrations. This can only be achieved through penetration of water in the interlayer space since the interlayer cations are fixed electrostatically by the negative charges of the layers (Madsen and Müller-Vonmoos 1989). The penetration of water into the space between clay layers induces the so-called osmotic swelling. The osmotic swelling depends mostly on ionic concentration, type of exchangeable ion, pH of the pore water and type of clay (Rodriguez-Navarro *et al.* 1997, 1998). Experiments to measure clay swelling in the laboratory have been performed and showed that the greatest part of the swelling takes place within the first two days (Madsen and Müller-Vonmoos 1989). A more in-depth description and experiments on the swelling behavior of clays can be found in the literature such as Madsen and Müller-Vonmoos (1989).

II.4 - Synergy between salts and clay minerals in stone deterioration

The degree of salt weathering of stones depends, among other things, on the properties of the rocks being affected (Cooke 1979). So it is possible that clay minerals play a role in the salt weathering susceptibility of stones (Harvey *et al.* 1978).

McGreevy and Smith (1984) investigated this issue and observed that laminated sandstones which contain smectite clays break down more readily than those with little clay. The authors suggested two possible explanations of how clay minerals might promote breakdown through salt crystallization. The first possibility is that the clays play an active and direct role in the stone decay through their swelling and complement the salt weathering effect but without synergic effect, the other one is an indirect effect where clay minerals enhance salt-related deterioration by contributing to an increase in microporosity of the stone which itself favors salt damage. They conclude that whatever the correct explanation is, it proves that weathering processes rarely occur in isolation and that many deterioration mechanisms have several origins.

On the other hand, the presence of salts in the material can have an influence on clay-induced deterioration. Rodriguez-Navarro *et al.* (1997, 1998) saw that the expansion of the fibrous clays of the Egyptian limestone they studied by Environmental Scanning Electron Microscope (ESEM) is strongly enhanced by the presence of NaCl. The presence of salts within the pore system of the stone promotes condensation of water at relative humidity values lower than 100%. For example, in the case of a mixture of NaCl and NaNO₃, each salt has a RH_{eq} around 75% but deliquescence of a mixture of both salts occurs at relative humidities around 60% (Arnold 1981; Price and Brimblecombe 1994). It means that liquid water can be present within the pore system of the stone at any relative humidity value above 60%. Thus if the RH goes above this value, damage to the stone by swelling may be produced. Therefore, the salts are not necessarily directly responsible for the stone deterioration if no salt crystallization exists but their presence enhances the problem of clay expansion by reducing the RH_{eq} even

when the relative humidity is not very high or when the RH changes are not very important (Rodriguez-Navarro *et al.* 1997, 1998).

The presence of soluble salts within the stone can also have a second effect on clay swelling. The solution they form when the water enters the pore system of the stone supplies ions that can act as counterions. Once hydrated they can also contribute to the swelling of the clays. Furthermore, they promote ion-exchange process between the inter-layer cations of the clays and the cations of the salts. The ion-exchange will foster higher decay through clay swelling if a less hydratable ion such as calcium is exchanged for a more hydratable ion such as sodium (Rodriguez-Navarro *et al.* 1997, 1998).

Chatterji, Christensen, and Overgaard (1979) sought to explain the damages suffered by Orthoceras limestone exposed to NaCl or Na₂SO₄ by the fact that the Ca-clay (smectite) present in the limestone is converted to Na-clay in the presence of an excess of sodium salts by an ion-exchange process. This process promotes the splitting and breakdown of clay-rich limestone, especially those where clays are concentrated along the bedding planes.

Rodriguez-Navarro *et al.* (1997, 1998) additionally proposed that the third possible action of an electrolyte is to create an electrical double layer at the clay-solution interface resulting in swelling due to electrostatic repulsion forces between the nearby fibrous clay particles. It is probably a combination of factors that could explain the enormous expansion of the Egyptian limestone studied (3% when immersed in water) which cannot be due to the crystalline swelling of the clays alone.

Rodriguez-Navarro *et al.* (1997, 1998) summarize well the different sequences of clay mineral swelling when salts are present. The initial swelling is due to the hydration of the negatively charged clay surface which can absorb polar liquid (water) as well as various ions present. However if sodium chloride, for example, is present within the stone, it offers a supply of sodium ions to the solution formed when water enters the pore system of the limestone. The sodium ions can act as counterions and, in turn, become hydrated and contribute to the swelling of single fibrous clay crystals (crystalline swelling). Once the hydration of the clay surface is completed, an electrical double layer will be formed, resulting in interparticle swelling due to electrostatic repulsion forces between nearby clay particles. This can create sufficient swelling pressure to damage the layered structure of the stone.

A last influence of salts on the swelling behavior of clay-rich stones was highlighted by Snethlage and Wendler (1996). They studied the hygric dilatation of a NaCl-contaminated sandstone in comparison to a salt-free stone. The salt-free stones behaved as expected, they expanded during wetting and contracted during drying. However, the salt-contaminated stones reacted the opposite way, contracting during wetting and expanding during drying. In addition, this dilatation was not reversible and the amount of dilatation increased from cycle to cycle. Snethlage and Wendler (1996) attempted to explain this unexpected behavior: “The contraction during the wetting phase can be relatively easily explained by the formation of dense hydration shells between the grains, which become denser as electrolytes become stronger. The expansion during the drying phase is still not clear. It could be explained either by the

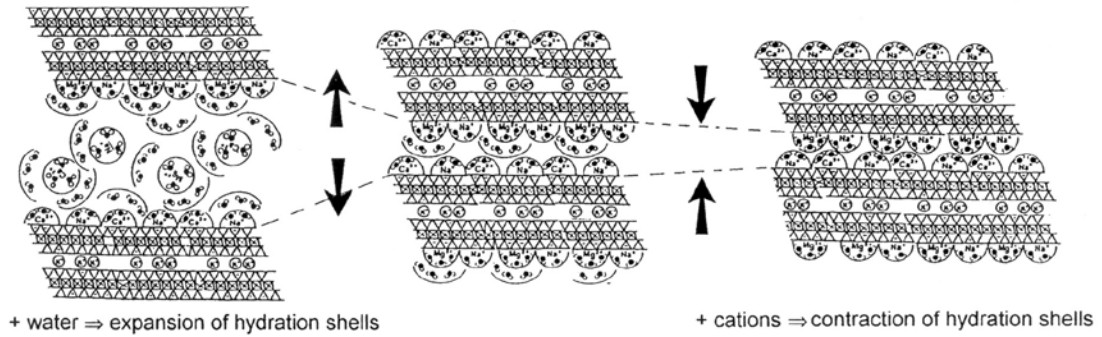


Figure II.7 *Expansion and contraction of clays in presence of salts.
From Sneathlaga and Wendler 1996.*

crystallization of salts in the coarse pores ... or by the formation of salt films which adhere tightly to the grains and push them apart while they are growing.”

Figure II.7 is a schematic representation of the expansion and contraction of clays in presence of salts. The supply of salt (cations) causes contraction, whereas the supply of water causes an expansion of the system. The more salts present, the stronger the contraction at constant moisture content. At constant salt content, the absorption of water will cause a decrease in salinity and the system will expand.

CHAPTER III

TREATMENTS FOR EGYPTIAN LIMESTONE

III.1 - Treating Egyptian limestone

Deterioration of Egyptian limestone in museums or in the field is generally due to multiple causes ranging from environmental conditions and geology of the limestone to building technology. It should always be addressed in a case-by-case basis. In the case of the eastern portion of the Ayyubid wall of Cairo, concerns such as the use of the nearby grounds for waste dumping and poor plumbing installed by inhabitants of the neighborhood against or in the wall, have to be addressed as part of the wall conservation plan. Nonetheless, as the abundant literature on Egyptian limestone shows, the geological nature of the stone, which naturally contains high concentration of both soluble salts and clay minerals, is a direct cause of concern and often pointed out as the main cause of decay. So the treatment of the stone itself is an issue which should be considered.

Numerous treatments addressing one or both issues (salts and clays) relevant to Egyptian limestone have been used in the past. However the published case studies of previous treatments are far from offering a perfect track record. Gauri (1981a) was, in fact, very optimistic when, after studying the great Sphinx and recommending restriction of the water movement and desalinization of the stone he affirmed that “both of these can be achieved easily with existing technologies”.

A review of possible treatments for Egyptian limestone is presented here. Other sources (Jedrzejewska 1970; Section française de l'IIC 1996) can be consulted for additional information on the subject of salt removal from porous stone.

III.1.1 - Consolidation treatments

III.1.1.a - Consolidating deteriorated stone

Several museums in Western Europe and North America have large collections of Egyptian limestone objects and their often-rapid deterioration in the museum environment lead to the investigation of treatments for several decades. Conservators were often confronted with objects whose surface deteriorated (flaking, powdering), while exhibiting salt efflorescences. The consolidation of the stone before any other treatment, such as cleaning and/or desalination, became a major issue for Egyptian limestone objects (Hanna 1984). However, performing stabilization of the weakened stone and preventing salt movement can be conflicting. If the consolidation treatment effectively secures the surface it may prevent other treatments, such as cleaning, to be carried out. If desalination and cleaning are carried out before consolidation then the probability of the sculpture suffering considerable surface loss is high (Bradley and Hanna 1986).

The traditional treatments of Egyptian limestone generally focused on the application of paraffin by immersion impregnation or of heated oils under vacuum (Charola, Wheeler, and Koestler 1982; Helms 1977). Many different materials have been used to consolidate stone, such as waxes, barium and calcium hydroxide, epoxies

and methacrylates (Hanna 1984). Miller (1992) offers an interesting review of the different practices at the British Museum for the consolidation of such decayed porous stones.

One of the most famous examples of consolidation treatment of Egyptian limestone is probably the case of the Abydos reliefs which have become at this point an involuntary depository of conservation trials and errors for the past century and has consequently generated an important body of literature. The Abydos reliefs, a set of Egyptian limestone bas-reliefs, were received by the Metropolitan Museum of Art in New York City in 1911. When they arrived at the museum, the reliefs had already suffered severe damage due to salt crystallization and began disintegrating within months of their installation. They were treated by various methods, each new method trying to succeed where the previous ones had failed. Not all sections of the reliefs were treated each time or in the same manner. None of the treatments were successful in stopping the deterioration of the stone by salt crystallization and clay swelling (Oddy, Hughes, and Baker 1976; Helms 1977; Charola, Wheeler, and Koestler 1982; Wheeler *et al.* 1984; Nunberg, Heywood, and Wheeler 1996). Previous treatments included: immersion of stones in molten paraffin (1911-13 and 1938-40), treatment with tung oil dissolved in carbon tetrachloride with lead or manganese oxides heated under vacuum (1911-13), beeswax (1943), PVACs (vinylite) to reattach some of the flaking (1957-59), barium ethyl sulphate (1975), epoxy impregnation (1975), and methyl trimethoxysilane consolidation (1984). Some of the sections were also set in iron-reinforced plaster and framed with angle iron for support in 1938-40 (Wheeler *et al.* 1984). None of these

treatments contributed to the stabilization of the panels and salts efflorescence continued to appear at their surface fostering further decay.

Fox (1984) was confronted with a similar problem, Coptic limestone reliefs from the Kevorkian collection at the Harvard University Art Museums. The surface of the fine-grained, very porous, fossiliferous limestone had been severely damaged due to the effects of fluctuating humidity upon salts, mainly sodium chloride, within the stones. Consolidation of the stones was seen as a necessity to improve the cohesiveness of the stone prior to any desalination treatments. To determine the most appropriate consolidant the author conducted experiments on limestone samples and found that around half of the consolidated samples showed sodium chloride recrystallization on the exterior surface four months after treatment. The consolidants seemed to foster further salt efflorescence. There is little doubt that salts also influence the durability of the consolidant.

Riecken and Sasse (1997) have investigated the durability of impregnation products (two different polymer agents: a hydrophobic and a non-hydrophobic polyurethane) for salt contaminated sandstones by measuring the biaxial bending strength through time. The authors found that the presence of salts can both influence the hardening process of the polymer and reduce the long-term durability of these products. It would appear that a critical salt concentration seems to exist for the tested stone/polymer combination. The salt crystals, initially covered like the surrounding stone by the polymer micro-layer which cannot be rendered totally impermeable, can take up moisture in the pores by osmotic process and expand in volume. This

phenomenon could crack the polymer film or reduce the adhesion between polymer and stone.

Wendler, Klemm, and Snethlage (1991) also underlined the fact that the presence of clays within the stone decreases the lifetime, already limited to 10-15 years, of consolidating and hydrophobing agents. There is a decrease in consolidant effectiveness with the increase of swelling clay minerals content. Alternating hygric swelling and shrinking effects are responsible for the loosening of contacts between the polysiloxane film and the mineral surface.

III.1.1.b - Salt encapsulation

Numerous times, consolidation has been perceived not as one of the first steps in a comprehensive conservation procedure of a weakened stone but as the last, and sometimes the only step in the conservation of Egyptian limestone. It was thought that a consolidant would not only harden the material but also render it impermeable to water, and therefore arrest the damaging cycles of salt crystallization and clay swelling. In a 1947 article, Coremans advocated elimination of soluble salts prior to consolidating objects by vacuum impregnation with heated paraffin (temperature not exceeding 90° - 100°C). His hope was to render the surface of the objects harder and impermeable.

It has also been believed that consolidants could be used to encapsulate the soluble salts and prevent their efflorescence avoiding the need for desalination after consolidation. This theory was revived in particular when silane consolidants appeared on the market. However, evidence of salt movement (efflorescence) following silane-consolidation was reported, even in an indoor situation (Bradley and Hanna 1986). For

encapsulation of salts to be successful, the consolidant would have to fill the pore structure completely at the surface of the stone - which is unlikely to occur since the amount of cured consolidant deposited in the stone is small compared with the pore volume - but also remain as an unbroken impermeable film through time.

Bradley and Hanna (1986) report on the cases of a limestone figure of the Ptolemaic period and a limestone panel from the tomb of Sri at Saqqara. Both objects were consolidated with methyl trimethoxy silane. Droplets soon appeared on the surface of the figure associated with the concentration of salts at or near to the stone surface. Furthermore, the surface of the panel was found to be more deteriorated and covered in a heavier efflorescence after two years in storage. Far from “encapsulating” the salts, the treatment with silane seems to have greatly enhanced salt mobility. As confidence in the concept of ‘encapsulation’ diminished, desalination began to be seen as a necessary treatment, although consideration was given to its possible damaging consequences (Miller 1992). Finally, consolidants have been proposed to be used as salt extractors. Based on experimental results, Fox (1984) suggested that perhaps consolidants could be used for the purpose of salt removal since they seemed to foster salt efflorescence.

The first reaction of a conservator facing a decayed stone is often to consolidate. Consolidants were advocated for the great Sphinx at Giza without much research (Saleh *et al.* 1992a, 1992b) or for a tomb from the twentieth dynasty near Saqqara (Shoeib, Roznerska, and Boryk-Józefowicz 1990). However, as illustrated in this section, past experiences show that consolidation treatments of Egyptian limestone have been seldom successful and at best, useless, so caution should be the rule.

III.1.2 - Salt removal methods

III.1.2.a - Mechanical removal

If thick salts crusts are present on the surface of the limestone, a mechanical removal can be considered as a first step in the treatment. However, it cannot be the only action taken since the salt crusts are the symptom of a high salt content within the stone. It is likely that efflorescence or salt crusts will reappear if no other action is taken. No reference to mechanical removal of salts from Egyptian limestone was found in the literature.

III.1.2.b - Water immersion

One of the simplest techniques of desalination of porous materials is water immersion. This apparently gentle treatment is based on the phenomenon of diffusion from the high salt concentration in the porous material to the water bath. The natural tendency is for the two concentrations to tend to the same value, resulting in the drawing out of the salts from the stone to the solution. The water is generally deionized to maximize the ion concentration difference between the bath and the stone interior. However, when the volumes involved are large, tap water is sometimes used. The British Museum generally uses ordinary London tap water for the washing process. This contains an average of 40 to 50 ppm of chloride, which obviously limits the removal of chlorides from the stone, but analyses have shown that by using this washing procedure the chloride content, at least in the outer layers of the stone, is significantly reduced (Oddy, Hughes, and Baker 1976). The water bath is regularly replaced and the

concentration of ions in the bath monitored. When the ion content is fairly constant from one bath to another, the stone is considered desalinated. The procedure of water immersion can also be used without changing the bath. The effectiveness of removal depends upon the distribution of salt in the stone and the depth of penetration of moisture into the stone, which in turn depends on the porosity of the stone (Bradley and Hanna 1986).

Coremans (1947) suggested a variation of the method by advocating the use of 80° alcohol instead of water to desalinate objects by soaking. The use of alcohol increases the length of the treatment. He argued that if the treatment takes a longer period of time, it has the advantage to be less damaging to friable surfaces.

The efficiency of the technique can be improved by using vacuum to extract salts from the stone while the stone is immersed in water or while water is run over the surface (Gauri 1983; Gauri, Holdren, and Vaughan 1986). The technique appears to remove the salts in the shortest possible time with the least expense but its harmlessness on a deteriorated surface has yet to be proven.

Desalination by water immersion can only be used for objects which can be immersed in tanks of reasonable size. Therefore, this technique is generally confined to museums objects or architectural parts which can be dismantled into relatively small pieces (tombstones, etc.). It is not possible, for obvious practical reasons, to use this technique in the field for structures as large as a city wall. In addition to practical impediments, this method can be very detrimental to any material sensitive to water. The clay-rich stones, such as most types of Egyptian limestone, unfortunately fall into this category. Several cases, including the Abydos reliefs case, have been reported of

Egyptian limestone sculptures disintegrating into powder on any prolonged contact with water (Charola, Wheeler, and Koestler 1982).

Studies have been performed to try to determine criteria to assess the suitability of stones for desalination by water immersion. Oddy, Hughes, and Baker (1976) studied the factors which can be used to predict whether Egyptian limestone sculptures may be cleaned and desalinated by washing. They found that a reliable estimation can be obtained by determining the soluble salt content and the percentage of acid-insoluble residue. This was achieved in practice by evaluating the results obtained through a close physical examination of the surface of the sculpture. Stones were divided into three classes: (1) stones which may almost invariably be soaked in water without coming to any harm. These have a soluble chloride content $<0.1\%$ and an acid-insoluble residue $<1\%$. (2) Sculptures in an unsound physical condition with flaking or powdery areas on the surface which cannot be cleaned and desalinated by immersion in water (soluble chloride content $>0.5\%$, acid-insoluble residue $>5\%$). (3) Undetermined cases (soluble chloride between $0.1 - 0.5\%$, acid-insoluble residue $1 - 5\%$). It is unclear how the authors came up with those numbers. However, the authors stress that analytical tests alone cannot be used to determine whether soaking in water would be harmful. They suggest that the surface of the stone should be tested by placing a swab of cotton wool soaked in distilled water on an unimportant part of the surface of several hours.

Barton and Blackshaw (1976) also tried to determine whether a stone sample was suitable for washing without resulting in catastrophic failure. By statistical analysis of the composition of 36 different Egyptian limestone sculptures, they showed that on

the basis of the combination of soluble chloride level and the acid-insoluble matter-level a good correlation was obtained allowing to determine its suitability for washing.

Bradley and Hanna (1986) used blocks of Caen stones to test desalination by water immersion after consolidation with silane. Reductions of up to 80% in the soluble chloride content were recorded and no visible damage was reported. However, it was observed that grains of stone became detached from the unconsolidated control stones despite the fact that the blocks were cut from sound undeteriorated stones. Desalination by soaking greatly reduced the salt content of the blocks but the damages caused by the treatment was sufficient to suggest that the technique should not be used on deteriorated limestone sculptures, even if previously consolidated.

III.1.2.c - Poulticing

Poulticing is the application of a wet neutral absorbing substance - clay mixes, tissues, paper products, cellulose powder, ashless floc, etc. - onto the surface of the stone. Desalination of the stone is due to the progressive drawing out of the water-soluble salts from inside the stone into the poultice substance as this dries. Once the poultice is totally dry, the soluble salts removed from the stone are caught inside it and the salt-laden poultice is removed from the surface of the stone. Several poultices can be applied in succession if necessary.

To avoid damage to the stone surface during the poulticing process, in particular if the surface is fragile and already deteriorated, and to facilitate the removal of the poultice, a sheet of Japanese paper is often inserted between the stone and the poultice

(Bradley and Hanna 1986). Poulticing can be combined with water immersion for a more thorough desalination (Oddy, Hughes, and Baker 1976).

The poulticing technique of desalination has been used successfully on deteriorated limestone sculptures. For example, Bradley and Hanna (1986) successfully treated a limestone figure of the Ptolemaic period from the British Museum by first consolidating the stone with methyl trimethoxysilane prior to a desalination treatment with a poultice of sepiolite and distilled water. Before applying the poultice, a separation layer of fine-mesh terylene netting was placed on the surface. However, there has been some discussion on the effectiveness of the technique because it is unlikely that moisture from the poultice penetrates into the stone to great depth (Bradley and Hanna 1986). On the other hand, as for any desalination procedure, it is generally not advisable to disturb dormant salts at deeper levels while removing active salts near the surface. Erratic conductivity meter readings from successive poultices where a steady downward trend might be expected are a sign of disturbance of deeper dormant salts.

One of the practical limitations of poulticing is the fact that it is very labor-intensive and it is generally reserved for museum objects. It is not considered practically feasible to poultice a surface as large as the city wall of Cairo along the new al-Azhar park (more than 7200 m²).

In addition, some poulticing treatments which first appeared to be successful, failed after several years. For example, two objects from the British Museum were treated by poulticing. The first one, an Egyptian limestone panel with figures in relief, had been desalinated by poulticing in 1985 (Hanna 1984), the other, an Egyptian limestone block statue, was consolidated and then desalinated by poulticing in 1987.

Both treatments appeared to be successful at first. However, in less than ten years after treatment, both presented renewed evidence of active decay with profuse efflorescences of needle-like crystals causing extensive detachment of flakes from the surface (Miller, 1992). Unsatisfactory results were also observed on one of the Abydos reliefs (Nunberg, Heywood, and Wheeler 1996), a decade after their poulticing and consolidation which first appeared successful (Wheeler *et al.* 1984).

III.1.2.d - Electro-osmosis

Electro-osmosis is another desalination technique based on the application of an electric current to a porous material containing salts. These, due to their ionic nature, will migrate respectively to the positive and negative electrodes inserted in the system and then removed once concentrated. There are some doubts regarding the effectiveness of the method.

III.1.3 - Environmental control

Review of the literature shows that numerous problems have been encountered with classic desalination treatments such as water immersion and poulticing of Egyptian limestone. They often exhibit efflorescence and other evidences of active deterioration a short time after treatment. One of the problems of these classic treatments is that they are water-based procedures and they introduce the very same element which is the most damaging to Egyptian limestone, causing clays to swell and salts to crystallize.

However, the situation in absence of any treatments is rarely better. Untreated Egyptian limestone objects often begin or continue to deteriorate, sometimes at a very rapid rate, even in a museum environment. Examples of catastrophic decay of Egyptian limestone objects in museum environment are numerous throughout the literature (Hanna 1984; Charola, Wheeler, and Koestler 1982; Wheeler *et al.* 1984; Bradley and Middleton 1988; Rodriguez-Navarro *et al.* 1997).

Employment of desalination techniques to eliminate salt-related decay mechanisms is clearly the wrong approach for some objects. For such cases, the solution appears to be to leave the salts in the stone and deactivate the decay mechanisms by humidity and temperature control. Environmental control of the objects is a passive form of treatment which addresses directly the very causes of deterioration: changing temperature and relative humidity. A strict control of the environment would avoid wet-dry cycles and assure a quasi-absence of dimensional change of the clays and cyclic crystallization of the soluble salts, drastically reducing the rate of deterioration of the stones.

Bradley and Middleton (1988) suggested environmental control to minimize deterioration of the Egyptian limestone sculptures considered at risk in the collections of the British Museum. The conditions the authors recommended were RH $45\% \pm 2\%$ and $19^\circ \pm 1^\circ\text{C}$. The museum, as a result of problems encountered with classic desalination treatments such as water immersion and poulticing, has now put a moratorium on active desalination treatments and opted for a using a combination of holding treatments and monitoring (Miller 1992).

A successful example of environmental control is that of an important group of partially metamorphosed limestone sculptures from Amaravati, India, in the British Museum collection. These had sustained degradation caused by internal pressures from the hydration of clay minerals in the past. As a result of storage in an air-conditioned environment, with relative humidity maintained between 30% and 40% and temperature at 17° to 21°C, it has now completed more than 18 years without further loss or weakening of the fabric (Miller 1992).

Another famous example is that of the Abydos reliefs. The reliefs have been subject to countless campaigns of treatments, consolidation and desalination during which an important number of known and unknown adhesives and consolidants were used. This made the choice of an appropriate adhesive/solvent system difficult because of interference from old adhesives. The conclusion reached was that a controlled environment was the most appropriate approach to stabilize the salts in the relief (Nunberg, Heywood and Wheeler 1996). These authors used both direct observation of samples from the back of the reliefs in conditioned environments and application of the computer model developed by Clegg (seen in Price and Brimblecombe 1994) to determine the temperature and relative humidity where the salts would remain most stable. The authors found that the salts would precipitate when exposed to a range of RH values between 60% and 28%. It should be noted that the experimental results did not fully agree with the computer model. The authors propose as a possible explanation that salts are separated during evaporation/crystallization cycles, which causes the salts to act individually.

Environmental control is now generally advocated for the conservation of stones with high-clay content. However, only stones of small enough in size can be placed in a controlled environment, so this approach is generally reserved to museum objects.

However, if total environmental control is not possible for outdoor immovable cultural heritage, partial control can be used. This includes using permanent or temporary shelters to reduce the amplitude of environmental parameters by covering the monument some parts of the day or the year. Such an approach was proposed for the Sphinx at Giza. Maekawa and Agnew (1996) proposed a night-time shelter to offer a temporary protection of the monument from dew condensation and wind erosion as an alternative to treatments such as consolidation or desalination of the stone. Tanimoto, Yoshimura, and Kondo (1993) also proposed a partial environmental control to protect the great Sphinx. They first suggested isolating the surrounding rock of the Sphinx with an impermeable diaphragm some 25-30 m below the surface to control seeping water. This proposed diaphragm would be produced by grouting through vertical drill holes beneath the Sphinx. They also proposed the installation of a removable or collapsible cover to minimize the effects of rainfall and high humidity. The size of this cover would be 25-30m high, 30-40 m wide and 90-100 m long. This removable/collapsible cover would also mitigate wind erosion. The total coverage time would be around 30-40 days an year, i.e. approximately 10%. Thus, the Sphinx would appear in the open air for 90% of the time. Removed or collapsed, the cover could be stored *in situ* or cased into the surrounding rock to remove it from the view of the tourists. However, environmental control of outdoor immovable cultural heritage is still a relatively difficult task, especially when the site is not an isolated monument, like the great Sphinx, but a

structure very much a part of the urban fabric such as the eastern section of the Ayyubid wall of Cairo.

III.1.4 - Protective treatments

Recently, new treatments have been suggested which aim to mitigate the action of salts as well as controlling the swelling of the clays (Pühringer and Engström 1985; Pühringer and Weber 1990; Wendler, Charola, and Fitzner 1996; Rodriguez-Navarro *et al.* 1997, 1998). Two of the possible alternative treatments make use of ion exchange resins and surfactants

III.1.4.a - Ion-exchange resins

Ion-exchange resins could be used to reduce the swelling capacity of clay minerals. Inner-crystalline swelling can be reduced by replacing interlayer cations, such as Na^+ , by other cations with fewer hydration layers (Ca^{2+} , Mg^{2+}). In theory, this should stabilize the clays by inducing aggregation and reduce swelling. The same effect could be obtained by replacing the interlayer cations by organic ions whose hydrocarbonate chain renders the surface more hydrophobic.

Chatterji, Christensen, and Overgaard (1979) showed through experiments that clays containing exchangeable calcium ion present in an Orthoceras limestone can be converted to sodium clays in the presence of excess sodium salts by an ion-exchange process. This conversion is favored if the corresponding calcium salt is highly insoluble. Studies indicate that sodium clays swell more than calcium clays causing overlying

materials to flake off (Chatterji, Christensen, and Overgaard 1979; Rodriguez-Navarro *et al.* 1997).

Due to the high ionic exchange capacity of the clays, it would be possible to replace sodium ions (supplied by the salts) with divalent cations and reduce clay swelling. In fact, lime washes have been extensively used to stabilize expansive clay-rich soils. Geotechnical engineers (Basma and Tuncer 1991) have taken advantage of the calcium ions from the lime ($\text{Ca}(\text{OH})_2$) which can replace other highly hydrated cations (i.e., Na^+ or K^+) in the clay structure (or adsorbed on the clay surface), thus reducing both the crystalline and the osmotic swelling capacity of the clays (Rodriguez-Navarro *et al.* 1997).

The idea of using ion-exchange resins to mitigate clay swelling has been mentioned several times in the literature (Rodriguez-Navarro *et al.* 1997, 1998) but an experimental study is yet to be carried out. One of the practical problems of the method is to find a way to exchange the cations without fostering decay on clay-rich stones which are water-sensitive.

III.1.4.b - Application of surfactant

Another alternative treatment is the application of surface-active agents or surfactants, to the surface of the stones. The surface active agents are adsorbed on the clay surface and influence the counter-ion distribution. They have therefore the capability to reduce the swelling capacity of the clays (Rodriguez-Navarro *et al.* 1997, 1998). In addition, surfactants have been reported to reduce the swelling capacity of

clays by forming hydrophobic coatings on the clay surface (Rodriguez-Navarro *et al.* 1997).

Wendler, Charola and Fitzner (1996) reported the use of surface-active compounds as anti-swelling agents for the clay-rich volcanic tuff from Eastern Island. Tuff is characterized by small capillary pores and large rates of hygric swelling, one of the main contributing factors to its deterioration. The degree of dilatation of untreated fine-grained stone reaches 1 mm/m when exposed to relative humidity over 80% and more than 2 mm/m when in contact with liquid water. Among the products tested as a protective agent was a surfactant, bifunctional Butyl Di-Ammonium Chloride (BDAC). The effectiveness of the treatment was determined by comparing the tests results obtained from treated and untreated material before and after artificial ageing. The surfactant enabled to reduce the hygric dilation significantly, and therefore prevented the loss of mechanical resistance, while the mechanical and hygric transport properties of the tuff, including liquid water absorption, remained unaffected.

III.2 - Surfactant impregnation as a conservation treatment

III.2.1 - Chemical characteristics of surfactants

III.2.1.a - Definition

Surfactants, or surface-active agents, belong to families of molecules which have a special propensity to adsorb at interfaces (liquid/solid, liquid/liquid or air/liquid interfaces) or to form colloidal aggregates in solution at a very low molar

concentrations so that their concentration is higher at the surface than in the bulk of the liquid (Porter 1994, 27; Myers 1999, 21).

III.2.1.b - Principal structural requirements for surface activity

Surface-active molecules have a characteristic chemical structure and possess two different chemical groups. Part of the molecule has little attraction for the surrounding phase (the solvent) and is called lyophobic. Other chemical units of the molecule have a strong attraction for the surrounding phase and are called lyophilic. However, most of the surfactants' literature is concerned with aqueous solvents and their interaction with another phase, so hydrophobic and hydrophilic are the terms commonly employed.

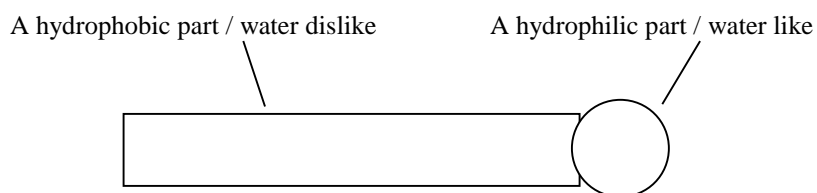


Figure III.1 Schematic representation of the basic structure of a surfactant.

The dual chemical nature of surfactants, referred as being amphiphilic (liking both), gives them the unusual property of having affinity for two essentially immiscible solvents (Myers 1999, 21).

III.2.1.c - Main classes of surfactants

Surfactants can be classified in several different ways. A widely used classification is the one based on the overall chemical structure of the surfactant

molecule, where the surfactants are primarily grouped according to the nature of the solubilizing functionality (lyophilic or hydrophilic group in aqueous solutions) and then, within each group, sub-groups are formed according to the nature of the lyophobic part of the molecule (Myers 1999, 24-25). In aqueous systems, the hydrophobic group generally includes a long-chain hydrocarbon and the hydrophilic group is an ionic or highly polar group that provides the water solubility to the molecule.

Surfactants can be divided into four types.

- Anionic surfactants. Their hydrophilic group carries a negative charge such as carboxyl (RCOO^-), sulphonate (RSO_3^-), or sulfate (ROSO_3^-).
- Cationic surfactants. Their hydrophilic group bears a positive charge as for example, the quaternary ammonium halides (R_4N^+).
- Nonionic surfactants. Their hydrophilic group has no charge but derives its water solubility from highly polar groups such as polyoxyethylene ($-\text{OCH}_2\text{CH}_2\text{O}-$), sugars or similar groups.
- Amphoteric (and zwitterionic) surfactants. The molecule is globally neutral but has, or can have, both a negative and a positive charge on its principal chain, as opposed to a counter ion M^+ or X^- . The sulfobetaines, $\text{RN}^+(\text{CH}_3)_2\text{CH}_2\text{CH}_2\text{CH}_2\text{SO}_3^-$, are an example of this class (Myers 1999, 25).

III.2.2 - Surfactant behavior

III.2.2.a - Concentration at interfaces

The lyophobic group (hydrophobic group in aqueous solvent) of a surfactant has no affinity for the dispersion medium. Consequently when a surface-active agent is dissolved in a solvent, the presence of the lyophobic group causes an unfavorable distortion of the liquid structure and increases the overall free energy of the system. Entropy is regained when surfactant molecules are transported to an interface of the solvent where they take the place of solvent molecules. Due to tendency of every system towards a state of minimum energy, surfactant molecules will therefore preferentially adsorb at interfaces. The formation of micelles is an alternative way to lower the energy of the system (Myers 1999, 22).

III.2.2.b - Spatial orientation of surfactant at interfaces

The amphiphilic nature of surfactant molecules not only results in their adsorption at interfaces but it will often result in a preferential orientation of the adsorbed molecules. These orient themselves, when possible, to minimize the overall interfacial energy of the system (Myers 1999, 22-23). In aqueous solutions containing organic solutes, the hydrophobic, non-polar, portion of the surfactant molecule are directed away from the aqueous phase, the bulk solvent phase, or at least lying along its interface (Myers 1999, 147).

However, the orientation of the adsorbed surfactant molecules from solution onto a surface also depends on its concentration. At low concentration, there is little

orientation of the molecules at the interface. As the concentration increases, the number of surfactant molecules increases and they begin to orient themselves depending on the nature of the hydrophilic group and of the surface in question. At the Critical Micelle Concentration (CMC), the number of surfactant molecules is

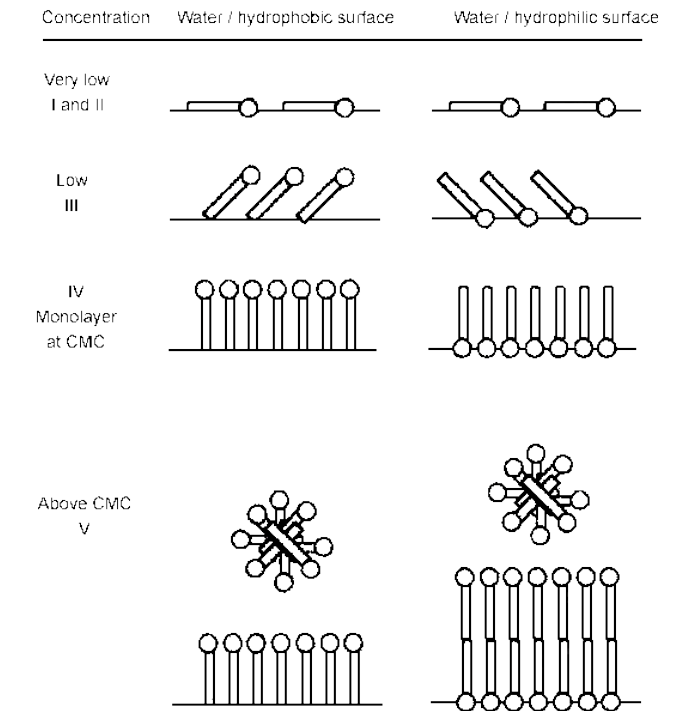


Figure III.2 Adsorption and concentration of surfactants.
From Porter 1994, 30.

sufficient to form a unimolecular layer at the interface. Above the CMC, there is no apparent change in adsorption at hydrophobic surfaces but at hydrophilic solid surfaces surfactant molecules can form multilayer ordered structures. In addition, the surfactant molecules in the solution will form an ordered structure, known as micelle, as long as the concentration is above the CMC (Porter 1994, 31).

III.2.2.c - Surface tension

Liquids assume the shape of minimal surface area, i.e. their final shape is determined by the state of equilibrium between the different forces acting upon the liquid: gravity, those which tend to keep the molecules together in a liquid state and those which tend to pull molecules out of the liquid into the adjacent vapor phase. The

surface tension can be seen as a measure of the “pulling” force which tends to give the liquid the minimum surface area for a given volume. In a more technical definition, the surface tension (or surface energy) is defined as “the amount of work required to increase the surface area of the liquid isothermally and reversibly by a unit amount” (Myers 1999, 141). The surface tension of water at 20°C is 72.8 mN.m⁻¹ (Myers 1999, 141).

The amphiphilic nature of surfactant molecules results in their adsorption at interfaces in order to decrease the free energy of the system. This leads to pronounced physical changes in the solution. Because less work is required to bring surfactant molecules to an interface than solvent molecules, the displacement of solvent molecules by adsorbed solutes at the interface decreases the surface tension of the liquid. This is one of the major consequences of the presence of a surfactant in a solution. The decrease of the liquid surface tension increases its spreading and wetting properties (Myers 1999, 22, 150).

The decrease in surface tension by surfactants is dependent on concentration. The more surfactant there is at the surface, up to complete coverage, the more pronounced is the change in surface tension. The surface tension falls to a minimum value at the CMC, where the surface is completely covered with a monolayer of surfactant molecules. The formation of multilayers has no significant effect, although, the surface tension does fall very slowly as the concentration increases (Porter 1994, 28-29, 31).

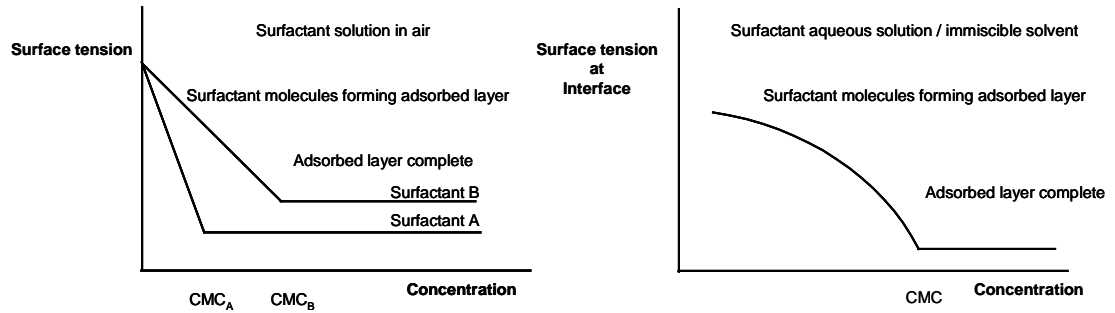


Figure III.3 Surface tension (left), and interfacial tension (right) versus surfactant concentration. From Porter 1994, 33.

There is a similar effect when the surfactant is present in a system of two immiscible liquids. The surfactant is adsorbed at their interface and reduces the surface tension, which in the case of two liquids is known as the interfacial tension. The variation of the interfacial tension versus concentration gives a similar curve to that of surface tension versus concentration and shows a discontinuity, the CMC which is characteristic of the surfactant (Porter 1994, 31, 33).

III.2.2.d - Presence of electrolytes

The surface tension of aqueous solutions varies with their composition. In particular if the second component is an inorganic electrolyte (salts) which requires significant solvation. The exact relationship between surface tension and concentration of the solute depends on the exact nature of the interaction between the two components but it is generally found that the addition of inorganic electrolytes to water results in an increase of the surface tension. The effect is not dramatic and requires rather high salt concentrations to become significant (Meyer 1999, 148).

The behavior of a surfactant in aqueous solution is affected by the presence of electrolytes. In the case of ionic surfactants, the electrolyte tends to reduce the

electrostatic repulsion between the ionic hydrophilic groups which leads to an increased tendency to form micelles. The CMC of the surfactant is therefore significantly decreased when electrolytes are present in the solution (Porter 1994, 38). For nonionic or amphoteric surfactants the addition of electrolytes to the solution hardly changes the CMC (Porter 1994, 36).

III.2.2.e - Effect of surfactant adsorption on solid surfaces

The effect of adsorption of a solvent onto a solid surface depends largely upon the dominant mechanism of adsorption. For a highly charged surface, if adsorption is the result of an ion exchange, the electrical nature of the surface will not be altered significantly. If, on the other hand, ion pairing becomes important, the potential of the surface can be completely neutralized. If the system is essentially stabilized by electrostatic repulsion such a reduction in surface potential will result in a loss of stability and eventual coagulation or flocculation of the particles (Myers 1999, 210).

In addition to changes of the electrical potential at the solid surface, surfactant adsorption by ion exchange or ion pairing results in the orientation of the surfactant molecules with their hydrophobic groups toward the aqueous phase. Therefore the solid surface becomes more hydrophobic and less easily wetted by water. The adsorption of surfactant to the more hydrophobic solid surface is however still possible by dispersion force interactions. When that occurs, the charge on the surface of the solid will be reversed, acquiring a charge opposite in sign to that of the original surface, because the hydrophilic group will now be oriented toward the aqueous phase. As a result, in a system normally wetted by water, the adsorption process reduces the wettability of the

solid surface, making its interaction with other less polar phases, such as air, more favorable (Myers 1999, 210).

It should be noted that the mode of action for most surfactants is extremely substrate specific and highly dependent on surfactant concentration and temperature. The effect of surfactants can be modified and enhanced by means of surfactant combinations, solvent combinations, complexones, ion exchangers, stabilizers and similar substances.

Because of the versatility of their actions, surfactants have numerous industrial applications ranging from detergents through defoaming agents to demulsifiers. They are also used to disperse aqueous suspensions of insoluble dyes and perfumes or to help dyes penetrate textiles evenly. Another use is the creation of foams for gas flooding in enhanced oil recovery. Through the literature of oil recovery, numerous data related to the adsorption of different types of surfactants on various rock types can be obtained (Mannhardt, Schramm, and Novosad 1992; Ivanova *et al.* 1993). Among the factors affecting the adsorption of surfactants onto rock are the chemical nature of the surfactant, the ionic strength of the aqueous phase and the presence of divalent cations, the rock type and the presence of clays in it.

III.2.3 - Action of surfactant on stone-water-clay-salt systems

III.2.3.a - Potential effects of surfactants upon salt deterioration

Surfactants have the ability to influence significantly the physical properties of a salt solution (viscosity, surface tension and vapor pressure). They can consequently

have a critical effect on the dynamics of solution flow and evaporation within the stone, and therefore on the degree of supersaturation, dynamics of precipitation and salt growth, and consequently the resulting damage to porous host materials (Rodriguez-Navarro and Doehne 1999).

In a brainstorming theoretical article, Pühringer and Engström (1985) enumerated the changes relevant to salt damage of stone induced by the addition of a surfactant. By reducing surface tension, increasing wettability of the surface and viscosity of salt solution films, surfactants reduce the liquid film thickness and lower the capillary transport capacity. Thus, overall transport capacity of the salt solution within the stone should be reduced. The change in surface energy of a salt solution should also influence the particle size and growth rate salts precipitated from saturated solutions. The control of the interfacial tension between liquid phase, salt formation and the substrate, will alter the moisture transfer to and from the surface of the salt, modifying the hydration and dehydration rates of the salts. It will also affect the adhesion of salt crystals to the substrate. Adhesion of the salt crystals to the substrate depends on the moisture in the pore system and on the contact surface between the salt film and substrate. The amount of moisture present depends in turn on the hydration / dehydration of the salt crystals. By modifying the hydration behavior of the salts, the surfactants could also modify the agglomeration of salt on a surface.

The theoretical effects of surfactants upon salts are numerous and the relationships between surface energy of a salt solution and the method of formation of salt structures has been known for quite some time. For example, surfactants have been used in floatation technology to control precipitation of salts and to enhance growth of

particle size or as anti-caking agents to prevent agglomeration in the manufacture of industrial salts. However, there still is insufficient detailed knowledge available to be able to use predictably surface-active substances for the control of processes involved in the formation of harmful salt deposits or ideal crystals. For instance, the ability of surfactants to lower the surface tension of liquid phases does not appear to have any relation to their ability in preventing agglomeration or growth on salt surfaces (Pühringer and Engström 1985).

III.2.3.b - Potential effects of surfactants upon clay deterioration

Lagaly and Weiss (1970) demonstrated that the cations between clay mineral layers were partially exchangeable against alkyl-ammonium ions, the degree of exchange being dependent on location and type of cation. This shows that surfactants have the potential to mitigate the swelling of the clays and consequently reduce stone deterioration.

Wendler, Klemm and Snethlage (1991) studied further the interaction between clay minerals with cationic surfactants. Their goal was to prevent, or at least reduce, the formation of hydration shells around the interlayers cations by blocking the negative charge centers of the clay mineral layers to which the cations are fixed. The hydration shell size depends on the type of cation and the amount of water available. This process is responsible for most of the swelling behavior of clay minerals. The authors worked on a clay-rich sandstone for which clay expansion was considered the main decay factor. After treating the stone with a bifunctional alkyl- α - ω -diammonium chloride surfactant, the dilatation of the stone was reduced by half. The decrease in swelling is

dependant on the surfactant concentration but the authors found that concentrations higher than 0.5 M were not desirable because of the induced color change to the stone. The postulated mechanism of interaction is that the surfactant ions replace the binding cations at the clay mineral interfaces. Apparently, the hydrophobic alkyl groups of the surfactant screen the contact forces between the mineral interfaces.

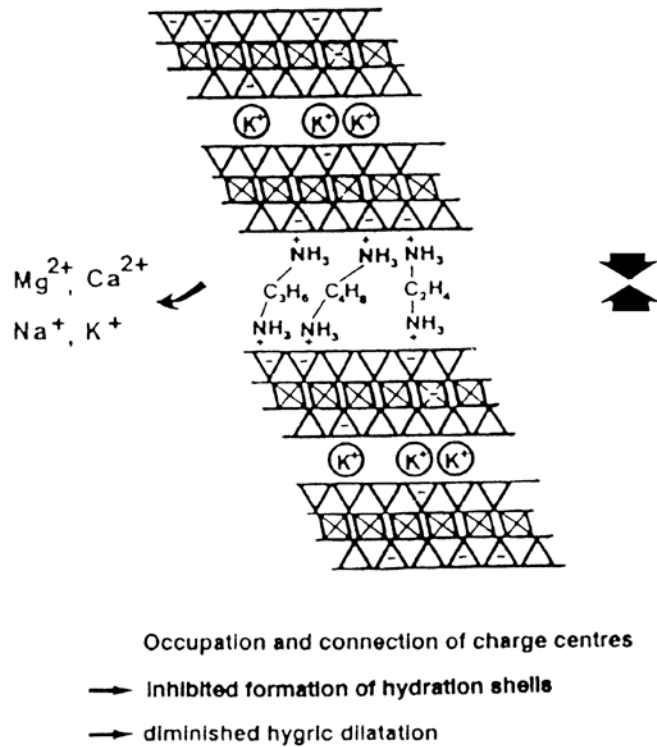


Figure III.4 Model of the ionic exchange of cations against bifunctional cationic surfactants on clay basal planes. From Wendler, Klemm, Sneathlge 1991.

This model was later confirmed by the cation exchange measured when desalted sandstone powder samples are dispersed in a butyl-diammonium chloride solution.

The authors also tested a combined treatment surfactant / water-repellent polysiloxane and a similar decrease in hydric dilatation was observed. A combined treatment may be particularly useful by combining the reduction of clay swelling with water repellency preventing the capillary uptake of water. Thus a two-fold effect on the weathering stability of stones can be achieved. The authors also suggest preparing aminosilane-modified siloxanes / silica gels to strengthen the binding of silica gels and polysiloxanes to the mineral surface. If the amino-groups are covalently integrated into

a silicon-organic network structure, a similar interaction with the clay mineral surface should be expected as in the case of isolated alkyl ammonium ions, but additionally the polymer should also be linked to the surface.

Although the use of surfactants seems very promising for clays and salt-rich stones, not enough experiments have been performed and research is truly needed. Some authors (Pühringer and Engström 1985) emphasize that certain combinations of surfactants with salts could accelerate deterioration.

III.2.3.c - Salt extraction by surfactants

Pühringer and Weber (1990) propose another, relatively unusual, use for surfactants: that of fostering “self-extraction” of salts from stones. Once efflorescence has been initiated, surfactants should promote further salt crystallization on the outside surface of the stone. According to their work, the formation of whiskers appears to be one of the most effective extraction mechanisms. Whiskers are formed on the outside surface of the stone through rapid growth by a screw dislocation (growth spiral) in their longitudinal axis. The object of the extraction method is to set up special boundary layers between the pore surfaces of the substrate material, the transferable salt solutions and the extracting liquids. This creates right charge conditions at the respective boundary surfaces for facilitating or accelerating mobilization of materials, primarily salt solutions. In addition, the vapor pressure outside the pore opening should be modified in the appropriate direction. Those two requirements can be achieved by using surface-active preparations which can create thin salt solution films capable of being transported through the pores by making use of both vapor pressure and surface-active

effects (charge conditions) in the boundary layer between liquids or materials which are in principle incompatible (immiscible).

The authors also propose pre-treatment of the stone with an apolar medium, which forms a barrier to avoid the redistribution of the salts and moisture into the stone during the application of the surfactant. They equally point out the possible risks of the method, mainly the hydration and/or crystallization of salts during extraction.

III.2.3.d - Sulphatation reaction of calcareous stone

Another effect of surfactants have been observed by Böke, Göktürk, and Caner-Saltik (1996). They studied the effects of three different surfactants (cationic, anionic and non-ionic) on the reaction of transformation of calcium carbonate into calcium sulfate. The experiments were carried out on different mixes of calcium carbonate / surfactant powder exposed to a flow of SO₂ gas. The results were monitored through FT-IR measurements of total sulfur content through time and sample weight increase. The results showed that the samples with added surfactants gained less weight and that their total sulphatation decreased significantly when compared with control samples. In all cases, the main sulphatation product was calcium sulfite hemi-hydrate while minute amounts of gypsum were produced. The authors suggest that the decrease in sulphatation may be due to the decrease in solubility of calcium carbonate when a surfactant is added.

III.2.4 - Surfactant treatment of the Ayyubid city wall of Cairo

The Ayyubid city wall of Cairo presents numerous conservation challenges which require different approaches. One of the main issues is the presence of a thick salt crust covering large areas of the wall. Large salt crystals were also present on the stone surface in lower areas previously buried. The salts, developed at the protected interface between the stone and the soil, have detached themselves from the stone substrate once this was expressed leaving a remarkably well-preserved stone surface.

The presence of salt crystals in such large quantities is a sign of an abundant source of salts from within the stone, the ground or from other sources. A surface cleaning of the wall to remove the salt crusts is a necessary first step in the wall treatment but it cannot be the only one since the cleaning of the wall does not address the issue of the source of the salts and it is very likely that efflorescences will soon reappear. However a desalination of the wall is practically unfeasible so an alternative *in situ* mitigation treatment to address salt and clay deterioration mechanisms should follow the surface cleaning treatment.

Few methods exist today to treat *in situ* Egyptian limestone, but the application of a surfactant solution is a promising one. Surfactants have the theoretical potential to mitigate the problems experienced by the Egyptian limestone. However, the application of the surfactant will also introduce a foreign chemical into the wall and the future consequences are not known. As the history of past failed conservation treatments shows, one can never be too careful when applying a new conservation method even if it is very promising.

Before any surfactant is used on the Ayyubid wall, further research is needed to better understand the action of the surfactant on the stone-water-salt-clay system and, more importantly, to give some indication of the drawback or potentially detrimental side-effects.

CHAPTER IV

LIMESTONE FROM THE AYYUBID CITY WALL OF CAIRO

IV.1 - Mineralogical and petrographic analysis

Two main types of limestone blocks can be found as veneer stone on the eastern section of the city wall of Cairo. The first is the original limestone from the Ayyubid period (12th century). The second type is the replacement stone installed in the 1950's by the Comité de Conservation des Monuments de l'Art Arabe.

The Ayyubid stone has a yellowish-buff color, whereas the Comité stone is whiter. They have similar chemical make-up with allochemical particles in a microcrystalline calcium carbonate matrix. Relevant results from previous examinations of samples both the Ayyubid and Comité stones taken from the eastern section of the Ayyubid wall of Cairo are included here (Dewey 2000). Detailed description of these stone samples is provided in Appendix A.

IV.1.1 - Texture

Both the Ayyubid stone and the Comité stone are fine-grained limestones but they are not equally homogeneous nor do they contain the same proportion of fossiliferous inclusions. The Ayyubid stone is highly fossiliferous while the Comité stone has a more homogenous matrix. The samples examined varied in condition from completely intact to completely disintegrated (Dewey 2000, 11-12, 21).

Thin-sections of a number of samples were examined. Some were dyed with Polysupra Kregersol Blue (Special-t Coatings) which allows salt identification. Figures IV.1 and IV.2 show examples of the range of texture and porosity found in the stones from the city wall. Figure IV.1 is a thin-section of Comité stone and shows a homogeneous fine-grained calcitic stone. The brown dots are iron inclusions within the stone. Small, well-distributed fossil fragments, primarily bioclasts can also be observed. However, not all stones, are equally homogeneous in texture. Figure IV.2 shows a thin section a fine-grained calcite matrix with abundant fossils (foraminifera) of what is probably original Ayyubid stone. Iron inclusions are clearly present. The thin section also exhibits a porosity composed of many small pores and some large pores. Micro-cracking is also visible through some of the foraminifera fossils.

IV.1.2 - Acid-insoluble residue

The amount of acid insoluble material was determined in six samples from both medieval Ayyubid stone and Comité replacement stone from the 1950s. The samples were crushed and 1M hydrochloric acid solution was added until effervescence ceased. The insoluble material was then filtered. The acid-insoluble fraction, which includes the clay minerals, varied between 1.5% and 8.8% (average 4.5%) (The results are presented in Table IV.1).

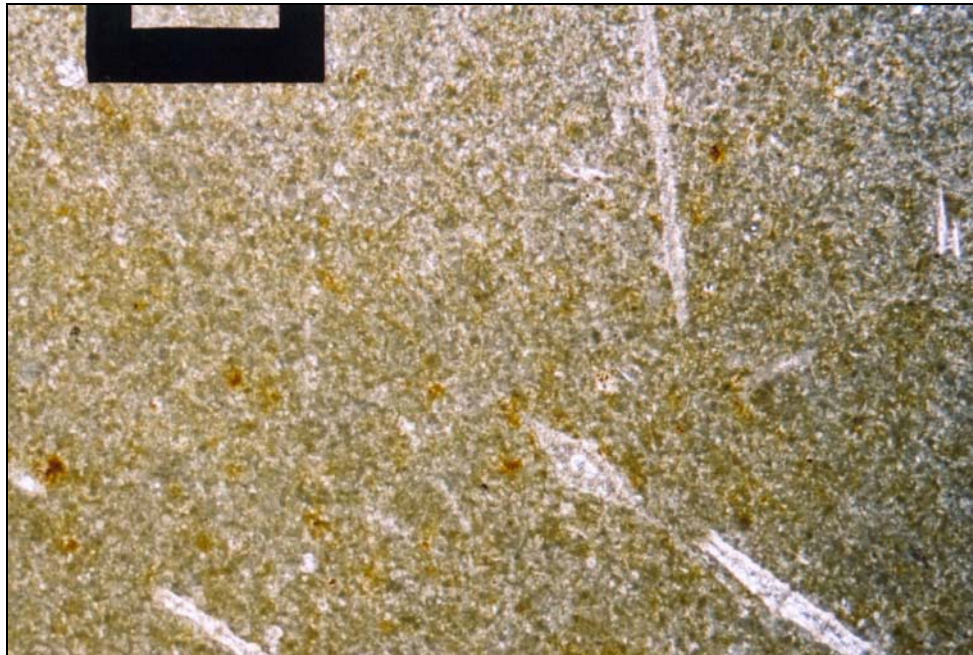


Figure IV.1 Thin section limestone (sample 5), Comité repair stone. Homogeneous fine-grained limestone, with small, well-distributed fossil fragments and iron inclusions. (From Dewey 2000, photo 3.12).

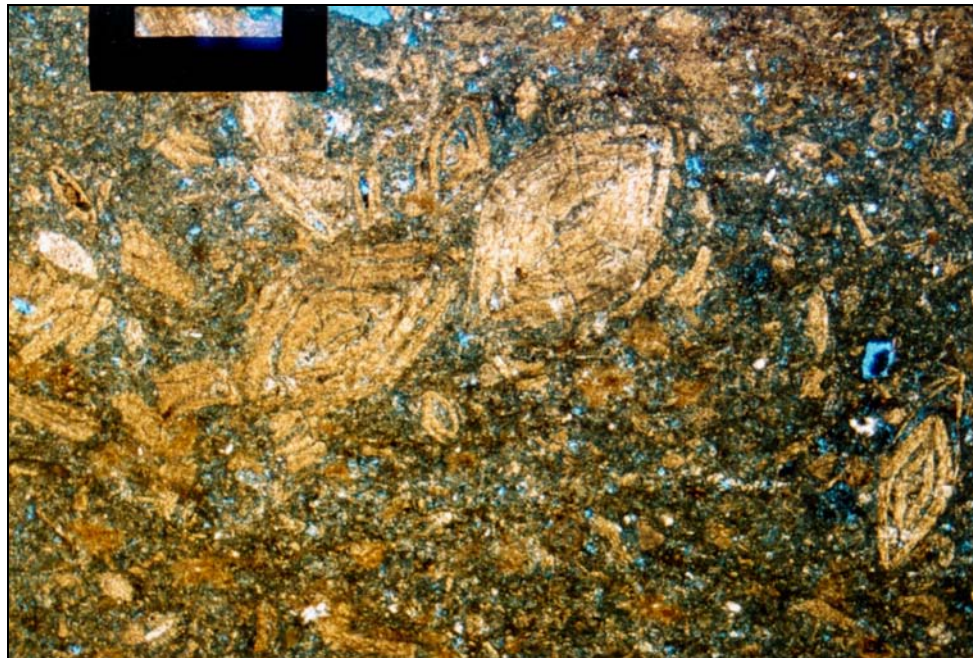


Figure IV.2 Thin section limestone (sample 14), appears to be original Ayyubid stone. Fine-grained calcite matrix with abundant fossils – some micro-cracked - and iron inclusions. Magnification $\times 25$. (From Dewey 2000, photo 1.17).

<i>Sample Number</i>	<i>Origin</i>	<i>Porosity (%)</i>	<i>Acid Insoluble Fraction (% w/w)</i>
12	Ayyubid?	3.5	1.5
14	Ayyubid?	10.8	2.4
15	Ayyubid?	6.0	4.0
16	Comité	/	8.8
17	Comité?	4.0	4.6
18	Comité?	/	5.9

Table IV.1 *Porosity and acid insoluble fraction of selected samples from the Cairo wall. See Appendix A for a complete description of each sample.*

The acid-insoluble fraction also includes iron oxides present in the iron oxides present in the stones, as seen in some thin sections, which give the limestones a yellowish tint (Dewey 2000, 21).

IV.2 - Physical properties

IV.2.1 - Density

The density of the two types of stone was measured by the Rock Engineering Laboratory of Cairo University. While the density of the Comité stone was 2.02 g.cm^{-3} , that of the Ayyubid stone was 2.08 g.cm^{-3} . These values are only indicative since they were obtained from just one sample per stone.

IV.2.2 - Porosity

Both types of stone have similar porosities. The Rock Engineering Laboratory of Cairo University (Rock Engineering Laboratory 1999b) determined porosity for both types of stone. Again, the values are indicative since only one sample per stone type was measured. The test method used was total immersion in boiling

water. The porosity for the Ayyubid Stone was found to be 18.83% while that for the Comité stone was 21.94%.

Apparent porosity was also determined through water absorption by total immersion (testing method not identified). For this purpose four small surface samples, representative of the types of stone, were used by Dewey (2000). The porosity of the samples varied from 3.5% to 10.8%, average 6.1% (see Table IV.1) (Dewey 2000). The large difference in the values obtained by Dewey as compared to those of the Rock Engineering Laboratory is probably due to the fact that Dewey measured the porosity on small surface flakes which may be less porous and because of their small size resulting in large experimental errors.

Two other thin sections illustrate the diversity of porosity type found among the stones of the Ayyubid wall. Figure IV.3 shows a thin section of a fine-grained calcite matrix with some large pores and many small pores. Microcracking and iron inclusions are present. Figure IV.4 shows tightly packed foraminifera and fossil fragments cemented by calcite matrix. The composition of the stone creates abundant small voids between the fossils as well as large voids inside them. The presence of fossils induces a peculiar pore-size distribution with an unusual proportion of large pores within a otherwise fine-grained limestone. The internal structure of some fossils, such as the bottom right foraminifera, has collapsed. In addition salt deposition is visible within both the matrix and the fossils.

Porosity, and in particular, the proportion of small pores in the stone is one of the factors recognized to affect the stone deterioration (Bradley and Middleton 1988; Miller 1992). Bradley and Middleton (1988) observed that the stones from

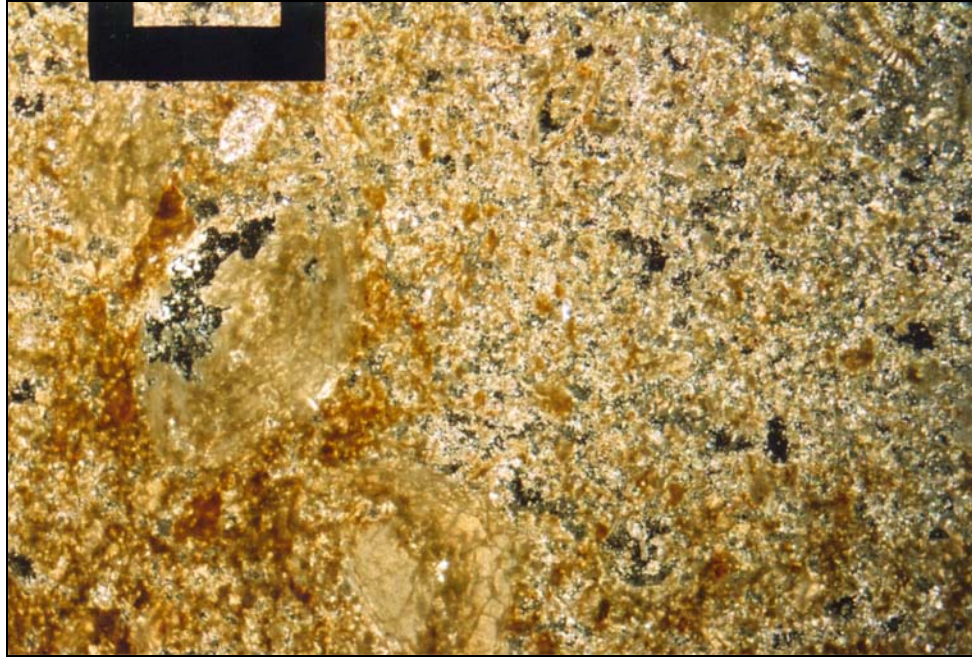


Figure IV.3 Thin section of limestone (sample 14), appears to be original Ayyubid stone. Fine-grained calcite matrix with iron inclusions, microcracking, many small pores and some large pores are present. Magnification $\times 25$. (From Dewey 2000, photo 1.16).

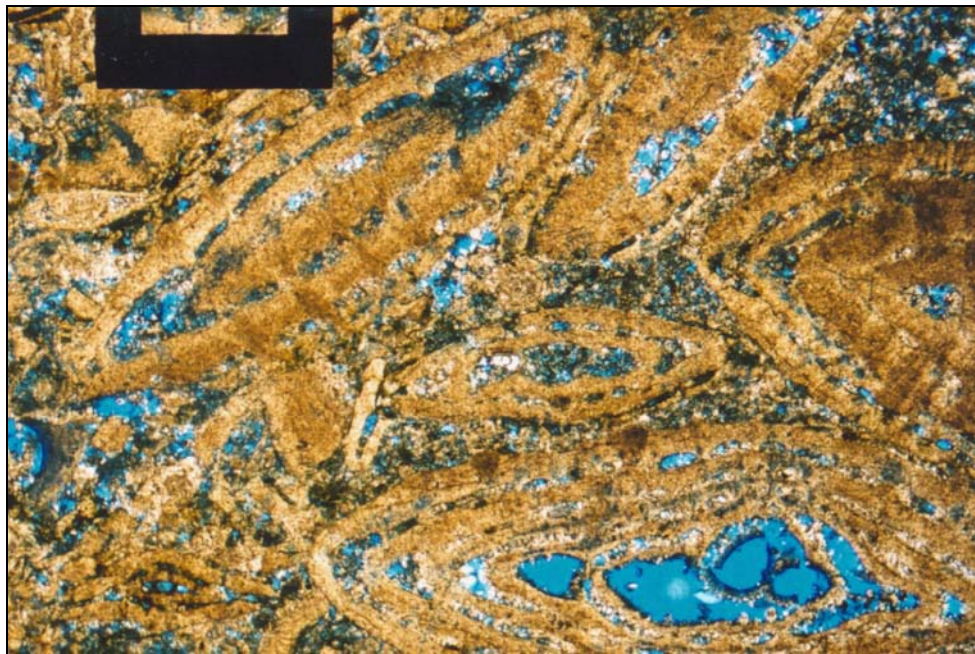


Figure IV.4 Thin section of limestone (sample 15), appears to be original Ayyubid stone. Tightly packed foraminifera and fossil fragments – some have collapsed internal structure - cemented by calcite matrix creating abundant small voids between the fossils as well as large voids inside them. Magnification $\times 25$. (From Dewey 2000, photo 1.12).

Thebes/Abydos deteriorated more quickly than stones from Cairo and from El Bersha. The first ones have textures in which the calcite is highly fragmented, occurring as dispersed grains and aggregates separated by fine grained clay and open pores, providing easy access for moisture, as well as greater surface area for chemical reaction, whereas the latter exhibit less fragmented textures, with solid islands of calcite separated by regions of higher porosity.

IV.2.3 - Micro-cracking and surface condition

A number of samples exhibit micro-cracks. These are probably due to progressive weathering of the limestone. Figure IV.5 is a thin section of a high porosity fine-grained limestone with an abundance of broken bioclasts and foraminifera. The microcracks are often associated with areas rich in salt. Figure IV.6 is an example of fine-grained limestone, probably an original Ayyubid stone, with many small pores showing microcracks and salt crystals.

In addition to the natural weathering of the limestone (cyclic salt crystallization and clay swelling), micro-cracking can also be due to the action of fire (thermal shock) or other short-term mechanical stresses. Micro-cracks in both the calcium carbonate matrix and the fossils are numerous. Figure IV.7 exhibits microcracking in a thin-section from a Comité stone. It displays an apparent “surface densification” around both the exterior surface and on the edges of the main microcrack. This surface densification may have been reflected in the low porosity values measured by Dewey (Table IV.1)



Figure IV.5 Thin section of limestone (sample 6), possibly original Ayyubid stone. High porosity fine-grained limestone with an abundance of broken bioclasts, foraminifera and microcracks. Magnification $\times 25$. (From Dewey 2000, photo 2.7).

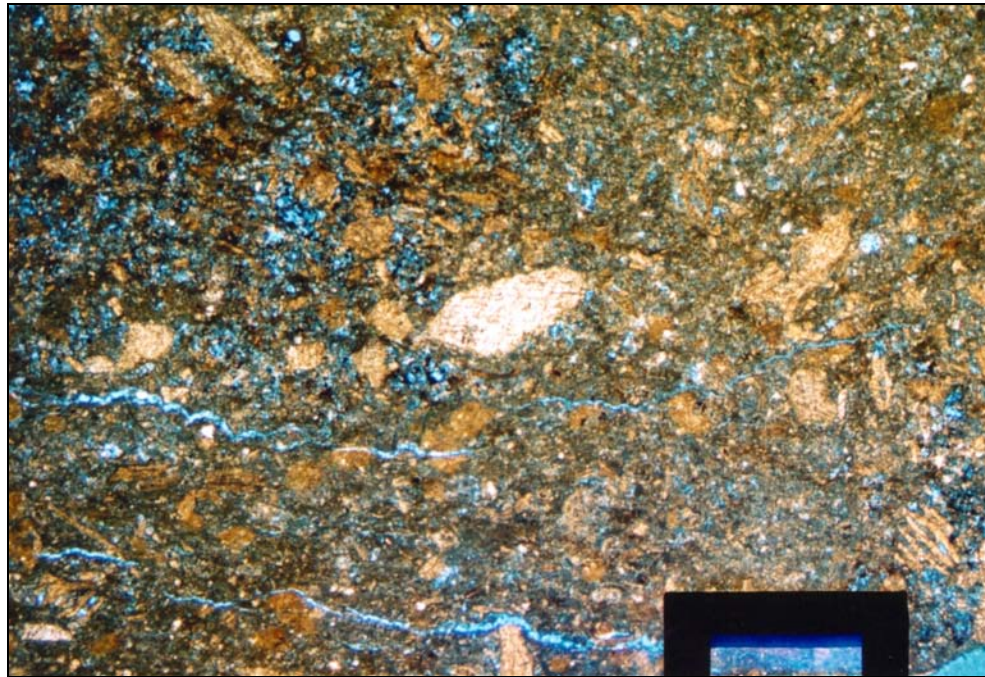


Figure IV.6 Thin section of limestone (sample 14), appears to be original Ayyubid stone. Fine-grained stone with many small pores, microcracks and salt crystals. Magnification $\times 25$. (From Dewey 2000, photo 1.25).

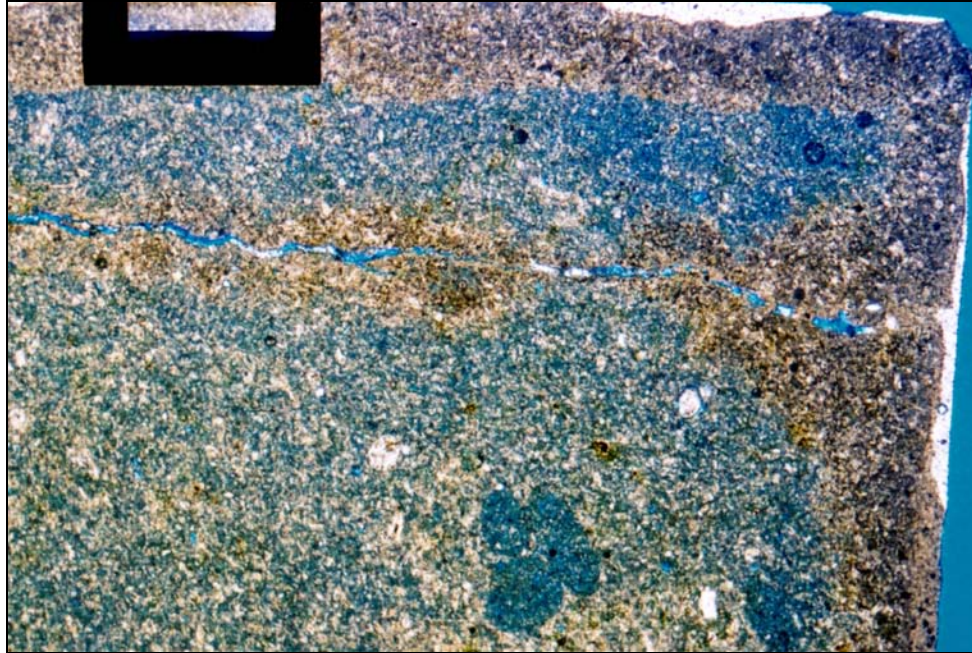


Figure IV.7 Thin section of limestone (sample 5), Comité repair stone. Fine-grained stone with microcracks and apparent densification of the outer surface. (From Dewey 2000, photo 3.19).

This could possibly be due to the recrystallization of salts just below the evaporation surface. It is probable that less soluble salts, such as gypsum, are part of this denser layer, whereas more soluble salts, such as halite, would preferentially crystallize on the outer surface forming the crusts observed on the wall surface.

IV.3 - Mechanical Properties

Additional mechanical tests were performed by the Rock Engineering Laboratory at Cairo University (Rock Engineering Laboratory 1999a). The test results are presented below:

		<i>Uniaxial Compressive Strength (kg.cm⁻²)</i>	<i>Young's Modulus (kg.cm⁻²)</i>	<i>Tensile Strength (kg.cm⁻²)</i>	<i>Double Sheer Strength (kg.cm⁻²)</i>
Ayyubid Stone	1	138	2400	40.8	58.0
	2	210	3000	40.6	73.3
	3	68	3200	31.0	81.9
	4	64	5000	35.6	62.5
	5	58	3222	39.2	40.1
Average		107.6	3364	37.5	63.1
Comité Stone	1	158	6077	33.6	22.3
	2	192	4400	46.1	15.9
	3	64	5000	33.6	29.5
	4	88	4615	27.8	18.2
	5	143	7777	29.6	25.2
Average		129	5574	34.1	22.2

Table IV.2 Mechanical properties of the historic limestone blocs.

It should be noted that kg.cm⁻² is in fact kilo force per cm⁻², i.e. 9.8 N.cm⁻².

The compressive strength of limestone is generally between 700 and 7000 N.cm⁻² for commercial modern fresh stones (Winkler 1975, 40). The values of the Ayyubid and Comité stones are on the low end of the compressive strength of limestone. They have relatively similar compressive strength although the Ayyubid stone weathered several centuries longer. Both stones have also similar tensile strength but the modulus of elasticity of the Ayyubid stone is much lower than that of the Comité stone.

IV.4 - Salt characterization

IV.4.1 - Salt deterioration pattern distribution

Salts are clearly visible to the naked eye on the exterior surface of the wall. They are present in different crystallization patterns. Figure IV.8 is a detail of the survey of salt deterioration patterns observed on the wall surface. As the drawing shows, the patterns are highly dependant on location on the wall. Four main conditions can be observed. The lower part of the wall, which was buried before the 1998 excavation, displays salt efflorescences as well as thin salt crusts (veils). Those veils are now falling off in large plaques leaving behind stones in very good condition, revealing original tooling marks (see Figure IV.10). This zone was probably damp during burial and due to its protected condition, experienced slow salt growth. This occurred within the burying material which explains the good preservation of the stone.

The next zone, just above grade level is characterized by very thick salt crusts, sometimes several centimeters thick, present at the surface and subsurface of the stone. This area, because of capillary rise of water, was sometimes damp and sometimes dry. The very variable environmental conditions have promoted salt growth creating thick salt crusts and surface damage.

Finally, the upper part of the wall is characterized by a particular salt condition, which can be qualified as a compact salt crust for lack of a more appropriate term. The condition is defined by the combination of a surface salt crust and salt growth within stone cracks penetrating deeper into the stone.

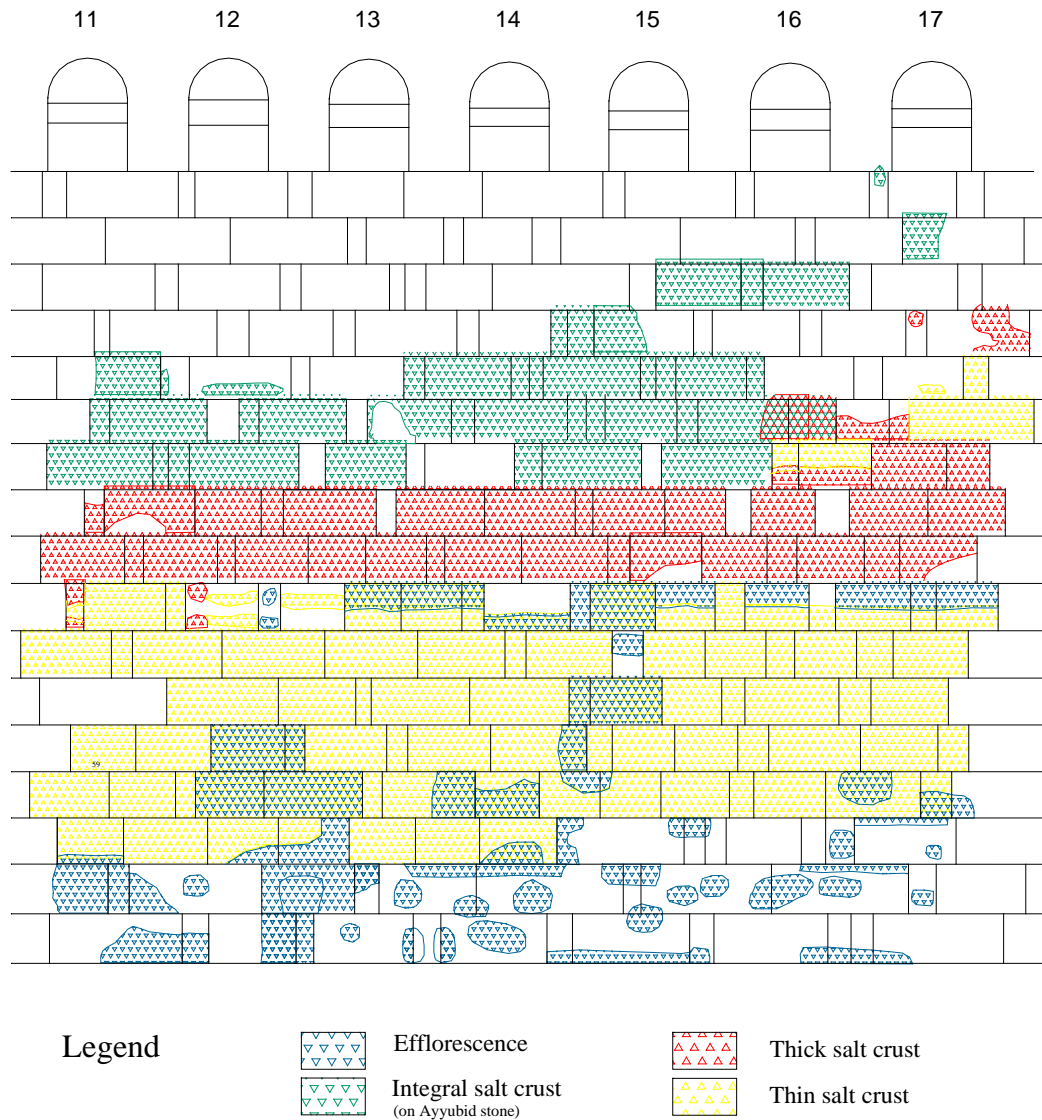


Figure IV.8 *Detail of the survey of salt deterioration patterns between tower 4 and 5 of the eastern section of the Ayyubid wall of Cairo.*

With the current exposure of the wall, the environmental conditions through out the wall have changed significantly so that salt deterioration locations will change.



Figure IV.9 Eastern section of the Ayyubid wall of Cairo between towers 3 and 4 looking North toward tower 4, showing the grade level before recent excavation, 2000.



Figure IV.10 Detail of the thin salt crusts (veil) falling off in large plaques from the surface of the stones, 2000.

The area of most concern is probably the lower portion of the wall, close to grade level where the thin crusts were previously found. The stones are in good condition but this area is likely to experience the most severely changing environmental conditions, fostering salt growth within the stone and inducing deterioration. Unless rising damp can be prevented, attention should be focused on this area for treatments aiming at mitigating moisture movement and the consequent salt growth and clay swelling.

IV.4.2 - Salt crystal growth

The thick layers of crystalline salt deposits can be several centimeters thick as shown in Figs IV.11 - IV.15. (*U sample refers to a unidentified surface flake*).



Figure IV.11 Layered salt crust on limestone from a surface flake (*U sample*). Total magnification $\times 2.5$.



Figure IV.12 *Detail of parallel columnar calcite crystals elongated perpendicularly to the layers, in previous sample (U sample). Total magnification $\times 6.25$.*

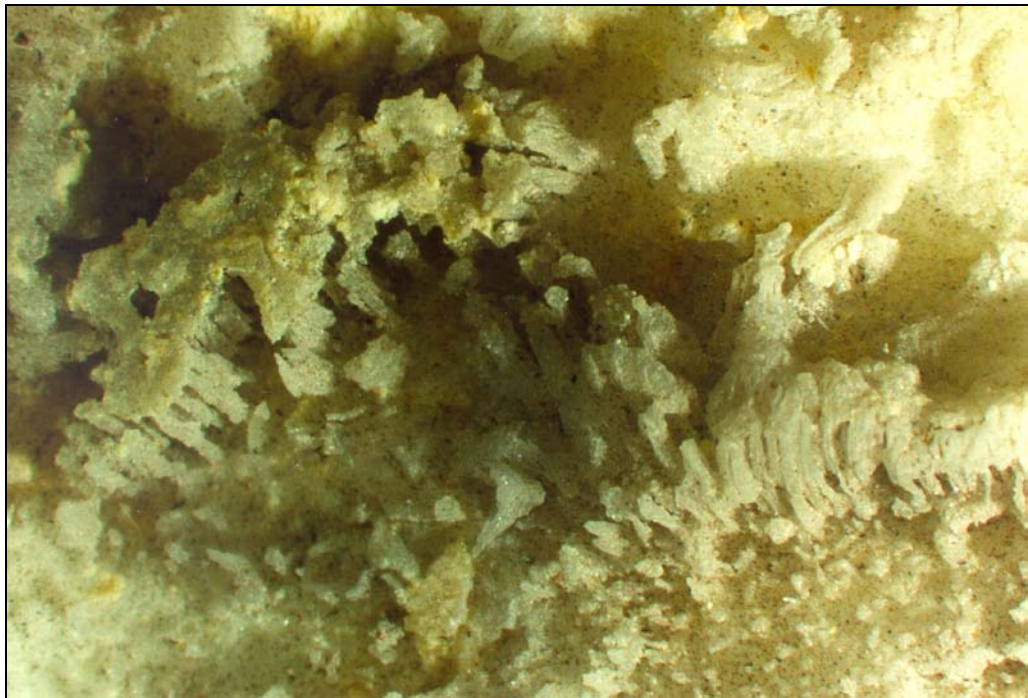


Figure IV.13 *Detail of parallel columnar calcite crystals view from above. (U sample). Total magnification $\times 1.875$.*



Figure IV.14 *Detail of typical layered sinter forms of parallel prisms and needle of calcite arranged in layers (U sample). Total magnification $\times 3.125$.*

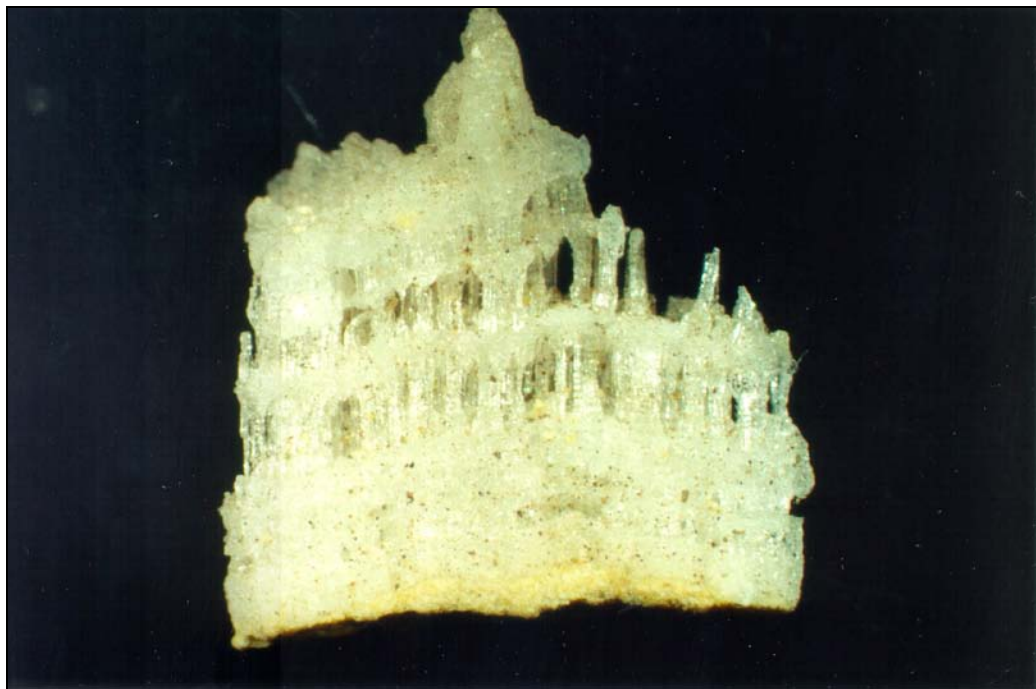


Figure IV.15 *Fragment of salt crystal detached from the stone exhibiting the characteristic parallel columnar crystals separated by horizontal layers (U sample). Total magnification $\times 3.125$.*

The salt crystals generally appear as layered crusts of columnar crystals. The development of such crusts is well known (Arnold and Kueng 1985). They are formed by layers of parallel prisms and needles of salt elongated perpendicularly to the layers.



Figure IV.16 Flaking and delamination of the stone surface caused by salt crystallization. Sample 9, possibly Comité repair stone from a recently excavated area. Total magnification $\times 5$.

Such crusts commonly develop where the walls are considerably humid and wet and where a high water supply is available (Arnold and Kueng 1985). Crust formation is generally associated with progressive loosening and spalling of the outermost layer of stone. Crusts generally continue to push away spalls and flakes of the stone (as seen in Fig. IV.16) in a continuous weathering process, stressing the stone surface. Because of their mode of formation and growth, salt crusts, in comparison to fluffy efflorescence, are particularly damaging to the stone.

Salt crusts on the Ayyubid city wall of Cairo are exceptional by their thickness, which can be well above a centimeter. They form under particular growth conditions, such as a steady supply of saline solution associated with a humid substrate. In terms of the future conservation of the wall, thick crusts are a proof of a continuous supply of salt from the ground to the wall, and/or a continuous supply of water which helps carry the salts already contained in the Egyptian limestone to the exterior surface of the wall.

IV.4.3 - Scanning Electron Microscopy

Scanning Electron Microscopy was performed on a surface flake from the city wall of Cairo between towers 4 and 5, sector 7-8 (unidentified stone type). By observation of the micromorphology, SEM enables to understand the deterioration mechanisms. Salt is easily distinguishable by its well-defined cubic shape (see Fig. IV.17).

SEM also enables a close observation of two distinctive phenomenons: the growth of salt from inside the pore of the stone, well illustrated in Figs. IV.18-19 and the growth of salt crystals within a fracture or micro-crack of the stone which exerts mechanical stress on the stone and fosters its decay (Figs. IV.18 and 20).

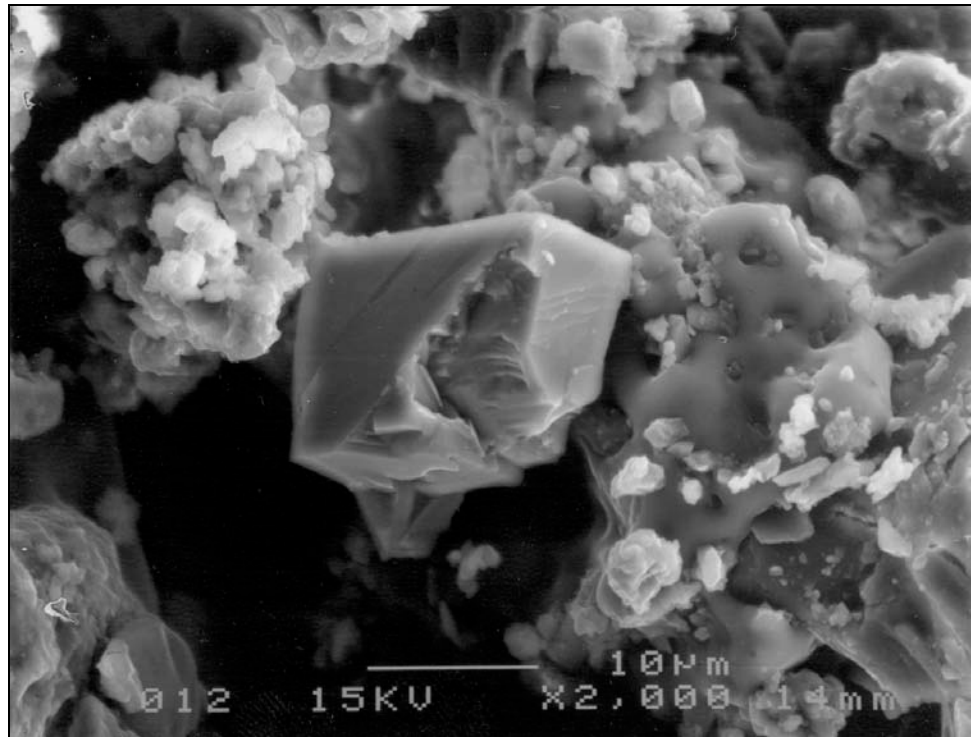


Figure IV.17 Scanning electron microphotography of a surface flake (Towers 4/5, sector 7/8) showing well-defined salt crystal covered by loose material. Magnification $\times 2000$.

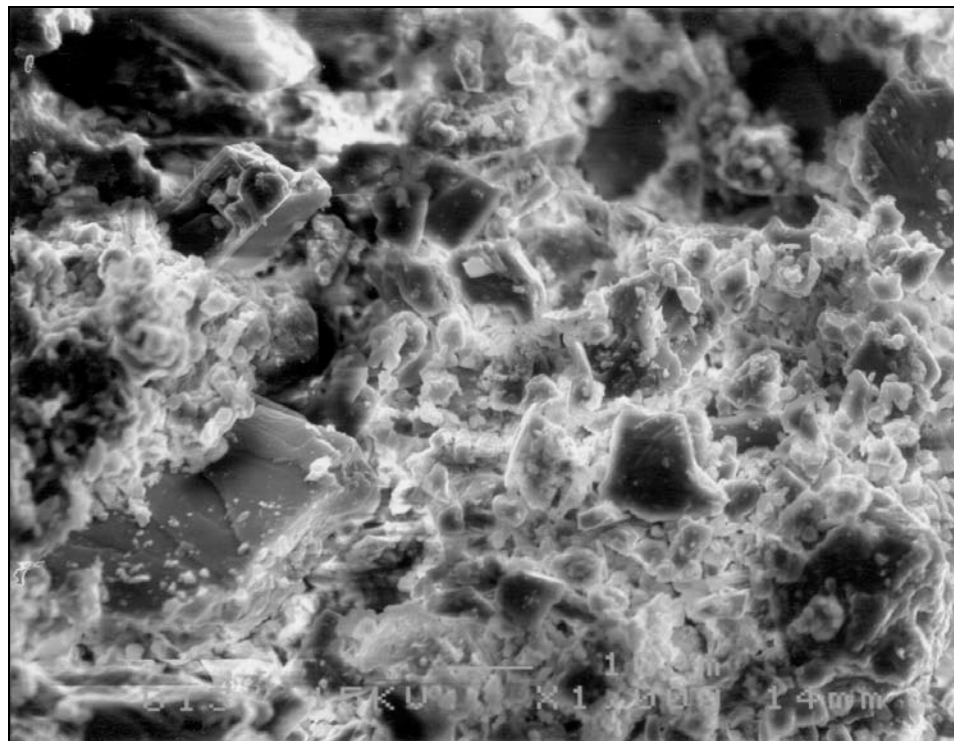


Figure IV.18 Scanning electron microphotography of a surface flake (Towers 4/5, sector 7/8) showing salt crystals growing from within pores and in a microcrack of the stone. Mag. $\times 2000$.

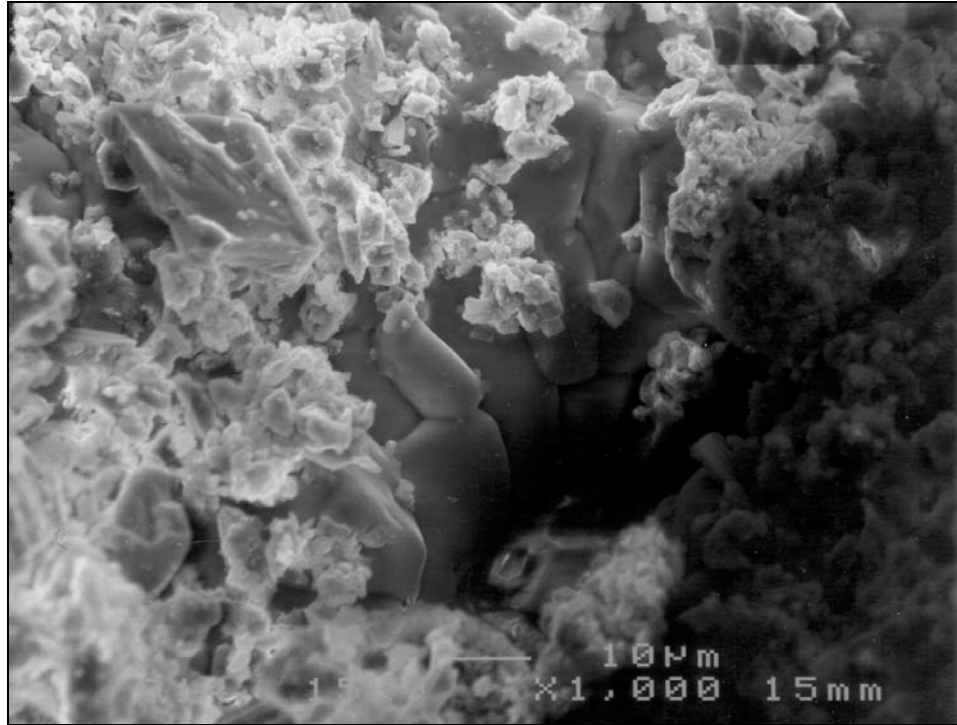


Figure IV.19 Scanning electron microphotography of a surface flake (Towers 4/5, sector 7/8) showing salt crystals growing out from a pore of the stone. Magnification $\times 1000$.

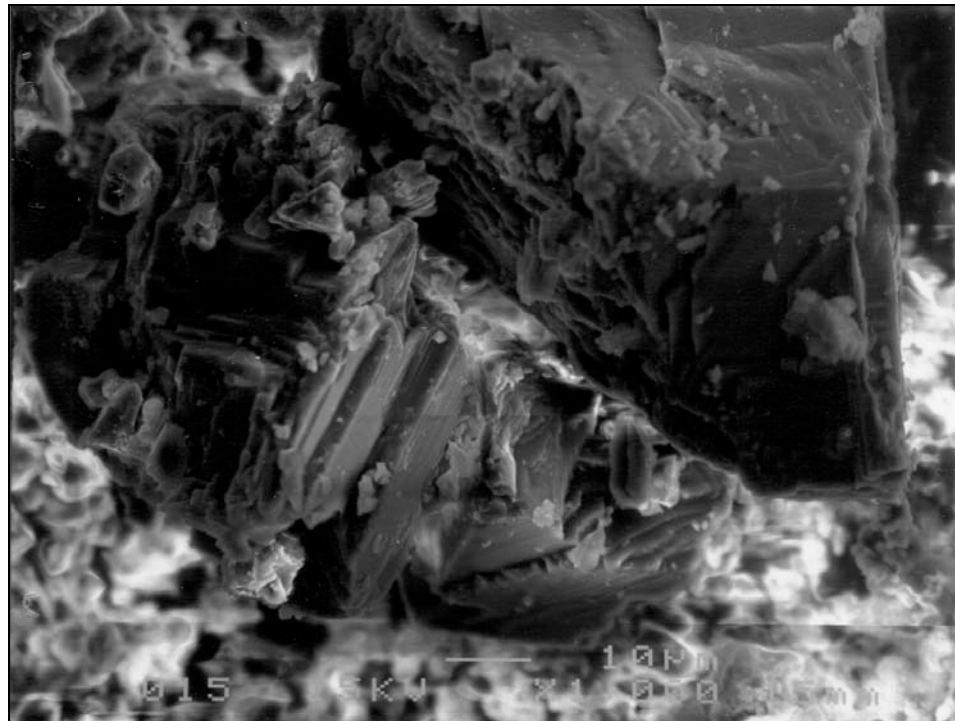


Figure IV.20 Scanning electron microphotography of a surface flake (Towers 4/5, sector 7/8) showing salt crystals growing out of a microcrack. Magnification $\times 1000$.

In addition to salt crusts on the stone surface, salt crystallized in micro- and macro-cracks within the stone as seen in Fig. IV.21. The blue dye treatment shows the salt deposits within the stone very clearly. They are well distributed within the voids of the matrix.

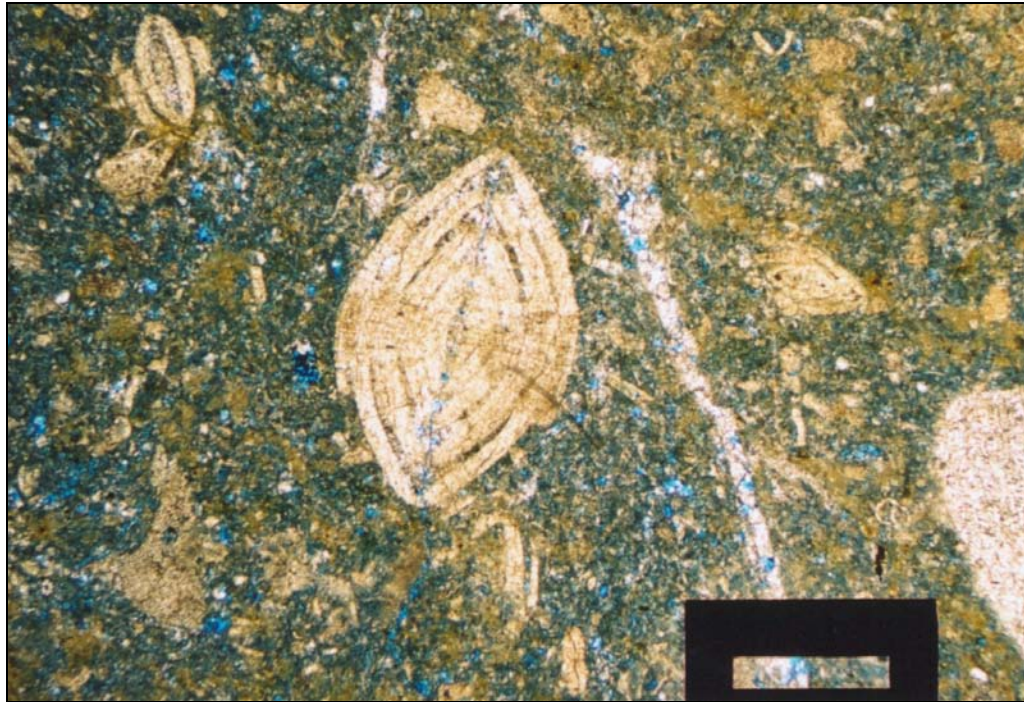


Figure IV.21 Thin section of limestone (sample 11) probably original Ayyubid stone. Coarse-grained matrix with a large amount of fossils and fossils fragments and high porosity. Salts are well distributed within the matrix voids. Magnification $\times 25$. (From Dewey 2000, photo 3.6).

IV.4.4 - Qualitative chemical analysis

Micro-chemical spot tests were performed by Dewey (2000) for preliminary salt identification. Eleven samples taken from the city wall from both Comité repair stone and Ayyubid original stone were analyzed and the results summarized in Table IV.3.

Chlorides were found in every analyzed sample. This is not surprising since halite is naturally present in Egyptian limestone. But chlorides could also have been brought through rising damp from the ground which is naturally rich in chlorides. Lucas (1915) analyzed soil samples around Cairo and found up to 20.25% of salt with an average of 5.46%. Chlorides may also come from the mortar used in the masonry construction.

<i>Sample Number</i>	<i>Origin</i>	<i>Sulfates</i>	<i>Chlorides</i>	<i>Nitrites</i>	<i>Nitrates</i>	<i>Carbonates</i>	<i>Phosphates</i>
2	Comité?	Ø	+++	+	Ø	Ø	+
3	Comité?	Ø	+++	+	+	+++	+
5	Comité	Ø	+++	+++	Ø	Ø	Ø
6	?	+	+++	+	Ø	+	+
9	Comité?	+	+++	Ø	Ø	+	+
12	Ayyubid?	+++	+++	+	Ø	Ø	+
14	Ayyubid?	+++	+++	+++	Ø	+	Ø
15	Ayyubid?	Ø	+++	+	Ø	+++	Ø
16	Comité	Ø	+++	+	Ø	+	Ø
17	Comité?	+	+++	+++	+++	Ø	Ø
18	Comité?	+	+++	+	Ø	+++	Ø

Table IV.3 *Micro-chemical spot tests of eleven samples (see Appendix A for a complete description of each sample). +++ Presence, + Traces, Ø, Absence.*

In addition to a consistent presence of chlorides, nitrites were positively detected in three out of eleven samples, with seven other samples showing traces. Nitrites generally originate from organic sources. Only one sample had traces of nitrates. This may be due to a testing error because nitrates may be reduced to nitrites if the sample is contaminated with nitrate reducing microorganisms and if the test is not carefully carried out (Borrelli 1994). The presence of nitrates and nitrites in stones from the eastern Ayyubid city wall can easily be explained by the fact that the area east of the wall has been used as a dumping ground for centuries, concentrating animal and human

trash. More recently, deficient plumbing and sewage lines of the houses adjacent to the west of the wall may also have contributed to this contamination.

Finally, traces of phosphates were found in 5 samples, while carbonates were found in three of the sample with traces in four of them. Carbonates are probably due to the presence of grains of limestone in the efflorescence samples (Dewey 2000, 11-12).

IV.5 - Salt distribution in the wall

Core samples from the Ayyubid wall were taken by the Rock Engineering Laboratory of Cairo University and analyzed to provide both a quantitative and a spatial analysis of salt distribution within the wall (Rock Engineering Laboratory 2000a).

IV.5.1 - Methodology

The core samples were obtained using 5-cm diameter diamond core bits. The core bits were 40 cm long and extensions were added to reach deeper inside the wall. Compressed air was used to blow out fine particles resulting from coring operation.

The first three samples were extracted from the front part of the wall, i.e., the east side of the wall, facing the park. The first core sample was taken at the base of the wall, around three courses above grade level (approximately 1 meter) (Fig. IV.22). This area was recently exposed (May 1999) and the coring was made through original Ayyubid veneer stone. The coring penetrated almost 160 cm inside the wall. The total length of the tested sample was 64.1 cm, the first 9 cm being the exterior veneer stone.



Figure IV.22 *Coring of the first core sample.
From Rock Engineering Laboratory 2000a.*

The difference between the length of the coring and the length of the sample is probably due to the voids existing inside the rubble core (R.E.L. 2000a, 2).

The second core was sampled a mid-height of the wall, approximately 3 meters above current grade (relation with previous grade unknown). The veneer stone at coring point was a Comité repair stone. The core penetrated almost 220 cm inside the wall and the total length of the tested sample was 73.5 cm, the veneer stone making-up the first 34 cm (R.E.L. 2000a, 9).

The third core sample was taken close to the top of the wall, approximately a meter from the top of the wall (fourth or fifth course down from the crenellation) on the vertical of the first coring place. The veneer stone at coring point was a original Ayyubid stone. The total cored length was almost 155 cm inside the wall and total

length of the sample was 101 cm, the stone veneer being the first 94 cm (R.E.L. 2000a, 15).

The last core sample was extracted from the backside of the wall, i.e., the west side of the wall, facing the city, on the same axis as the third sample. It provides some information on the side of the wall on which houses abutt. The total core length was almost 145 cm inside the wall and the total length of the sample was 71.5 cm, the stone veneer being the first 14 cm (R.E.L. 2000a, 21).

The core samples were then divided into sections and chemical analysis was performed on each section to analyze the main constituents and types of salts present in the sample. In addition, XRD analysis was performed on three sections of each cored sample: the first two centimeters of veneer stone, last two centimeters of veneer stone and the two centimeters immediately following the veneer stone, in the rubble core.

IV.5.2 - Results

IV.5.2.a - Salt content

The main results of the Rock Engineering Laboratory analysis are shown in Tables IV.4 and IV.5, additional results are presented in Appendix B. The results show that the soluble salt content never falls below 3.5% at any point in the wall, whatever coring depth or height.

At the low coring point, the water soluble salt content is relatively stable in the veneer stone around 4.5%, then the value peaks at 7.0% in the two centimeters

immediately following the stone before remaining relatively stable around 4.6% in the interior of the wall.

At the middle coring point, the water-soluble salt content is higher in average than at the low coring point. The salt content in the veneer stone varies between 5.4% and 6.7% (average 5.85%). In the rubble core the salt content varies between 4.8% and 6.0% (average 5.44%).

At the high coring point, the water soluble salt content is lower than at the low and middle coring points, between 3.5% and 4.7% (average 4.2%) in the veneer stone and 4.52% in the rubble core (only one value).

The high core sample taken from the back (west) side of the wall shows a much higher percentage of soluble salts in the veneer stone than the eastern face of the wall, between 8.4% and 15.20% (average 11.2%).

<i>Sample Number</i>		<i>Length of the core section (cm)</i>	<i>Water Soluble Salts (% wt)</i>	<i>Acid Insoluble Residue (% wt)</i>
LOW POINT				
Veneer Stone	1	2.00	4.58	0.50
	2	2.00	4.37	1.00
	3	5.00	4.56	1.00
	4	5.00	7.00	1.00
	5	10.00	4.71	43.00
	6	10.00	4.80	1.00
	7	10.00	4.21	41.00
	8	10.00	4.82	1.00
MIDDLE POINT				
Veneer Stone	1	2.00	6.70	0.50
	2	2.00	5.40	1.00
	3	5.00	5.50	0.50
	4	5.00	6.00	0.50
	5	10.00	6.00	1.00
	6	10.00	5.50	0.50
	7	10.00	6.00	1.00
	8	10.00	4.80	55.00
	9	10.00	5.80	24.00
	10	10.00	5.60	17.00
	11	10.00	5.00	0.50
HIGH POINT				
Veneer Stone	1	2.00	4.46	---
	2	2.00	4.53	0.50
	3	5.00	3.55	---
	4	5.00	3.57	0.50
	5	10.00	3.56	---
	6	10.00	4.63	0.50
	7	10.00	4.53	0.50
	8	10.00	4.71	0.50
	9	10.00	4.70	1.00
	10	10.00	4.55	0.50
	11	10.00	3.67	0.50
	12	10.00	3.58	0.50
	13	10.00	4.52	18.00
BACK POINT				
Veneer Stone	1	2.00	15.20	0.50
	2	2.00	15.00	0.50
	3	5.00	13.00	0.50
	4	5.00	13.00	0.50
	5	10.00	8.40	---
	6	10.00	8.60	1.20
	7	10.00	9.20	---
	8	10.00	8.60	0.50
	9	10.00	9.60	1.00

Table IV.4 *Water-soluble salt content and acid insoluble residue content of the core samples.*

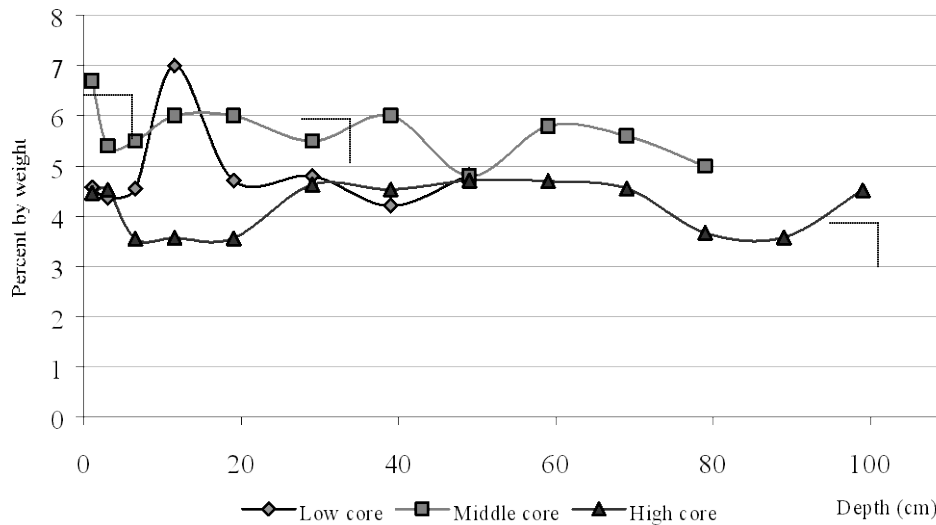


Figure IV.23 Water-soluble salt content of the three core samples in function of the depth of penetration of the coring. Dotted lines mark the end of the veneer stone.

From the outside to the inside of the wall, the concentration of the salts decreases slightly at the low point. The decrease is more obvious at the middle point but the salt content at the high point is quasi stable. For the core sample from the back of the wall (west side) the soluble salt content decreases significantly, nearly by half, from the outside to the inside of the wall.

The concentrations of Cl^- , NH_4^+ , and SO_4^{2-} , were also reported (see Table IV.5). However, it is unclear how the sum of the percentages of these three ions can be higher than the total amount of water-soluble salts present. For this reason only general comments can be made.

Sample Number		Cl (% per weight)	NH ₄ ⁺ (% per weight)	SO ₄ ²⁻ (% per weight)
LOW POINT				
Veneer Stone	1	0.30	5.84	---
	2	0.30	6.21	---
	3	0.40	6.21	---
4	0.20	6.33	---	
5	0.20	2.35	0.02	
6	0.20	3.77	---	
7	0.30	1.32	4.12	
8	0.50	4.99	4.12	
MIDDLE POINT				
Veneer Stone	1	0.50	6.45	0.14
	2	0.10	5.23	2.05
	3	0.54	5.23	0.98
	4	0.40	5.85	3.14
	5	0.20	5.97	1.52
	6	0.20	4.99	1.02
7	0.20	3.03	0.10	
8	0.20	1.56	4.12	
9	0.30	2.78	0.21	
10	0.20	4.74	0.18	
11	0.20	4.74	0.10	
HIGH POINT				
Veneer Stone	1	4.60	5.13	0.37
	2	2.70	4.40	0.21
	3	2.46	4.74	0.45
	4	2.10	5.18	3.03
	5	0.60	5.43	0.27
	6	0.70	5.13	0.51
	7	0.80	4.74	0.16
	8	1.20	4.35	0.06
	9	1.10	4.79	---
	10	0.50	5.13	0.25
	11	0.50	3.28	0.08
	12	0.86	5.72	0.43
13	2.00	4.45	0.27	
BACK POINT				
Veneer Stone	1	7.31	3.89	2.87
	2	3.80	3.77	3.40
	3	4.60	3.89	2.64
	4	3.10	3.52	2.39
5	1.10	4.13	---	
6	3.40	5.72	2.05	
7	0.80	3.77	0.20	
8	3.20	4.49	---	
9	3.20	4.49	0.31	

Table IV.5 Chlorides, ammonium and sulfates content of the core samples.

The percentage of chlorides in the veneer stone increases with the height of the coring point from 0.3% at the low and middle coring point to 1.5% at the high coring point. At the low and middle coring point, this percentage is almost stable with the depth of coring but significantly decreases with depth at the high point.

The percentage of ammonium is several times higher than that of chlorides whatever the coring point or the depth in the wall is. The ammonium content decreases with the height of the coring point. It varies in the veneer stone from 6.1% at low point to 5.7% at middle point, to 4.8% at high point. The presence of ammonium results from activities of microorganisms which decompose nitrogenous organic materials such as proteins.

Finally the sulfate content is very variable from one coring height to the other for the same coring depth, and can vary between 0% and 4% from one 10-cm coring section to the next. In average the sulfates content in the veneer stone is 0% at the low coring point, 1.5% at the middle point and 5% at the high point. This suggests that the main source of sulfates is likely to be air pollution, and hence the sulfate content increases with exposure to pollution, which correlates with the wall height.

The back façade coring point (west side of the wall) is very different from the three front coring points in terms of salt content. It not only has a much higher percentage of total water soluble salts, 15.2%, but the chloride content is proportionally much higher. In the veneer stone, the average ion contents are respectively 4.7% for Cl^- , 3.8% for NH_4^+ , and 2.8% for SO_4^{2-} .

IV.5.2.b - Acid-insoluble residue

The acid-insoluble residue content, which includes the clay minerals, is always below 1% in the veneer stone. In the rubble part of the wall, values vary enormously from one section of the core to another, ranging, from one 10-cm to another, between 1% and 55%, an indication of the diverse nature of the materials used for the core of the wall.

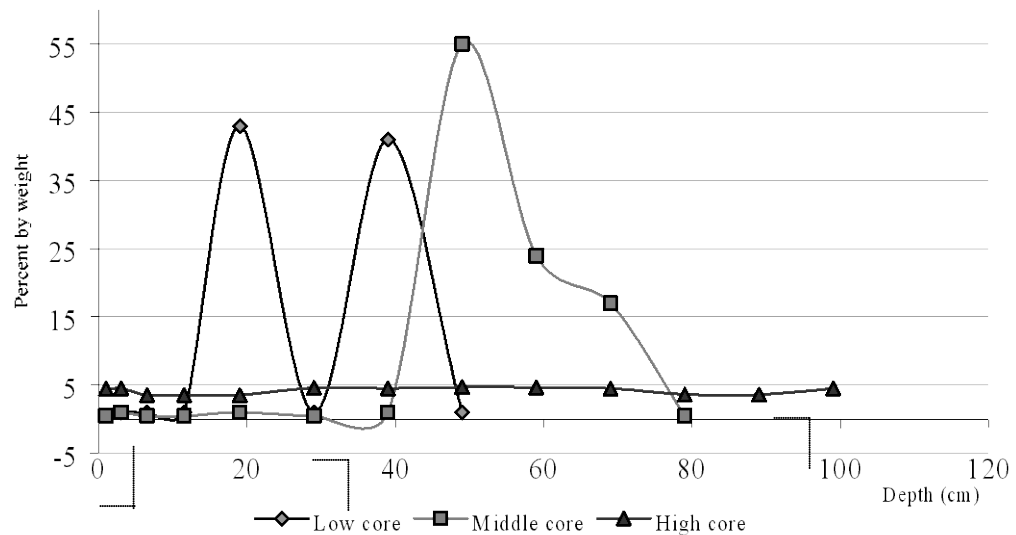


Figure IV.24 Acid insoluble residue content for the three core samples in function of the depth of penetration of the coring. Dotted lines mark the end of the veneer stone.

IV.5.2.c - X-Ray Diffraction analysis

X-Ray Diffraction analysis was performed on three distinct sections inside the wall for each coring sample: in the two first centimeters of the veneer stone, the two last centimeters of the veneer stone and in the two centimeters directly following the veneer stone. The results are summarized in Table IV.6.

		<i>Core sample 1 Low</i>	<i>Core sample 2 Middle</i>	<i>Core sample 3 High</i>	<i>Core sample 4 Back</i>
<i>First two centimeters of vener stone</i>	Stone	Calcite ++++ Dolomite ++ Quartz +	Calcite ++++	Calcite ++++ Dolomite ++++	Calcite ++++ Dolomite ++ Quartz ++
	Salts	Halite ++ NH ₄ Cl ++	Halite ++	Halite ++ NH ₄ Cl ++ Thenardite ++	Halite ++ NH ₄ Cl ++ Thenardite ++
<i>Last two centimeters of vener stone</i>	Stone	Calcite ++++ Dolomite + Quartz +	Calcite ++++ Dolomite ++ Quartz ++	Calcite ++++ Dolomite ++ Quartz ++	Calcite ++++ Dolomite ++ Quartz +
	Salts	Halite ++ NH ₄ Cl ++	Mascagnite ++ Halite ++	Halite ++ NH ₄ Cl + Thenardite +	Halite ++ Thenardite ++ NH ₄ Cl ++
<i>Two centimeters after the stone</i>	Stone	Calcite ++++ Dolomite + Quartz +	Calcite ++++ Dolomite ++++ Quartz ++	Calcite ++++ Quartz ++++ Feldspar ++ Dolomite ++	Calcite ++++ Dolomite ++ Quartz +
	Salts	Halite +	Halite +	Halite ++ NH ₄ Cl ++ Thenardite +	Halite ++ NH ₄ Cl ++

Table IV.6 Results of the XRD analysis performed on the core samples.

Where NH₄Cl: Ammonium chloride,
 Calcite: calcium carbonate (CaCO₃),
 Dolomite: calcium magnesium carbonate (CaMg(CO₃)₂),
 Halite: sodium chloride (NaCl),
 Mascagnite: ammonium sulfate ((NH₄)₂SO₄),
 Thenardite: sodium sulfate (Na₂SO₄),
 Quartz: silicon oxide (SiO₂).

The type of salt found by XRD agrees with literature data on the order of occurrence - sodium chloride (halite), always present, then ammonium chloride, anhydrous sodium sulphate (thenardite), and more rarely ammonium sulfate.

IV.5.3 - Discussion

The acid insoluble residue, including clay minerals, was always found to be below 1% in veneer stones, both in the Comité (middle coring point) and in the

Ayyubid stone (other coring points). This is a relatively low percentage for Egyptian limestone which can easily exhibit a two-digit clay minerals content. A percentage of acid insoluble residue below 1% is considered “safe” for the stone, i.e. will not be the major cause of the stone deterioration according to the literature (Oddy, Hughes, and Baker 1976; Hanna 1984; Bradley and Middleton 1988; Miller 1992). This low percentage of clay minerals is a very positive point for the conservation of the city wall of Cairo.

The water-soluble salt content was found to be above 3.5% at any point in the coring samples. The respective average content in the veneer stone is 4.5% (low point), 5.85% (middle point), 4.2% (high point), and 11.2% (back point). The middle coring point in the front side of the wall corresponded to a Comité stone and showed a higher percentage of water-soluble salts than the two Ayyubid stones (low and high coring points). Since no other water-soluble salts content analyses were performed on the two stone types, it is difficult to know if the higher salt content of the Comité stone is a local condition (more likely) or a characteristic of the stone. Whatever the stone, the water-soluble salt content is high. According to the literature, it is high enough to consider salt deterioration the main decay mechanism. Even a soluble salt content of 0.1% or above has been considered as “high” (Miller 1992).

The percentage of ranges between 0.1% and 4.6% in veneer stone depending on the height of the coring point for the front (east) side stones, and between 3.1% and 7.3% for the back (west) veneer stone. Whereas the percentage of ammonium ranges between 4.8% and 6.1% in average for the veneer stone of the front side and 3.8% for the back side. The presence of ammonium, nitrates and nitrites, the latter detected by

microchemical tests, is due to microbial or bacterial activity: first reduction of nitrogen-containing material to ammonium and further re-oxidation to nitrites and nitrates completing the organic cycle for nitrogen (Caneva, Nugari, and Salvadori 1991).

XRD analysis detected only the presence of ammonium salts but not that of any nitrate salts. This may be due to the fact that the XRD pattern of sodium nitrate (sodaniter or nitraite) (JCPDS 7-271) has a pattern practically identical to that of calcite (JCPDS 5-0586) so that it is easily obscured. Nitrites oxidize easily to nitrates and hence are less frequently found.

The percentage of individual ions is particularly relevant with regards to the susceptibility of stone to deterioration. Chloride content, rather than that of the total soluble salts is often considered the determining factor when assessing quality of Egyptian limestone and likelihood of its rapid deterioration. Hanna (1984) considers that a stone with a concentration of chloride above 0.1% needs desalination. Whereas Oddy, Hughes, and Baker (1976) found that stones with a soluble chloride content above 0.5% are in the category of showing catastrophic deterioration if immersed in water. Finally Bradley and Middleton (1988) studied a number of Egyptian limestone samples and found that the undeteriorated stones had a chloride content between 0.01% and 1.2% whereas the chloride content of the deteriorated stones varied between 0.3% and 2.4%. In light of the literature references, it is clear that the percent of chlorides is relatively high and is a major cause of concern for conservation of the wall. In addition the analysis showed the presence of a high nitrogen bearing compounds content (NO_3^- , NO_2^- , NH_4^+). Bradley and Middleton (1988) concluded that a high proportion of nitrates is an aggravating factor in a stone with a high level of soluble salts.

The evolution of the salt content as a function of core depth is not very clear. It is difficult to see a real pattern which could give an indication about the source of the salts. A possible explanation is that the partial burial of the wall fostered an increase in capillary rise resulting in a fairly homogeneous distribution. The upper part is slightly lower in salt content towards the interior as would be expected from air pollution.

The core sample from the back (west) side of the wall clearly shows that the salt content decreases with the depth of penetration. The probable explanation for this observation is that the back side of the wall was never buried, thus surface evaporation of water was continuous, the water helping the migration of the salts towards the exterior surface of the wall. It is therefore expected to have a higher concentration of salts closer to the surface than deeper into the wall. Also, much of the salts are apparently contributed by human activities and the contamination proceeds from the surface inwards.

Overall, the top portion of the wall contains less water, therefore has less salt, with the exception of sulfates resulting from air pollution. The middle section of the wall was only partially buried. Hence, this area concentrated salts due to crystallization cycles induced by the enhanced capillary rise of the covered lower section. The bottom part of the wall was covered longer and provided a more stable and moist environment with very slow crystal growth. The pattern of the salt deterioration revealed by the condition survey is consistent with the data from the coring samples.

CHAPTER V

CONSERVATION TREATMENT OF EGYPTIAN LIMESTONE

V.1 - Materials

V.1.1 - Overview of the experiment

The goal of the tests was to assess the influence of the action of the surfactant, butyl- α - ω -diammonium chloride or BDAC, on two types of Egyptian limestone, with or without salts, when submitted to wet-dry cycling. The stone cubes were first impregnated with different combinations of salt and surfactant solutions. The capillarity and drying rates were measured during the impregnation process. After their preparation the samples were submitted to wet-dry cycling while their weight and the length each of their three dimensions were monitored.

V.1.2 - Stone samples

To study the effect a surfactant treatment could have on the limestone of the eastern section of the Ayyubid city wall of Cairo, tests were performed on recently quarried Egyptian limestone. The quarry, located close to Cairo, is of the Muquattam Hill rock formation. It is exploited by Naguib Bros. Co., apparently does not have a particular name.

The quarry has different beds and two types of limestone were selected, a nummulitic and a non-nummulitic one². These stone are being considered for replacement along the lower courses of the Ayyubid wall where most of the veneer stones have been lost leaving the upper veneer stones without proper structural support.

V.1.2.a - Replacement stone characteristics

The basic characteristics of the two types of replacement limestone have been measured by the Rock Engineering Laboratory of Cairo University and are given in Tables V.1-3 (Rock Engineering Laboratory 2000b). The corresponding values for the historic stones are also given for comparison (Rock Engineering Laboratory 1999a, 1999b).

<i>Stone Type</i>	<i>Density (g.cm⁻³)</i>	<i>Water Absorption (Percent by weight)</i>	<i>Porosity (Percent by volume)</i>
Non-nummulitic (L)	2.00	9.65	24.60
Nummulitic (F)	2.10	6.62	20.34
Ayyubid	2.08	N/A	18.33
Comité	2.02	N/A	21.94

Table V.1 *Physical characteristics of the historic and replacement stones.*

Note to Table V.1: Porosity was measured by total immersion in boiling water (the data were obtained from only one sample per stone type).

<i>Stone Type</i>	<i>Compressive Strength (kg.cm⁻²)</i>	<i>Young's Modulus (kg.cm⁻²)</i>	<i>Tensile Strength (kg.cm⁻²)</i>
Non-nummulitic (L)	126.02	4700	12.00
Nummulitic (F)	100.90	3800	10.13
Ayyubid	107.6	3364	37.5
Comité	129	5574	34.1

Table V.2 *Mechanical characteristics of the historic and replacement stones.
(Note: 1 kg.cm⁻² = 9.8 N.cm⁻²).*

² A nummulitic stone is a stone containing a genus of fossil foraminiferous cephalopods belonging to the order Polythalamia, found abundantly in the Tertiary strata (*Oxford English Dictionary* s.v nummulite).

Note to Table V.2: The replacement stone data come from only one sample per type; the historic stone data are the average of 5 values for each type.

Stone Type	<i>Acid Insoluble Residue</i>	<i>CaO</i>	<i>MgO</i>	<i>Fe₂O₃</i>	<i>Loss On Ignition</i>	<i>Total Soluble Salts</i>	<i>Cl</i>	<i>SO₄²⁻</i>	<i>NH₄⁺</i>
	<i>Percent per weight</i>								
Non-nummulitic (L)	2.5	50.05	0.80	1.0	39.25	5.4	0.80	0.16	3.99
Nummulitic (F)	3.5	50.49	0.60	0.60	39.60	6.8	0.90	0.26	4.30

Table V.3 Chemical analysis of the replacement stones.

V.1.2.b - Experimental samples

Small cubes approximately 5×5×5 cm³ were used as test samples. Nineteen cubes of each stone type were cut in Cairo and shipped to the University of Pennsylvania³. Throughout the rest of the chapter the nummulitic stone will be identified by the letter F for fossiliferous and the non-nummulitic stone by the letter L for limestone. Each sample was also coded by a number reflecting the treatment received.

The faces of each cube are identified as Top, Bottom, Front, Back, Right or Left according to its position in relation to the cube number as

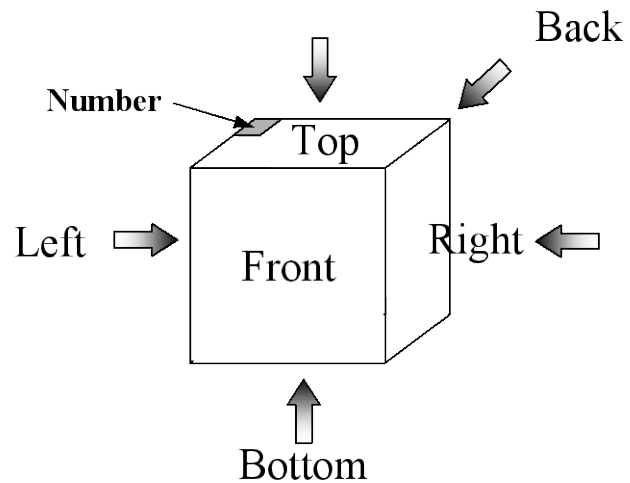


Figure V.1 Identification of each cube face.

³ Most of the cube edges were chipped by mechanical contact with neighboring cubes during transport due to poor packing, the cubes having been left loose in the card box. The transport may have mechanically stressed the cubes.

indicated in Fig. V.1.

The orientation of the bedding planes were not taken into consideration when the samples were cut. However an effort was made to guess this orientation before numbering the samples, so that the bedding planes should be parallel to the Top and Bottom faces of the cubes.

V.1.3 - Salt

Some of the limestone cubes were impregnated with sodium chloride. The product utilized was sodium chloride crystal certified ACS (Fisher Scientific). Key physical properties of sodium chloride are given in the Table V.4 below.

Sodium Chloride	Molecular weight	58.44 g.mol ⁻¹
	Density	2.1654
	Solubility in cold water (0°C)	35.7 g per 100cc.
	Solubility in hot water (100°C)	39.12 g per 100cc.
Saturated Sodium Chloride Solution	Concentration (20 °C)	26.41 % per weight
	Density (20 °C)	1.1978 g.cm ⁻¹
	Surface tension (20 °C)	8.35 Pa
	Viscosity (20 °C)	1.986 mPoise
	Vapor pressure (20 °C)	1.7634 kPa
Distilled water	Vapor pressure (20 °C)	2.3388 kPa

Table V.4 Main physical properties of sodium chloride and its saturated solution. From Handbook of Chemistry and Physics 1995 and Rodriguez-Navarro and Doehne 1999.

V.1.4 - Surfactant

The surfactant chosen for the experiment was butyl- α - ω -diammonium chloride (BDAC), C₄H₈(NH₃⁺)₂(Cl)₂, which has been known to reduce the degree of swelling of various clay containing materials without changing their hydric transport properties (Lagaly and Weiss 1970; Sneath, Wendler, and Klemm 1995; Wendler, Klemm, and

Snethlage 1991). Wendler, Charola and Fitzner (1996) successfully used a bifunctional alkyl- α - ω -diammonium chloride surfactant to reduce the swelling of the clay-rich volcanic tuff from Easter Island. Butyl- α - ω -diammonium chloride is the common name of the surfactant, however the compound should be called 1,4-diaminobutane dihydrochloride (CAS 333-93-7) when the nomenclature rules of the International Union of Pure and Applied Chemistry (IUPAC) are followed.

The BDAC is sold as a white crystalline solid and very hygroscopic. The toxicological properties of the chemical have not been investigated, so care should be taken when manipulating the product to prevent opportunities for direct contact with the skin or eyes and to prevent inhalation. Appropriate protective equipment should be worn when manipulating this chemical.

The experiment used a 4% per weight aqueous solution of 1,4-diaminobutane dihydrochloride (Acros Organics) [molecular weight 161.08 g.mol⁻¹]. The density of a 4% aqueous solution is 1.04g.cm⁻³.

V.2 - Methodology

V.2.1 - Treatment procedures

Of the nineteen cubes of each stone type, nummulitic (F) and non-nummulitic (L), one sample of each was kept as control (numbered 0). The eighteen other samples were then divided into six groups of three, and each group was prepared in a different way. Identical procedures were used for both types of stone. Fifteen samples were subjected to capillary rise and subsequent total immersion in either water (3 samples),

saturated solution of sodium chloride (9) or surfactant (3), while three were impregnated with the surfactant by brushing. Six of the nine samples impregnated with the saturated solution of NaCl were then re-treated with surfactant, either by immersion or by brushing. The complete treatment matrix is presented Table V.5.

V.2.2 - Capillary absorption

V.2.2.a - Parameters

During impregnation, the capillary rise was monitored to obtain two parameters for each type of stone and each type of solution. The first parameter is the capillary water absorption rate, that is the amount of water absorbed per unit surface, expressed in g.cm^{-2} , as a function of time, at room temperature and pressure, by a sample which has its support surface in contact with a solution. The second parameter, the capillary absorption coefficient, is derived from the first one. It is the angular coefficient, expressed in $\text{g.cm}^{-2}.\text{s}^{-1/2}$, of the initial straight segment of the capillary absorption curve. The procedure follows the standard Normal 11/85 with few variations described later.

V.2.2.b - Sample preparation

Prior to any treatment the samples were dried in an oven (Fisher Scientific Isotemp 500 series) around 60°C for 24 hours. After 24 hours the stones were taken out of the oven and left to cool in a desiccator prior to weighing (Balance Denver Instrument XE-510).

<i>Preparation Type</i>	<i>Sample Number</i>	<i>Impregnation 1</i>	<i>Drying 1</i>	<i>Impregnation 2</i>	<i>Drying 2</i>
Water (Control)	1	Capillary absorption followed by total immersion for 24 hours in water.	Air-drying followed by 60°C oven drying.	/	/
	2	Capillary absorption monitored.	Drying rate monitored.		
	3				
NaCl	4	Capillary absorption followed by total immersion for 24 hours in saturated solution of NaCl.	Air-drying followed by 60°C oven drying.	/	/
	5	Capillary absorption monitored.	Drying rate monitored.		
	6				
Brushed BDAC	7	BDAC brushed 14 times in all faces.	Air-drying followed by 60°C oven drying.	/	/
	8				
	9				
Immersed BDAC	10	Capillary absorption followed by total immersion for 24 hours in 4% solution of BDAC.	Air-drying followed by 60°C oven drying.	/	/
	11	Capillary absorption monitored.	Drying rate monitored.		
	12				
NaCl + Brushed BDAC	13	Capillary absorption followed by total immersion for 24 hours in saturated solution of NaCl.	Air-drying followed by 60°C oven drying.	BDAC brushed 14 times in all faces	Air-Drying
	14	Capillary absorption monitored.	Drying rate monitored.		
	15				
NaCl + Immersed BDAC	16	Capillary absorption followed by total immersion for 24 hours in saturated solution of NaCl.	Air-drying. Drying rate monitored.	Capillary absorption followed by total immersion for 24 hours in 4% solution of BDAC.	Air-drying followed by 60°C oven drying.
	17	Capillary absorption monitored.		Capillary absorption monitored.	Drying rate monitored.
	18				

Table V.5 Matrix of treatments for of the limestone cubes.

The procedure of drying in the oven and cooling was repeated until constant weight was attained. The weight is considered constant when the difference between two successive weightings at 24-hour interval is equal or less than 0.1% of the weight of the sample. The samples attained constant weights after 48 hour of drying. The evolution of the sample weight through time is presented in Appendix D.

V.2.2.c - Experimental procedure

Each of the fifteen samples that were to be impregnated by capillary rise was set on glass beads in a plastic container with one of three solutions: water, saturated sodium chloride or 4% aqueous solution of BDAC. The Bottom face, as defined in Fig. V.1, was placed in contact with the solution at $t = 0$. The containers were prepared in such way that the solutions were kept just at the level of the top of the glass beads throughout the capillary rise experiment. Samples impregnated with the same solution shared the same container. Care was taken that the samples never touched each other or the edges of the container to avoid preferential paths for capillary rise. To reduce the evaporation of the solution during capillary rise and to decrease the influence of changes in environmental conditions (relative humidity and temperature) the containers were covered with tight lids. However, they were not hermetically sealed to avoid, in the case of water, condensation on the faces of the cubes.

At given interval the samples were taken out of the containers and the wet surface (Bottom face) was patted dry with a damp paper towel and the samples were weighed. After weighing the samples were immediately returned to their container.

The test was continued until the variation in the amount of absorbed water in two successive weighings at a 24-hour interval was equal or less than 1% of the amount of total water or solution absorbed. The capillary rise was stopped after 72 hours, at the point where for most samples the difference in water absorbed was less than 1%. However, for some samples, notably those with NaCl, the difference was between 1 and 2%. The decision to stop capillary rise impregnation after 3 days was taken because of time constraints and the fact that the purpose of the experiment was the impregnation of the samples.

V.2.3 - Total immersion

The samples impregnated by capillary rise were then immersed for 24 hours in their respective solution (water, saturated solution of NaCl or 4% solution of BDAC).

V.2.4 - Drying

V.2.4.a - Parameters

After the 24-hour total immersion, the samples were dried and their loss of weight by evaporation was monitored. More precisely, the variation of water content of the material over time, at constant temperature and relative humidity was measured and expressed as a percentage of the dry weight of the sample. From these measurement the drying index can be calculated. The Drying index is the ratio between the integral of the drying curve and the maximum water content multiplied by the final time. The final time is the hypothetical time required for the loss of water values to reach the asymptote

they are tending to. The procedure followed the standard Normal 29/88 with few variations outlined hereafter.

V.2.4.b - Experimental procedure

The saturated samples were removed from their solution and patted dry with a damp paper towel. Their weights were recorded and they were immediately placed on metal grids. The grids were elevated several inches to provide good air circulation underneath the cubes to allow them to dry.

Their weights were recorded at given intervals. It was decided not to use a desiccator but to let the samples air-dry because of the difficulty to assure equal relative humidity in a desiccator when so many very humid samples are placed into it. The samples closer to the desiccating agent tend to dry faster than the samples far from it. In contrast, when the samples are left to dry at room environmental conditions, all cubes are in exactly the same temperature and relative humidity even if these vary (RH between 31% and 40%, temperature between 19° and 21°C).

The cubes were weighed several times during the first 24 hours then weighed once each 24-hour intervals while the following formula applies:

$$0.90 \leq \frac{m_0 - m_{i-1}}{m_0 - m_i} \leq 1.0$$

where m_0 is the weight (g) of the sample at time t_0 (h),

m_{i-1} is the weight (g) of the sample at time t_{i-1} (h),

m_i is the weight (g) of the sample at time t_i (h),

The air-drying of the samples was stopped after 96 hours even though the above formula still applied to some samples, i.e. the NaCl treated ones, because of time constraints.

The samples were then dried in an oven (Fisher Scientific Isotemp 500 series) around 60°C until constant weight. The weight is considered constant when the difference between two weighings taken at a 24-hour interval is equal or less than 0.01% of the weight of the dry sample. The samples were oven-dried 96 hours after which the difference between weighings was less than 0.01% for most samples. Those treated with NaCl saturated solution still showed a larger difference but oven-drying was discontinued due to time constraints.

V.2.5 - Application of surfactant by brushing

Samples (7, 8 and 9) were treated with a 4% aqueous solution of BDAC applied to all their faces by brushing with a soft painter's brush. A total of 14 applications was made over a 5-day period. Each application consisted of a single brush stroke on every area of the six faces of each cube. The cubes absorbed the solution very well and within seconds of application the cubes' surfaces were dry. Around 130 ml of surfactant solution was absorbed by the six cubes (three per stone type), adding up to 21.7 ml per cube. After the application of the surfactant by brushing the samples were oven-dried at 60°C.

V.2.6 - Application of surfactant to salt impregnated samples

For six samples of each stone type (13 through 18), a second impregnation with surfactant followed the salt impregnation. Those samples, which had first been impregnated with a saturated solution of sodium chloride, were treated with the surfactant.

V.2.6.a - Capillary absorption and total immersion

The first three samples (16, 17, 18) received the surfactant by capillary absorption followed by total immersion as described in section V.2.2 and V.2.3. However they were not oven dried prior to the second impregnation, but only after it to insure that each sample was only submitted to one oven-drying phase at 60°C. Oven-drying mechanically stresses stones, therefore each sample was submitted only once to oven drying during their preparation. The samples were dried, following the same procedure described in section V.2.4.

V.2.6.b - Application by brushing

The other three samples (13, 14, 15) received the surfactant by brushing over a 4-day period following the procedure described in section V.2.5. The samples had already been air-dried and oven-dried at the end of the first impregnation phase so they were only air-dried after the brush application of the surfactant. The consequence of not oven-drying the samples 13, 14, and 15 at the end of the preparation is they were more humid than all of the other stone cubes when they start cycling.



Figure V.2 Prepared samples before cycling. On the right, nummulitic samples, on the left non-nummulitic samples, displayed for each stone type by increasing sample number from top to bottom, left to right.

Figure V.2 presents all the samples after preparation and before cycling.

V.2.7 - Cycling

V.2.7.a - Environmental conditions

After their preparation, all the samples were subjected to wet-dry cycling. In the wet condition, the samples were placed on plastic racks in closed containers. A solution filled the bottom third of the container to impose a fixed relative humidity in the chamber. First, a saturated solution of sodium chloride which equilibrates at a relative humidity of 75% was used. Since the samples exhibited very little changes after 24 hours at this relative humidity, it was decided to replace it with deionized water which would result in a relative humidity close to 100%. It was assumed that the

relative humidity was between 90% and 100% because the plastic containers were not perfectly sealed and were regularly opened for monitoring of the stones.

For the first cycle, the samples were left 6 days in the humidity chamber (one day with a saturated solution of sodium chloride followed by five days with a solution of distilled water) and then taken out of the humidity chamber. The following humidity periods were reduced to only three days. A 3-day period was found to be a good balance between the requirement of sufficient time for the stones to pick up moisture and the time constraints of a practical experiment.

The drying period was equally 3-day long. The two first days the samples were placed on metallic grids and left to air-dry, then they were placed in a desiccator for the last 24 hours. Thus, the total length of a cycle was six days: three days in the humidity chamber alternating with three days of drying.

V.2.7.b - Measurements

Both the weight and the change of dimensions of cubes were monitored. Care was taken to measure them always in the same order. When the samples were kept in the humidity chamber, six at a time were removed from this controlled environment for measurements. The samples were weighed to the centigram (Balance Denver Instrument XE-510) and the length of each face in each of the three dimensions of the cube was measured (respectively Top-Bottom, Front-Back and Right-Left following the conventions of Fig. V.1). These measurements were made using a dial length comparator (Humboldt Mfg Co. Model H-3250, see Fig.V.3) and following an adapted

version of the ASTM standard C490-97: Standard Practice for Use of Apparatus for the Determination of Length Change of Hardened Cement Paste, Mortar and Concrete.

The ASTM standard is designed to measure the length of prismatic test specimens $1 \times 1 \times 1\frac{1}{4}$ inches. In order to measure changes in length of 5 cm^3 cubes, a two parts extension was built (see Fig. V.4).

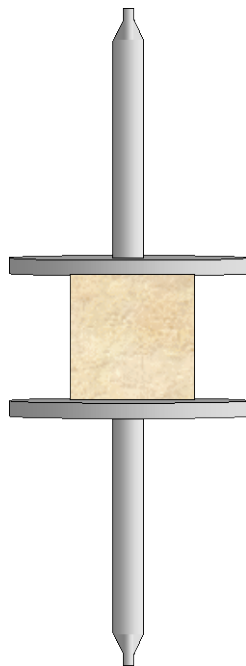


Figure V.4 Two parts extension of the length comparator with a cube in measurement position.



Figure V.3 Humboldt length comparator with dial indicator. Model H-3250.

The instrument records length change, that is an increase or decrease in the linear dimension of a sample. The comparator instrument is made of two main parts: a frame including the base, upright and adjustable anvil and a dial micrometer indicator with movable anvil. The dial micrometer is graduated to read in 0.0001-inch units with a total range of 0.400 inches.

Once a day, before each series of measurements, the length comparator is calibrated and adjusted using the standard Invar test bar provided with the instrument⁴. The central part of the reference bar is covered with electric tape to minimize the effect of temperature change during handling. The test bar is placed between the anvils and the bottom anvil is adjusted so that the dial micrometer is set to 0.20". Adjustment is made by loosening the hex locking nut on the elevating screw at the base and by adjusting the anvil. The lock nut at the base is then tightened. In addition, the scale around the circumference of the dial, which measures 0.0001" increments, may be rotated and locked with a set screw and therefore reset to zero at any indication of the needle pointer. This procedure enables to calibrate the instrument with the standard bar to 0.2000".

After calibration of the length comparator, each cubic sample is placed on the circular platform of the bottom extension. The upper extension, already placed in the upper anvil, is then very slowly and carefully lowered to allow contact between the upper circular platform and the cubic stone sample. The cubic samples are then centered top and bottom on the disc platforms. The platforms-cube assembly is then rotated slowly between the anvils while the comparator reading is taken. The minimum reading of the dial is recorded. The extension parts are always used at the same place (top or bottom) for each measurement. In addition, cubes are oriented the same way each time a dimension is measured.

⁴ Invar is the proprietary name of an alloy of iron or steel (about 64%) and nickel (about 36%), which has a very small coefficient of expansion (*Oxford English Dictionary*, s.v Invar).

V.3 - Results

V.3.1 - Capillary rise

V.3.1.a - Capillary Absorption Rate

Weight changes of the samples over time serve to calculate the amount of water (or solution) absorbed by the sample per unit surface (M_i) at a time t_i by using the

following equation: $M_i = \frac{m_i - m_0}{S}$

where m_i is the weight (g) of the sample at time t_i ,

m_0 is the weight (g) of the sample at time t_0 ,

S is the surface of the sample in contact with the solution (cm^2).

Note: the surface of the sample was calculated by measuring the two dimensions of the face in contact with the solution with a caliper (General MG) with a precision of 1/20th of a millimeter.

The graph of average values M_i for each type of stone and each type of impregnation solution as a function of $\sqrt{t_i}$ is plotted in Fig. V.5. All experimental data are presented in Appendix E.

It should be noted that the capillary rise for the first impregnation of all samples was of 72 hours but only 48 hours for the second impregnation (samples 16, 17, and 18).

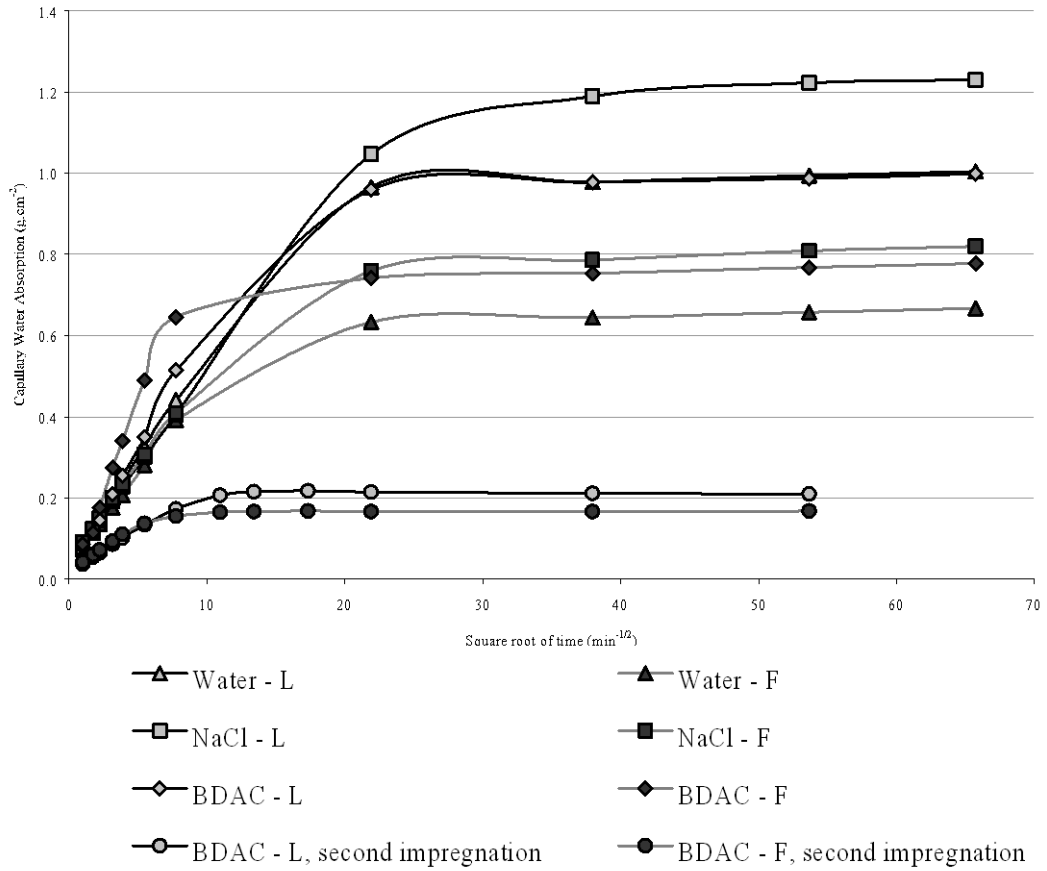


Figure V.5 Graph of the average values of the Capillary Water Absorption (g.cm^{-2}) per stone and impregnation solution type.

V.3.1.b - Capillary Absorption Coefficient

The capillary absorption coefficient AC is represented by the tangent of the linear segment of the capillary absorption curve. AC is obtained from the graphs of the capillary water absorption as a function of the square root of time and is expressed in $\text{g.cm}^{-2}.\text{s}^{-1/2}$. Table V.6 gives the average capillary absorption coefficient per stone and impregnation solution type. The value for each sample can be found in Appendix E.

<i>Impregnation Solution</i>	Deionized Water		Saturated Sodium Chloride		4 % BDAC		BDAC Second Impregnation	
	L	F	L	F	L	F	L	F
<i>Stone type</i>								
Capillary Absorption Coefficient ($\text{g.cm}^{-2}.\text{s}^{-1/2}$)	0.0547 (± 0.0051)	0.0457 (± 0.0194)	0.0461 (± 0.0102)	0.0474 (± 0.0216)	0.0648 (± 0.0036)	0.0871 (± 0.0179)	0.0202 (± 0.0066)	0.0215 (± 0.046)
<i>Linear Regression Coefficient R²</i>	0.9998	0.9992	0.9996	0.9990	0.9984	0.9923	0.9957	0.9933
<i>Last point of the linear regression (min.)</i>	60	60	480	60	60	60	60	30

Table V.6 Average values of the capillary absorption coefficient per stone and impregnation solution type. Standard deviations are given between brackets.

V.3.1.c - Total immersion

After capillary absorption, the samples were immersed in their respective solution for 24 hours. The average weight gain in percent of the dry weight per stone and impregnation solution type after 24-hour of total immersion is reported in Table V.7 together with the last value measured by capillary absorption.

<i>Impregnation Solution</i>	Deionized Water		Saturated Sodium Chloride		4 % BDAC		BDAC Second Impregnation	
	L	F	L	F	L	F	L	F
<i>Max. value for capillary absorption</i>	10.13 (± 0.18)	6.30 (± 0.66)	11.79 (± 0.38)	7.49 (± 0.85)	10.12 (± 0.31)	7.36 (± 0.62)	1.79 (± 0.11)	1.50 (± 0.08)
<i>After 24 hour total immersion</i>	10.28 (± 0.19)	6.41 (± 0.68)	11.24 (± 0.41)	7.02 (± 0.62)	10.18 (± 0.30)	7.51 (± 0.65)	1.29 (± 0.11)	1.25 (± 0.08)

Table V.7 Average weight gain in percent of the dry weight per stone and impregnation solution type. Standard deviations are given between brackets.

V.3.2 - Drying

V.3.2.a - Residual Water Content

Measurement of the sample weights over time enables the calculation of the residual water content with the following equation: $Q_i = \frac{m_i - m_d}{m_d} \times 100$

Where Q_i is the water content at time t_i , given as percent of the final dry weight,

m_i is the weight (g) of the sample at time t_i (min.),

m_d is the weight (g) of the dry sample at the end of the test.

Figure V.6 shows the average values Q_i , of the residual water content, as a function of time t_i for each type of stone and each type of impregnation solution. It should be noted that since samples 16, 17, and 18 were not oven-dried before their second impregnation, the “dry” weights were extrapolated using the average loss of water during oven-drying of the other samples impregnated with the same saturated solution of sodium chloride (samples 4, 5,6, 13,14, and 15). For comparison, the actual weight loss as a function of time for each type of stone and each type of impregnation solution is shown in Fig. V.7. All the experimental data are given in Appendix F.

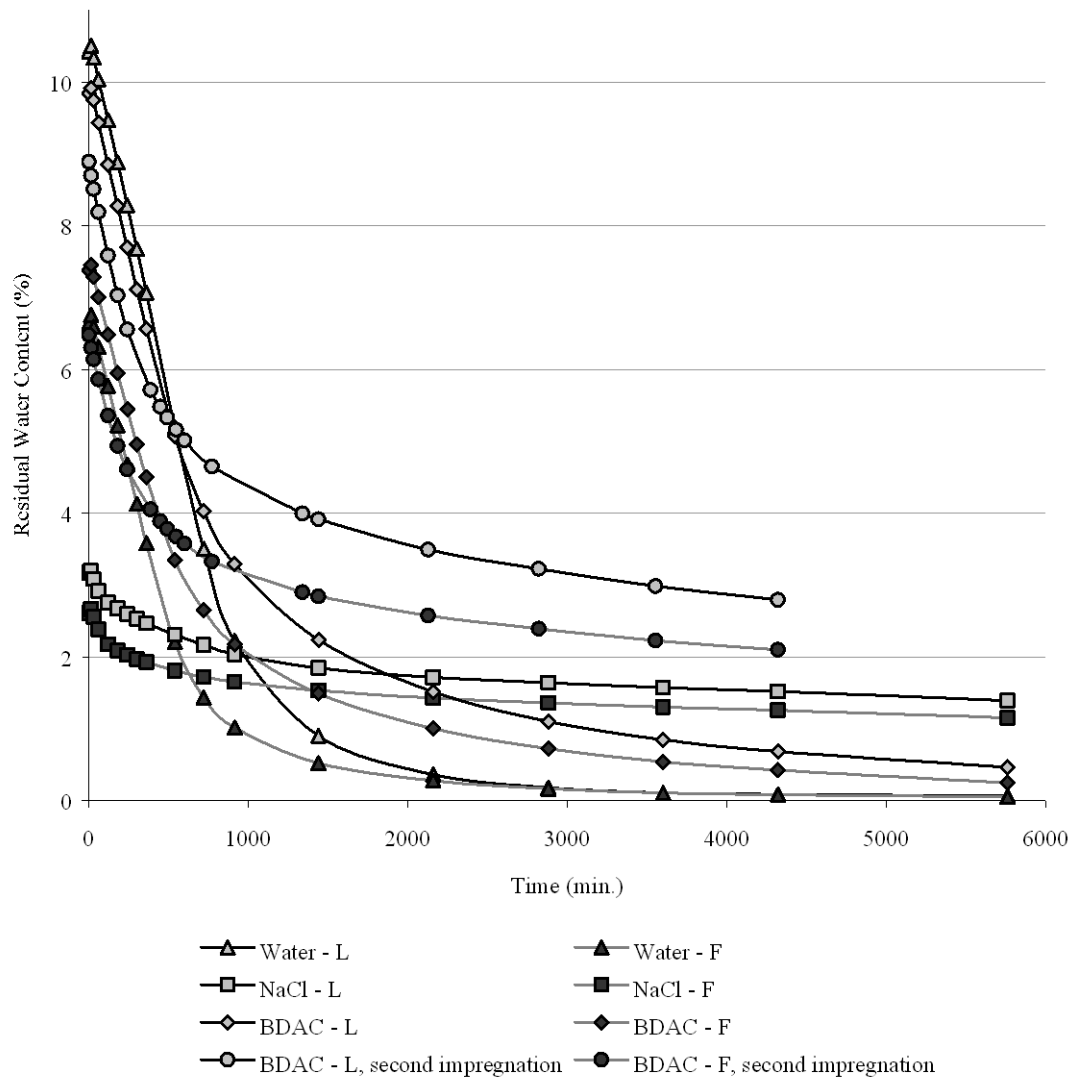


Figure V.6 Graph of the average values of the Residual Water Content (%) per stone and impregnation solution type.

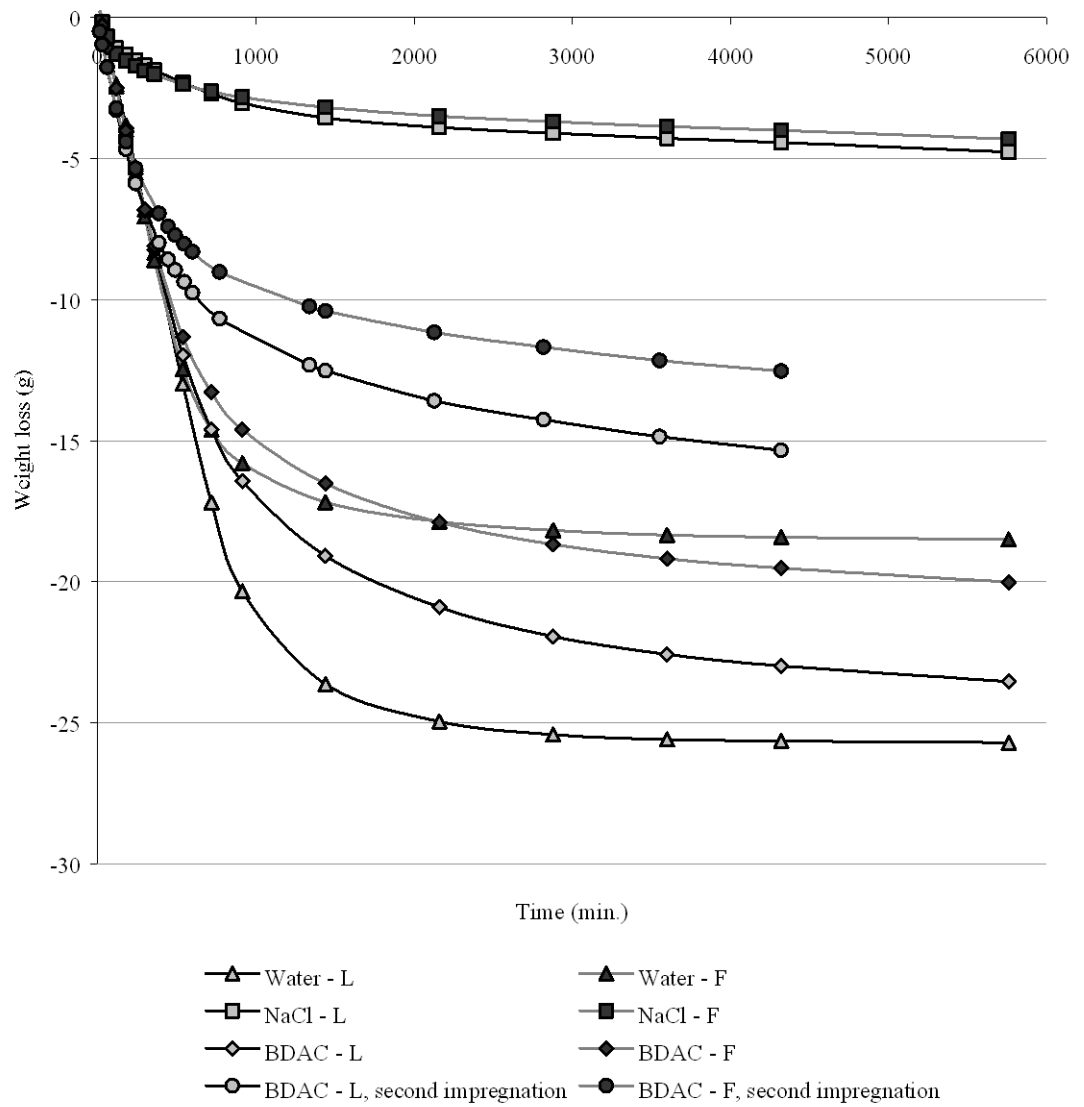


Figure V.7 Graph of the average values weight loss per stone and impregnation solution type.

V.3.2.b - Drying Index

The Drying Index (DI) is calculated with the following equation:

$$DI = \frac{\int_{t_0}^{t_f} f(Q_i) dt}{Q_{\max} \times t_f}$$

Where $f(Q_i, t)$ is equation of the water content expressed as a percent of the final dry weight as a function of time,

Q_{\max} is the initial water content, expressed as percentage of the final dry weight

t_f is the final time (min.) of the test, before the sample are placed in the oven,

t_0 is the initial time of the test, i.e. $t_0 = 0$

Since $f(Q_i, t)$ is not an explicit equation, the calculation of the integral has to be approximated. There are numerous methods to approximate integrals. The method chosen here is to approximate each segment of the curve by a straight line and calculate the integral as the sum of the integrals of each segment. The following equation detailed the approximation.

$$\int_{t_0}^{t_f} f(Q_i) dt \approx \sum_{i=0}^{n-1} \int_{t_i}^{t_{i+1}} f_i(Q_i) dt = \sum_{i=0}^{n-1} (t_{i+1} - t_i) \times (Q_{i+1} - Q_0) + 0.5 \times \frac{Q_{i+1} - Q_i}{t_{i+1} - t_i}$$

Table V.8 gives the average drying index per stone and impregnation solution type. The values of the drying index for each individual sample can be found in Appendix F.

<i>Impregnation Solution</i>	Deionized Water		Saturated Sodium Chloride		4 % BDAC		BDAC Second Impregnation	
	<i>Stone type</i>	L	F	L	F	L	F	L
<i>Initial maximum solution content</i> Q_{max} (%)	10.43 (±0.19)	6.65 (±0.65)	3.17 (±0.25)	2.61 (±0.22)	9.85 (±0.28)	7.38 (±0.66)	8.89 (±0.26)	6.48 (±0.65)
<i>Final time of the test (min) t_f</i>	5760	5760	5760	5760	5760	5760	4320	4320
<i>Drying Index at t_f</i>	0.083 (±0.001)	0.074 (±0.002)	0.519 (±0.024)	0.518 (±0.044)	0.152 (±0.008)	0.133 (±0.011)	0.401 (±0.013)	0.404 (±0.007)

Table V.8 Average values of the Drying Index per stone and impregnation solution type. Standard deviations are given between brackets.

V.3.3 - Cycling

The effect of the wet-dry cycling on each sample was followed by two types of measurements: weight and length changes. For the latter the changes along the three dimensions were taken into account.

From the measurements of the sample weights through time the weight difference was calculated with the following equation:

$$\Delta M(\%) = \frac{(M_i - M_0)}{M_0} \times 100$$

where $\Delta M(\%)$ is the weight difference at time t_i given as a percent of the initial weight,

M_0 is the weight (g) of the sample at the beginning of cycling ($t_0 = 0$),

M_i is the weight (g) of the sample at time t_i .

The weight differences of the non-nummulitic and the nummulitic samples over time during cycling for each type of impregnation solution are shown Figures V.8 and V.9. All the experimental data are presented in Appendix G.

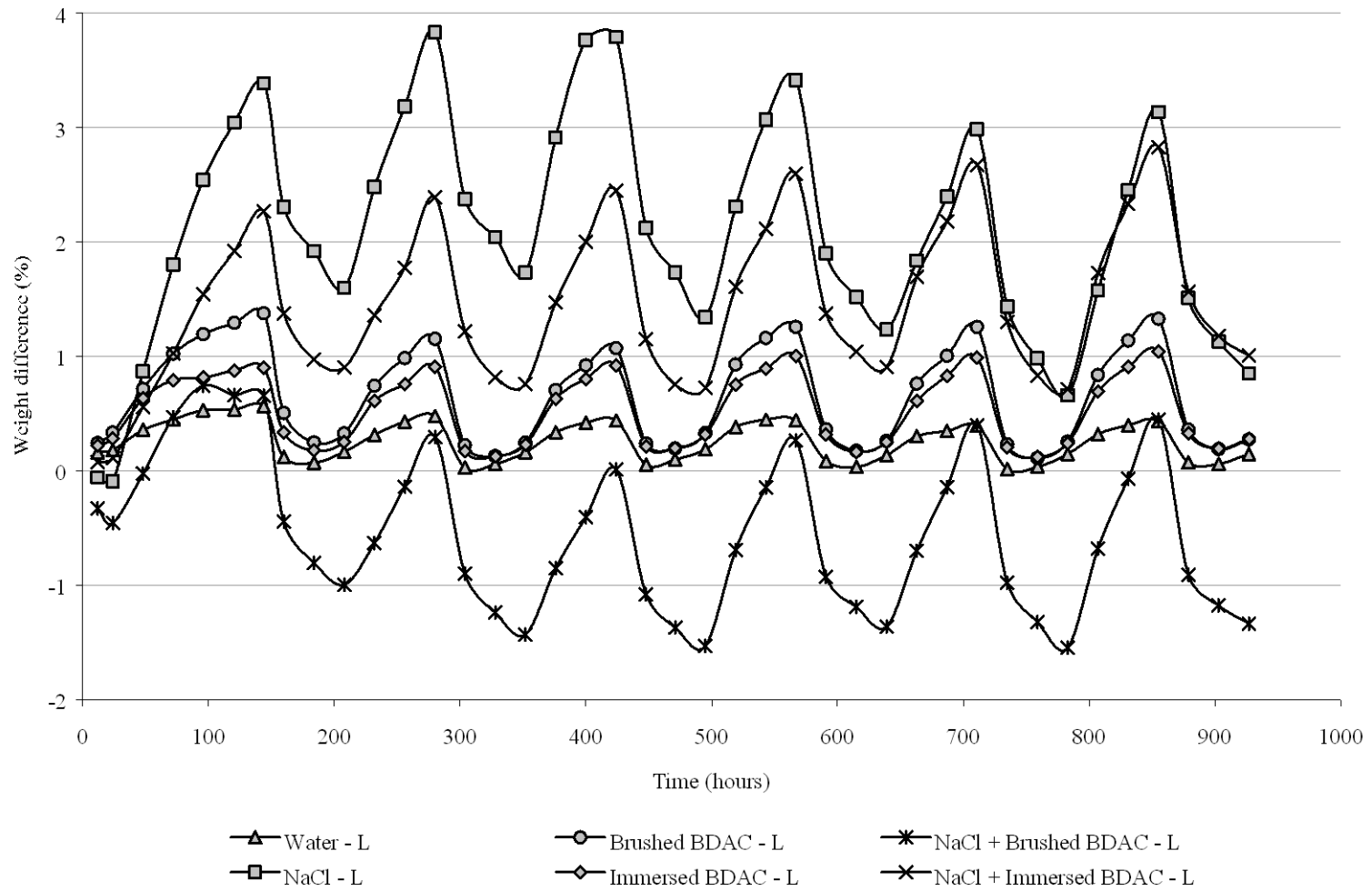


Figure V.8 Average weight difference per preparation treatment during cycling, non-nummular stones.

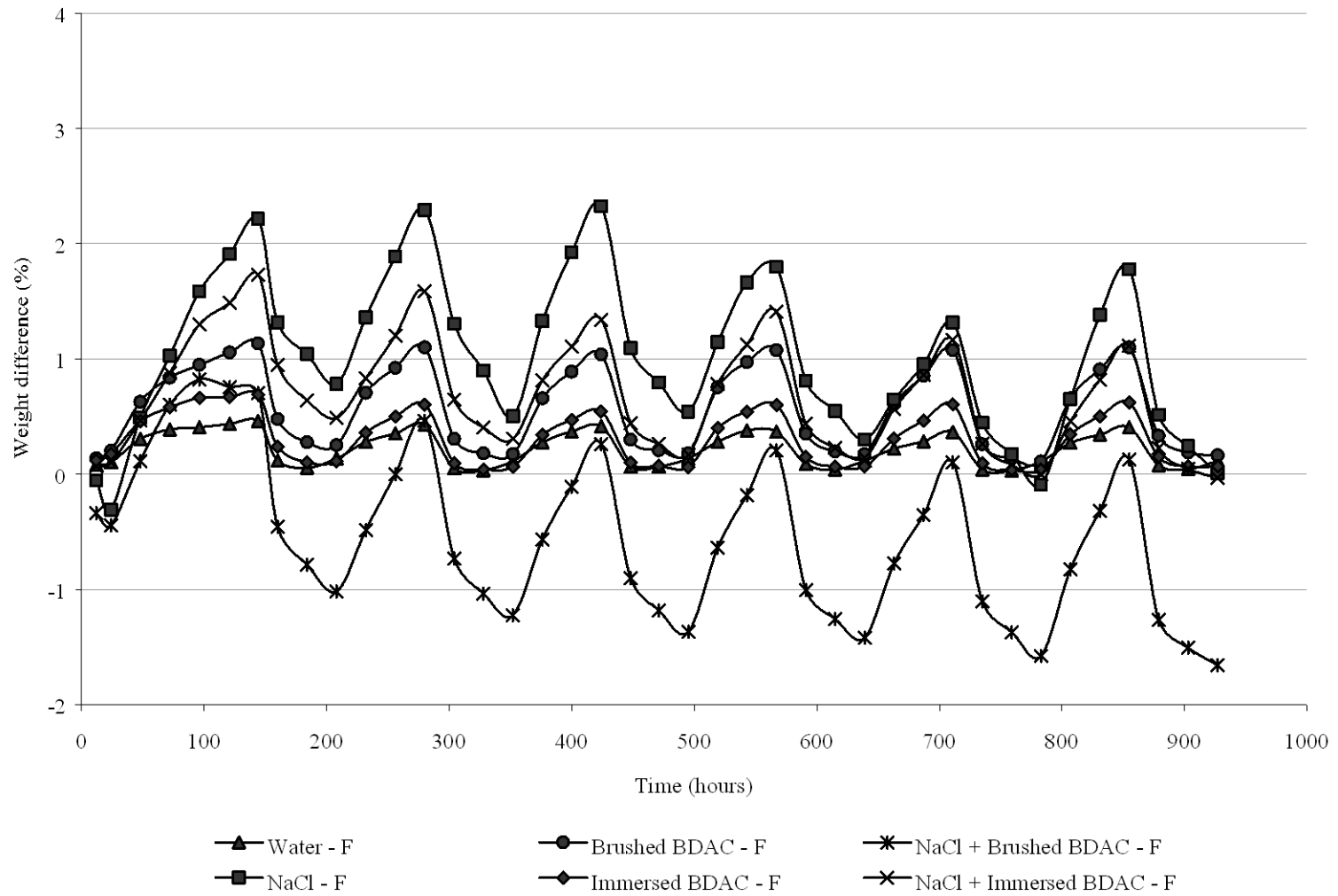


Figure V.9 Average weight difference per preparation treatment during cycling, nummulitic stones.

For the changes along the three dimensions, to facilitate interpretation, the three changes in length were added, equivalent of the change length of a “flattened” cube.

The following equation was used:

$$\Delta L(\%) = \left[\frac{(l_{1,i} - l_{1,0})}{l_{1,0}} + \frac{(l_{2,i} - l_{2,0})}{l_{2,0}} + \frac{(l_{3,i} - l_{3,0})}{l_{3,0}} \right] \times 100$$

where $\Delta L(\%)$ is the sum of the change in length of each dimension given in percent at time t_i ,

$l_{j,0}$ is the comparator reading of the j dimension of sample at the beginning of cycling ($t_0 = 0$) in inches. ($j=1$ Top-Bottom, $j=2$ Front-Back, $j=3$ Right-Left),

$l_{j,i}$ is the comparator reading of the j dimension of sample at time t_i in inches. ($j=1$ for Top.Bottom, $j=2$ for Front-Back, $j=3$ for Right-Left),

The length change values for each sample is reported to the nearest 0.001% and averages to the nearest 0.01%.

The length differences of the non-nummulitic and the nummulitic samples over time during cycling for each type of impregnation solution are shown Figure V.10 and V.11 respectively. All the experimental data are presented in Appendix G.

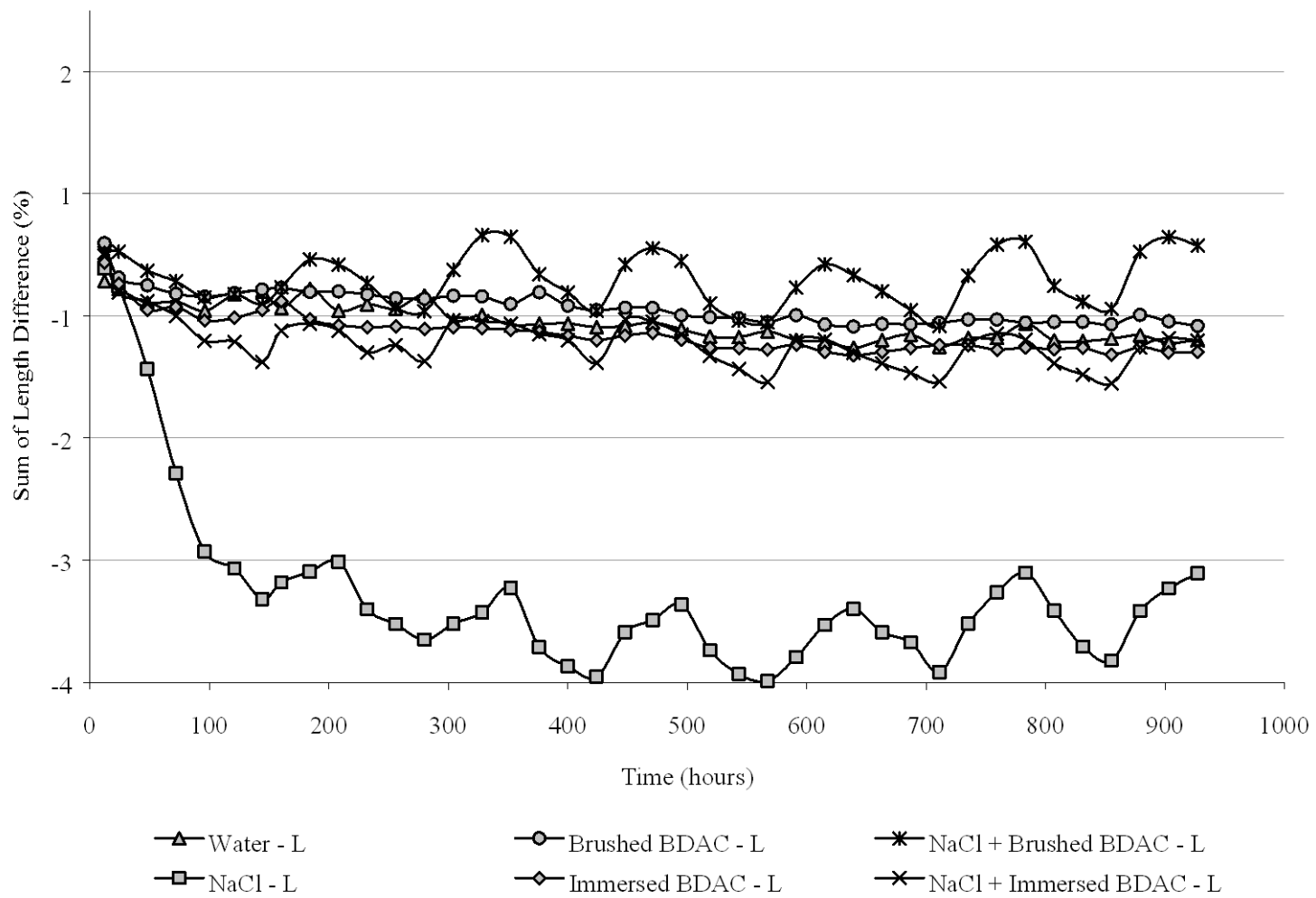


Figure V.10 Average sum of length difference per preparation treatment during cycling, non-nummulitic stones.

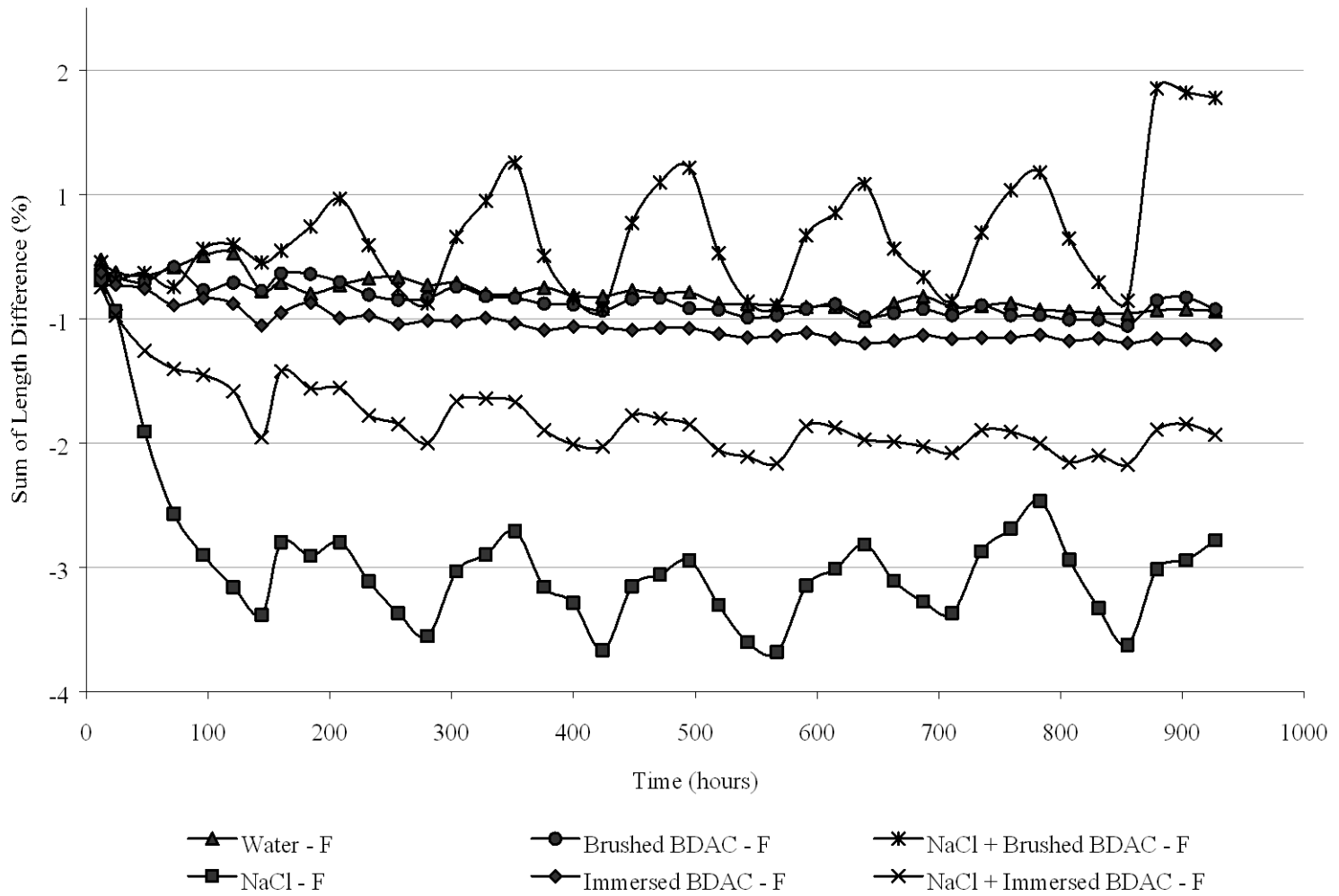


Figure V.11 Average sum of length difference per preparation treatment during cycling, nummulitic stones.

V.4 - Discussion

V.4.1 - Sample preparation

Both types of limestone showed similar behavior, in terms of absorption and drying.

A comparison of the average weight gain for each type of stone and each type of impregnation solution after each preparation phase is presented Table V.9. The values for each individual sample are given in Appendix C.

Preparation	Sample Number	% Weight difference of original weight			
		After first Impregnation	After first Drying	After second Impregnation	After second Drying
Water (Control)	L-1-2-3	10.28 (± 0.19)	-0.14 (± 0.003)	/	/
	F-1-2-3	6.41 (± 0.68)	-0.22 (± 0.04)	/	/
NaCl	L-4-5-6	11.14 (± 0.69)	7.76 (± 0.48)	/	/
	F-4-5-6	6.72 (± 0.08)	3.99 (± 0.10)	/	/
Brushed BDAC	L-7-8-9	0.84 (± 0.05)	0.34 (± 0.01)	/	/
	F-7-8-9	1.21 (± 0.12)	0.30 (± 0.04)	/	/
Immersed BDAC	L-10-11-12	10.18 (± 0.30)	0.30 (± 0.03)	/	/
	F-10-11-12	7.51 (± 0.65)	0.11 (± 0.03)	/	/
NaCl + Brushed BDAC	L-13-14-15	11.21 (± 0.32)	7.81 (± 0.16)	10.50 (± 0.39)	/
	F-13-14-15	6.97 (± 0.06)	4.17 (± 0.36)	6.42 (± 0.02)	/
NaCl + immersed BDAC	L-16-17-18	11.38 (± 0.19)	7.91 (± 0.26)*	10.83 (± 0.19)	1.78 (± 0.08)
	F-16-17-18	7.68 (± 0.89)	5.04 (± 0.75)*	7.57 (± 0.81)	1.02 (± 0.14)

Table V.9 Average differences in percent between the weights of the samples before preparation and at the difference preparation stages. Standard deviations are given between brackets.

Notes to the Table V.9:

First impregnation: after 24-hour immersion or after surfactant brushing.

First drying: after 96 hour of oven drying except for samples 16, 17, 18. Those samples were not oven dried before their second immersion.

(*) The values reported are extrapolated from the average loss of water during oven drying of the other NaCl-impregnated samples.

This table also outlines the differences during preparation. The control samples, impregnated with water did not change in weight throughout the procedure. All the samples impregnated first with the saturated solution of sodium chloride (4-6, 13-18) show weight gain after capillarity rise and drying (around 7.5-8 % for the non-nummulitic stones and around 4-5% for the nummulitic type). This gain is the combination of both the weight of the salt crystallized within the pore space and any solution remaining due to imperfect drying of the samples.

Samples either brushed or immersed in BDAC display similar weight gains after drying (around 0.3% except for the immersed, less porous, nummulitic stones which showed a lower weight increase) equivalent of the weight of the surfactant effectively remaining within the stone.

Samples first impregnated with NaCl and then brushed with the surfactant display a significant weight gain after the application of BDAC which reflects the fact that they were not oven-dried.

Samples impregnated with both NaCl and subsequently BDAC showed a much smaller weight gain. This may be due to the fact that the second impregnation released salt from the stones into the surfactant solution, effectively decreasing the salt content of those samples to about one third of the original amount.

The difference in pore space and pore-size distribution between the two stone types was clearly evidenced during the impregnation with the saturated NaCl solution. The pattern of salt crystallization is notably different between them.



Figure V.12 Back sides of non-nummulitic samples L4, L5, and L6 (from left to right) after impregnation with saturated solution of NaCl and following drying.



Figure V.13 Back sides of nummulitic samples F4, F5, and F6 (from left to right) after impregnation with saturated solution of NaCl and following drying.

The non-nummulitic stones are far more homogeneous and the salt crystallization pattern developed on the surface reflects the original vertical gradient of capillary rise (see Fig. V.12).



Figure V.14 Back side of non-nummulitic samples L4 after impregnation with saturated solution of NaCl and following drying showing preferential salt crystallization pattern.

The nummulitic samples have a far less homogeneous texture due to the high density of fossils. With the evaporation of water, the salts crystallize preferentially where the fossils are, as seen in Fig. V.13 and in a close-up in Fig. V.14.

The internal voids within the fossils seem to offer a preferential path for the evaporation of water. The water carries with it the dissolved salts which then crystallize on the fossils' surface.

V.4.2 - Capillary rise

Both types of limestone have similar absorption rates (capillary absorption coefficient) but all non-nummulitic stones (L) have higher total capillary water absorption (asymptotical value of the curves Fig. V.5) than the nummulitic stones (F) regardless the impregnation solution. This observation correlates with the higher porosity of the non-nummulitic stones (24,6%) compared with the nummulitic one (20.3%).

The comparison of the values obtained with different solutions can at first be misleading. The Normal standard recommends reporting the capillary absorption as a gain in mass by area in contact with the solution. This approach is only valid when all impregnation solutions have the same density. In this particular case, the capillary absorption data should be divided by the density of each solution in order to compare them. The table below provides capillary water absorption at $t = 48$ hours.

<i>Impregnation Solution</i>	Deionized Water		Saturated Sodium Chloride		4 % BDAC		BDAC Second Impregnation	
	Density ($g.cm^{-3}$)							
<i>Stone type</i>	L	F	L	F	L	F	L	F
Capillary Water Absorption at $t= 48$ H ($cm^3.cm^{-2}$)	0.9938	0.6576	1.0209	0.6755	0.9488	0.7382	0.2013	0.1618
Capillary Water Absorption at $t= 48$ H ($g.cm^{-2}$)	0.9938	0.6576	1.2228	0.8091	0.9868	0.7677	0.2094	0.1683

Table V.10 Average values of the capillary water absorption per stone and impregnation solution type. Standard deviations are given between brackets.

When the capillary water absorption is considered in terms of volume absorbed the initial apparent differences between the impregnation solutions are greatly reduced. Nonetheless, the differences between the different impregnation solutions are significant in term of the capillarity absorption coefficient. This parameter represents the initial rate of absorption in function of time (see Table V.6). Whatever the type of stone, the initial absorption is always faster with the BDAC solution than with water or with the saturated solution of sodium chloride. The differences between the salt solution and pure water are much smaller. It should be pointed out that except for water the

initial absorption is slightly higher for the less porous nummulitic stone than for the non-nummulitic one reflecting difference in their pore-size distribution.

The differences in capillary absorption coefficient can be explained by the increased wettability provided by the surfactant. The difference between the salt and pure water solution likely reflects the increased density and viscosity of the saturated sodium chloride solution but these factors have a relatively small effect.

After capillary rise, the samples were fully immersed in their respective solutions for 24 hours. The samples immersed in deionized water or in aqueous solution of BDAC gain weight after a 24-hour immersion. However, the samples immersed in the saturated solution of sodium chloride do not behave as expected. Their full immersion leads to a slight decrease of the weight of the samples. This is probably due to the fact that during capillary rise sodium chloride crystallizes on the surface of the stone. When the stones are fully immersed in the saturated solution, the surface deposit is removed resulting in the observed weight decrease.

The samples 16, 17 and 18 were impregnated with the surfactant after their impregnation with the saturated NaCl solution. The rate of absorption of the surfactant is notably slower (see Fig. V.5). This can be explained by the fact that the samples had not been oven dried and that both salt and moisture already occupied part of the pore space, resulting in less and slower absorption of BDAC.

V.4.3 - Drying

Both types of limestone have a similar drying rate. The non-nummulitic limestone (L) absorbed a higher amount of solution in the impregnation phase and therefore starts the drying phase with a higher residual water content than the non-nummulitic limestone (F). For each impregnation solution, the residual water content of the non-nummulitic limestone is consequently always higher than for the nummulitic stone. However this difference tends to decrease with time. As seen in the rapidly merging curves of the water impregnated stones (see Fig. V.6). For these, the critical moisture content⁵ was reached in less than a day of drying (approximately 17/18 hours).

When comparison between the different impregnation solutions is made, the curves are really more similar than they appear. First because the drying curves are based on the weight changes of the samples and the solutions do not have the same density. In addition, even when samples are completely dry, samples impregnated with BDAC or NaCl will obviously have increased their weight from their initial ones. After the initial drying, the residual water content of the samples impregnated with NaCl is always higher than those impregnated with BDAC or those impregnated with water because of moisture retention. The initial water content of the NaCl-impregnated stone is deceptively low, not because little solution was absorbed but because after 96 hours of oven drying, these samples were far from dry, as evidenced by not satisfying the criteria of the 0.01% difference between weighings. The samples impregnated with BDAC dry somewhat slower (critical moisture content is reached after some 20 hours

⁵ The critical moisture content is the transition point between the drying mechanism relying on capillarity and the one relying on diffusion.

of drying) than those impregnated with water but both of them dried much faster than the NaCl-impregnated stones.

The drying curves of the twice-impregnated samples (16, 17, 18) are interesting in two ways. The samples dry faster than those impregnated only with NaCl. This is due to the significant loss of salt during the second immersion. Furthermore, the amount of BDAC remaining in the stone appears to be smaller than when applied by brushing (see Table V.9). The actual amount retained in the twice treated samples could not be easily detected.

V.4.4 - Cycling

V.4.4.a - Weight changes during cycling

Table V.11 summarizes some characteristics values of the weight changes of the samples during cycling. Amplitude of each individual cycle is given Appendix H.

As expected, the samples gain weight during the humid phase and lose it during drying. Both types of limestone, non-nummulitic (L) and nummulitic (F), present similar profiles of changes in weight during the cycling which depends on their treatment. However the non-nummulitic stones exhibit a higher initial gain of weight (initial uptake) as well as larger amplitude for each cycle. The amplitude is the absolute value of the difference between the higher and the lower measurements of the weight difference of two consecutive cycles. The difference between the two types of stone during cycling directly reflects the difference in porosity of the two stone types: 24.60% for non-nummulitic and 20.34% nummulitic one.

Preparation	Sample Number	% Weight difference of original weight		
		Initial uptake	Max amplitude	Average amplitude per cycle
Water (Control)	L-1-2-3	0.56	0.49	0.41 (± 0.04)
	F-1-2-3	0.46	0.41	0.36 (± 0.03)
NaCl	L-4-5-6	3.39	2.47	2.16 (± 0.24)
	F-4-5-6	2.22	1.87	1.56 (± 0.27)
Brushed BDAC	L-7-8-9	1.38	1.22	1.05 (± 0.11)
	F-7-8-9	1.13	0.99	0.91 (± 0.04)
Immersed BDAC	L-10-11-12	0.90	0.93	0.81 (± 0.06)
	F-10-11-12	0.69	0.59	0.54 (± 0.03)
NaCl + Brushed BDAC	L-13-14-15	0.74	1.99	1.69 (± 0.21)
	F-13-14-15	0.82	1.84	1.64 (± 0.12)
NaCl + immersed BDAC	L-16-17-18	2.27	2.11	1.74 (± 0.21)
	F-16-17-18	1.73	1.28	1.16 (± 0.09)

Table V.11 Characteristic values of the percentual weight changes during wet-dry cycling. Standard deviations are given between brackets.

For both stone types, the samples presenting the highest initial moisture uptake are those impregnated with a saturated NaCl solution, then those salt-impregnated and treated with a surfactant by immersion, followed by the samples treated only with surfactant brushed, then immersed. The samples impregnated only with water presented the smallest initial gain of weight. The stones treated with NaCl followed by brushed BDAC are abnormally placed on the graphs because these samples were not initially as dry as the others. This is clearly shown on the mostly negative weight difference these samples exhibit during cycling. Therefore this data will not be included in initial moisture uptake discussion.

There is a very important difference between the samples only impregnated with water and those impregnated with NaCl saturated solution. The presence of salt increases the initial moisture uptake by 505% and 382% for the non-nummulitic and

nummulitic samples respectively. The application of BDAC has two opposite effects depending on whether the sample contained salt or not. On salt-impregnated samples it reduces the initial moisture uptake by as much as 22% (nummulitic) and 33% (non-nummulitic). On the other hand, for non-salt impregnated samples, the application of BDAC promotes initial moisture absorption. The latter increases by 61% and 50% for non-nummulitic and nummulitic samples respectively when the surfactant was applied by immersion reflecting the residual amount of surfactant in the sample. When the surfactant is brushed on the sample surface the initial moisture absorption increased by 146% for both stones.

The comparison of the maximum amplitude of cycling and the average cycling amplitude shows similar trends to that of the initial moisture uptake. Impregnation of the stones with NaCl results in a tremendous increase in the amplitude observed between consecutive cycles. The average amplitude increases by 427% for non-nummulitic stone and 333% for nummulitic ones.

A decrease in average amplitude for the salt-impregnated samples is observed when they were also treated with surfactant. The amount of this decrease depends on the stone type and the method of application of the surfactant. For the non-nummulitic stone the decrease is similar regardless of the application method of the surfactant while for the nummulitic one a significant decrease was noticed only when the surfactant was applied by immersion. Since this decrease could also be due to the amount of salts present, the actual effect of the surfactant is difficult to evaluate.

Examination of the curves plotted in Figure V.8 and V.9 shows that the amount of moisture uptake is less for salt-impregnated samples when they have been brushed

with a surfactant. However, this effect decreases with on-going cycling, especially for non-nummulitic stones. It is evident that the texture of the stone influences significantly the effect of the surfactant.

V.4.4.b - Length changes during cycling

Table V.12 summarizes some characteristics values of the sum of the length changes of the samples during cycling. Amplitude of each individual cycle is given Appendix H.

Preparation	Sample Number	% Sum of length difference of original length		
		Initial decrease	Max amplitude	Average amplitude per cycle
Water (Control)	L-1-2-3	-0.30	0.24	0.13 (± 0.06)
	F-1-2-3	-0.28	0.33	0.10 (± 0.09)
NaCl	L-4-5-6	-2.82	0.81	0.60 (± 0.15)
	F-4-5-6	-2.88	1.16	0.81 (± 0.17)
Brushed BDAC	L-7-8-9	-0.35	0.12	0.06 (± 0.03)
	F-7-8-9	-0.28	0.23	0.14 (± 0.05)
Immersed BDAC	L-10-11-12	-0.54	0.23	0.09 (± 0.06)
	F-10-11-12	-0.56	0.18	0.08 (± 0.05)
NaCl + Brushed BDAC	L-13-14-15	-0.41	0.69	0.54 (± 0.10)
	F-13-14-15	-0.25	1.71	1.05 (± 0.29)
NaCl + immersed BDAC	L-16-17-18	-0.88	0.51	0.37 (± 0.06)
	F-16-17-18	-1.45	0.58	0.34 (± 0.12)

Table V.12 Characteristic values of the percentual sum of length changes during wet-dry cycling. Standard deviation is given between brackets.

During cycling, the salt-impregnated samples contract during wetting and expand in drying. This behavior, opposite to that of non salt-impregnated stones, had already been observed on sandstones by Wendler and Rückert-Thümling (1993). They explain this by the formation of denser hydration shells between the grains, resulting in

a contraction of the clay layers. During the drying phase the clays appear to return to their original state, i.e., expanding from the previous contraction.

For the salt-impregnated samples, two separate aspects of the graphs can be considered, the initial contraction and the amplitude of the cyclic contraction. The salt-impregnated samples brushed with surfactant cannot be taken into consideration for the discussion on initial contraction of the samples, as they were not as dry as the others so their initial contraction is smaller than it should be. The salt-impregnated samples show a considerably higher initial contraction than those which had been also immersed in surfactant. The contraction is reduced by 69 % for the non-nummulitic samples and by 50% for the nummulitic ones. However, this may be partly due to the fact that the samples immersed in the surfactant contain significantly less salt as previously highlighted in the general discussion on sample preparation.

When the average amplitude of the cyclic contraction is considered, the application of the surfactant seems to have ambivalent results. For the non-nummulitic stones, the average amplitude of change between two consecutive cycles decreases by 10% or 38% depending on whether the surfactant was applied by brushing or immersion. Whereas for the nummulitic stones the average amplitude of change decreases by 58% when the surfactant is applied by immersion but increases by 30% when the surfactant is applied by brushing.

Both types of limestone, non-nummulitic (L) and nummulitic (F) present similar profiles of change in length during wet-dry cycling. However, the less porous stone, the nummulitic one, generally displays higher changes in length during cycling, even though it absorbs less moisture than the more porous, non-nummulitic stone.

The samples impregnated only with water or surfactant hardly display variation in length during cycling, their average amplitude being under 0.15%. The samples however show a tendency to shrink over time as the number of cycles increases. This shrinking could be attributed to the presence of inherent salts (around 6%) in the stones (see Table V.3). Overall, the surfactant-impregnated samples (whatever the method) consistently show less contraction than the samples impregnated with water.

Brushing on of the surfactant does not appear to reduce the change in length for either of the salt-impregnated stones. In the case of the nummulitic stones, this is consistent with the fact that the moisture uptake was not affected. However, the non-nummulitic stones showed a significant decrease (for a 99.5% confidence level) in moisture absorption as confirmed by the application the statistical *t*-test.

Immersion in surfactant for salt-impregnated samples of both types reduces the change in length. This change follows the decrease in moisture absorption for the nummulitic stone, explained by a reduction in salt content. However, the non-nummulitic stones show a far smaller reduction of moisture uptake, even though it is presumed that salt has been lost. This reflects the importance of the stone texture on the influence of the surfactant.

An unusual phenomenon is also observed for the samples treated with NaCl and immersed in BDAC. During the wetting phase of the cycling, the samples progressively contract over the length of the cycle as expected. However during the drying phase after the initial expansion of the first day of drying, the samples slowly contract again rather than continuing their expansion. This effect can be attributed to the presence of the surfactant since samples treated only with sodium chloride continue to expand.

CONCLUSION

More than eight centuries after its construction, the eastern section of the Ayyubid city wall of Cairo is undergoing a comprehensive conservation intervention. One of the issues is the presence of very large amounts of salt. The different deterioration patterns found on the wall surface are likely to require different treatments. For example, thick salt crusts should be removed mechanically thus avoiding the use of water which could enhance salt migration and clay swelling.

Due to the nature of Egyptian limestone as well as the natural and social environment of the wall, an *in situ* mitigation treatment for the salts and the clay minerals contained in the stone is the most logical option. It should consider the introduction of a moisture barrier at the base of the wall as well as addressing any other water infiltration points. This should be complemented with protective treatments for the stone. Among those recently investigated, the application of a surfactant was seen the most promising. This work focused on the application on one such conservation treatment.

The experimental program aimed to evaluate the action of the surfactant, butyl- α - ω -diammonium chloride (BDAC), on two types of Egyptian limestone, a nummulitic and a non-nummulitic one, considered for replacement veneer stones. Although the general behavior of both stones is very similar the porosity of each stone influences the magnitude of the changes observed during the experiment.

In terms of weight gain, the action of the surfactant depends on whether salts are present or not. For salt-impregnated samples, the application of the surfactant by both immersion and brushing reduces the amplitude of weight difference during the cycling. For nummulitic stones, the reduction is significantly larger for samples immersed in the surfactant than in samples brushed with the surfactant. This can be explained by the fact that the immersed samples contained less salts. However, the reduction in amplitude is almost identical for both brushed and immersed surfactant for the non-nummulitic samples reflecting the similar amount of surfactant retained. On samples not previously impregnated with sodium chloride, the surfactant, whatever its application mode was, has the action of increasing the amplitude of weight difference during cycling.

In terms of length changes, the application of the surfactant by either method does not affect the behavior of the samples significantly, which, like the control samples do not display a significant cyclic variation. On salt-impregnated, samples for both types of stones, the brushed surfactant has no significant effect on the length change, but the latter is importantly reduced for immersion application. This is probably due to the fact that the samples contain less salts.

The experimental results obtained can be summarized as follows:

- Both stones considered for replacement do not appear to have a significant clay content (acid insoluble residue approximately 3% by weight).
- Both stones do contain a high amount of soluble salts (approximately 6 to 7% by weight).
- The porosity of the stone influences the amount of surfactant retained, particularly when applied by immersion.

- The application of the surfactant does not change the color of the stone significantly.
- The application of surfactant appeared to reduce powdering of salt-impregnated stones, particularly the non-nummulitic ones.
- The surfactant applied reduces the amount of moisture absorbed during wet-dry cycling.
- The surfactant does not appear to have a long-term effect in reducing moisture absorption, particularly for the non-nummulitic one.

As usual, the experiment also raised new questions which should be addressed in future research. The main ones are:

- Determine depth of penetration of the surfactant for both application method.
- Determine why the amount of surfactant remaining in the non-nummulitic stone is the same regardless of application method.
- Determine why there is no significant change in moisture absorption cycle amplitude between salt-impregnated samples treated with surfactant by brushing and by immersion even though the latter has significantly less salts (as reflected in the decrease in the length change).
- Research the unusual contraction suffered by the salt and surfactant-impregnated samples during the drying cycles.
- Research whether the application of the surfactant by poulticing significantly affects the rate of salt extraction.
- Research the effect of a combined surfactant-lime water application.

- Research the long-term effectiveness of the surfactant in moisture absorption reduction.

On the basis of the results obtained it is premature to recommend the application of a surfactant as protective treatment for the Ayyubid city wall of Cairo, although it appears to reduce moisture absorption. The review of past conservation treatments of Egyptian limestone warns us to take a cautious approach in the application of any new treatment.

APPENDIX A

DESCRIPTION OF THE SAMPLES FROM THE AYYUBID CITY WALL

The description of the samples come from the on-site survey forms of each sample (Fong, 1999).

Sample 1

Site: East wall – park side. Tower 5.

Location: South façade between course numbers 6 and 7 beneath crenellation number 3 (South → North).

Sample description: is this a coating – possibly plaster, or is this decayed, transformed stone now delaminating? It looks like a coating. Could this be remnants of some plaster work done for an accretion against park side of wall in this location?

Removal: Hand. K. Fong. 21.10.98.

Sample 2

Site: East wall – park side. Tower 3 / Tower 4.

Location: Course number 9 within area of previous repairs just above what appears to be a previous fill line. Extreme salt deposits in this area. Thick crusts and crystals. High deterioration (flaking, crumbling in salt saturated area).

Sample description: Salt deposit. Sample 2 was removed just above sample 3.

Removal: Hand. K. Fong. 22.10.98.

Sample 3

Site: East wall – park side. Tower 3 / Tower 4.

Location: Course 10 within what appears to be previous fill/grade line. This area appears to be an area of previous repair (Comité stone work). High salt infestation in this area.

Sample description: Salt infested stone flakes.

Removal: Hand. K. Fong. 22.10.98.

Sample 4

Site: East wall – park side. Tower 5 / Tower 6 - 1.

Location: taken from horizontal crenellation joint between numbers 2 and 3 of crenellation. This area is thought to have been re-pointed by the Comité.

Sample description: Extruded mortar.

Removal: Hand. K. Fong. 22.10.98.

Sample 5

Site: East wall – park side. Tower 10.

Location: Near horizontal joint between course numbers 8 and 9. Taken from bottom of course 8. The sample, taken from approximately 3 meters from top of the wall, comes from an area that was completely exposed in the 1950's and recovered 5-10 years later until 1998 when the park excavation began.

Sample description: Repair stone.

Removal: Hand. K. Fong. 24.10.98.

Sample 6

Site: East wall – Rampart/parapet wall. Tower 9 / Tower 10 - 4.

Location: Course number 1, facing stone just south of crenellation number 10 (North → South) (same location as number 8). Sample taken from back of park side stretcher stone.

Sample description: Back side of this stone is eroded as is facing stone of parapet wall in this location. Detached stone fragment of highly eroded stone.

Removal: Hand, much dirt behind detached fragment. K. Fong. 4.11.98.

Sample 7

Site: East wall – Parapet. Tower 9 / Tower 10 - 4.

Location: Course 1 beneath northwest corner of crenellation number 10 (North → South). Top third of mortar joint between two stretchers.

Sample description: This is possibly original mortar.

Removal: Screw driver. K. Fong. 4.11.98.

Sample 8

Site: East wall – Parapet wall. Tower 9 / Tower 10 - 4.

Location: Course number 1, just south of crenellation number 10 (North → South) (same location as number 6).

Sample description: Exterior mortar between two stretchers. Mortar extremely soft, highly deteriorated – disaggregated. Is this intra-wall joint mortar different from pointing mortar?

Removal: Hand and screwdriver. K. Fong. 4.11.98.

Sample 9

Site: East wall – park side. Tower 8 / Tower 9.

Location: course number 2, north end of large stratified trash overhang. Course number 3 is now covered with dirt and trash. Was this area recently excavated (since April 1998)?

Sample description: Highly deteriorated, flaking stone. Repair stone?

Removal: Hand and screwdriver. K. Fong. 4.11.98.

Sample 10

Site: East wall – park side. Tower 8.

Location: Northeast elevation of tower, course number 3.

Sample description: Joint mortar. Stones on either side of joint appear to be original and in stable condition, suggesting original mortar.

Removal: Hand. K. Fong. 4.11.98.

Sample 11

Site: East wall – parapet. Tower 8 / Tower 9 - 1.

Location: Parapet elevation, south end of course number 1 of crenellation number 3 (South → North).

Sample description: Alveolar erosion of what is believed to be original stone.

Removal: Hammer and chisel. K. Fong. 4.11.98.

Sample 12

Site: East wall – park side. Tower 8.

Location: North façade of the tower, course number 4, stretcher number 2 (West → East).

Sample description: Color change in stone, delaminating fragment. This appears to be original stone.

Removal: Hand. K. Fong. 4.11.98.

Sample 13

Site: East wall – park side. Tower 8.

Location: South façade, course number 1, stretcher number 1 (West → East).

Sample description: Mortar behind stretcher, intra-wall construction. Exposed bedding mortar from behind a limestone stretcher and the rubble core, located on several feet away from Sample 12.

Removal: Hand. K. Fong. 4.11.98.

Sample 14

Site: East wall – park side. Tower 5 / Tower 6 - 1.

Location: Course 1 (within 42 centimeters from the top), beneath crenellation number 5 (South → North). The area appears to have been covered for a significant amount of time (40-50 years) until 1998 when the park excavation began.

Sample description: Delaminating stretcher, appears to be original stone.

Removal: Masonry hammer. K. Fong. 4.11.98.

Samples 15

Site: East wall – park side. Tower 5.

Location: Southeast façade of tower, course number 10 (midway between the top and the current grade), beneath crenellation numbers 4 and 5, stretcher stone.

Sample description: Highly fossiliferous stone, highly decayed, active condition. Flaking stones are not nearly as decayed. Eroded stone face is lightly dusted

with dirt but clearly yellow (indicating relatively recent exposure). This appears to be original stone.

Removal: Hand. K. Fong. 4.11.98.

Sample 16

Site: East wall – park side. Tower 4 / Tower 5 - 4.

Location: Course number 4, just north of crenellation number 6 (North → South), header stone.

Sample description: Repair Comité stone. The surface of this stone is by appearance, smooth and continuous, however upon very close inspection it is slightly blistered. The stone easily compresses beneath gentle finger pressure. The stone is severely flaking and disaggregated beneath the surface skin (only paper thin). The stone lacks all internal cohesion to a depth of approximately 5 mm. The flanking stones are also Comité repair stones. The surface finish chisel marks are still visible on these flanking stones.

Removal: Hand. K. Fong. 4.11.98.

Sample 17

Site: East wall – park side. Tower 3 / Tower 4 - 5.

Location: Course number 8, beneath crenellation number 11 (North → South).

Sample taken from what appears to be just in the middle of or just above a previous fill line.

Sample description: fractured, delaminating severe flaking and salt infestation curtain wall stone. Deterioration in this area is so severe that it is impossible to visually ascertain whether this is original or repair stone. Entire surrounding area of the wall is Comité work. What is happening on Community and rampart side of the wall. Is there an accretion that is draining into the wall?

Removal: Hand. K. Fong. 4.11.98.

Sample 18

Site: East wall – park side. Tower 3 / Tower 4 - 5.

Location: Course number 10, beneath crenellation number 12 (North → South), beneath previous fill line.

Sample description: Comité repair stone. Severe flaking and salt infestation.

Removal: Hand and screwdriver. K. Fong. 4.11.98.

APPENDIX B

CORE SAMPLES ANALYSES

From the report of the Rock Engineering Laboratory of Cairo University (R.E.L. 2000a).

Core Sample 1 - Low coring point, front side

<i>Sample Number</i>	<i>Length (cm)</i>	<i>Material Type</i>	<i>Moisture Content (% by weight)</i>
Outer Surface	3.30	Rock	2.02
2	8.10	Rock	2.05
3	6.90	Rock	2.39
4	4.60	Rock Frag.	2.65
5	4.30	Red Brick	12.60
6	2.10	Red Brick + Mortar	4.02
7	4.10	Mortar	4.98
8	4.00	Rock Frag.	2.90
9	2.10	Rock Frag.	3.35
10	3.10	Rock Frag.	3.92
11	3.50	Rock Frag. + Mortar	6.91
12	2.50	Rock Frag. + Mortar	8.51
13	5.00	Rock Frag.	6.61
14	2.00	Rock Frag.	3.11
15	3.50	Rock Frag.	3.51
16	5.00	Rock Frag.	10.37
17	---	Ground Mortar	6.36

Table B.1 *Moisture content of sections from core sample 1, low coring point front side.*

Core Sample 2 - Middle coring point, front side

<i>Sample Number</i>	<i>Length (cm)</i>	<i>Material Type</i>	<i>Moisture Content (% by weight)</i>
Outer Surface	11.00	Rock	1.80
2	4.00	Rock	1.77
3	7.00	Rock	1.96
4	9.50	Rock	2.21
5	5.50	Rock	1.52
6	8.00	Rock	2.55
7	5.50	Mortar	6.33
8	5.00	Mortar	12.95
9	---	Ground Mortar	6.27
10	---	Rock Frag.	3.58
11	3.00	Red Brick	0.40
12	8.00	Rock	1.82
13	7.00	Rock	1.14

Table B.2 *Moisture content of sections from core sample 2, middle coring point, front side.*

Core Sample 3 - High coring point, front side

<i>Sample Number</i>	<i>Length (cm)</i>	<i>Material Type</i>	<i>Moisture Content (% by weight)</i>
Outer Surface	16.00	Rock	1.45
2	8.00	Rock	0.56
3	---	Rock	0.56
4	6.50	Rock	2.07
5	3.00	Rock	2.27
6	5.00	Rock	1.62
7	9.00	Rock	2.04
8	12.50	Rock	2.60
9	12.00	Rock	1.10
10	7.00	Rock	1.09
11	10.00	Rock	1.57
12	7.00	Rock	3.68
13	5.00	Rock	1.43

Table B.3 *Moisture content of sections from core sample 3, high coring point, front side.*

Core Sample 4 - Back side coring point

<i>Sample Number</i>	<i>Length (cm)</i>	<i>Material Type</i>	<i>Moisture Content (% by weight)</i>
Outer Surface	7.50	Rock	1.15
2	8.50	Rock	1.18
3	12.50	Rock	0.32
4	9.00	Rock	2.16
5	13.50	Rock + Mortar	2.63
6	13.00	Rock	0.51
7	4.00	Rock + Mortar	2.56
8	3.50	Rock + Mortar	2.96

Table B.4 *Moisture content of sections from core sample 4, back side coring point.*

APPENDIX C

SAMPLE WEIGHT CHANGES DURING PREPARATION

<i>Impregnation Solution</i>	<i>Sample Number</i>	<i>After initial drying</i>	<i>After Immersion 1</i>	<i>After Drying 1</i>	<i>After Immersion 2</i>	<i>After Drying 2</i>
Water	L1	249.50	274.86	249.17	/	/
	L2	250.06	275.51	249.72	/	/
	L3	245.18	270.93	244.84	/	/
NaCl	L4	252.52	278.63	271.01	/	/
	L5	245.69	274.06	264.53	/	/
	L6	247.91	276.51	268.43	/	/
Brushed BDAC	L7	249.16	251.12	249.96	/	/
	L8	249.95	252.14	250.80	/	/
	L9	246.16	248.24	247.02	/	/
Immersed BDAC	L10	249.54	275.79	250.33	/	/
	L11	251.36	276.55	252.04	/	/
	L12	249.35	274.27	250.14	/	/
NaCl + Brushed BDAC	L13	258.07	286.23	278.29	284.18	/
	L14	248.35	276.08	267.31	274.38	/
	L15	249.38	278.16	269.23	276.57	/
NaCl + Immersed BDAC	L16	245.47	273.72	265.02*	272.41	249.60
	L17	248.67	276.41	267.64*	275.07	253.22
	L18	247.25	275.59	267.37*	274.20	251.76
Water	F1	285.29	301.66	284.54	/	/
	F2	278.18	297.90	277.59	/	/
	F3	280.80	298.82	280.31	/	/
NaCl	F4	279.38	298.00	290.66	/	/
	F5	285.12	304.17	296.68	/	/
	F6	288.21	307.85	299.36	/	/
Brushed BDAC	F7	283.74	287.21	284.56	/	/
	F8	273.80	277.43	274.74	/	/
	F9	289.60	292.75	290.36	/	/
Immersed BDAC	F10	286.01	307.78	286.43	/	/
	F11	268.50	290.25	268.72	/	/
	F12	287.48	307.05	287.80	/	/
NaCl + Brushed BDAC	F13	283.95	303.69	294.64	302.21	/
	F14	279.77	299.13	292.17	297.73	/
	F15	283.75	303.74	296.03	301.90	/
NaCl + Immersed BDAC	F16	287.09	306.20	299.07*	306.14	289.55
	F17	279.30	302.16	294.75*	301.71	282.44
	F18	283.43	306.69	298.77*	306.25	286.51

Table C.1 Weights of the samples before preparation and at the difference preparation stages.

<i>Impregnation Solution</i>	<i>Sample Number</i>	<i>After Immersion 1</i>	<i>After Drying 1</i>	<i>After Immersion 2</i>	<i>After Drying 2</i>
Water	L1	10.16	-0.13	/	/
	L2	10.18	-0.14	/	/
	L3	10.50	-0.14	/	/
NaCl	L4	10.34	7.32	/	/
	L5	11.55	7.67	/	/
	L6	11.54	8.28	/	/
Brushed BDAC	L7	0.79	0.32	/	/
	L8	0.88	0.34	/	/
	L9	0.84	0.35	/	/
Immersed BDAC	L10	10.52	0.32	/	/
	L11	10.02	0.27	/	/
	L12	9.99	0.32	/	/
NaCl + Brushed BDAC	L13	10.91	7.84	10.12	/
	L14	11.17	7.63	10.48	/
	L15	11.54	7.96	10.90	/
NaCl + Immersed BDAC	L16	11.51	7.96*	10.97	1.68
	L17	11.16	7.63*	10.62	1.83
	L18	11.46	8.14*	10.90	1.82
Water	F1	5.74	-0.26	/	/
	F2	7.09	-0.21	/	/
	F3	6.42	-0.17	/	/
NaCl	F4	6.66	4.04	/	/
	F5	6.68	4.05	/	/
	F6	6.81	3.87	/	/
Brushed BDAC	F7	1.22	0.29	/	/
	F8	1.33	0.34	/	/
	F9	1.09	0.26	/	/
Immersed BDAC	F10	7.61	0.15	/	/
	F11	8.10	0.08	/	/
	F12	6.81	0.11	/	/
NaCl + Brushed BDAC	F13	6.95	3.76	6.43	/
	F14	6.92	4.43	6.42	/
	F15	7.04	4.33	6.40	/
NaCl + Immersed BDAC	F16	6.66	4.17*	6.64	0.86
	F17	8.18	5.53*	8.02	1.12
	F18	8.21	5.41*	8.05	1.09

Table C.2 *Differences in percent between the weights of the samples before preparation and at the difference preparation stages.*

Notes to the Table C.1 and C.2:

First impregnation: after 24-hour immersion or after surfactant brushing.

First drying: after 96 hour of oven drying except for samples 16, 17, 18.

(*) Those samples (16, 17, 18) were not oven dried before their second immersion. The values reported are extrapolated from the average loss of water during oven drying of the other NaCl-impregnated samples.

APPENDIX D

INITIAL DRYING RESULTS

<i>Sample Number</i>	<i>Weight in grams</i>			<i>Weight Difference</i>	<i>Weight Difference</i>
	<i>0 hours</i>	<i>24 hours</i>	<i>48 hours</i>	<i>0 / 24 Hours</i>	<i>24 / 48 Hours</i>
				<i>in percent by weight</i>	
L0	250.49	/	/	/	/
L1	250.01	249.54	249.50	0.188	0.016
L2	250.66	250.10	250.06	0.224	0.016
L3	245.65	245.20	245.18	0.184	0.008
L4	253.86	252.56	252.52	0.515	0.016
L5	246.35	245.71	245.69	0.260	0.008
L6	248.47	247.93	247.91	0.218	0.008
L7	250.13	249.24	249.16	0.357	0.032
L8	250.57	249.97	249.95	0.240	0.008
L9	246.71	246.19	246.16	0.211	0.012
L10	250.40	249.57	249.54	0.333	0.012
L11	252.24	251.39	251.36	0.338	0.012
L12	249.96	249.37	249.35	0.237	0.008
L13	259.36	258.10	258.07	0.488	0.012
L14	249.26	248.37	248.35	0.358	0.008
L15	250.09	249.41	249.38	0.273	0.012
L16	246.16	245.52	245.47	0.261	0.020
L17	249.19	248.71	248.67	0.193	0.016
L18	247.93	247.28	247.25	0.263	0.012
F0	296.21	/	/	/	/
F1	286.41	285.34	285.29	0.375	0.018
F2	278.73	278.23	278.18	0.180	0.018
F3	281.58	280.86	280.80	0.256	0.021
F4	280.40	279.45	279.38	0.340	0.025
F5	286.35	285.16	285.12	0.417	0.014
F6	288.81	288.25	288.21	0.194	0.014
F7	284.35	283.80	283.74	0.194	0.021
F8	275.03	273.86	273.80	0.427	0.022
F9	290.21	289.66	289.60	0.190	0.021
F10	286.52	286.05	286.01	0.164	0.014
F11	269.58	268.55	268.50	0.384	0.019
F12	287.96	287.52	287.48	0.153	0.014
F13	284.53	283.99	283.95	0.190	0.014
F14	281.09	279.83	279.77	0.450	0.021
F15	284.27	283.80	283.75	0.166	0.018
F16	288.09	287.15	287.09	0.327	0.021
F17	279.63	279.34	279.30	0.104	0.014
F18	283.90	283.48	283.43	0.148	0.018

Table D.1 *Variation of the sample weight during the initial drying before sample preparation.*

APPENDIX E

CAPILLARY ABSORPTION AND TOTAL IMMERSION RESULTS

Preparation Solution Sample Number	Dimensions (cm)		Surface (cm ²)	Time (hours)												After 24 hours of full immersion	
	Front	Right		0	1/60	1/20	1/12	1/6	0.25	0.5	1	8	24	48	72		
	-Back	-Left		Time (min)													
			0	1	3	5	10	15	30	60	480	1440	2880	4320			
Deionized Water	L1	5.025	4.990	25.075	249.50	251.28	252.33	253.12	254.58	255.61	257.82	260.49	273.54	273.89	274.27	274.51	274.86
	L2	5.000	4.975	24.875	250.06	251.70	252.55	253.16	254.28	255.13	257.13	260.08	274.18	274.50	274.88	275.15	275.51
	L3	4.980	4.935	24.576	245.18	247.30	248.49	249.38	250.97	252.08	254.30	257.35	269.57	269.88	270.27	270.54	270.93
Saturated NaCl	L4	5.090	5.030	25.603	252.52	254.37	255.19	255.66	256.47	257.12	258.66	260.75	273.96	279.14	280.37	280.60	278.63
	L5	5.010	5.050	25.301	245.69	247.39	248.44	249.21	250.56	251.58	253.81	257.24	274.00	274.57	275.43	275.57	274.06
	L6	4.990	5.005	24.975	247.91	249.76	250.75	251.45	252.64	253.60	255.78	258.30	275.46	276.79	277.48	277.61	276.51
4% BDAC	L10	4.030	5.045	20.330	249.54	251.56	252.76	253.67	255.39	256.58	259.27	262.52	274.59	275.02	275.34	275.68	275.79
	L11	5.010	4.970	24.900	251.36	253.12	254.02	254.60	256.09	257.23	259.04	263.81	275.44	275.89	276.11	276.40	276.55
	L12	4.975	4.995	24.850	249.35	251.41	252.20	253.05	254.64	255.77	258.51	262.96	273.13	273.60	273.78	274.07	274.27
Saturated Sodium Chloride	L13	5.045	5.025	25.351	258.07	259.31	259.98	260.43	261.13	261.70	262.96	264.72	279.38	286.47	287.16	287.33	286.23
	L14	4.970	4.980	24.751	248.35	250.03	250.76	251.32	252.41	253.16	254.56	256.27	268.67	276.64	277.72	277.89	276.08
	L15	4.995	4.985	24.900	249.38	250.88	251.69	252.48	253.63	254.47	255.98	257.99	274.99	278.86	279.75	279.90	278.16
	L16	4.990	5.030	25.100	245.47	247.68	248.79	249.47	250.55	251.24	252.54	254.68	272.28	274.13	274.72	274.85	273.72
	L17	4.995	5.015	25.050	248.67	251.16	252.45	253.22	255.01	256.27	258.94	263.19	276.14	276.59	277.09	277.24	276.41
	L18	4.995	4.990	24.925	247.25	249.26	250.24	250.85	252.17	253.04	255.03	257.58	273.76	276.00	276.60	276.74	275.59

Table E.1 Weight (g) over time during capillarity absorption, non-nummulitic samples (L).

Preparation	Solution	Sample	Number	Dimensions (cm)		Surface (cm ²)	Time (hours)										After 24 hours of full immersion		
				Front	Right		0	1/60	1/20	1/12	1/6	0.25	0.5	1	8	24		48	72
				-Back	-Left		0	1	3	5	10	15	30	60	480	1440		2880	4320
Deionized Water	F1	5.190	5.090	26.417	285.29	288.23	289.50	290.24	291.23	291.90	293.39	295.15	300.58	300.90	301.27	301.50	301.66		
	F2	5.060	5.160	26.110	278.18	280.23	281.26	282.02	283.58	284.84	288.00	292.94	296.72	297.02	297.40	297.66	297.90		
	F3	5.055	5.170	26.134	280.80	282.28	282.68	282.94	283.53	284.01	285.30	287.39	297.40	297.64	297.98	298.24	298.82		
Saturated NaCl	F4	5.205	5.035	26.207	279.38	281.51	282.49	283.15	284.38	285.25	286.95	289.47	298.13	298.80	299.42	299.53	298.00		
	F5	5.180	5.120	26.522	285.12	287.58	288.58	289.24	290.54	291.42	293.43	296.65	304.27	304.46	304.72	304.77	304.17		
	F6	5.215	5.155	26.883	288.21	289.48	290.46	291.03	292.30	293.17	294.90	297.37	307.64	308.03	308.40	308.50	307.85		
4% BDAC	F10	5.080	5.050	25.654	286.01	288.65	288.66	290.61	293.82	295.87	300.35	305.87	306.69	306.94	307.27	307.56	307.78		
	F11	5.075	5.130	26.035	268.50	270.65	270.65	272.17	274.03	275.30	278.05	282.09	288.56	288.95	289.35	289.63	290.25		
	F12	5.225	5.215	27.248	287.48	289.54	291.83	293.23	295.96	297.95	302.57	305.41	305.69	306.00	306.37	306.63	307.05		
Saturated Sodium Chloride	F13	5.195	5.185	26.936	283.95	286.53	287.58	288.28	289.74	290.89	293.47	297.10	303.58	304.28	304.80	305.05	303.69		
	F14	5.170	5.160	26.677	279.77	281.33	281.76	282.10	282.88	283.47	284.89	286.82	298.90	299.82	300.44	300.65	299.13		
	F15	5.110	5.090	26.010	283.75	285.65	286.05	286.35	287.15	287.76	287.85	288.62	303.89	305.03	305.85	306.36	303.74		
	F16	5.170	5.125	26.496	287.09	290.30	291.39	292.25	293.57	294.39	296.02	298.25	306.46	307.15	307.92	308.27	306.20		
	F17	5.240	5.160	27.038	279.30	282.73	284.00	285.01	286.95	288.36	291.26	294.74	302.50	303.26	304.02	304.41	302.16		
	F18	5.150	5.155	26.548	283.43	286.82	287.75	288.68	290.49	291.90	294.99	299.54	307.19	308.16	309.10	309.70	306.69		

Table E.2 Weight (g) over time during capillarity absorption, nummulitic samples (F).

Preparation Solution Sample Number	Dimensions (cm)		Surface (cm ²)	Time (hours)														After 24 hour of full immersion	
	Front -Back	Right -Left		Time (min)															
				0	1/60	1/20	1/12	1/6	0.25	0.5	1	2	3	5	8	24	48		
0	1	3	5	10	15	30	60	120	180	300	480	1440	2880						
4% BDAC	L16	4.990	5.030	25.100	268.66	269.49	269.81	269.97	270.35	270.65	271.49	272.59	273.64	273.9	273.98	273.88	273.76	273.72	272.41
	L17	4.995	5.015	25.050	271.51	272.58	273.18	273.6	274.35	274.9	275.65	276.28	276.56	276.62	276.61	276.55	276.45	276.43	275.07
	L18	4.995	4.990	24.925	271.03	271.72	272.01	272.15	272.56	272.83	273.43	274.31	275.31	275.59	275.67	275.62	275.6	275.54	274.20
	F16	5.170	5.125	26.496	302.49	303.73	304.22	304.44	304.84	305.21	305.72	306.18	306.52	306.59	306.61	306.57	306.55	306.63	306.14
	F17	5.240	5.160	27.038	298.12	299.26	299.8	300.11	300.65	301.08	301.78	302.31	302.52	302.55	302.61	302.58	302.58	302.63	301.71
	F18	5.150	5.155	26.548	302.19	303.19	303.62	304.01	304.81	305.39	306.34	306.81	307.04	307.05	307.12	307.05	307.08	307.1	306.25

Table E.3 Weight (g) over time during capillarity absorption, second impregnation of samples 16, 17, and 18.

Preparation Solution Sample Number	Dimensions (cm)		Surface (cm ²)	Time (min)												After 24 hours of full immersion	
	Front	Right		0	1	3	5	10	15	30	60	480	1440	2880	4320		
	-Back	-Left		Square root of time (min ^{-1/2})													
			0.00	1.00	1.73	2.24	3.16	3.87	5.48	7.75	21.91	37.95	53.67	65.73			
Deionized Water	L1	5.025	4.990	25.075	0.0710	0.1129	0.1444	0.2026	0.2437	0.3318	0.4383	0.9587	0.9727	0.9878	0.9974	1.0114	0.0710
	L2	5.000	4.975	24.875	0.0653	0.0992	0.1235	0.1681	0.2020	0.2817	0.3992	0.9610	0.9737	0.9888	0.9996	1.0139	0.0653
	L3	4.980	4.935	24.576	0.0849	0.1325	0.1682	0.2318	0.2763	0.3652	0.4873	0.9766	0.9890	1.0046	1.0154	1.0310	0.0849
Saturated NaCl	L4	5.090	5.030	25.603	0.0907	0.1309	0.1539	0.1937	0.2255	0.3010	0.4035	1.0512	1.3051	1.3654	1.3767	1.2801	0.0907
	L5	5.010	5.050	25.301	0.0673	0.1089	0.1394	0.1929	0.2333	0.3216	0.4574	1.1212	1.1437	1.1778	1.1833	1.1235	0.0673
	L6	4.990	5.005	24.975	0.0739	0.1134	0.1413	0.1888	0.2271	0.3142	0.4148	1.0998	1.1529	1.1804	1.1856	1.1417	0.0739
4% BDAC	L10	4.030	5.045	20.330	0.0794	0.1265	0.1623	0.2298	0.2766	0.3823	0.5100	0.9842	1.0011	1.0137	1.0270	1.0314	0.0794
	L11	5.010	4.970	24.900	0.0695	0.1050	0.1279	0.1868	0.2318	0.3032	0.4916	0.9508	0.9686	0.9773	0.9887	0.9946	0.0695
	L12	4.975	4.995	24.850	0.0817	0.1131	0.1468	0.2099	0.2548	0.3635	0.5401	0.9436	0.9623	0.9694	0.9809	0.9889	0.0817
Saturated Sodium Chloride	L13	5.045	5.025	25.351	0.0485	0.0747	0.0924	0.1198	0.1421	0.1914	0.2602	0.8340	1.1114	1.1384	1.1451	1.1020	0.0485
	L14	4.970	4.980	24.751	0.0673	0.0966	0.1190	0.1627	0.1928	0.2489	0.3174	0.8144	1.1339	1.1772	1.1840	1.1114	0.0673
	L15	4.995	4.985	24.900	0.0595	0.0917	0.1230	0.1686	0.2020	0.2619	0.3417	1.0163	1.1698	1.2051	1.2111	1.1420	0.0595
	L16	4.990	5.030	25.100	0.1100	0.1653	0.1991	0.2529	0.2872	0.3519	0.4584	1.3345	1.4266	1.4560	1.4625	1.4062	0.1100
	L17	4.995	5.015	25.050	0.0992	0.1506	0.1813	0.2526	0.3028	0.4092	0.5785	1.0944	1.1123	1.1323	1.1382	1.1052	0.0992
	L18	4.995	4.990	24.925	0.0803	0.1195	0.1439	0.1966	0.2314	0.3109	0.4128	1.0594	1.1489	1.1728	1.1784	1.1325	0.0803

Table E.4 Capillarity Water Absorption (g.cm⁻²), non-nummulitic samples (L).

Preparation Solution Sample Number	Dimensions (cm)		Surface (cm ²)	Time (min)												After 24 hours of full immersion	
	Front	Right		0	1	3	5	10	15	30	60	480	1440	2880	4320		
	-Back	-Left		Square root of time (min ^{-1/2})													
			0.00	1.00	1.73	2.24	3.16	3.87	5.48	7.75	21.91	37.95	53.67	65.73			
Deionized Water	F1	5.190	5.090	26.417	0.1091	0.1563	0.1838	0.2205	0.2454	0.3007	0.3661	0.5676	0.5795	0.5933	0.6018	0.6077	0.1091
	F2	5.060	5.160	26.110	0.0774	0.1164	0.1451	0.2040	0.2516	0.3710	0.5576	0.7004	0.7117	0.7261	0.7359	0.7450	0.0774
	F3	5.055	5.170	26.134	0.0563	0.0715	0.0814	0.1038	0.1221	0.1712	0.2507	0.6314	0.6406	0.6535	0.6634	0.6854	0.0563
Saturated NaCl	F4	5.205	5.035	26.207	0.0806	0.1177	0.1427	0.1893	0.2222	0.2866	0.3819	0.7098	0.7351	0.7586	0.7628	0.7048	0.0806
	F5	5.180	5.120	26.522	0.0928	0.1305	0.1553	0.2044	0.2375	0.3133	0.4347	0.7220	0.7292	0.7390	0.7409	0.7183	0.0928
	F6	5.215	5.155	26.883	0.0477	0.0846	0.1060	0.1538	0.1865	0.2515	0.3444	0.7305	0.7451	0.7590	0.7628	0.7384	0.0477
4% BDAC	F10	5.080	5.050	25.654	0.1002	0.1006	0.1746	0.2965	0.3743	0.5444	0.7539	0.7850	0.7945	0.8071	0.8181	0.8264	0.1002
	F11	5.075	5.130	26.035	0.0821	0.0821	0.1401	0.2112	0.2597	0.3647	0.5189	0.7660	0.7809	0.7961	0.8068	0.8305	0.0821
	F12	5.225	5.215	27.248	0.0763	0.1612	0.2131	0.3142	0.3880	0.5591	0.6644	0.6748	0.6862	0.7000	0.7096	0.7252	0.0763
Saturated Sodium Chloride	F13	5.195	5.185	26.936	0.0956	0.1345	0.1604	0.2145	0.2572	0.3527	0.4873	0.7274	0.7533	0.7726	0.7818	0.7314	0.0956
	F14	5.170	5.160	26.677	0.0579	0.0738	0.0864	0.1154	0.1372	0.1899	0.2615	0.7096	0.7437	0.7667	0.7745	0.7181	0.0579
	F15	5.110	5.090	26.010	0.0718	0.0869	0.0982	0.1284	0.1515	0.1549	0.1840	0.7608	0.8039	0.8349	0.8541	0.7552	0.0718
	F16	5.170	5.125	26.496	0.1186	0.1589	0.1907	0.2394	0.2697	0.3300	0.4124	0.7157	0.7412	0.7697	0.7826	0.7061	0.1186
	F17	5.240	5.160	27.038	0.1276	0.1748	0.2124	0.2846	0.3370	0.4449	0.5743	0.8630	0.8912	0.9195	0.9340	0.8503	0.1276
	F18	5.150	5.155	26.548	0.1271	0.1619	0.1968	0.2646	0.3175	0.4333	0.6039	0.8906	0.9270	0.9622	0.9847	0.8719	0.1271

Table E.5 Capillarity Water Absorption (g.cm⁻²), nummulitic samples (F).

Preparation Solution Sample Number	Dimensions (cm)		Surface (cm ²)	Time (min)													After 24 hour of full immersion		
	Front -Back	Right -Left		Square root of time (min ^{-1/2})															
				0	1	3	5	10	15	30	60	120	180	300	480	1440		2880	
4% BDAC	L16	4.990	5.030	25.100	0.0413	0.0572	0.0652	0.0841	0.0991	0.1409	0.1956	0.2479	0.2608	0.2648	0.2598	0.2539	0.2519	0.1867	0.0413
	L17	4.995	5.015	25.050	0.0426	0.0665	0.0833	0.1131	0.1351	0.1649	0.1900	0.2012	0.2036	0.2032	0.2008	0.1968	0.1960	0.1418	0.0426
	L18	4.995	4.990	24.925	0.0276	0.0392	0.0448	0.0611	0.0719	0.0959	0.1311	0.1710	0.1822	0.1854	0.1834	0.1826	0.1802	0.1267	0.0276
	F16	5.170	5.125	26.496	0.0458	0.0639	0.0721	0.0868	0.1005	0.1193	0.1363	0.1489	0.1515	0.1522	0.1508	0.1500	0.1530	0.1349	0.0458
	F17	5.240	5.160	27.038	0.0424	0.0625	0.0740	0.0941	0.1101	0.1361	0.1559	0.1637	0.1648	0.1670	0.1659	0.1659	0.1678	0.1335	0.0424
	F18	5.150	5.155	26.548	0.0375	0.0536	0.0682	0.0982	0.1200	0.1556	0.1732	0.1818	0.1822	0.1848	0.1822	0.1833	0.1841	0.1522	0.0375

Table E.6 Capillarity Water Absorption (g.cm⁻²), second impregnation of samples 16, 17, and 18.

Preparation solution	Sample Type	Time (min)											After 24 hours of full immersion
		1	3	5	10	15	30	60	480	1440	2280	4320	
		<i>Square root of time (min^{-1/2})</i>											
		1.00	1.73	2.24	3.16	3.87	5.48	7.75	21.91	37.95	53.67	65.73	
Deionized Water	L	0.0737	0.1149	0.1453	0.2009	0.2406	0.3262	0.4416	0.9654	0.9785	0.9938	1.0041	1.0188
	F	0.0810	0.1147	0.1367	0.1761	0.2064	0.2810	0.3914	0.6332	0.6439	0.6576	0.6670	0.6794
Saturated Sodium Chloride	L	0.0774	0.1168	0.1437	0.1921	0.2271	0.3012	0.4050	1.0472	1.1894	1.2228	1.2294	1.1716
	F	0.0911	0.1248	0.1499	0.1994	0.2351	0.3063	0.4094	0.7588	0.7855	0.8091	0.8198	0.7549
4% BDAC	L	0.0769	0.1149	0.1457	0.2088	0.2544	0.3497	0.5139	0.9595	0.9773	0.9868	0.9989	1.0050
	F	0.0862	0.1146	0.1759	0.2740	0.3406	0.4894	0.6457	0.7419	0.7539	0.7677	0.7782	0.7940

Preparation solution	Sample Type	Time (min)											After 24 hours of full immersion	
		1	3	5	10	15	30	60	120	180	300	480		1440
		<i>Square root of time (min^{-1/2})</i>												
		1.00	1.73	2.24	3.16	3.87	5.48	7.75	10.95	13.42	17.32	21.91	37.95	53.67
4% BDAC	L	0.0372	0.0543	0.0644	0.0861	0.1020	0.1339	0.1722	0.2067	0.2155	0.2178	0.2147	0.2111	0.2094
	F	0.0419	0.0600	0.0714	0.0931	0.1102	0.1370	0.1551	0.1648	0.1662	0.1680	0.1664	0.1683	0.1402

Table E.7 Average values of the Capillarity Absorption ($\text{g}\cdot\text{cm}^{-2}$) per stone and impregnation solution type. (a) Above, first impregnation, (b) below, second impregnation of samples 16, 17 and 18 only.

<i>Preparation solution</i>	<i>Sample Number</i>	<i>Capillary Absorption Coefficient (g.cm⁻².s^{-1/2})</i>	<i>Linear Regression Coefficient R²</i>	<i>Last of the linear regression (min.)</i>
Deionized Water	L1	0.0550	0.9966	60
	L2	0.0495	0.9996	60
	L3	0.0597	0.9966	60
Saturated Sodium Chloride	L4	0.0459	0.9995	60
	L5	0.0569	0.9998	30
	L6	0.0510	0.9984	60
4 % BDAC	L10	0.0646	0.9977	60
	L11	0.0614	0.9886	60
	L12	0.0686	0.9963	60
Saturated Sodium Chloride	L13	0.0376	0.9966	480
	L14	0.0353	0.9986	480
	L15	0.0454	0.9986	480
	L16	0.0500	0.9888	60
	L17	0.0698	0.9994	30
	L18	0.0495	0.9985	60
Deionized Water	F1	0.0369	0.9804	60
	F2	0.0657	0.9957	30
	F3	0.0288	0.9893	60
Saturated Sodium Chloride	F4	0.0444	0.9975	60
	F5	0.0503	0.9996	60
	F6	0.0439	0.9978	60
4 % BDAC	F10	0.1035	0.9896	60
	F11	0.0680	0.9915	60
	F12	0.0899	0.9758	60
Saturated Sodium Chloride	F13	0.0584	0.9996	60
	F14	0.0308	0.9977	60
	F15	0.0282	0.9892	15
	F16	0.0431	0.9880	60
	F17	0.0673	0.9965	60
	F18	0.0719	0.9983	60
BDAC Second Impregnation	L16	0.0215	0.9950	120
	L17	0.0279	0.9838	30
	L18	0.0146	0.9980	120
	F16	0.0184	0.9923	15
	F17	0.0209	0.9906	30
	F18	0.0273	0.9943	30

Table E.8 Capillary absorption coefficient per stone and impregnation solution type.

APPENDIX F

DRYING RESULTS

<i>Preparation Solution Sample Number</i>	<i>Time (hours)</i>	<i>After immersion</i>	<i>0.25</i>	<i>0.5</i>	<i>1</i>	<i>2</i>	<i>3</i>	<i>4</i>	<i>5</i>	<i>6</i>	<i>9</i>	<i>12</i>
	<i>Time (min.)</i>	<i>0</i>	<i>15</i>	<i>30</i>	<i>60</i>	<i>120</i>	<i>180</i>	<i>240</i>	<i>300</i>	<i>360</i>	<i>540</i>	<i>720</i>
	<i>RH (%)</i>	<i>37</i>	<i>40</i>	<i>39</i>	<i>37</i>	<i>36.5</i>	<i>36</i>	<i>36</i>	<i>36</i>	<i>35</i>	<i>35</i>	<i>34</i>
	<i>Temp. (°C)</i>	<i>19</i>	<i>20</i>	<i>20</i>	<i>20.5</i>	<i>20.5</i>	<i>20.5</i>	<i>20.5</i>	<i>21</i>	<i>21</i>	<i>21</i>	<i>21</i>
<i>Water</i>	<i>L1</i>	274.86	274.94	274.56	273.80	272.37	270.87	269.37	267.81	266.25	261.54	257.38
	<i>L2</i>	275.51	275.72	275.31	274.58	273.17	271.74	270.28	268.80	267.31	262.74	258.62
	<i>L3</i>	270.93	271.22	270.75	270.04	268.63	267.19	265.72	264.25	262.73	258.07	253.76
<i>Saturated NaCl</i>	<i>L4</i>	278.63	278.94	278.57	278.26	277.79	277.58	277.41	277.26	277.13	276.75	276.42
	<i>L5</i>	274.06	274.09	273.88	273.45	272.91	272.68	272.48	272.28	272.10	271.61	271.17
	<i>L6</i>	276.51	276.73	276.45	275.95	275.51	275.29	275.10	274.93	274.78	274.37	274.02
<i>Brushed BDAC</i>	<i>L7</i>	Samples were impregnated by brushing the surfactant onto them, so drying rate could not be measured										
	<i>L8</i>											
	<i>L9</i>											
<i>BDAC</i>	<i>L10</i>	275.79	275.96	275.47	274.70	273.19	271.74	270.27	268.78	267.38	263.58	260.90
	<i>L11</i>	276.55	276.72	276.29	275.51	274.05	272.69	271.26	269.82	268.46	264.75	262.08
	<i>L12</i>	274.27	274.50	274.11	273.32	271.88	270.37	268.92	267.46	266.08	262.39	259.83
<i>Saturated Sodium Chloride</i>	<i>L13</i>	286.23	286.23	285.90	285.46	285.06	284.85	284.66	284.49	284.34	283.92	283.55
	<i>L14</i>	276.08	276.20	275.86	275.39	274.97	274.77	274.58	274.42	274.27	273.87	273.52
	<i>L15</i>	278.16	278.17	277.90	277.44	277.02	276.78	276.54	276.32	276.13	275.62	275.13
	<i>L16</i>	273.72	273.82	273.51	273.01	272.60	272.34	272.08	271.87	271.68	271.16	270.75
	<i>L17</i>	276.41	276.41	276.05	275.54	275.14	274.91	274.69	274.50	274.35	273.92	273.55
	<i>L18</i>	275.59	275.57	275.26	274.80	274.46	274.27	274.06	273.88	273.75	273.34	273.04

Table F.1a Weight over time during drying, non-nummulitic samples (L). Part I.

<i>Preparation Solution Sample Number</i>	<i>Time (hours)</i>	15.25	24	36	48	60	72	96	<i>Oven Drying 60°C</i>			
	<i>Time (min.)</i>	915	1440	2160	2880	3600	4320	5760				
	<i>RH (%)</i>	34	34	36	35	34	33	31	<i>24 H</i>	<i>48 H</i>	<i>72H</i>	<i>96H</i>
	<i>Temp. (°C)</i>	21	21	20	21	21	20	20				
<i>Water</i>	<i>L1</i>	254.48	251.44	250.10	249.64	249.46	249.4	249.34	249.16	249.15	249.11	249.17
	<i>L2</i>	255.44	252.03	250.64	250.16	249.99	249.94	249.88	249.71	249.71	249.67	249.72
	<i>L3</i>	250.36	246.95	245.69	245.25	245.08	245.03	244.98	244.82	244.83	244.78	244.84
<i>Saturated NaCl</i>	<i>L4</i>	276.09	275.66	275.39	275.19	275.02	274.88	274.58	273.36	272.33	271.74	271.01
	<i>L5</i>	270.74	270.06	269.60	269.40	269.23	269.08	268.77	267.41	266.24	265.49	264.53
	<i>L6</i>	273.71	273.16	272.77	272.58	272.41	272.28	271.99	270.81	269.82	269.20	268.43
<i>Brushed BDAC</i>	<i>L7</i>							251.12	249.97	249.97	249.92	249.96
	<i>L8</i>	Weight of the samples after BDAC brushing ►						252.14	250.82	250.81	250.77	250.80
	<i>L9</i>							248.24	247.01	247.03	246.98	247.02
<i>BDAC</i>	<i>L10</i>	259.05	256.38	254.52	253.44	252.76	252.31	251.71	250.50	250.32	250.31	250.33
	<i>L11</i>	260.23	257.57	255.76	254.73	254.09	253.68	253.13	252.04	252.05	252.04	252.04
	<i>L12</i>	258.02	255.40	253.62	252.63	252.03	251.65	251.15	250.27	250.13	250.12	250.14
<i>Saturated Sodium Chloride</i>	<i>L13</i>	283.20	282.78	282.49	282.30	282.13	281.99	281.68	280.57	279.62	279.04	278.29
	<i>L14</i>	273.22	272.72	272.41	272.19	271.99	271.82	271.45	270.15	268.99	268.26	267.31
	<i>L15</i>	274.68	274.06	273.67	273.47	273.28	273.12	272.79	271.62	270.64	270.02	269.23
	<i>L16</i>	270.38	269.81	269.43	269.26	269.10	268.97	268.70	Samples were not oven-dried before their second impregnation. The 96 H values (dry sample weight) were extrapolated from the average loss of water during oven drying of the other NaCl impregnated samples ►			265.02
	<i>L17</i>	273.24	272.80	272.47	272.26	272.07	271.90	271.36				267.64
	<i>L18</i>	272.79	272.36	272.05	271.82	271.62	271.45	271.08				267.37

Table F.1b Weight over time during drying, non-nummulitic samples (L). Part II.

<i>Preparation Solution Sample Number</i>	<i>Time (hours)</i>	<i>After immersion</i>	<i>0.25</i>	<i>0.5</i>	<i>1</i>	<i>2</i>	<i>3</i>	<i>4</i>	<i>5</i>	<i>6</i>	<i>9</i>	<i>12</i>
	<i>Time (min.)</i>	<i>0</i>	<i>15</i>	<i>30</i>	<i>60</i>	<i>120</i>	<i>180</i>	<i>240</i>	<i>300</i>	<i>360</i>	<i>540</i>	<i>720</i>
	<i>RH (%)</i>	<i>37</i>	<i>40</i>	<i>39</i>	<i>37</i>	<i>36.5</i>	<i>36</i>	<i>36</i>	<i>36</i>	<i>35</i>	<i>35</i>	<i>34</i>
	<i>Temp. (°C)</i>	<i>19</i>	<i>20</i>	<i>20</i>	<i>20.5</i>	<i>20.5</i>	<i>20.5</i>	<i>20.5</i>	<i>21</i>	<i>21</i>	<i>21</i>	<i>21</i>
<i>Water</i>	<i>F1</i>	301.66	302.22	301.57	300.78	299.21	297.61	296.01	294.46	292.93	289.62	288.10
	<i>F2</i>	297.90	298.07	297.70	296.91	295.41	293.90	292.38	290.82	289.26	284.83	282.02
	<i>F3</i>	298.82	299.08	298.68	297.90	296.42	294.92	293.42	291.91	290.37	286.54	284.39
<i>Saturated NaCl</i>	<i>F4</i>	298.00	298.18	297.84	297.32	296.79	296.55	296.35	296.17	296.04	295.68	295.44
	<i>F5</i>	304.17	304.28	303.91	303.45	302.93	302.74	302.62	302.53	302.45	302.25	302.09
	<i>F6</i>	307.85	307.79	307.46	306.97	306.35	306.09	305.90	305.73	305.59	305.19	304.88
<i>Brushed BDAC</i>	<i>F7</i>	Samples were impregnated by brushing the surfactant onto them, so drying rate could not be measured										
	<i>F8</i>											
	<i>F9</i>											
<i>BDAC</i>	<i>F10</i>	307.78	308.06	307.65	306.83	305.37	303.84	302.41	301.03	299.74	296.45	294.38
	<i>F11</i>	290.25	290.38	289.87	289.11	287.68	286.16	284.75	283.37	282.08	278.78	276.64
	<i>F12</i>	307.05	307.26	306.75	305.98	304.52	303.03	301.61	300.23	298.96	295.90	294.20
<i>Saturated Sodium Chloride</i>	<i>F13</i>	303.69	303.38	303.27	302.71	302.12	301.81	301.60	301.40	301.23	300.76	300.40
	<i>F14</i>	299.13	298.83	298.54	298.01	297.35	297.04	296.85	296.68	296.55	296.23	296.05
	<i>F15</i>	303.74	303.77	303.53	303.00	302.35	302.08	301.88	301.69	301.57	301.16	300.90
	<i>F16</i>	306.20	306.72	306.27	305.76	305.19	304.96	304.81	304.65	304.54	304.23	303.98
	<i>F17</i>	302.16	302.74	302.37	301.83	301.23	300.98	300.80	300.64	300.53	300.21	299.96
	<i>F18</i>	306.69	307.43	306.92	306.39	305.74	305.48	305.3	305.12	304.98	304.57	304.28

Table F.2a Weight over time during drying, nummulitic samples (F). Part I.

<i>Preparation Solution Sample Number</i>	<i>Time (hours)</i>	15.25	24	36	48	60	72	96	<i>Oven Drying 60°C</i>			
	<i>Time (min.)</i>	915	1440	2160	2880	3600	4320	5760				
	<i>RH (%)</i>	34	34	36	35	34	33	31	<i>24 H</i>	<i>48 H</i>	<i>72H</i>	<i>96H</i>
	<i>Temp. (°C)</i>	21	21	20	21	21	20	20				
<i>Water</i>	<i>F1</i>	287.21	286.02	285.38	285.08	284.89	284.80	284.70	284.55	284.55	284.52	284.54
	<i>F2</i>	280.58	279.02	278.27	277.96	277.81	277.75	277.69	277.58	277.59	277.56	277.59
	<i>F3</i>	283.19	281.80	281.11	280.80	280.64	280.56	280.47	280.31	280.32	280.30	280.31
<i>Saturated NaCl</i>	<i>F4</i>	295.27	294.95	294.63	294.45	294.28	294.15	293.87	292.65	291.82	291.30	290.66
	<i>F5</i>	301.95	301.68	301.44	301.24	301.06	300.92	300.61	299.27	298.20	297.51	296.68
	<i>F6</i>	304.62	304.23	303.85	303.64	303.46	303.32	303.00	301.66	300.67	300.08	299.36
<i>Brushed BDAC</i>	<i>F7</i>							287.21	284.62	284.57	284.55	284.56
	<i>F8</i>	Weight of the samples after BDAC brushing ►						277.43	274.81	274.75	274.74	274.74
	<i>F9</i>							292.75	290.49	290.37	290.36	290.36
<i>BDAC</i>	<i>F10</i>	293.01	291.04	289.61	288.76	288.21	287.86	287.33	286.45	286.43	286.42	286.43
	<i>F11</i>	275.14	272.89	271.35	270.51	269.98	269.63	269.11	268.73	268.72	268.71	268.72
	<i>F12</i>	293.10	291.56	290.43	289.76	289.33	289.04	288.60	287.83	287.81	287.80	287.80
<i>Saturated Sodium Chloride</i>	<i>F13</i>	300.11	299.67	299.30	299.10	298.91	298.77	298.44	297.09	296.04	295.38	294.64
	<i>F14</i>	295.89	295.66	295.45	295.29	295.14	295.03	294.80	293.83	293.13	292.68	292.17
	<i>F15</i>	300.68	300.32	300.01	299.83	299.67	299.53	299.23	298.05	297.18	296.66	296.03
	<i>F16</i>	303.79	303.44	303.19	303.02	302.88	302.78	302.52	Samples were not oven-dried before their second impregnation. The 96 H values (dry sample weight) were extrapolated from the average loss of water during oven drying of the other NaCl impregnated samples ►			299.07
	<i>F17</i>	299.76	299.42	299.10	298.88	298.68	298.52	298.15				294.75
	<i>F18</i>	304.03	303.59	303.17	302.93	302.73	302.56	302.21				298.77

Table F.2b Weight over time during drying, nummulitic samples (L). Part II.

<i>Preparation Solution Sample Number</i>	<i>Time (hours)</i>	<i>After immersion</i>	<i>0.25</i>	<i>0.5</i>	<i>1</i>	<i>2</i>	<i>3</i>	<i>4</i>	<i>6.45</i>	<i>7.45</i>	<i>8.2</i>	<i>9.1</i>
	<i>Time (min.)</i>	<i>0</i>	<i>15</i>	<i>30</i>	<i>60</i>	<i>120</i>	<i>180</i>	<i>240</i>	<i>387</i>	<i>447</i>	<i>492</i>	<i>547</i>
	<i>RH (%)</i>	32	32	32	32	32	32	32	32	33	33	34
	<i>Temp. (°C)</i>	20	20	20	20	20	20	20	20	20	21	20
<i>Saturated NaCl</i>	<i>L16</i>	272.41	271.91	271.45	270.64	269.12	267.72	266.53	264.42	263.83	263.46	263.04
	<i>L17</i>	275.07	274.60	274.14	273.35	271.85	270.48	269.27	267.15	266.55	266.16	265.74
	<i>L18</i>	274.20	273.71	273.24	272.41	270.86	269.46	268.25	266.15	265.57	265.19	264.77
	<i>F16</i>	306.14	305.60	305.15	304.36	302.97	301.86	301.04	299.66	299.26	298.98	298.72
	<i>F17</i>	301.71	301.24	300.78	300.00	298.56	297.32	296.31	294.61	294.11	293.78	293.45
	<i>F18</i>	306.25	305.75	305.27	304.43	302.93	301.68	300.69	298.99	298.50	298.17	297.85

<i>Preparation Solution Sample Number</i>	<i>Time (hours)</i>	<i>10</i>	<i>12.9</i>	<i>22.9</i>	<i>24</i>	<i>35.45</i>	<i>47</i>	<i>59.2</i>	<i>72</i>	<i>Oven Drying 60°C</i>			
	<i>Time (min.)</i>	<i>600</i>	<i>772</i>	<i>1339</i>	<i>1440</i>	<i>2127</i>	<i>2820</i>	<i>3552</i>	<i>4320</i>				
	<i>RH (%)</i>	<i>34</i>	<i>34</i>	<i>38</i>	<i>38</i>	<i>44</i>	<i>44</i>	<i>51</i>	<i>44</i>	<i>24 H</i>	<i>48 H</i>	<i>72H</i>	<i>96H</i>
	<i>Temp. (°C)</i>	<i>20</i>	<i>21</i>	<i>21</i>	<i>21</i>	<i>21</i>	<i>21</i>	<i>21</i>	<i>21</i>				
<i>Saturated NaCl</i>	<i>L16</i>	262.66	261.75	260.11	259.90	258.85	258.18	257.58	257.09	253.85	251.74	250.3	249.60
	<i>L17</i>	265.36	264.39	262.74	262.53	261.47	260.80	260.22	259.75	256.95	255.22	254.01	253.22
	<i>L18</i>	264.40	263.52	261.88	261.68	260.61	259.92	259.30	258.81	255.60	253.63	252.45	251.76
	<i>F16</i>	298.49	297.89	296.85	296.71	296.06	295.64	295.26	294.95	292.64	291.11	290.17	289.55
	<i>F17</i>	293.14	292.35	291.01	290.84	290.01	289.44	288.92	288.52	285.87	284.20	283.11	282.44
	<i>F18</i>	297.55	296.81	295.52	295.34	294.53	293.95	293.44	293.03	290.1	288.34	287.18	286.51

Table F.3 Weight over time during drying, after second impregnation for samples 16, 17, and 18.

<i>Preparation Solution Sample Number</i>	<i>Time (hours)</i>	<i>After immersion</i>																		
	<i>Time (min.)</i>	0.25	0.5	1	2	3	4	5	6	9	12	15.25	24	36	48	60	72	96		
<i>Water</i>	<i>L1</i>	10.31	10.34	10.19	9.88	9.31	8.71	8.11	7.48	6.85	4.96	10.31	3.29	2.13	0.91	0.37	0.19	0.12	0.09	
	<i>L2</i>	10.33	10.41	10.25	9.96	9.39	8.82	8.23	7.64	7.04	5.21	10.33	3.56	2.29	0.93	0.37	0.18	0.11	0.09	
	<i>L3</i>	10.66	10.77	10.58	10.29	9.72	9.13	8.53	7.93	7.31	5.40	10.66	3.64	2.25	0.86	0.35	0.17	0.10	0.08	
<i>Saturated NaCl</i>	<i>L4</i>	2.81	2.93	2.79	2.68	2.50	2.42	2.36	2.31	2.26	2.12	2.00	1.87	1.72	1.62	1.54	1.48	1.43	1.32	
	<i>L5</i>	3.60	3.61	3.53	3.37	3.17	3.08	3.01	2.93	2.86	2.68	2.51	2.35	2.09	1.92	1.84	1.78	1.72	1.60	
	<i>L6</i>	3.01	3.09	2.99	2.80	2.64	2.56	2.48	2.42	2.37	2.21	2.08	1.97	1.76	1.62	1.55	1.48	1.43	1.33	
<i>BDAC</i>	<i>L10</i>	10.17	10.24	10.04	9.74	9.13	8.55	7.97	7.37	6.81	5.29	10.17	4.22	3.48	2.42	1.67	1.24	0.97	0.79	
	<i>L11</i>	9.72	9.79	9.62	9.31	8.73	8.19	7.63	7.05	6.51	5.04	9.72	3.98	3.25	2.19	1.48	1.07	0.81	0.65	
	<i>L12</i>	9.65	9.74	9.58	9.27	8.69	8.09	7.51	6.92	6.37	4.90	9.65	3.87	3.15	2.10	1.39	1.00	0.76	0.60	
<i>Saturated Sodium Chloride</i>	<i>L13</i>	2.85	2.85	2.73	2.58	2.43	2.36	2.29	2.23	2.17	2.02	1.89	1.76	1.61	1.51	1.44	1.38	1.33	1.22	
	<i>L14</i>	3.28	3.33	3.20	3.02	2.87	2.79	2.72	2.66	2.60	2.45	2.32	2.21	2.02	1.91	1.83	1.75	1.69	1.55	
	<i>L15</i>	3.32	3.32	3.22	3.05	2.89	2.80	2.72	2.63	2.56	2.37	2.19	2.02	1.79	1.65	1.57	1.50	1.44	1.32	
	<i>L16</i>	3.28	3.32	3.20	3.02	2.86	2.76	2.66	2.59	2.51	2.32	2.16	2.02	1.81	1.66	1.60	1.54	1.49	1.39	
	<i>L17</i>	3.28	3.28	3.14	2.95	2.80	2.72	2.63	2.56	2.51	2.35	2.21	2.09	1.93	1.80	1.73	1.65	1.59	1.39	
	<i>L18</i>	3.08	3.07	2.95	2.78	2.65	2.58	2.50	2.44	2.39	2.23	2.12	2.03	1.87	1.75	1.67	1.59	1.53	1.39	

Table F.4 Residual Water Content over time during drying, non-nummulitic samples (L).

Preparation Solution Sample Number	Time (hours)	After immersion	0.25	0.5	1	2	3	4	5	6	9	12	15.25	24	36	48	60	72	96
	Time (min.)	0	15	30	60	120	180	240	300	360	540	720	915	1440	2160	2880	3600	4320	5760
Water	F1	6.02	6.21	5.99	5.71	5.16	4.59	4.03	3.49	2.95	1.79	1.25	0.94	0.52	0.30	0.19	0.12	0.09	0.06
	F2	7.32	7.38	7.24	6.96	6.42	5.88	5.33	4.77	4.20	2.61	1.60	1.08	0.52	0.24	0.13	0.08	0.06	0.04
	F3	6.60	6.70	6.55	6.28	5.75	5.21	4.68	4.14	3.59	2.22	1.46	1.03	0.53	0.29	0.17	0.12	0.09	0.06
Saturated NaCl	F4	2.53	2.59	2.47	2.29	2.11	2.03	1.96	1.90	1.85	1.73	1.64	1.59	1.48	1.37	1.30	1.25	1.20	1.10
	F5	2.52	2.56	2.44	2.28	2.11	2.04	2.00	1.97	1.94	1.88	1.82	1.78	1.69	1.60	1.54	1.48	1.43	1.32
	F6	2.84	2.82	2.71	2.54	2.33	2.25	2.18	2.13	2.08	1.95	1.84	1.76	1.63	1.50	1.43	1.37	1.32	1.22
BDAC	F10	7.45	7.55	7.41	7.12	6.61	6.08	5.58	5.10	4.65	3.50	2.78	2.30	1.61	1.11	0.81	0.62	0.50	0.31
	F11	8.01	8.06	7.87	7.59	7.06	6.49	5.97	5.45	4.97	3.74	2.95	2.39	1.55	0.98	0.67	0.47	0.34	0.15
	F12	6.69	6.76	6.58	6.32	5.81	5.29	4.80	4.32	3.88	2.81	2.22	1.84	1.31	0.91	0.68	0.53	0.43	0.28
Saturated Sodium Chloride	F13	3.07	2.97	2.93	2.74	2.54	2.43	2.36	2.29	2.24	2.08	1.95	1.86	1.71	1.58	1.51	1.45	1.40	1.29
	F14	2.38	2.28	2.18	2.00	1.77	1.67	1.60	1.54	1.50	1.39	1.33	1.27	1.19	1.12	1.07	1.02	0.98	0.90
	F15	2.60	2.61	2.53	2.35	2.13	2.04	1.98	1.91	1.87	1.73	1.65	1.57	1.45	1.34	1.28	1.23	1.18	1.08
	F16	2.38	2.56	2.41	2.24	2.05	1.97	1.92	1.86	1.83	1.72	1.64	1.58	1.46	1.38	1.32	1.27	1.24	1.15
	F17	2.51	2.71	2.58	2.40	2.20	2.11	2.05	2.00	1.96	1.85	1.77	1.70	1.58	1.47	1.40	1.33	1.28	1.15
	F18	2.65	2.90	2.73	2.55	2.33	2.25	2.19	2.13	2.08	1.94	1.85	1.76	1.61	1.47	1.39	1.33	1.27	1.15

Table F.5 Residual Water Content over time during drying, nummulitic samples (F).

<i>Preparation Solution Sample Number</i>	<i>Time (hours)</i>	<i>After immer- sion</i>	0.25	0.5	1	2	3	4	6.45	7.45	8.2	9.1	10	12.9	22.9	24	35.45	47	59.2	72	
	<i>Time (min.)</i>		0	15	30	60	120	180	240	387	447	492	547	600	772	1339	1440	2127	2820	3552	4320
<i>Saturated Sodium Chloride</i>	<i>L16</i>	<i>Residual Water Content (%)</i>	9.14	8.94	8.75	8.43	7.82	7.26	6.78	5.94	5.70	5.55	5.38	5.23	4.87	4.21	4.13	3.71	3.44	3.20	3.00
	<i>L17</i>		8.63	8.44	8.26	7.95	7.36	6.82	6.34	5.50	5.26	5.11	4.94	4.79	4.41	3.76	3.68	3.26	2.99	2.76	2.58
	<i>L18</i>		8.91	8.72	8.53	8.20	7.59	7.03	6.55	5.72	5.49	5.33	5.17	5.02	4.67	4.02	3.94	3.52	3.24	2.99	2.80
	<i>F16</i>		5.73	5.54	5.39	5.11	4.63	4.25	3.97	3.49	3.35	3.26	3.17	3.09	2.88	2.52	2.47	2.25	2.10	1.97	1.86
	<i>F17</i>		6.82	6.66	6.49	6.22	5.71	5.27	4.91	4.31	4.13	4.02	3.90	3.79	3.51	3.03	2.97	2.68	2.48	2.29	2.15
	<i>F18</i>		6.89	6.72	6.55	6.25	5.73	5.29	4.95	4.36	4.18	4.07	3.96	3.85	3.59	3.14	3.08	2.80	2.60	2.42	2.28

Table F.6 *Residual Water Content over time during drying, after second impregnation for samples 16, 17, and 18.*

Sample Number	Preparation solution	Time (hours)	After immersion																		
		Time (min.)	0	15	30	0.5	1	2	3	4	5	6	9	12	15.25	24	36	48	60	72	96
L	F	L	F	Residual Water Content (%)																	
				L	F	L	F	L	F	L	F	L	F	L	F	L	F	L	F	L	F
				10.43	10.51	10.34	10.04	9.47	8.89	8.29	7.68	7.07	5.19	3.50	2.23	0.90	0.36	0.18	0.11	0.09	0.06
				6.65	6.76	6.59	6.31	5.77	5.23	4.68	4.13	3.58	2.21	1.43	1.01	0.52	0.28	0.17	0.11	0.08	0.05
				9.85	9.92	9.75	9.44	8.85	8.28	7.70	7.12	6.57	5.08	4.03	3.29	2.24	1.51	1.10	0.85	0.68	0.46
				7.38	7.46	7.29	7.01	6.49	5.95	5.45	4.96	4.50	3.35	2.65	2.18	1.49	1.00	0.72	0.54	0.42	0.25
				3.17	3.20	3.08	2.92	2.76	2.67	2.60	2.53	2.47	2.31	2.17	2.04	1.84	1.72	1.64	1.57	1.52	1.39
				2.61	2.67	2.55	2.38	2.17	2.09	2.03	1.97	1.93	1.81	1.72	1.65	1.53	1.43	1.36	1.30	1.26	1.15

Sample Number	Solution	Time (hours)	After immersion																			
		Time (min.)	0	15	30	0.5	1	2	3	4	6.45	7.45	8.2	9.1	10	12.9	22.9	24	35.45	47	59.2	72
L	F	L	F	Residual Water Content (%)																		
				L	F	L	F	L	F	L	F	L	F	L	F	L	F	L	F	L	F	
				8.89	8.70	8.52	8.19	7.59	7.04	6.56	5.72	5.48	5.33	5.17	5.02	4.65	4.00	3.91	3.49	3.22	2.99	2.79
				6.48	6.30	6.14	5.86	5.36	4.94	4.61	4.05	3.89	3.78	3.67	3.58	3.33	2.90	2.84	2.58	2.39	2.23	2.10

Table F.7 Average values of the Residual Water Content (%) per stone and impregnation solution type. (a) Above, first impregnation. (b) Below, second impregnation of samples 16, 17, and 18 only.

<i>Preparation Solution</i>	<i>Sample Number</i>	<i>Initial maximum water content Q_{max} (%)</i>	<i>Final time of the test (min) t_f</i>	<i>Drying Index at t_f</i>
Deionized Water	L1	10.31	5760	0.083
	L2	10.33	5760	0.084
	L3	10.66	5760	0.082
Saturated Sodium Chloride	L4	2.81	5760	0.548
	L5	3.60	5760	0.520
	L6	3.01	5760	0.518
4 % BDAC	L10	10.17	5760	0.160
	L11	9.72	5760	0.150
	L12	9.65	5760	0.145
Saturated Sodium Chloride	L13	2.85	5760	0.505
	L14	3.28	5760	0.552
	L15	3.32	5760	0.480
	L16	3.28	5760	0.495
	L17	3.28	5760	0.516
	L18	3.08	5760	0.535
Deionized Water	F1	6.02	5760	0.075
	F2	7.32	5760	0.071
	F3	6.60	5760	0.075
Saturated Sodium Chloride	F4	2.53	5760	0.513
	F5	2.52	5760	0.597
	F6	2.84	5760	0.504
4 % BDAC	F10	7.45	5760	0.144
	F11	8.01	5760	0.121
	F12	6.69	5760	0.135
Saturated Sodium Chloride	F13	3.07	5760	0.493
	F14	2.38	5760	0.444
	F15	2.60	5760	0.491
	F16	2.38	5760	0.554
	F17	2.51	5760	0.547
	F18	2.65	5760	0.523
BDAC Second Impregnation	L16	9.14	4320	0.413
	L17	8.63	4320	0.387
	L18	8.91	4320	0.401
	F16	5.73	4320	0.401
	F17	6.82	4320	0.399
	F18	6.89	4320	0.412

Table F.8 *Drying Index per stone and impregnation solution type.*

APPENDIX G

WET-DRY CYCLING RESULTS

Sample number	Time (day)																																								
	0	0.5	1	2	3	4	5	6	7	8	9	10	11	12	13	14	15	16	17	18	19	20	21	22	23	24	25	26	27	28	29	30	31	32	33	34	35	36	37	38	39
	Time (hours)																																								
	0	12	24	48	72	96	120.75	144	160	184	208	232	256	280	304	328	352	376	400	424	448	471	495	519	543	567	591	615	639	663	687	711	735	759	783	807	831	855	879	903	927
L1 W	249.34	249.77	249.81	250.26	250.50	250.70	250.78	250.83	249.66	249.53	249.77	250.15	250.42	250.58	249.40	249.49	249.73	250.18	250.39	250.44	249.47	249.59	249.80	250.30	250.32	250.37	249.45	249.33	249.57	250.06	250.22	250.26	249.27	249.32	249.60	250.05	250.23	250.31	249.42	249.39	249.59
TB	1.9630	1.9612	1.9597	1.9602	1.9610	1.9587	1.9599	1.9617	1.9599	1.9594	1.9594	1.9646	1.9630	1.9649	1.9589	1.9621	1.9593	1.9586	1.9591	1.9592	1.9591	1.9593	1.9597	1.9597	1.9592	1.9592	1.9584	1.9577	1.9576	1.9579	1.9581	1.9581	1.9583	1.9585	1.9593	1.9577	1.9580	1.9603	1.9622	1.9588	1.9595
FB	1.9642	1.9621	1.9646	1.9614	1.9605	1.9609	1.9639	1.9632	1.9615	1.9602	1.9602	1.9612	1.9603	1.9603	1.9601	1.9606	1.9593	1.9609	1.9608	1.9599	1.9591	1.9608	1.9588	1.9603	1.9596	1.9605	1.9594	1.9583	1.9588	1.9593	1.9596	1.9587	1.9597	1.9583	1.9592	1.9592	1.9594	1.9612	1.9584	1.9592	1.9589
RL	1.9541	1.9544	1.9532	1.9523	1.9536	1.9518	1.9522	1.9526	1.9521	1.9522	1.9521	1.9518	1.9514	1.9553	1.9517	1.9516	1.9518	1.9511	1.9515	1.9516	1.9517	1.9507	1.9513	1.9499	1.9500	1.9516	1.9508	1.9509	1.9495	1.9504	1.9506	1.9505	1.9503	1.9509	1.9514	1.9516	1.9500	1.9498	1.9504	1.9502	1.9511
L2 W	249.88	250.28	250.33	250.82	251.08	251.28	251.30	251.34	250.18	250.06	250.30	250.69	251.00	251.09	249.96	250.04	250.29	250.74	250.97	251.03	250.02	250.14	250.35	250.87	251.09	251.07	250.15	250.03	250.28	250.71	250.82	250.96	249.98	250.04	250.30	250.76	250.99	251.08	250.12	250.09	250.30
TB	1.9559	1.9542	1.9542	1.9538	1.9530	1.9532	1.9561	1.9529	1.9529	1.9564	1.9527	1.9519	1.9525	1.9527	1.9516	1.9514	1.9513	1.9514	1.9511	1.9513	1.9514	1.9519	1.9512	1.9505	1.9513	1.9516	1.9502	1.9512	1.9502	1.9511	1.9509	1.9501	1.9511	1.9511	1.9518	1.9512	1.9510	1.9506	1.9511	1.9503	1.9502
FB	1.9639	1.9614	1.9610	1.9606	1.9607	1.9608	1.9612	1.9606	1.9603	1.9608	1.9601	1.9600	1.9598	1.9600	1.9600	1.9594	1.9599	1.9592	1.9595	1.9597	1.9597	1.9591	1.9594	1.9590	1.9592	1.9592	1.9592	1.9588	1.9583	1.9588	1.9588	1.9590	1.9589	1.9586	1.9596	1.9590	1.9589	1.9586	1.9589	1.9585	1.9583
RL	1.9564	1.9560	1.9543	1.9539	1.9536	1.9532	1.9541	1.9541	1.9538	1.9559	1.9535	1.9539	1.9534	1.9534	1.9536	1.9535	1.9532	1.9531	1.9534	1.9530	1.9532	1.9529	1.9529	1.9524	1.9524	1.9524	1.9526	1.9523	1.9524	1.9522	1.9529	1.9520	1.9524	1.9526	1.9525	1.9524	1.9521	1.9521	1.9521	1.9522	1.9521
L3 W	244.99	245.37	245.42	245.80	245.98	246.18	246.14	246.23	245.26	245.14	245.39	245.71	245.98	246.09	245.05	245.13	245.39	245.80	245.98	246.00	245.11	245.21	245.45	245.89	246.12	246.05	245.24	245.11	245.37	245.68	245.75	245.92	245.07	245.10	245.40	245.77	245.95	246.05	245.21	245.17	245.40
TB	1.9491	1.9482	1.9483	1.9466	1.9466	1.9474	1.9470	1.9487	1.9477	1.9496	1.9473	1.9468	1.9469	1.9468	1.9464	1.9466	1.9465	1.9469	1.9460	1.9463	1.9462	1.9467	1.9460	1.9448	1.9448	1.9452	1.9452	1.9452	1.9458	1.945	1.9464	1.9443	1.9459	1.9458	1.9468	1.9442	1.9449	1.9441	1.9453	1.9453	1.9454
FB	1.9507	1.9494	1.9481	1.9483	1.9490	1.9480	1.9478	1.9483	1.9474	1.9494	1.9478	1.9473	1.9475	1.9488	1.9479	1.9477	1.9466	1.9472	1.9475	1.9469	1.9469	1.9471	1.9472	1.9463	1.9467	1.9463	1.9461	1.9463	1.9459	1.9470	1.9467	1.9465	1.9462	1.9461	1.9484	1.9462	1.9463	1.9462	1.9463	1.9459	1.9462
RL	1.9547	1.9524	1.9519	1.9518	1.9514	1.9511	1.9508	1.9520	1.9509	1.9515	1.9518	1.9506	1.9512	1.9501	1.9501	1.9500	1.9502	1.9502	1.9501	1.9493	1.9504	1.9509	1.9496	1.9498	1.9492	1.9490	1.9491	1.9493	1.9487	1.9492	1.9495	1.9485	1.9492	1.9501	1.9498	1.9493	1.9499	1.9487	1.9485	1.9491	1.9495
L4 W	269.97	269.82	269.73	272.70	275.76	278.49	279.36	279.24	275.84	274.71	273.77	276.25	278.17	279.05	274.61	273.54	272.66	276.29	278.57	278.92	273.93	272.77	271.86	275.18	277.62	278.69	273.97	272.87	272.03	273.53	275.12	277.00	272.36	271.00	270.12	273.17	275.55	277.54	272.77	271.63	270.80
TB	1.9234	1.9230	1.9216	1.9204	1.9131	1.9124	1.9115	1.9126	1.9143	1.9157	1.9158	1.9126	1.9120	1.9125	1.9143	1.9146	1.9158	1.9133	1.9124	1.9122	1.9149	1.9146	1.9141	1.9126	1.9110	1.9110	1.9121	1.9138	1.9137	1.9122	1.9108	1.9108	1.9137	1.9148	1.9175	1.9133	1.9124	1.9113	1.9139	1.9141	1.9153
FB	1.9864	1.9836	1.9833	1.9753	1.9684	1.9657	1.9649	1.9634	1.9651	1.9660	1.9691	1.9641	1.9651	1.9625	1.9627	1.9654	1.9688	1.9606	1.9612	1.9606	1.9653	1.9656	1.9679	1.9634	1.9612	1.9608	1.9622	1.9644	1.9652	1.9630	1.9625	1.9623	1.9653	1.9656	1.9675	1.9642	1.9630	1.9609	1.9638	1.9658	1.9680
RL	1.9955	2.0001	1.9965	1.9957	1.9917	1.9818	1.9801	1.9780	1.9780	1.9799	1.9801	1.9775	1.9769	1.9773	1.9793	1.9796	1.9797	1.9774	1.9770	1.9753	1.9765	1.9784	1.9780	1.9757	1.9754	1.9760	1.9754	1.9764	1.9773	1.9762	1.9770	1.9751	1.9773	1.9802	1.9801	1.9789	1.9768	1.9782	1.9789	1.9809	1.9808
L5 W	263.14	262.97	262.89	265.32	267.98	269.99	271.83	273.37	270.37	269.25	268.35	270.77	272.62	274.82	271.00	270.18	269.39	272.65	274.8	274.64	269.97	268.92	267.75	269.65	271.21	271.88	268.31	267.36	266.66	268.31	270.14	272.01	267.78	266.57	265.67	268.13	271.02	273.08	268.21	267.16	266.40
TB	1.9763	1.9756	1.9758	1.9723	1.9692	1.9609	1.9581	1.9570	1.9590	1.9608	1.9605	1.9583	1.9542	1.9544	1.9557	1.9553	1.9559	1.9541	1.9534	1.9524	1.9557	1.9568	1.9573	1.9533	1.9528	1.9523	1.9556	1.9561	1.9564	1.9545	1.9543	1.9536	1.9577	1.9596	1.9595	1.9562	1.9553	1.9542	1.9579	1.9600	1.9599
FB	1.9974	1.9956	1.9941	1.9878	1.9746	1.9698	1.9703	1.9664	1.9680	1.9675	1.9680	1.9651	1.9644	1.9617	1.9631	1.9630	1.9658	1.9606	1.9598	1.9595	1.9611	1.9618	1.9633	1.9624	1.9616	1.9607	1.9551	1.9642	1.9648	1.9648	1.9628	1.9598	1.9626	1.9648	1.9664	1.9638	1.9591	1.9592	1.9620	1.9629	1.9652
RL	1.9791	1.9765	1.9793	1.9737	1.9676	1.9628	1.9621	1.9598	1.9600	1.9608	1.9607	1.9593	1.9578	1.9579	1.9583	1.9596	1.9607	1.9579	1.9571	1.9567	1.9588	1.9598	1.9609	1.9596	1.9583	1.9579	1.9601	1.9623	1.9640	1.9641	1.9640	1.9597	1.9618	1.9628	1.9635	1.9633	1.9607	1.9601	1.9626	1.9637	1.9628
L6 W	267.26	267.10	267.01	269.31	271.06	272.25	273.53	274.84	272.59	271.75	271.02	273.16	275.03	277.12	273.72	272.95	272.14	274.69	277.09	277.11	273.43	272.52	271.46	273.99	276.08	277.11	273.27	272.28	271.53	273.20	274.27	275.22	271.69	270.64	269.84	271.64	273.40	274.80	271.43	270.60	269.94
TB	1.9696	1.9683	1.9662	1.9618	1.9577	1.9552	1.9551	1.9553	1.9547	1.9549	1.9542	1.9528	1.9533	1.9531	1.9534	1.9526	1.9542	1.9526	1.9505	1.9508	1.9535	1.9540	1.9549	1.9521	1.9511	1.9501	1.9577	1.956	1.9569	1.9537	1.9532	1.9507	1.9527	1.9547	1.9552	1.9530	1.9521	1.9516	1.9548	1.9553	1.9553
FB	1.9803	1.9800	1.9780	1.9718	1.9673	1.9646	1.9632	1.9602	1.9612	1.9600	1.9617	1.9588	1.9589	1.9565	1.9570	1.9581	1.9589	1.9563	1.9554	1.9543	1.9561	1.9560	1.9579	1.9557	1.9535																

Sample number	Time (day)																																								
	0	0.5	1	2	3	4	5	6	7	8	9	10	11	12	13	14	15	16	17	18	19	20	21	22	23	24	25	26	27	28	29	30	31	32	33	34	35	36	37	38	39
	Time (hours)																																								
	0	12	24	48	72	96	120.75	144	160	184	208	232	256	280	304	328	352	376	400	424	448	471	495	519	543	567	591	615	639	663	687	711	735	759	783	807	831	855	879	903	927
L10 W	250.49	251.08	251.25	252.17	252.68	252.81	252.95	253.02	251.49	251.04	251.22	252.11	252.52	252.88	251.01	250.87	251.18	252.17	252.64	252.93	251.13	251.07	251.45	252.66	253.08	253.31	251.43	251.01	251.27	252.11	252.73	253.25	251.12	250.87	251.22	252.28	252.98	253.39	251.43	251.07	251.32
TB	1.9582	1.9609	1.9558	1.9539	1.9544	1.9543	1.9549	1.9564	1.9553	1.9551	1.9541	1.9553	1.9541	1.9536	1.9545	1.9542	1.9537	1.9533	1.9537	1.9534	1.9538	1.9534	1.9528	1.9529	1.9526	1.9526	1.9531	1.9525	1.9520	1.9526	1.9533	1.9537	1.9539	1.9529	1.9530	1.9528	1.9527	1.9525	1.9531	1.9528	1.9525
FB	1.9567	1.9554	1.9538	1.9525	1.9532	1.9528	1.9518	1.9534	1.9523	1.9523	1.9521	1.9520	1.9523	1.9518	1.9513	1.9522	1.9515	1.9521	1.9514	1.9514	1.9509	1.9527	1.9512	1.9503	1.9510	1.9510	1.9512	1.9508	1.9503	1.9502	1.9501	1.9519	1.9505	1.9505	1.9520	1.9511	1.9511	1.9504	1.9512	1.9505	1.9508
RL	1.9700	1.9686	1.9681	1.9689	1.9659	1.9659	1.9655	1.9653	1.9738	1.9654	1.9654	1.9649	1.9648	1.9659	1.9647	1.9656	1.9655	1.9655	1.9647	1.9647	1.9650	1.9646	1.9643	1.9641	1.9642	1.9638	1.9646	1.9643	1.9636	1.9634	1.9647	1.9644	1.9643	1.9646	1.9644	1.9641	1.9646	1.9639	1.9643	1.9644	1.9641
L11 W	252.23	252.76	252.89	253.79	254.19	254.22	254.38	254.44	253.00	252.62	252.81	253.71	254.05	254.49	252.61	252.50	252.73	253.80	254.24	254.56	252.73	252.67	252.95	254.14	254.44	254.76	252.97	252.6	252.78	253.72	254.34	254.77	252.71	252.49	252.77	254.1	254.6	254.96	253.02	252.67	252.86
TB	1.9633	1.9619	1.9618	1.9600	1.9592	1.9597	1.9601	1.9594	1.9600	1.9598	1.9596	1.9593	1.9592	1.9594	1.9595	1.9588	1.9591	1.9590	1.9591	1.9588	1.9591	1.9589	1.9591	1.9586	1.9585	1.9580	1.9582	1.9578	1.9576	1.9582	1.9585	1.9581	1.9593	1.9581	1.9581	1.9582	1.9579	1.9581	1.9581	1.9581	1.9579
FB	1.9678	1.9670	1.9664	1.9650	1.9692	1.9644	1.9644	1.9647	1.9648	1.9643	1.9644	1.9638	1.9648	1.9641	1.9644	1.9647	1.9643	1.9640	1.9639	1.9631	1.9640	1.9639	1.9632	1.9633	1.9632	1.9636	1.9634	1.9630	1.9625	1.9629	1.9627	1.9632	1.9635	1.9625	1.9631	1.9633	1.9633	1.9629	1.9628	1.9627	1.9633
RL	1.9604	1.9609	1.9598	1.9582	1.9577	1.9569	1.9576	1.9581	1.9571	1.9579	1.9569	1.9569	1.9577	1.9571	1.9580	1.9572	1.9571	1.9564	1.9566	1.9567	1.9565	1.9562	1.9569	1.9559	1.9553	1.9559	1.9566	1.9564	1.9552	1.9562	1.9559	1.9559	1.9560	1.9561	1.9560	1.9559	1.9561	1.9559	1.9558	1.9560	1.9553
L12 W	250.29	250.83	251.01	251.81	252.10	252.12	252.28	252.33	251.04	250.69	250.89	251.80	252.14	252.49	250.69	250.59	250.82	251.77	252.18	252.45	250.77	250.76	251.00	251.88	252.21	252.48	250.99	250.66	250.84	251.77	252.19	252.44	250.73	250.56	250.84	251.85	252.29	252.54	251.02	250.73	250.92
TB	1.9439	1.9435	1.9434	1.9414	1.9420	1.9412	1.9420	1.9410	1.9414	1.9412	1.9412	1.9409	1.9407	1.9410	1.9412	1.9405	1.9407	1.9412	1.9405	1.9401	1.9404	1.9405	1.9411	1.9401	1.9400	1.9398	1.9401	1.9395	1.9402	1.9399	1.9399	1.9396	1.9397	1.9397	1.9395	1.9394	1.9396	1.9394	1.9400	1.9393	1.9402
FB	1.9587	1.9579	1.9565	1.9551	1.9551	1.9554	1.9550	1.9554	1.9548	1.9552	1.9551	1.9546	1.9548	1.9547	1.9545	1.9544	1.9549	1.9545	1.9543	1.9545	1.9547	1.9550	1.9542	1.9542	1.9543	1.9538	1.9534	1.9535	1.9538	1.9539	1.9536	1.9538	1.9534	1.9537	1.9535	1.9539	1.9535	1.9532	1.9542	1.9535	1.9533
RL	1.9599	1.9589	1.9592	1.9574	1.9571	1.9566	1.9571	1.9586	1.9572	1.9566	1.9562	1.9561	1.9560	1.9556	1.9560	1.9558	1.9559	1.9557	1.9556	1.9552	1.9556	1.9558	1.9552	1.9547	1.9549	1.9548	1.9551	1.9544	1.9553	1.9547	1.9553	1.9548	1.9548	1.9550	1.9547	1.9547	1.9551	1.9544	1.9549	1.9546	1.9547
L13 W	284.18	283.31	282.97	284.45	286.05	286.38	286.03	286.00	282.59	281.42	280.91	282.16	283.63	284.94	281.25	280.21	279.76	281.34	282.67	283.91	280.61	279.75	279.42	281.62	283.23	284.64	281.07	280.28	279.90	282.1	283.59	284.86	280.83	279.73	279.14	281.47	283.21	284.67	280.93	280.16	279.75
TB	1.9707	1.9706	1.9697	1.9688	1.9700	1.9681	1.9684	1.9675	1.9693	1.9706	1.9698	1.9691	1.9667	1.9678	1.9691	1.9717	1.9701	1.9679	1.9674	1.9670	1.9697	1.9705	1.9688	1.9664	1.9662	1.9682	1.9664	1.9683	1.9691	1.9686	1.9676	1.9663	1.9685	1.9701	1.9696	1.9677	1.9666	1.9676	1.9689	1.9698	1.9700
FB	1.9869	1.9872	1.9874	1.9869	1.9833	1.9830	1.9817	1.9829	1.9829	1.9845	1.9850	1.9833	1.9831	1.9816	1.9841	1.9845	1.9847	1.9840	1.9829	1.9812	1.9844	1.9848	1.9845	1.9829	1.9810	1.9809	1.9824	1.9839	1.9828	1.9806	1.9809	1.9800	1.9838	1.9857	1.9843	1.9823	1.9812	1.9807	1.9842	1.9856	1.9836
RL	1.9643	1.9656	1.9650	1.9629	1.9635	1.9623	1.9631	1.9625	1.9631	1.9629	1.9635	1.9626	1.9617	1.9613	1.9634	1.9665	1.9650	1.9642	1.9631	1.9629	1.9643	1.9650	1.9645	1.9622	1.9621	1.9618	1.9641	1.9645	1.9635	1.9639	1.9633	1.9626	1.9645	1.9656	1.9657	1.9642	1.9629	1.9624	1.9646	1.9654	1.965
L14 W	274.38	273.43	273.08	274.26	275.59	276.29	276.02	276.05	272.92	271.92	271.41	272.42	273.85	275.11	271.73	270.76	270.27	271.89	273.15	274.35	271.23	270.4	270.03	272.32	273.82	274.88	271.58	270.84	270.40	272.16	273.82	275.32	271.49	270.52	269.96	272.34	274.04	275.49	271.68	270.93	270.53
TB	1.9546	1.9538	1.9539	1.9527	1.9520	1.9509	1.9519	1.9522	1.9527	1.9541	1.9537	1.9512	1.9513	1.9514	1.9534	1.9549	1.9542	1.9522	1.9511	1.9502	1.9531	1.9538	1.9524	1.9511	1.9502	1.9508	1.9527	1.9529	1.9525	1.9510	1.9506	1.9502	1.9516	1.9538	1.9542	1.9521	1.9513	1.9501	1.9512	1.9533	1.9525
FB	1.9559	1.9552	1.9557	1.9536	1.9530	1.9532	1.9514	1.9512	1.9515	1.9535	1.9536	1.9536	1.9496	1.9503	1.9523	1.9548	1.9544	1.9527	1.9513	1.9494	1.9525	1.9544	1.9535	1.9494	1.9492	1.9485	1.9510	1.9527	1.9522	1.9511	1.9495	1.9487	1.9529	1.9535	1.9543	1.9490	1.9481	1.9483	1.9523	1.9532	1.9531
RL	1.9592	1.9599	1.9598	1.9591	1.9599	1.9584	1.9583	1.9570	1.9589	1.9606	1.9593	1.9594	1.9586	1.9581	1.9602	1.9612	1.9621	1.9600	1.9596	1.9580	1.9606	1.9613	1.9607	1.9608	1.9594	1.9577	1.9592	1.9610	1.9594	1.9601	1.9589	1.9569	1.9605	1.9625	1.9624	1.9618	1.9617	1.9597	1.9627	1.9631	1.9631
L15 W	276.57	275.63	275.27	276.21	277.43	278.67	278.61	278.58	275.89	275.06	274.47	275.28	276.49	277.53	274.63	273.79	273.14	274.78	275.92	276.97	274.25	273.52	272.9	275.40	276.82	277.82	274.71	274.07	273.45	275.02	276.53	278.26	274.63	273.82	273.11	275.62	277.28	278.69	274.90	274.19	273.68
TB	1.9640	1.9635	1.9635	1.9624	1.9617	1.9612	1.9622	1.9620	1.9627	1.9657	1.9642	1.9615	1.9613	1.9615	1.9637	1.9657	1.9653	1.9616	1.9608	1.9612	1.9637	1.9650	1.9639	1.9603	1.9593	1.9600	1.9633	1.9647	1.9639	1.9613	1.9606	1.9594	1.9612	1.9633	1.9638	1.9610	1.9597	1.9604	1.9639	1.9640	1.9646
FB	1.9629	1.9627	1.9636	1.9623	1.9604	1.9597	1.9603	1.9584	1.9598	1.9616	1.9619	1.9615																													

Sample number	Time (day)																																									
	0	0.5	1	2	3	4	5	6	7	8	9	10	11	12	13	14	15	16	17	18	19	20	21	22	23	24	25	26	27	28	29	30	31	32	33	34	35	36	37	38	39	
	Time (hours)																																									
	0	12	24	48	72	96	120.75	144	160	184	208	232	256	280	304	328	352	376	400	424	448	471	495	519	543	567	591	615	639	663	687	711	735	759	783	807	831	855	879	903	927	
F1	W	284.61	284.84	284.9	285.47	285.66	285.72	285.81	285.88	284.96	284.79	285.02	285.39	285.56	285.76	284.77	284.72	284.96	285.34	285.59	285.69	284.81	284.80	285.02	285.36	285.59	285.59	284.87	284.74	284.97	285.30	285.47	285.60	284.76	284.72	284.95	285.38	285.54	285.69	284.85	284.76	284.98
	TB	1.9943	1.9952	1.9943	1.9946	1.9930	1.9923	1.9934	1.9911	1.9936	1.9931	1.9940	1.9943	1.9937	1.9937	1.9934	1.9931	1.9933	1.9942	1.9923	1.9922	1.9936	1.9933	1.9933	1.9927	1.9924	1.9919	1.9923	1.9920	1.9921	1.9928	1.9933	1.9924	1.9928	1.9927	1.9921	1.9923	1.9931	1.9924	1.9928	1.9923	1.9929
	FB	2.0419	2.0396	2.0368	2.0378	2.0378	2.0365	2.0386	2.0371	2.0396	2.0368	2.0383	2.0378	2.0376	2.0377	2.0375	2.0361	2.0367	2.0365	2.0370	2.0371	2.0369	2.0362	2.0362	2.0354	2.0362	2.0356	2.0368	2.0352	2.0354	2.0356	2.0356	2.0365	2.0358	2.0370	2.0361	2.0358	2.0353	2.0365	2.0356	2.0353	2.0357
	RL	2.0262	2.0258	2.0275	2.0259	2.0234	2.0237	2.0252	2.0243	2.0251	2.0242	2.0254	2.0261	2.0234	2.0254	2.0265	2.0253	2.0235	2.0237	2.0240	2.0251	2.0250	2.0253	2.0260	2.0247	2.0240	2.0252	2.0241	2.0226	2.0213	2.0232	2.0246	2.0229	2.0244	2.0259	2.0246	2.0233	2.0223	2.0230	2.0242	2.0245	2.0235
F2	W	277.64	277.86	277.90	278.61	278.84	278.86	278.96	279.05	277.96	277.76	278.01	278.46	278.68	278.93	277.75	277.70	277.94	278.43	278.72	278.88	277.78	277.78	278.00	278.44	278.72	278.69	277.84	277.71	277.94	278.24	278.42	278.68	277.71	277.69	277.92	278.40	278.63	278.82	277.82	277.73	277.93
	TB	2.0110	2.0123	2.0090	2.0110	2.0091	2.0199	2.0103	2.0104	2.0107	2.0085	2.0106	2.0096	2.0105	2.0087	2.0106	2.0089	2.0097	2.0108	2.0103	2.0094	2.0090	2.0107	2.0107	2.0091	2.0100	2.0089	2.0094	2.0093	2.0086	2.0101	2.0093	2.0092	2.0083	2.0089	2.0088	2.0087	2.0088	2.0086	2.0088	2.0091	2.0088
	FB	2.0084	2.0073	2.0082	2.0076	2.0065	2.0060	2.0085	2.0073	2.0061	2.0062	2.0064	2.0061	2.0066	2.0051	2.0063	2.0078	2.0076	2.0073	2.0066	2.0060	2.0061	2.0058	2.0056	2.0061	2.0058	2.0065	2.0061	2.0070	2.0055	2.0062	2.0060	2.0046	2.0051	2.0053	2.0053	2.0052	2.0049	2.0047	2.0043	2.0049	2.0051
	RL	2.0234	2.0228	2.0243	2.0226	2.0230	2.0224	2.0230	2.0233	2.0233	2.0225	2.0217	2.0219	2.0224	2.0226	2.0228	2.0222	2.0220	2.0225	2.0221	2.0218	2.0219	2.0220	2.0214	2.0213	2.0209	2.0214	2.0214	2.0222	2.0206	2.0215	2.0227	2.0216	2.0209	2.0212	2.0216	2.0214	2.0214	2.0206	2.0208	2.0216	2.0211
F3	W	280.40	280.63	280.72	281.16	281.41	281.51	281.57	281.61	280.72	280.56	280.78	281.16	281.38	281.57	280.55	280.51	280.71	281.22	281.47	281.58	280.61	280.62	280.79	281.23	281.52	281.46	280.68	280.54	280.72	280.99	281.15	281.44	280.53	280.52	280.71	281.17	281.37	281.58	280.64	280.55	280.71
	TB	2.0030	2.0025	2.0026	2.0039	2.0026	2.0020	2.0018	2.0017	2.0015	2.0021	2.0016	2.0044	2.0052	2.0027	2.0018	2.0019	2.0016	2.0031	2.0015	2.0014	2.0021	2.0015	2.0013	2.0008	2.0016	2.0009	2.0007	2.0008	2.0004	2.0013	2.0012	2.0012	2.0016	2.0011	2.0012	2.0004	2.0009	2.0004	2.0012	2.001	2.0009
	FB	1.9907	1.9916	1.9900	1.9875	1.9996	1.9976	1.9997	1.9877	1.9879	1.9885	1.9883	1.9880	1.9904	1.9890	1.9883	1.9873	1.9872	1.9871	1.9874	1.9872	1.9884	1.9867	1.9886	1.9875	1.9861	1.9873	1.9872	1.9871	1.9862	1.9863	1.9881	1.9874	1.9882	1.9865	1.9856	1.9878	1.9872	1.9869	1.9873	1.9871	1.9870
	RL	2.0335	2.0336	2.0319	2.0322	2.0319	2.0321	2.0333	2.0327	2.0320	2.0323	2.0321	2.0334	2.0325	2.0336	2.0323	2.0317	2.0323	2.0319	2.0321	2.0327	2.0328	2.0327	2.0317	2.0319	2.0323	2.0307	2.0313	2.0317	2.0312	2.0323	2.0320	2.0320	2.0313	2.0311	2.0311	2.0308	2.0308	2.0316	2.0312	2.0308	2.0307
F4	W	289.69	289.54	289.46	291.95	294.41	296.41	297.43	298.4	295.10	294.19	293.33	295.71	297.34	298.75	296.00	294.22	293.22	296.39	298.30	299.06	294.91	294.12	293.12	296.06	298.23	298.51	294.60	293.71	292.83	294.37	295.88	297.41	293.64	292.68	291.69	295.01	298.04	298.71	293.75	292.89	292.14
	TB	2.0453	2.0448	2.0430	2.0338	2.0255	2.0238	2.0257	2.0240	2.0271	2.0266	2.0280	2.0241	2.0247	2.0237	2.0271	2.0283	2.0274	2.0259	2.0250	2.0201	2.0241	2.0234	2.0215	2.0189	2.0187	2.0188	2.0218	2.0233	2.0240	2.0210	2.0191	2.0187	2.0237	2.0246	2.0251	2.0222	2.0219	2.0190	2.0226	2.0232	2.0225
	FB	2.0612	2.0576	2.0556	2.0459	2.0383	2.0398	2.0303	2.0276	2.0294	2.0309	2.0330	2.0292	2.0284	2.0289	2.0311	2.0335	2.0364	2.0298	2.0284	2.0270	2.0289	2.0309	2.0339	2.0286	2.0271	2.0273	2.0331	2.0341	2.0352	2.0295	2.0278	2.0269	2.0311	2.0342	2.0382	2.0289	2.0299	2.0266	2.0289	2.0308	2.0315
	RL	2.0061	2.0040	2.0043	2.0001	1.9987	1.9971	1.9978	1.9963	2.0085	1.9990	2.0017	2.0006	1.9986	1.9984	2.0095	2.0012	2.0034	2.0003	2.0094	1.9969	1.9988	2.0005	2.0038	2.0001	1.9983	1.9975	2.0002	2.0017	2.0044	2.0017	2.0021	1.9999	2.0040	2.0048	2.0089	2.0057	1.9955	1.9948	1.9978	1.9967	2.0029
F5	W	295.52	295.33	293.23	296.62	297.86	299.51	300.34	301.07	298.63	297.79	297.08	298.41	299.83	300.86	297.77	296.83	295.02	297.77	299.85	301.51	297.76	296.77	296.09	297.37	298.92	299.46	296.65	295.89	295.19	295.95	296.66	297.76	295.49	294.7	294.05	295.93	298.04	299.69	295.93	295.07	294.40
	TB	2.0536	2.0494	2.0494	2.0418	2.0357	2.0306	2.0281	2.0264	2.0312	2.0332	2.0311	2.0293	2.0247	2.0227	2.0261	2.0284	2.0293	2.0276	2.0239	2.0224	2.0285	2.0304	2.0297	2.0272	2.0232	2.0211	2.0242	2.0263	2.0269	2.0271	2.0234	2.0227	2.0276	2.0306	2.0312	2.0260	2.0234	2.0224	2.0297	2.0291	2.0291
	FB	2.0372	2.0345	2.0325	2.0302	2.0287	2.0257	2.0252	2.0250	2.0255	2.0264	2.0279	2.0252	2.0233	2.0222	2.0260	2.0262	2.0282	2.0255	2.0224	2.0225	2.0253	2.0254	2.0253	2.0252	2.0228	2.0221	2.0243	2.0268	2.0296	2.0259	2.0253	2.0252	2.0274	2.0282	2.0316	2.0292	2.0257	2.0222	2.0254	2.0270	2.0296
	RL	2.0213	2.0295	2.0287	2.0190	2.0178	2.0156	2.0163	2.0145	2.0170	2.0168	2.0181	2.0171	2.0162	2.0146	2.0161	2.0186	2.0213	2.0194	2.0157	2.0156	2.0184	2.0202	2.0206	2.0191	2.0161	2.0156	2.0203	2.0201	2.0214	2.0220	2.0204	2.0210	2.0224	2.0231	2.0234	2.0222	2.0185	2.0181	2.0234	2.0221	2.0229
F6	W	298.32	298.17	298.10	299.27	300.32	301.56	302.58	303.59	301.40	300.71	300.01	301.38	302.99	304.12	301.22	300.37	299.69	301.04	302.31	303.43	300.49	299.62	299.07	300.14	300.99	301.36	299.38	298.74	298.10	298.86	299.32	299.89	298.27	297.61	296.93	298.28	299.56	300.72	298.35	297.65	297.00
	TB	2.0463	2.0437	2.0419	2.0374	2.0330	2.0296	2.0272	2.0238	2.0304	2.0277	2.0262	2.0253	2.0234	2.0196	2.0213	2.0241	2.0243	2.021	2.0185	2.0175	2.0221	2.0209	2.0214	2.0182	2.0183	2.0175	2.0224	2.0215	2.0215	2.0204	2.0205	2.0201	2.0228	2.0240	2.0231	2.0201	2.0177	2.0141	2.0205	2.0222	2.0233
	FB	2.0618	2.0593	2.0542	2.0460	2.0383	2.0376	2.0336	2.0344	2.0360	2.0359	2.0362	2.0336	2.0312	2.0309	2.0327	2.0361	2.0369	2.0325	2.0325	2.0306	2.0335	2.0329	2.0357	2.0344	2.0304	2.0304	2.0343	2.0336	2.0363	2.0340	2.0332	2.0320	2.0352	2.0349	2.0343	2.0344	2.0336	2.0322	2.0350	2.0360	2.0338
	RL	2.0374	2.0356	2.0333	2.0294	2.0270	2.0228	2.0224	2.0211	2.0235	2.0257	2.0266	2.0250	2.0233	2.0215	2.0243	2.0263	2.0271	2.0246	2.0229	2.0230	2.0274	2.0282	2.0277	2.0260	2.0246	2.0242	2.0266	2.0281	2.0283	2.0279	2.0275	2.0272	2.0299	2.0309	2.0332	2.0313	2.0300	2.0287	2.0320	2.0328	2.0341
F7	W	284.66	285.04	285.23	286.45	286.98	287.19	287.55	287.73	285.93	285.38	285.3	286.59	287.18	287.67	285.45	285.11	285.08	286.30	286.97	287.39	285.40	285.16	285.10	286.40	287.07	287.36	285.50	285.10	285.03	286.15	286.77	287.37	285.24	284.93	284.87	286.2					

Sample number	Time (day)																																								
	0	0.5	1	2	3	4	5	6	7	8	9	10	11	12	13	14	15	16	17	18	19	20	21	22	23	24	25	26	27	28	29	30	31	32	33	34	35	36	37	38	39
	Time (hours)																																								
	0	12	24	48	72	96	120.75	144	160	184	208	232	256	280	304	328	352	376	400	424	448	471	495	519	543	567	591	615	639	663	687	711	735	759	783	807	831	855	879	903	927
F10 W	287.01	288.01	289.01	290.01	291.01	292.01	293.01	294.01	295.01	296.01	297.01	298.01	299.01	300.01	301.01	302.01	303.01	304.01	305.01	306.01	307.01	308.01	309.01	310.01	311.01	312.01	313.01	314.01	315.01	316.01	317.01	318.01	319.01	320.01	321.01	322.01	323.01	324.01	325.01	326.01	327.01
TB	2.1369	2.1363	2.1348	2.1319	2.1317	2.1316	2.1330	2.1318	2.1328	2.1325	2.1320	2.1325	2.1317	2.1317	2.1313	2.1311	2.1332	2.1314	2.1314	2.1313	2.1317	2.1318	2.1307	2.1316	2.1318	2.1311	2.1313	2.1313	2.1306	2.1314	2.1322	2.1314	2.1311	2.1307	2.1315	2.1313	2.1312	2.1309	2.1312	2.1317	2.1297
FB	2.0053	2.0044	2.0037	2.0041	2.0022	2.0015	2.0022	2.0020	2.0024	2.0022	2.0024	2.0023	2.0023	2.0013	2.0015	2.0017	2.0016	2.0013	2.0013	2.0012	2.0011	2.0013	2.0010	2.0007	2.0007	2.0002	2.0012	2.0004	2.0002	2.0004	2.0009	2.0004	2.0009	2.0006	2.0005	2.0006	2.0007	2.0003	2.0004	2.0003	2.0004
RL	2.0122	2.0111	2.0103	2.0098	2.0082	2.0080	2.0087	2.0087	2.0083	2.0083	2.0087	2.0081	2.0077	2.0074	2.0078	2.0082	2.0074	2.0076	2.0075	2.0071	2.0076	2.0079	2.0077	2.0071	2.0067	2.0078	2.0073	2.0067	2.0072	2.0072	2.0074	2.0067	2.0073	2.0073	2.0066	2.0079	2.0069	2.0073	2.0065	2.0076	2.0075
F11 W	269.50	270.50	271.50	272.50	273.50	274.50	275.50	276.50	277.50	278.50	279.50	280.50	281.50	282.50	283.50	284.50	285.50	286.50	287.50	288.50	289.50	290.50	291.50	292.50	293.50	294.50	295.50	296.50	297.50	298.50	299.50	300.50	301.50	302.50	303.50	304.50	305.50	306.50	307.50	308.50	309.50
TB	2.0179	2.0172	2.0163	2.0170	2.0157	2.0251	2.0175	2.0150	2.0163	2.0153	2.0158	2.0151	2.0145	2.0146	2.0149	2.0153	2.0144	2.0142	2.0150	2.0145	2.0149	2.0151	2.0149	2.0144	2.0148	2.0144	2.0152	2.0141	2.0143	2.0147	2.0140	2.0145	2.0137	2.0141	2.0142	2.0138	2.0147	2.0146	2.0145	2.0140	2.0140
FB	1.9973	1.9955	1.9952	1.9940	1.9942	1.9946	1.9939	1.9918	1.9933	1.9920	1.9930	1.9938	1.9927	1.9928	1.9937	1.9920	1.9932	1.9921	1.9933	1.9936	1.9920	1.9922	1.9938	1.9933	1.9921	1.9931	1.9930	1.9932	1.9927	1.9914	1.9923	1.9916	1.9930	1.9931	1.9925	1.9915	1.9923	1.9920	1.9926	1.9911	1.9916
RL	2.0133	2.0129	2.0124	2.0115	2.0131	2.0099	2.0103	2.0094	2.0102	2.0183	2.0101	2.0105	2.0095	2.0102	2.0102	2.0107	2.0102	2.0096	2.0099	2.0095	2.0095	2.0100	2.0092	2.0095	2.0091	2.0094	2.0095	2.0094	2.0089	2.0093	2.0090	2.0088	2.0090	2.0081	2.0094	2.0088	2.0090	2.0087	2.0096	2.0095	2.0087
F12 W	288.48	289.48	290.48	291.48	292.48	293.48	294.48	295.48	296.48	297.48	298.48	299.48	300.48	301.48	302.48	303.48	304.48	305.48	306.48	307.48	308.48	309.48	310.48	311.48	312.48	313.48	314.48	315.48	316.48	317.48	318.48	319.48	320.48	321.48	322.48	323.48	324.48	325.48	326.48	327.48	328.48
TB	2.0231	2.0227	2.0230	2.0221	2.0213	2.0204	2.0228	2.0200	2.0208	2.0201	2.0199	2.0203	2.0206	2.0202	2.0208	2.0199	2.0202	2.0197	2.0201	2.0202	2.0202	2.0194	2.0192	2.0198	2.0191	2.0193	2.0192	2.0190	2.0188	2.0186	2.0182	2.0197	2.0191	2.0198	2.0200	2.0190	2.0193	2.0177	2.0188	2.0190	2.0189
FB	2.0357	2.0343	2.0330	2.0337	2.0340	2.0324	2.0335	2.0319	2.0328	2.0331	2.0325	2.0331	2.0328	2.0339	2.0320	2.0340	2.0326	2.0327	2.0315	2.0323	2.0323	2.0322	2.0331	2.0312	2.0312	2.0315	2.0321	2.0313	2.0309	2.0318	2.0319	2.0321	2.0320	2.0322	2.0315	2.0317	2.0315	2.0318	2.0314	2.0311	2.0313
RL	2.0412	2.0406	2.0403	2.0429	2.0383	2.0389	2.0378	2.0384	2.0384	2.0383	2.0382	2.0382	2.0378	2.0393	2.0388	2.0398	2.0374	2.0381	2.0384	2.0381	2.0374	2.0379	2.0381	2.0373	2.0376	2.0371	2.0367	2.0371	2.0366	2.0368	2.0383	2.0372	2.0370	2.0373	2.0381	2.0368	2.0370	2.037	2.0373	2.0379	2.0372
F13 W	284.95	285.95	286.95	287.95	288.95	289.95	290.95	291.95	292.95	293.95	294.95	295.95	296.95	297.95	298.95	299.95	300.95	301.95	302.95	303.95	304.95	305.95	306.95	307.95	308.95	309.95	310.95	311.95	312.95	313.95	314.95	315.95	316.95	317.95	318.95	319.95	320.95	321.95	322.95	323.95	324.95
TB	2.0025	2.0017	2.0024	2.0024	2.0011	2.0009	2.0092	2.0092	2.0026	2.0041	2.0056	2.0038	2.0008	2.0006	2.0020	2.0047	2.0073	2.0011	1.9987	1.9987	2.0036	2.0061	2.0068	2.0000	1.9975	2.0002	2.0031	2.0049	2.0039	2.0029	2.0004	1.9990	2.0024	2.0057	2.0068	2.0029	1.9987	1.9979	2.0166	2.0169	2.0128
FB	2.0412	2.0403	2.0393	2.0399	2.0394	2.0395	2.0401	2.0396	2.0430	2.0444	2.0489	2.0430	2.0394	2.0378	2.0445	2.0485	2.0532	2.0444	2.0397	2.0381	2.0436	2.0486	2.0495	2.0436	2.0390	2.0373	2.0446	2.0458	2.0521	2.0430	2.0416	2.0390	2.0440	2.0469	2.0469	2.0440	2.0395	2.0371	2.0484	2.0494	2.0525
RL	2.0264	2.0261	2.0251	2.0265	2.0245	2.0234	2.0236	2.0269	2.0268	2.0297	2.0299	2.0284	2.0262	2.0254	2.0280	2.0294	2.0345	2.0297	2.0286	2.0281	2.0298	2.0292	2.0315	2.0316	2.0266	2.0272	2.0311	2.0324	2.0356	2.0310	2.0291	2.0263	2.0304	2.0313	2.0351	2.0319	2.0286	2.0295	2.0339	2.0334	2.0347
F14 W	280.77	281.77	282.77	283.77	284.77	285.77	286.77	287.77	288.77	289.77	290.77	291.77	292.77	293.77	294.77	295.77	296.77	297.77	298.77	299.77	300.77	301.77	302.77	303.77	304.77	305.77	306.77	307.77	308.77	309.77	310.77	311.77	312.77	313.77	314.77	315.77	316.77	317.77	318.77	319.77	320.77
TB	2.0115	2.0129	2.0111	2.0105	2.0108	2.0161	2.0134	2.0112	2.0129	2.0134	2.0119	2.0109	2.0099	2.0088	2.0136	2.0153	2.0153	2.0109	2.0084	2.0079	2.0140	2.0140	2.0146	2.0094	2.0086	2.0092	2.0120	2.0134	2.0128	2.0101	2.0077	2.0082	2.0126	2.0137	2.0149	2.0106	2.0087	2.0083	2.0210	2.0207	2.0167
FB	2.0445	2.0448	2.0437	2.0431	2.0332	2.0445	2.0439	2.0431	2.0448	2.0448	2.0462	2.0434	2.0406	2.0410	2.0450	2.0462	2.0494	2.0428	2.0400	2.0402	2.0477	2.0479	2.0499	2.0429	2.0408	2.0399	2.0440	2.0443	2.0463	2.0420	2.0402	2.0401	2.0449	2.0469	2.0477	2.0427	2.0397	2.0400	2.0513	2.0522	2.0531
RL	2.0220	2.0202	2.0190	2.0184	2.0179	2.0181	2.0207	2.0178	2.0169	2.0197	2.0208	2.0209	2.0189	2.0174	2.0193	2.0210	2.0226	2.0211	2.0171	2.0154	2.0207	2.0239	2.0254	2.0239	2.0209	2.0176	2.0211	2.0232	2.0261	2.0220	2.0204	2.0191	2.0222	2.0253	2.0255	2.0249	2.0218	2.0201	2.0266	2.0284	2.0301
F15 W	284.75	285.75	286.75	287.75	288.75	289.75	290.75	291.75	292.75	293.75	294.75	295.75	296.75	297.75	298.75	299.75	300.75	301.75	302.75	303.75	304.75	305.75	306.75	307.75	308.75	309.75	310.75	311.75	312.75	313.75	314.75	315.75	316.75	317.75	318.75	319.75	320.75	321.75	322.75	323.75	324.75
TB	2.0410	2.0415	2.0409	2.0401	2.0405	2.0416	2.0438	2.0398	2.0437	2.0459	2.0461	2.0432	2.0407	2.0404	2.0448	2.0473	2.0470	2.0407	2.0394	2.0400	2.0438	2.0482	2.0463	2.0420	2.0387	2.0390	2.0438	2.0446	2.0446	2.0427	2.0420	2.0394	2.0434	2.0464	2.0464	2.0422	2.0400	2.0389	2.0572	2.0557	2.0556
FB	2.0068	2.0071	2.0052	2.0056	2.0041	2.0063	2.0089	2.0074	2.0074	2.0069	2.0140	2.0072	2.0033	2.0032	2.0092	2.0100	2.0096	2.0047	2.0034	2.0029	2.0080	2.0117	2.0123	2.0031	2.0016	2.0025	2.0047	2.0058	2.0072	2.0033	2.0032	2.0022	2.0051	2.0091	2.0097	2.0037	2.0021	2.0019	2.0134	2.0095	2.0083
RL	2.0206	2.0191	2.0187	2.0219	2.0299	2.0299	2.0184	2.0184	2.0212	2.0222	2.0214	2.0212	2.0209	2.0191	2.0197	2.0213	2.0235	2.0215	2.0207	2.0196	2.0216	2.0232	2.0235	2.0216	2.0207	2.0197	2.0224	2.0233	2.0234	2.0233	2.0219	2.0216	2.0231	2.0237	2.0245	2.0224	2.0248	2.0211	2.0303	2.0304	2.0302
F16 W	288.09	289.09	290.09	291.09	292.09	293.09	294.09	295.09	296.09	297.09	298.09	299.09	300.09	301.09	302.09	303.09	304.09	305.09	306.09	307.09	308.09	309.09	310.09	311.09	312.09	313.09	314.09	315.09	316.09	317.09	318.09	319.09	320.09	321.09	322.09	323.09					

Preparation Solution	Sample Type	Time (day)																																							
		0.5	1	2	3	4	5	6	7	8	9	10	11	12	13	14	15	16	17	18	19	20	21	22	23	24	25	26	27	28	29	30	31	32	33	34	35	36	37	38	39
		Time (hours)																																							
		12	24	48	72	96	120.75	144	160	184	208	232	256	280	304	328	352	376	400	424	448	471	495	519	543	567	591	615	639	663	687	711	735	759	783	807	831	855	879	903	927
Water (Control)	L	0.16	0.18	0.36	0.45	0.53	0.54	0.56	0.12	0.07	0.17	0.31	0.43	0.48	0.03	0.06	0.16	0.34	0.42	0.44	0.05	0.10	0.19	0.38	0.45	0.44	0.08	0.03	0.14	0.30	0.35	0.39	0.01	0.03	0.15	0.32	0.40	0.43	0.07	0.06	0.15
	F	0.08	0.10	0.31	0.39	0.41	0.44	0.46	0.12	0.05	0.14	0.28	0.35	0.43	0.05	0.03	0.11	0.28	0.37	0.42	0.07	0.07	0.14	0.28	0.38	0.37	0.09	0.04	0.12	0.22	0.28	0.36	0.04	0.03	0.11	0.27	0.34	0.41	0.08	0.05	0.12
NaCl	L	-0.06	-0.09	0.87	1.80	2.54	3.04	3.39	2.31	1.92	1.60	2.48	3.18	3.83	2.37	2.04	1.73	2.91	3.76	3.79	2.12	1.73	1.34	2.31	3.07	3.41	1.90	1.52	1.23	1.84	2.40	2.98	1.44	0.98	0.66	1.57	2.45	3.13	1.51	1.13	0.85
	F	-0.06	-0.31	0.49	1.03	1.59	1.91	2.22	1.32	1.04	0.78	1.36	1.89	2.29	1.30	0.90	0.50	1.33	1.92	2.32	1.10	0.80	0.54	1.15	1.66	1.80	0.81	0.55	0.30	0.65	0.95	1.32	0.45	0.17	-0.09	0.65	1.38	1.78	0.52	0.24	0.01
Brushed BDAC	L	0.24	0.34	0.72	1.02	1.19	1.29	1.38	0.50	0.25	0.33	0.74	0.98	1.15	0.22	0.13	0.24	0.71	0.92	1.07	0.24	0.19	0.33	0.93	1.16	1.26	0.36	0.17	0.26	0.76	1.00	1.26	0.23	0.11	0.26	0.84	1.14	1.33	0.36	0.19	0.27
	F	0.14	0.20	0.63	0.84	0.95	1.06	1.13	0.48	0.28	0.25	0.71	0.92	1.10	0.31	0.18	0.17	0.66	0.89	1.04	0.30	0.21	0.18	0.75	0.97	1.08	0.35	0.20	0.17	0.61	0.86	1.08	0.26	0.14	0.11	0.66	0.91	1.10	0.33	0.19	0.16
Immersed BDAC	L	0.22	0.28	0.63	0.79	0.82	0.88	0.90	0.33	0.18	0.25	0.61	0.76	0.91	0.17	0.13	0.23	0.63	0.80	0.92	0.22	0.20	0.32	0.75	0.89	1.00	0.32	0.17	0.25	0.61	0.83	0.99	0.21	0.12	0.24	0.69	0.91	1.05	0.33	0.19	0.28
	F	0.12	0.18	0.46	0.58	0.66	0.67	0.69	0.24	0.10	0.11	0.36	0.50	0.60	0.10	0.04	0.07	0.34	0.47	0.55	0.10	0.07	0.06	0.40	0.55	0.60	0.15	0.06	0.07	0.31	0.47	0.61	0.09	0.04	0.04	0.35	0.50	0.62	0.15	0.07	0.07
NaCl + Brushed BDAC	L	-0.33	-0.46	-0.03	0.47	0.74	0.66	0.66	-0.45	-0.80	-1.00	-0.63	-0.14	0.29	-0.90	-1.24	-1.43	-0.85	-0.40	0.01	-1.08	-1.37	-1.53	-0.69	-0.15	0.27	-0.93	-1.19	-1.36	-0.70	-0.14	0.40	-0.98	-1.32	-1.55	-0.68	-0.07	0.45	-0.91	-1.18	-1.34
	F	-0.34	-0.44	0.11	0.60	0.82	0.76	0.71	-0.46	-0.79	-1.02	-0.48	0.00	0.46	-0.73	-1.03	-1.22	-0.56	-0.11	0.26	-0.90	-1.18	-1.37	-0.64	-0.18	0.20	-1.01	-1.25	-1.42	-0.77	-0.35	0.10	-1.10	-1.37	-1.58	-0.83	-0.32	0.13	-1.26	-1.51	-1.66
NaCl + immersed BDAC	L	0.08	0.11	0.56	1.02	1.54	1.92	2.27	1.37	0.97	0.90	1.36	1.78	2.39	1.22	0.82	0.76	1.47	2.00	2.45	1.15	0.75	0.73	1.61	2.12	2.59	1.37	1.04	0.91	1.70	2.18	2.67	1.30	0.84	0.71	1.73	2.33	2.83	1.56	1.18	1.01
	F	0.07	0.10	0.47	0.88	1.30	1.49	1.73	0.95	0.64	0.49	0.83	1.20	1.59	0.65	0.41	0.31	0.82	1.11	1.34	0.44	0.26	0.17	0.78	1.13	1.41	0.44	0.23	0.14	0.57	0.86	1.16	0.27	0.08	0.00	0.46	0.82	1.11	0.23	0.05	-0.03

Figure G.5 Average difference in percent between the sample weight at $t=0$ and at $t=i$ per stone and impregnation solution type.

Preparation Solution	Sample Type	Time (day)																																							
		0.5	1	2	3	4	5	6	7	8	9	10	11	12	13	14	15	16	17	18	19	20	21	22	23	24	25	26	27	28	29	30	31	32	33	34	35	36	37	38	39
		Time (hours)																																							
		12	24	48	72	96	120.75	144	160	184	208	232	256	280	304	328	352	376	400	424	448	471	495	519	543	567	591	615	639	663	687	711	735	759	783	807	831	855	879	903	927
Water (Control)	L	-0.22	-0.28	-0.39	-0.38	-0.46	-0.32	-0.30	-0.43	-0.28	-0.46	-0.41	-0.44	-0.34	-0.54	-0.50	-0.58	-0.57	-0.56	-0.59	-0.58	-0.56	-0.61	-0.67	-0.67	-0.63	-0.70	-0.72	-0.76	-0.70	-0.66	-0.75	-0.68	-0.68	-0.57	-0.70	-0.71	-0.69	-0.66	-0.72	-0.69
	F	-0.03	-0.13	-0.15	-0.09	0.00	0.03	-0.28	-0.21	-0.30	-0.23	-0.18	-0.17	-0.23	-0.21	-0.30	-0.31	-0.25	-0.32	-0.32	-0.27	-0.30	-0.29	-0.38	-0.38	-0.40	-0.41	-0.40	-0.51	-0.38	-0.32	-0.41	-0.40	-0.38	-0.43	-0.44	-0.46	-0.46	-0.43	-0.43	-0.44
NaCl	L	-0.12	-0.27	-0.94	-1.79	-2.43	-2.57	-2.82	-2.68	-2.59	-2.52	-2.90	-3.02	-3.15	-3.02	-2.93	-2.73	-3.21	-3.37	-3.46	-3.09	-2.99	-2.87	-3.24	-3.43	-3.49	-3.29	-3.03	-2.90	-3.09	-3.17	-3.42	-3.02	-2.77	-2.61	-2.92	-3.21	-3.32	-2.92	-2.73	-2.61
	F	-0.19	-0.44	-1.41	-2.07	-2.40	-2.66	-2.88	-2.30	-2.41	-2.30	-2.62	-2.87	-3.05	-2.53	-2.40	-2.21	-2.66	-2.79	-3.17	-2.65	-2.56	-2.45	-2.81	-3.10	-3.18	-2.65	-2.52	-2.32	-2.61	-2.78	-2.87	-2.37	-2.19	-1.97	-2.44	-2.83	-3.13	-2.52	-2.44	-2.28
Brushed BDAC	L	0.09	-0.19	-0.25	-0.32	-0.35	-0.32	-0.29	-0.27	-0.31	-0.30	-0.33	-0.36	-0.36	-0.34	-0.34	-0.40	-0.31	-0.42	-0.45	-0.43	-0.44	-0.50	-0.51	-0.52	-0.55	-0.50	-0.57	-0.59	-0.57	-0.57	-0.56	-0.53	-0.53	-0.56	-0.55	-0.55	-0.57	-0.49	-0.55	-0.58
	F	-0.12	-0.17	-0.21	-0.09	-0.27	-0.21	-0.28	-0.14	-0.14	-0.21	-0.31	-0.35	-0.34	-0.24	-0.32	-0.34	-0.38	-0.39	-0.44	-0.34	-0.33	-0.42	-0.43	-0.49	-0.48	-0.42	-0.43	-0.39	-0.49	-0.46	-0.42	-0.47	-0.40	-0.47	-0.47	-0.51	-0.51	-0.56	-0.36	-0.33
Immersed BDAC	L	-0.07	-0.24	-0.45	-0.43	-0.54	-0.52	-0.45	-0.38	-0.53	-0.58	-0.60	-0.59	-0.61	-0.59	-0.60	-0.62	-0.63	-0.66	-0.70	-0.66	-0.64	-0.70	-0.76	-0.76	-0.78	-0.73	-0.79	-0.82	-0.80	-0.76	-0.74	-0.74	-0.78	-0.76	-0.77	-0.77	-0.82	-0.76	-0.80	-0.80
	F	-0.13	-0.23	-0.26	-0.40	-0.33	-0.38	-0.56	-0.45	-0.37	-0.50	-0.48	-0.55	-0.52	-0.52	-0.49	-0.54	-0.59	-0.57	-0.57	-0.59	-0.58	-0.58	-0.62	-0.65	-0.64	-0.61	-0.66	-0.70	-0.68	-0.64	-0.66	-0.65	-0.65	-0.63	-0.68	-0.66	-0.70	-0.66	-0.67	-0.71
NaCl + Brushed BDAC	L	0.02	0.02	-0.13	-0.22	-0.35	-0.32	-0.41	-0.26	-0.04	-0.08	-0.23	-0.44	-0.46	-0.13	0.16	0.14	-0.16	-0.31	-0.46	-0.08	0.05	-0.05	-0.40	-0.54	-0.55	-0.27	-0.08	-0.17	-0.30	-0.45	-0.58	-0.17	0.08	0.10	-0.26	-0.39	-0.45	0.02	0.14	0.07
	F	-0.05	-0.18	-0.13	-0.25	0.06	0.09	-0.05	0.05	0.24	0.47	0.09	-0.26	-0.38	0.16	0.45	0.75	0.01	-0.34	-0.42	0.27	0.60	0.71	0.02	-0.36	-0.39	0.17	0.35	0.58	0.06	-0.17	-0.36	0.19	0.53	0.67	0.14	-0.21	-0.36	1.35	1.32	1.27
NaCl + immersed BDAC	L	-0.01	-0.31	-0.38	-0.50	-0.70	-0.71	-0.88	-0.62	-0.57	-0.62	-0.80	-0.74	-0.87	-0.53	-0.55	-0.56	-0.65	-0.70	-0.89	-0.53	-0.55	-0.65	-0.83	-0.93	-1.04	-0.71	-0.70	-0.80	-0.89	-0.97	-1.04	-0.74	-0.65	-0.70	-0.89	-0.98	-1.06	-0.76	-0.68	-0.70
	F	-0.25	-0.48	-0.76	-0.90	-0.95	-1.08	-1.45	-0.92	-1.06	-1.06	-1.28	-1.35	-1.50	-1.16	-1.14	-1.17	-1.40	-1.51	-1.53	-1.28	-1.30	-1.35	-1.56	-1.61	-1.67	-1.36	-1.38	-1.47	-1.49	-1.53	-1.58	-1.40	-1.41	-1.50	-1.65	-1.60	-1.67	-1.39	-1.35	-1.44

Figure G.6 Average sum of the length difference in percent between the sample lengths at $t=0$ and at $t=i$ per stone and impregnation solution type.

APPENDIX H

STATISTICAL ANALYSIS OF THE WET-DRY CYCLING RESULTS

<i>Preparation Solution</i>	<i>Sample number</i>	<i>Initial uptake</i>	<i>Amplitude 1</i>	<i>Amplitude 2</i>	<i>Amplitude 3</i>	<i>Amplitude 4</i>	<i>Amplitude 5</i>	<i>Amplitude 6</i>	<i>Amplitude 7</i>	<i>Amplitude 8</i>	<i>Amplitude 9</i>	<i>Amplitude 10</i>	<i>Amplitude 11</i>	<i>Maximum amplitude</i>	<i>Average amplitude</i>	<i>Standard deviation - average amplitude</i>
Water (Control)	L-1-2-3	0.56	0.49	0.41	0.45	0.41	0.39	0.39	0.41	0.36	0.38	0.42	0.37	0.49	0.41	0.04
	F-1-2-3	0.46	0.41	0.37	0.40	0.38	0.35	0.31	0.34	0.32	0.33	0.38	0.36	0.41	0.36	0.03
NaCl	L-4-5-6	3.39	1.79	2.23	2.10	2.06	2.45	2.07	2.18	1.75	2.32	2.47	2.28	2.47	2.16	0.24
	F-4-5-6	2.22	1.43	1.51	1.79	1.82	1.78	1.26	1.50	1.02	1.41	1.87	1.77	1.87	1.56	0.27
Brushed BDAC	L-7-8-9	1.38	1.13	0.90	1.02	0.94	0.88	1.06	1.08	1.08	1.15	1.22	1.14	1.22	1.05	0.11
	F-7-8-9	1.13	0.88	0.85	0.93	0.87	0.86	0.90	0.90	0.90	0.97	0.99	0.94	0.99	0.91	0.04
Immersed BDAC	L-10-11-12	0.90	0.72	0.73	0.78	0.79	0.72	0.80	0.83	0.82	0.87	0.93	0.85	0.93	0.81	0.06
	F-10-11-12	0.69	0.59	0.50	0.56	0.50	0.48	0.54	0.54	0.54	0.57	0.58	0.55	0.59	0.54	0.03
NaCl + Brushed BDAC	L-13-14-15	0.74	1.74	1.29	1.72	1.44	1.54	1.79	1.63	1.76	1.94	1.99	1.78	1.99	1.69	0.21
	F-13-14-15	0.82	1.84	1.48	1.69	1.49	1.63	1.57	1.62	1.52	1.68	1.70	1.79	1.84	1.64	0.12
NaCl + immersed BDAC	L-16-17-18	2.27	1.36	1.49	1.63	1.69	1.73	1.87	1.69	1.77	1.96	2.11	1.82	2.11	1.74	0.21
	F-16-17-18	1.73	1.24	1.10	1.28	1.03	1.17	1.24	1.27	1.02	1.17	1.12	1.15	1.28	1.16	0.09

Table H.1 Characteristic values of the percentual weight changes during wet-dry cycling. By convention all the amplitude are positive values.

<i>Preparation Solution</i>	<i>Sample number</i>	<i>Initial uptake</i>	<i>Amplitude 1</i>	<i>Amplitude 2</i>	<i>Amplitude 3</i>	<i>Amplitude 4</i>	<i>Amplitude 5</i>	<i>Amplitude 6</i>	<i>Amplitude 7</i>	<i>Amplitude 8</i>	<i>Amplitude 9</i>	<i>Amplitude 10</i>	<i>Amplitude 11</i>	<i>Maximum amplitude</i>	<i>Average amplitude</i>	<i>Standard deviation - average amplitude</i>
Water (Control)	L-1-2-3	0.46	0.18	0.16	0.24	0.10	0.04	0.11	0.13	0.06	0.19	0.14	0.05	0.24	0.13	0.06
	F-1-2-3	0.28	0.33	0.02	0.14	0.11	0.05	0.12	0.14	0.00	0.11	0.08	0.03	0.33	0.10	0.09
NaCl	L-4-5-6	2.82	0.30	0.64	0.42	0.73	0.59	0.62	0.59	0.52	0.81	0.72	0.71	0.81	0.60	0.15
	F-4-5-6	2.88	0.58	0.75	0.85	0.96	0.72	0.74	0.87	0.55	0.90	1.16	0.84	1.16	0.81	0.17
Brushed BDAC	L-7-8-9	0.35	0.07	0.09	0.02	0.11	0.02	0.12	0.06	0.07	0.04	0.04	0.08	0.12	0.06	0.03
	F-7-8-9	0.28	0.14	0.21	0.11	0.19	0.10	0.16	0.11	0.09	0.08	0.16	0.23	0.23	0.14	0.05
Immersed BDAC	L-10-11-12	0.54	0.16	0.23	0.02	0.11	0.05	0.13	0.04	0.06	0.06	0.08	0.06	0.23	0.09	0.06
	F-10-11-12	0.56	0.18	0.17	0.05	0.10	0.03	0.08	0.08	0.06	0.04	0.07	0.03	0.18	0.08	0.05
NaCl + Brushed BDAC	L-13-14-15	0.41	0.37	0.42	0.62	0.62	0.51	0.61	0.47	0.51	0.69	0.55	0.59	0.69	0.54	0.10
	F-13-14-15	0.25	0.51	0.84	1.13	1.18	1.13	1.11	0.98	0.94	1.03	1.03	1.71	1.71	1.05	0.29
NaCl + immersed BDAC	L-16-17-18	0.88	0.31	0.31	0.34	0.35	0.36	0.51	0.35	0.34	0.39	0.41	0.37	0.51	0.37	0.06
	F-16-17-18	1.45	0.53	0.58	0.36	0.38	0.25	0.39	0.30	0.22	0.18	0.27	0.32	0.58	0.34	0.12

Table H.2 Characteristic values of the percentual sum of length changes during wet-dry cycling. By convention all the amplitude are positive values.

t-Test

The test serves, among other purposes, to compare the means of two sets of data. For this purpose the following experimental *t* is calculated.

$$t = \left[\frac{(\bar{x} - \bar{y})}{s} \right] \times \sqrt{\frac{M \times N}{M + N}}$$

where \bar{x} and \bar{y} are the means of the two sets,

s is the pooled standard deviation, and

M and N are the number of measurements within each set.

If the calculated *t* is larger than the one listed in the table at the desired confidence level, there is a significant difference between the two means.

Standard deviation from pooled data

The pooled standard deviation obtained is a much better estimate than each individual *s*. The pooled standard deviation is calculated with the following equation:

$$s = \sqrt{\frac{\sum_{j=1}^{j=k} \sum (x_i - \bar{x}_j)^2}{N - k}}$$

where *k* is the number of samples (1 to *k*), and

N is the sum of all measurements (*N*₁ to *N*_{*k*}).

t-Test for average amplitude per cycle of the percentual weight changes during wet-dry cycling

In this specific case for the *t*-test, M=N=11,

for the standard deviation of the pooled data, N=22, k=2,

degrees of freedom = 10.

Degrees of freedom	Confidence levels (%)			
	90	95	99	99.5
10	1.812	2.228	3.169	3.581

Table H.3 Values of *t* for 10 degrees of freedom for various confidence levels.

L-4-5-6 and L-13-14-15 – Weight change

The calculated values are $s_{\text{pooled}} = 0.222$, $t = 4.858 > 3.581$.

Therefore there is a significant difference between the two means, with a confidence level of 99.5%.

L-4-5-6 and L-16-17-18 – Weight change

The calculated values are $s_{\text{pooled}} = 0.222$, $t = 4.380 > 3.581$.

Therefore there is a significant difference between the two means, with a confidence level of 99.5%.

L-13-14-15 and L-16-17-18 – Weight change

The calculated values are $s_{\text{pooled}} = 0.208$, $t = 0.564 < 1.812$.

Therefore there is not a significant difference between the two means, with a confidence level of 90%.

BIBLIOGRAPHY

- ABD EL-HADY, M. M. 1988. Infra-red Investigations on Monumental Limestone Samples. In *Proceedings of the Sixth International Congress on Deterioration and Conservation of Stone, 12-14 September 1988, Toruń*. Edited by J. Ciabach. Toruń: Nicholas Copernicus University Press Department. 387-394.
- . 1995. Conservation Problems of Islamic Architectural Heritage in Cairo [Egypt]. In *Conservation, Preservation and Restoration: Traditions, Trends and Techniques*. Edited by G. Kamalakar, V. Pandit Rao, and M. Veerender. Hyderabad, India: Birla Archeological and Cultural Research Institute. 63-70.
- ABD EL-HADY, M. M., and R. KRZYWOBLOCKA-LAUROV. 1985. The Durability of Limestone Employed in Roman Theater and Qait Bay's Citadel in the Marine Environment in Alexandria, Egypt. In *Proceedings of the Fifth International Congress on Deterioration and Conservation of Stone, 25-27 September 1985, Lausanne*. Edited by G. Félix. Lausanne: Presses polytechniques romandes. 307-312.
- AGA KAHN TRUST FOR CULTURE. 1998. Three Pilot Projects for Conservation and Urban Revitalization in Cairo's al-Darb al-Ahmar District: Scope of Work and Current Status of Activities. *Historic Cities Support Programme Technical Brief* no. 1
- AMERICAN SOCIETY FOR THE TESTING OF MATERIALS. 1990. ASTM C157-89: Standard Test Method for Length Change of Hardened Hydraulic-Cement, Mortar and Concrete. In *1990 Annual Book of ASTM Standards*. Section 4 – Construction, Vol. 04.01 Cement, Lime, Gypsum. West Conshohocken, PA: ASTM.
- . 1998. ASTM C490-97: Standard Practice for Use of Apparatus for the Determination of Length Change of Hardened Cement Paste, Mortar and Concrete. In *1998 Annual Book of ASTM Standards*. Section 4 – Construction, Vol. 04.01 Cement, Lime, Gypsum. West Conshohocken, PA: ASTM.
- . 1998. ASTM C1012-97: Standard Test Method for Length Changes of Hydraulic-cement Mortars exposed to a Sulfate Solution. In *1998 Annual Book of ASTM Standards*. Section 4 – Construction, Vol. 04.01 Cement, Lime, Gypsum. West Conshohocken, PA: ASTM.
- ANTONIOU, J. 1998. *Historic Cairo: a walk through the Islamic city*. Cairo: The American University in Cairo Press.
- ARNOLD, A. 1981. Nature of Reactions of Saline Minerals in Walls. In *Conservation of Stone 2: Preprints of the Contributions to the International Symposium, 27-30 October 1981, Bologna*. Edited by R. Rossi-Manaresi. Bologna: Centro per la Conservazione delle Sculture all'aperto. 13-23.
- ARNOLD, A., and A. KUENG. 1985. Crystallization and Habits of Salt Efflorescences on Walls I: Methods of Investigation and Habits. In *Proceedings of the Fifth International Congress on Deterioration and Conservation of Stone, 25-27 September 1985, Lausanne*. Edited by G. Félix. Lausanne: Presses polytechniques romandes. 255-267.
- ARNOLD A., and K. ZEHNDER. 1985. Crystallizations and Habits of Salt Efflorescences on Walls II: Conditions of Crystallization. In *Proceedings of the Fifth International Congress on Deterioration*

- and Conservation of Stone, 25-27 September 1985, Lausanne.* Edited by G. Félix. Lausanne: Presses polytechniques romandes. 269-277.
- . 1990. Salt Weathering on Monuments. In *Proceedings of the First International Symposium on the Conservation of Monuments in the Mediterranean Basin: The Influence of Coastal Environment and Salt Spray on Limestone and Marble, 7-10 June 1989, Bari.* Edited by F. Zezza. Brescia, Italy: Grafo Edizioni. 31-58.
- ASH, M., and I. ASH, comps. 1997. *Handbook of industrial surfactants: an international guide to more than 21,000 products by trade name, composition, application, and manufacturer.* 2nd ed. Aldershot, England: Gower.
- BARANSKI, M., and T. KOWALSKI. 1989. Protection of the Basilica Tetrastyle at Ashmunein. In *Reports from Ashmunein: Polish-Egyptian Archeological and Preservation Mission at El Ashmunein.* Vol. 1. Warszawa: Prakonie Konservacj Zabytków. 20-28.
- BARTON, N. G., and S. M. BLACKSHAW. 1976. A Statistical Evaluation of the Analyses Carried out on Egyptian Limestone. *Lithoclastia*, no 2: 11-16.
- BASMA, A. A., and E. R. TUNCER. 1991. Effect of Lime on Volume Change and Compressibility of Expansive Clays. *Transportation Research Record* 1295: 52-61.
- BEDARIDA, F., L. ZEFIRO, and C. PONTIGGIA. 1976. Holographic Control of Diffusion Coefficients in water Solutions: Crystal Growth from Solutions. In *Proceedings of the International Conference on Applications of Holography and Optical Data Processing, 23-26 August 1976, Jerusalem.* Edited by E. Marom, A.A. Friesem, and E. Wiener-Avneer. Oxford: Pergamon Press. 259-266.
- BENNEMA, P. 1984. Crystal Growth from Solution: Theory and Experimentation. *Journal of Crystal Growth* 24/25: 76-83.
- BIENFAIT, M., and R. KERN. 1964. Etablissement de la forme d'équilibre d'un cristal (méthode de Lemlein-Kija). *Bulletin de la Société Française de Minéralogie and Cristallographie* 87: 604-613.
- BÖKE, H., H. GÖKTÜRK, and E. N. CANER-SALTIK. 1996. Effect of Some Surfactants on the Sulphation Reaction of Calcareous Stone. In *Proceedings of the Eighth International Congress on Deterioration and Conservation of Stone, 30 September – 4 October 1996, Berlin.* Edited by J. Riederer. Berlin: Möller Druck und Verlag. 401-406.
- BONNET, S., and B. PERRIN. 1999. Influence de la présence des ions chlorures sur les propriétés à l'équilibre de différents mortiers. *Materials and Structures / Matériaux et Constructions* 32 (August-Septembre): 492-499.
- BORRELLI, E. 1994. Un caso singolare nell'analisi dei sali solubili: la riduzione dei nitrati a nitriti (Unexpected reduction of nitrates to nitrites during the analyses of soluble salts). In *Proceedings of the Third International Symposium on the Conservation of Monuments in the Mediterranean Basin. Stone and Monuments: Methodologies for the Analyses of Weathering and Conservation, 22-25 June 1994, Venice.* Edited by V. Fassina, H. Ott, and F. Zezza. Venice: Soprintendenza ai Beni Artistici e Storici di Venezia. 151-154.
- BRADLEY, S. M., and S. B. HANNA. 1986. The Effect of Soluble Salt Movements on the Conservation of an Egyptian Limestone Standing Figure. In *Case Studies in the Conservation of Stone and Wall Paintings: Preprints of the Contribution to the Bologna Congress, 21-26 September 1986.* Edited by N.S. Brommelle and P. Smith. London: The International Institute for Conservation of Historic and Artistic Works. 57-61.

- BRADLEY, S. M., and A. P. MIDDLETON. 1988. A Study of the Deterioration of Egyptian Limestone Sculpture. *Journal of the American Institute for Conservation* 27, no. 2: 64-86.
- BUILDING RESEARCH ESTABLISHMENT. 1975. The Decay and Conservation of Stone Masonry. *BRE Digest* 177 (May).
- CAMAITI, M., F. FRATINI, E. LUPPICHINI, and C. MANGANELLI DEL FÀ. 1995. La pulitura di superfici lapidee "restaurate" (Cleaning of previously restored stone surfaces). In *Proceedings of a Symposium on Cleaning of Architectural Surfaces, 3-6 July 1995, Bressanone. (Scienza e beni culturali* 11). Padova: Libreria Progetto Editore. 387-396.
- CAMUFFO, D. 1993. Controlling the Aeolian Erosion of the Great Sphinx. *Studies in Conservation* 38, no. 3 (august): 198-205.
- CANER, E. N., and N. J. SEELEY. 1978. The Clay Minerals and the Decay of Limestone. In *International Symposium on Deterioration and Protection of Stone Monuments*. Paris: UNESCO/RILEM. 1-34.
- CANEVA, G., M. P. NUGARI, and O. SALVADORI. 1991. Biology in the Conservation of Works of Art. Rome: International Centre for the Study of the Preservation and the Restoration of Cultural Property (ICCROM).
- CASANOVA, P. 1894-97. *Histoire et description de la citadelle du Caire*. Paris: E. Leroux. Mémoires publiés par les membres de la mission archéologique française au Caire. Tome 6. Fasc. 4-5.
- CHAROLA, A. E. 2000. Salts in the Deterioration of Porous Materials: An Overview. *Journal of the American Institute for Conservation*. In press.
- CHAROLA, A. E., G. E. WHEELER, and R. J. KOESTLER. 1982. Treatment of the Abydos Reliefs: Preliminary Investigations. In *Proceedings of the Fourth International Congress on the Deterioration and Preservation of Stone Objects, 7-9 July 1982, Louisville*. Edited by K. L. Gauri, and J. A. Gwinn. Louisville, Kentucky: The University of Louisville. 77-88.
- CHATTERJI S., P. CHRISTENSEN, and G. OVERGAARD. 1979. Mechanisms of Breakdown of Natural Stones caused by Sodium Salts. In *Proceedings of the Third International Congress on the Deterioration and Preservation of Stones, 24-27 October 1979, Venice*. Padova: Università degli Studi di Padova. 131-34.
- CLIFTON, J. R., ed. 1986. *Cleaning Stone and Masonry: a Symposium Sponsored by ASTM Committee E-6 on Performance of Building Constructions, 18 April 1983, Louisville, Kentucky*. (ASTM Special Technical Publication 935) Philadelphia: ASTM.
- COMITÉ DE CONSERVATION DES MONUMENTS DE L'ART ARABE.
 Exercice 1894. Fascicule onzième. *Procès-Verbaux des Séances - Rapports de la Deuxième Commission*. 2nd ed. Le Caire: Imprimerie Nationale, 1908.
 Exercice 1897. Fascicule quatorzième. *Procès-Verbaux des Séances - Rapports de la Deuxième Commission*. Le Caire: Imprimerie centrale J. Barbier, 1898.
 Exercice 1898. Fascicule quinzième. *Procès-Verbaux des Séances - Rapports de la Section Technique*. Le Caire: Imprimerie centrale J. Barbier, 1900.
 Exercice 1899. Fascicule seizième. *Procès-Verbaux des Séances - Rapports de la Section Technique*. Le Caire: Imprimerie de l'Institut Français d'Archéologie Orientale, 1899.
 Exercice 1900. Fascicule dix-septième. *Procès-Verbaux des Séances - Rapports de la Section Technique*. Le Caire: Imprimerie de l'Institut Français d'Archéologie Orientale, 1900.
 Exercice 1901. Fascicule dix-huitième. *Procès-Verbaux des Séances - Rapports de la Section Technique*. Le Caire: Imprimerie de l'Institut Français d'Archéologie Orientale, 1901.

Exercice 1902. Fascicule dix-neuvième. *Procès-Verbaux des Séances - Rapports de la Section Technique*. Le Caire: Imprimerie de l'Institut Français d'Archéologie Orientale, 1902.

Exercice 1907. Fascicule vingt-quatrième. *Procès-Verbaux des Séances - Rapports de la Section Technique*. Le Caire: Imprimerie de l'Institut Français d'Archéologie Orientale, 1908.

Exercice 1908. Fascicule vingt-cinquième. *Procès-Verbaux des Séances - Rapports de la Section Technique*. Le Caire: Imprimerie de l'Institut Français d'Archéologie Orientale, 1909.

Exercice 1911. Fascicule vingt-huitième. *Procès-Verbaux des Séances - Rapports de la Section Technique*. Le Caire: Imprimerie de l'Institut Français d'Archéologie Orientale, 1912.

Exercice 1912. Fascicule vingt-neuvième. *Procès-Verbaux des Séances - Rapports de la Section Technique*. Le Caire: Imprimerie de l'Institut Français d'Archéologie Orientale, 1913.

Exercice 1913. Fascicule trentième. *Procès-Verbaux des Séances - Rapports de la Section Technique*. Le Caire: Imprimerie de l'Institut Français d'Archéologie Orientale, 1914.

Comptes rendus des exercices 1915-1919. Fascicule trente-deuxième. Le Caire: Imprimerie de l'Institut Français d'Archéologie Orientale, 1922.

Exercice 1920-1924. Fascicule trente-troisième. *Procès-Verbaux des Séances - Rapports de la Section Technique*. Imprimerie de l'Institut Français d'Archéologie Orientale, 1928.

Exercice 1925-1926. Fascicule trente-quatrième. *Procès-Verbaux des Séances - Rapports de la Section Technique*. Imprimerie F.E. Noury & Fils, 1933.

Exercice 1927-1929. Fascicule trente-cinquième. *Procès-Verbaux des Séances - Rapports de la Section Technique*. Imprimerie F.E. Noury & Fils, 1934.

Comptes rendus des exercices 1930-1932. Fascicule trente-sixième. *Procès-Verbaux des Séances - Rapports de la Section Technique*. Le Caire: Imprimerie F.E. Noury & Fils, 1936.

Exercice 1933-1935. Fascicule trente-septième. *Procès-Verbaux des Séances du Comité et Rapports de la Section Technique*. Le Caire: Imprimerie Nationalew, Būlūk, 1940.

Exercice 1936-1940. Fascicule trente-huitième. *Procès-Verbaux des Séances du Comité et Rapports de la Section Technique*. Le Caire: Imprimerie Nationalew, Būlūk, 1944.

CONSEIL SUPÉRIEUR DU SERVICE DE CONSERVATION DES MONUMENTS ARABES.

[19??]. Exercices 1941-45. Fascicule trente-neuvième. *Procès-Verbaux des Séances du Conseil Supérieur et Rapports du Comité Permanent*. Le Caire: Imprimerie Université Fouad I^{er}.

COOKE, R. M. 1981. Salt Weathering in Deserts. *Proceedings of the Geologists Association* 92: 1-16.

COOKE, R. U. 1979. Laboratory Simulation of Salt Weathering Processes in Arid Environments. *Earth Surface Processes* 4: 347-359.

COREMANS, P. 1947. L'altération et le traitement des calcaires égyptiens infectés de sels solubles. *Chronique d'Egypte, Bulletin périodique de la fondation égyptologique reine Elisabeth* 22: 119-122.

CRESWELL, K. A. C. 1952. *Fortification in Islam before A.D. 1250*. London: Geoffrey Cumberlege.

———. 1952-59. *The Muslim Architecture of Egypt*. Oxford: Clarendon Press.

DELGADO RODRIGUES, J. 1977. Estimation of the Content of Clay Minerals and its Significance in Stone Decay. In *Proceedings of the Second International Symposium on Deterioration of Building Stones, 27 September – 1 October 1976, Athens*. Athens: Université technique nationale. 105-8.

Description de l'Egypte, ou recueil des observations et des recherches qui ont été faites en Egypte pendant l'expédition de l'Armée française. 1993. Publiée par les ordres de Napoléon Bonaparte. Paris: Bibliothèque de l'Image.

DEWEY, C. [2000]. *The Ayyubid City Wall of Cairo: Stone Characterization and Analysis*. Unpublished report prepared for the Aga Kahn Trust for Culture.

- DOSSETT, J. W. 1998. *Composite Repair of Sandstone*. Master of Science in Historic Preservation Thesis, University of Pennsylvania.
- DUNN, J. R., and P. P. HUDEC. 1966. Water, Clay and Rock Soundness. *The Ohio Journal of Science* 66 (2): 153-68.
- . [1988?]. Frost and Sorption effects in Argillaceous Rocks. *Dunn Geosciences Corporation*.
- DUTTLINGER, W., and D. KNÖFEL. 1990. Chemical and Mineralogical Investigations of Decay Phenomena at the Curbs of the Wells in Bad Nauheim. In *Proceedings of the First International Symposium on the Conservation of Monuments in the Mediterranean Basin: The Influence of Coastal Environment and Salt Spray on Limestone and Marble, 7-10 June 1989, Bari*. Edited by F. Zezza. Brescia, Italy: Grafo Edizioni. 71-79.
- FÉLIX, C., and V. FURLAN. 1994. Variations dimensionnelles de grès et calcaires liées à leur consolidation avec un silicate d'éthyle (Dimensional variations of sandstone and limestone in connection with their consolidation with ethyl silicate). In *Proceedings of the Third International Symposium on the Conservation of Monuments in the Mediterranean Basin. Stone and Monuments: Methodologies for the Analyses of Weathering and Conservation, 22-25 June 1994, Venice*. Edited by V. Fassina, H. Ott, and F. Zezza. Venice: Soprintendenza ai Beni Artistici e Storici di Venezia. 855-859.
- First International Symposium on the Great Sphinx towards Global Treatment of the Sphinx, Cairo, 29 February – 3 March 1992*. 1992. *Studies in Egyptian Culture* no. 9. n.p: Waseda University.
- FONG, K.. [1999?]. *Al-Darb Al-Ahamar: The Wall*. Unpublished Report.
- FOX, J. C. 1984. Choosing a Consolidant for Limestone: Preliminary Considerations. In *Papers Presented at the Art Conservation Training Programs Conference, 2-4 May 1984*. Cambridge, Massachusetts: Center for Conservation and Technical Studies. 55-74.
- FURLAN, V., and Y. HOUST. 1983. Cristallisation de sels et dégâts de matériaux (Salt crystallization and deterioration of materials). Parts 1 and 2. *Chantiers/Suisse* 14, no. 3: 225-228; no. 4: 317-320.
- FURLAN, V., and R. PANCELLA. 1981. Propriétés d'un grès tendre traité avec des silicates d'éthyle et un polymère acrylique (Properties of a soft sandstone treated with ethyl silicates and an acrylic polymer). In *Conservation of Stone 2: Preprints of the Contributions to the International Symposium, 27-30 October 1981, Bologna*. Edited by R. Rossi-Manaresi. Bologna: Centro per la Conservazione delle Sculture all'aperto. 645-663.
- . 1983. Effects of Water on the Properties of a Calcareous Sandstone Consolidated with Synthetic Resins. In *Materials Science and Restoration: Proceedings of the International Colloquium, 6-8 September 1983, Esslingen*. Edited by F.H. Wittmann. Lausanne: Edition Lack und Chemie. 335-340.
- GALAN, E. 1990. Carbonate Rocks: Alteration and Control of Stone Quality: Some Considerations. In *Proceedings of the First International Symposium on the Conservation of Monuments in the Mediterranean Basin: The Influence of Coastal Environment and Salt Spray on Limestone and Marble, 7-10 June 1989, Bari*. Edited by F. Zezza. Brescia, Italy: Grafo Edizioni. 249-254.
- GAURI, K. L. 1981a. The Deterioration of Ancient Stone Structures in Egypt. In *Prospection et Sauvegarde des Antiquités de l'Égypte: Actes de la Table Ronde organisée à l'occasion du Centenaire de l'Institut Français d'Archéologie Orientale, 8-12 Janvier 1981*. Edited by N.-C. Grimal. Bibliothèque d'Étude, t.88. Le Caire: Institute Francais d'Archeologie Orientale du Caire. 13-18.

- . 1981b. Deterioration of the Stone of the Great Sphinx. *Newsletter of the American Research Center in Egypt* 144 (Spring). 35-47.
- . 1983. Removal of Water Soluble Salts from Masonry and Porosimetry of a Pharaonic Veneer Stone from the Sphinx. *Newsletter of the American Research Center in Egypt* 124 (Winter), 19-27.
- GAURI, K. L., A. N. CHOWDHURY, N. P. KULSHRESHTHA, and A. R. PUNURU. 1988. Geologic Features and the Durability of Limestones at the Sphinx. In *Engineering Geology of Ancient Works, Monuments and Historical Site: Preservation and Protection: Proceedings of an International Symposium Organized by the Greek National Group of IAEG, 19-23 September 1988, Athens*. Vol. 2. Edited by P. G. Marinou, and G. C. Kouki. Rotterdam: A. A. Balkema. 723-729.
- GAURI, K. L., G. C. HOLDREN, and W. C. VAUGHAN. 1986. Cleaning Efflorescence from Masonry. In *Cleaning Stone and Masonry: a Symposium Sponsored by ASTM Committee E-6 on Performance of Building Constructions, 18 April 1983, Louisville, Kentucky*. (ASTM Special Technical Publication 935). Edited by J. R. Clifton. Philadelphia: ASTM. 3-13.
- GAURI, K. L., and A. R. PUNURU. 1990. Characterization and Durability of Limestones Determined through Mercury Intrusion Porosimetry. In *Proceedings of the First International Symposium on the Conservation of Monuments in the Mediterranean Basin: The Influence of Coastal Environment and Salt Spray on Limestone and Marble, 7-10 June 1989, Bari*. Edited by F. Zezza. Brescia, Italy: Grafo Edizioni. 255-258.
- Handbook of Chemistry and Physics*. 1995. 75th ed. Edited by David R. Lide. Boca Raton: CRC Press.
- HANNA, S. B. 1984. The Use of Organo-silanes for the Treatment of Limestone in an Advanced State of Deterioration. In *Adhesives and Consolidants: Preprints of the Contribution to the Paris Congress, 2-8 September 1984*. Edited by N. S. Brommelle, E. M. Pye, P. Smith, and G. Thomson. London: The International Institute for Conservation of Historic and Artistic Works. 171-176.
- HARRELL, J. A. 1992. Ancient Egyptian Limestone Quarries: a Petrological Survey. *Archaeometry* 34, no. 2 (August): 195-211.
- HARVEY, R. D., J. W. BAXTER, G. S. FRASER, and C. B. SMITH. 1978. Absorption and Other Properties of Carbonate Rock Affecting Soundness of Aggregate. In *Decay and Preservation of Stone*. Edited by E. M. Winkler. *Engineering Geology Case Histories* 11: 7-16.
- HAZLEHURST, T. H., JR., H. C. MARTIN, and L. BREWER. 1936. The Creeping of Saturated Salt Solutions. *Journal of Physical Chemistry* 40 (4): 439-452.
- HELMI, F. M. 1988. Deterioration Phenomenon in the North Temple of Karanis, near Fayoum, Egypt. In *Proceedings of the Sixth International Congress on Deterioration and Conservation of Stone, 12-14 September 1988, Torun*. Edited by J. Ciabach. Torun: Nicholas Copernicus University Press Department. 166-174.
- . 1990. Study of Salt Problem in the Sphinx, Giza, Egypt. In *Preprints of the Ninth Triennial Meeting of the ICOM Committee for Conservation, 26-31 August 1990, Dresden, German Democratic Republic*. Edited by K. Grimstad. Los Angeles: ICOM Committee for Conservation. 326-329.
- HELMS, G. M. 1977. Conservation of Egyptian Limestone: the Abydos Reliefs. In *Students Papers Presented at the Third Annual Art Conservation Training Programs Conference, 8-11 May 1977, Queen's University, Kingston, Canada*. 40-51.

- HUGHES, R. 1988. *The Sphinx and its conservation*. London: Ove Arup & Partners.
- HUMBOLDT MFG. CO. 1998. *H-3250 Length Comparator with Dial Indicator User Guide*. Booklet Manuel. Norridge, Illinois: Humboldt Mfg. Co.1-7.
- HUME, W. F. 1925- *Geology of Egypt*. Cairo: Government Press.
- IMAM, M. M. 1999. Lithostratigraphy, Microfacies and Depositional Environments of the Miocene in the Area Between Wadi el Tayiba and Wadi Sidri, West-Central Sinai, Egypt. *Neues Jahrbuch für Geologie und Palaontologie-Monatshefte* 7 (July): 409-439.
- IVANOVA N. I., L. I. LOPATINA, V. A. KURBATSKII, and E. D. SHCHUKIN. 1993. Adsorption of Nonionic Surfactants from Aqueous-Solutions on the Surface of Limestone. *Russian Journal of Applied Chemistry* 66, no. 7, part 2: 1260-1262.
- IVANOVA N. I., and E. D. SHCHUKIN. 1993. Mixed Adsorption of Ionic and Nonionic Surfactants on Calcium Carbonate. *Colloids and Surfaces A: Physicochemical and Engineering Aspects* 76: 109-113.
- JABŁOŃSKA-SZYSZKO, M., and B. RUDNIKA. 1988. Study of the Reasons for the Destruction of the Antique Building Stone in Paimyra. In *Proceedings of the Sixth International Congress on Deterioration and Conservation of Stone, 12-14 September 1988, Toruń*. Edited by J. Ciabach. Toruń: Nicholas Copernicus University Press Department. 207-215.
- JARMONTOWICZ, A. 1988. Identification of the Minerals in Egyptian Ancient Monuments by Infrared Spectroscopy. In *Proceedings of the Sixth International Congress on Deterioration and Conservation of Stone, 12-14 September 1988, Toruń*. Edited by J. Ciabach. Toruń: Nicholas Copernicus University Press Department. 411-417.
- JEDRZEJEWSKA, H. 1970. Removal of Soluble Salts from Stone. In *Preprints of the Contributions to the New York Conference on Conservation of Stone and Wooden Objects, 7 - 13 June 1970*. 2nd ed. Vol. 1, *Conservation of Stone*. London: The International Institute for Conservation of Historic and Artistic Works. 19-34.
- JURKIEWICZ, R. 1989. Preliminary Studies on Conservation Programme for the Basilica in Ashmunein. In *Reports from Ashmunein: Polish-Egyptian Archeological and Preservation Mission at El Ashmunein*. Vol. 1. Warszawa: Prakonie Konservacj Zabytków. 11-19.
- KABESH, M. L. A., and M. MAMDOUH M. HAMADA. 1956. *Limestones of the Cairo neighborhood*. Geological Survey of Egypt. Cairo: Les Editions Universitaires d'Egypte.
- LAGALY, G., and A. WEISS. 1970. Über die Bildung sequenziosomer glimmerartiger Schichtsilicate (Formation of sequence isomers of mica type layer silicates). *Zeitschrift für Naturforschung* 25b: 572-576.
- LAUGHLIN, R. G. 1994. *The aqueous phase behavior of surfactants*. London: Academic Press.
- LEHMANN, J. 1987. The Methodology for the Cleaning and Desalting of Stone Objects in Goluchow Castle Museum. In *Preprints of the Eight Triennial Meeting of the ICOM Committee for Conservation, 6-11 September 1987, Sydney, Australia*. Vol.2. Los Angeles: The Getty Conservation Institute. 487-491.

- LEWIN, S. Z. 1982. The Mechanism of Masonry Decay through Crystallization. In *Conservation of Historic Stone Buildings and Monuments*. Washington, D.C.: National Academy Press. 120-144.
- LUCAS, A. 1915. *Disintegration and preservation of building stones in Egypt*. Cairo: Ministry of Finances.
- MACKENZIE, N. D. 1992. *Ayyubid Cairo: a topographical study*. Cairo: The American University in Cairo.
- MADSEN, F. T., and M. MÜLLER-VONMOOS. 1989. The Swelling Behavior of Clays. *Applied Clay Science* 4, no.2: 143-56.
- MAEKAWA, S., and N. H. AGNEW. 1996. Investigation on Environmentally Driven Deterioration of the Great Sphinx and Concepts for Protection. In *Archeological Conservation and its Consequences: Preprints of the Contribution to the Copenhagen Congress, 26-30 August 1996*. Edited by A. Roy, and P. Smith. London: International Institute for Conservation of Historic and Artistic Works. 116-120.
- MANNHARDT K., L. L. SCHRAMM, and J. J. NOVOSAD. 1992. Adsorption of Anionic and Amphoteric Foam-Forming Surfactants on Different Rock Types. *Colloids and Surfaces* 68 (1-2): 37-53.
- MCEWAN, D. M. C., and J. J. WILSON. 1980. Interlayer and Intercalation Complexes of Clay Minerals. In *Crystal Structures of Clay Minerals and Their X-Ray Identification*. Edited by G. W. Brindley and G. Brown. London: Mineralogical Society. 197-248.
- MCGREEVY, J. P., and B. J. SMITH. 1984. The Possible Role of Clay Minerals in Salt Weathering. *Catena* 11: 169-75.
- MEINECKE, M., ed. 1980. *Islamic Cairo: architectural conservation and urban development of the historic centre: Proceedings of a seminar organized by the Goethe Institut, 1-5 October 1978, Cairo*. London: Art and Archaeology Research Papers.
- MIDDLETON, A. P., and S. M. BRADLEY. 1989. Provenancing of Egyptian Limestone Sculpture. *Journal of Archeological Science* 16: 475-88.
- MILLER, E. 1992. Current Practice at the British Museum for the Consolidation of Decayed Porous Stones. *The Conservator* 16: 78-84.
- MITTAL, K. L., ed. 1979. *Solution chemistry of surfactants*. New York: Plenum Press.
- Monuments of Egypt: the Napoleonic edition: the complete archaeological plates from La Description de l'Egypte*. 1987. Edited with introduction and notes by C. C. Gillispie, and M. Dewachter. Princeton, N.J.: Princeton Architectural Press.
- MOORE, D. M., and R. C. REYNOLDS, JR. 1989. *X-Ray Diffraction and the Identification and Analysis of Clay Minerals*. New York: Oxford University Press.
- MYERS, D. 1999. *Surfaces, interfaces, and colloids*. 2nd ed. New York: Wiley-VCH Publishers.
- NORMAL. 1985. 11/85. Capillary Water Absorption and Capillary Absorption Coefficient. Original in Italian, draft translation by A. E. Charola. Photocopy.
- . 1988. 29/88. Measurement of the Drying Index. Original in Italian, draft translation by A. E. Charola. Photocopy.

- NUNBERG, S., A. HEYWOOD, and G. WHEELER. 1996. Relative Humidity Control as an Alternative Approach to Preserving an Egyptian Limestone Relief. In *Le dessalement des matériaux poreux: Septièmes journées d'études de la SFIIC, 9-10 mai 1996, Poitiers*. Champs-sur-Marne: Section Française de l'Institut International de Conservation des oeuvres d'art. 127-35.
- ODDY, W. A., M. J. HUGHES, and S. BAKER. 1976. The Washing of Limestone Sculptures from Egypt and the Middle East. *Lithoclastia* no.2: 3-10.
- PAGÈS, J-L. 1994. *Silhouette urbaine: l'exemple du Caire*. Paris: Institut d'aménagement et d'urbanisme de la région d'Ile-de-France.
- PANCELLA, R., and V. FURLAN. 1985. Propriétés d'un grès tendre traité avec des résines synthétiques. 1^{ère}, 2^{ème} parties (Properties of a soft sandstone treated with synthetic resins. Parts 1 and 2). *Chantiers* 16, no. 4: 295-98, no. 5: 409-13.
- PAUTY, E. 1931. La défense de l'ancienne ville du Caire et de ses monuments. *Bulletin de l'institut français d'archéologie orientale* 31. 135-176.
- PORTER, M. R. 1994. *Handbook of surfactants*. 2d ed. London: Blackie Academic & Professional.
- PRICE C., and P. BRIMBLECOMBE. 1994. Preventing Salt Damage in Porous Materials. In *Preventive Conservation Practice, Theory and Research: Preprints of the Contributions to the Ottawa Congress, 12-16 September 1994*. Edited by A. Roy and P. Smith. London: International Institute for Conservation of Historic and Artistic Works. 90-93.
- PÜHRINGER, J., and L. ENGSTRÖM. 1985. Unconventional Methods for the Prevention of Salt Damage. In *Proceedings of the Fifth International Congress on Deterioration and Conservation of Stone, 25-27 September 1985, Lausanne*. Edited by G. Félix. Lausanne: Presses polytechniques romandes. 241-250.
- PÜHRINGER, J., and J. WEBER. 1990. A Model for Salt Extraction: Some Principles. In *Preprints of the Ninth Triennial Meeting of the ICOM Committee for Conservation, 26-31 August 1990, Dresden, German Democratic Republic*. Edited by K. Grimstad. Los Angeles: ICOM Committee for Conservation. 355-360.
- RASHED M. A., and K. N. SEDIEK. 1997. Petrography, Diagenesis and Geotechnical Properties of the El-rufuf Formation (Thebes Group), El-kharga Oasis, Egypt. *Journal of African Earth Sciences* 25, no. 3 (October): 407-423.
- REYNOLDS-BALL, E. A. [1897a]. *Cairo of yesterday and to-day: the city of the caliphs; a popular study of Cairo and its environs and the Nile and its antiquities*. Boston: Dana Estates & Cie.
- . [1897b]. *The city of the caliphs, a popular study of Cairo and its environs and the Nile and its antiquities*. Boston, Estes and Lauriat.
- RIECKEN, B., and H. R. SASSE. 1997. Durability of Impregnation Products for Salt Contaminated Natural Stones. In *Structural Studies, Repairs and Maintenance of Historical Buildings: Proceedings of the Fifth International Conference on Structural Studies, repairs and Maintenance of Historical Buildings (STREMAH, San Sebastian, Spain)*. Edited by S. Sánchez-Beitia, and C. A. Brebbia. Boston: Computational Mechanics Publications. 203-212.

- RILEM. [1978?]. Test N°II.5: Evaporation Curve. In *International Symposium on Deterioration and Protection of Stone Monuments. Experimental Methods. Part II – Tests defining the properties connected with the presence and the movement of water*. Paris: UNESCO/RILEM.
- . [1978?]. Test N°II.6: Water Absorption Coefficient (Cappilarity). In *International Symposium on Deterioration and Protection of Stone Monuments. Experimental Methods. Part II – Tests defining the properties connected with the presence and the movement of water*. Paris: UNESCO/RILEM.
- . [1978?]. Test N°II.7: Linear Strain due to Water Absorption. In *International Symposium on Deterioration and Protection of Stone Monuments. Experimental Methods. Part II – Tests defining the properties connected with the presence and the movement of water*. Paris: UNESCO/RILEM.
- ROCK ENGINEERING LABORATORY. 1999a. Unpublished 12 December 1999 testing results. Cairo: Mining Department, Faculty of Engineering, Cairo University.
- . 1999b. Unpublished 19 December 1999 testing results RE-25. Cairo: Mining Department, Faculty of Engineering, Cairo University.
- . 2000a. Unpublished 3 January 2000 report RE-26. Cairo: Mining Department, Faculty of Engineering, Cairo University.
- . 2000b. Unpublished 3 March 2000 testing results RE-36. Cairo: Mining Department, Faculty of Engineering, Cairo University.
- RODRIGUEZ-NAVARRO, C., and E. DOEHNE. 1999. Salt Weathering: Influence of Evaporation Rate, Supersaturation and Crystallization Pattern. *Earth Surface Processes and Landforms* 24, (3): 191-209.
- RODRIGUEZ-NAVARRO, C., E. HANSEN, E. SEBASTIAN, and W. S. GINELL. 1997. The Role of Clays in the Decay of Ancient Egyptian Limestone Sculptures. *Journal of the American Institute for Conservation* 36 (2): 151-63.
- RODRIGUEZ-NAVARRO C., E. SEBASTIAN, E. DOEHNE, and W. S. GINELL. 1998. The Role of Sepiolite-Palygorskite in the Decay of Ancient Egyptian Limestone Sculptures. *Clays and Clay Minerals* 46 (4): 414-422.
- SAID, R, ed. 1990. *The Geology of Egypt*. Rotterdam: A.A Balkema Publishers.
- SAID, R. 1962. *The Geology of Egypt*. New York: Elsevier.
- SALEH, S. A., F. M. HELMI, M. M. KAMAL, and A.-F. E. EL-BANNA. 1992a. Consolidation Study of Limestone: Sphinx, Giza, Egypt. In *Proceedings of the Seventh International Congress on Deterioration and Conservation of Stone, 15-18 June 1992, Lisbon, Portugal*. Vol. 2. Edited by J. Delgado Rodrigues, F. Henriques, and F. Telmo Jeremias. Lisbon: Laboratório Nacional de Engenharia Civil. 791-800.
- . 1992b. Artificial Weathering of Treated Limestone: Sphinx, Giza, Egypt. In *Proceedings of the Seventh International Congress on Deterioration and Conservation of Stone, 15-18 June 1992, Lisbon, Portugal*. Vol. 2. Edited by J. Delgado Rodrigues, F. Henriques, and F. Telmo Jeremias. Lisbon: Laboratório Nacional de Engenharia Civil. 781-89.
- AL-SAYYAD, N. 1981. *Streets of Islamic Cairo: a configuration of urban themes and patterns*. Cambridge, Massachusetts: Aga Khan Program for Islamic Architecture.

- SCHÄFER, S. 1995. Grundlagen wäßriger Reinigung nach Richard Wolbers (Basic principles of aqueous cleaning according to Richard Wolbers). *Zeitschrift für Kunsttechnologie und Konservierung* 9 (1): 139-54.
- SCHAFFER, R. J. [1932] 1972. The weathering of natural building stones. *Building Research Special Report*, no. 18.
- SCHRAMM L., K. MANNHARDT, and J. NOVOSAD. 1991. Electrokinetic Properties of Reservoir Rock Particles. *Colloids And Surfaces* 55 (April): 309-331.
- SECTION FRANÇAISE DE L'INSTITUT INTERNATIONAL DE CONSERVATION DES OEUVRES D'ART. 1996. *Le dessalement des matériaux poreux: Septièmes journées d'études de la SFIIC, 9-10 mai 1996, Poitiers* (The desalting of porous materials: Seventh study days of the SFIIC, 9-10 May 1996, Poitiers). Champs-sur-Marne: Section Française de l' Institut International de Conservation des oeuvres d'art.
- SELWITZ, C. 1990. Deterioration of the Great Sphinx: an Assessment of the Literature. *Antiquity* 64: 853-859.
- SHOEIB, A. S. A., M. ROZNEKSKA, and K. BORYK-JÓZEFOWICZ. 1990. Weathering Effects on an Ancient Egyptian Limestone which has been Affected by Salt. In *Proceedings of the First International Symposium on the Conservation of Monuments in the Mediterranean Basin: The Influence of Coastal Environment and Salt Spray on Limestone and Marble, 7-10 June 1989, Bari*. Edited by F. Zezza. Brescia, Italy: Grafo Edizioni. 203-208.
- SNETHLAGE R., and E. WENDLER. 1996. Moisture Cycles and Sandstone Degradation. In *Saving Our Architectural Heritage: the Conservation of Historic Stone Structures: Report of the Dahlem Workshop, 3-8 March 1996, Berlin*. Edited by N. S. Baer, and R. Snethlage. Chichester: John Wiley & Sons.
- SNETHLAGE R., E. WENDLER, and D. D. KLEMM. 1995. Tenside im Gesteinsschutz-bisherige resultate mit einem neuen Konzept zur erhaltung von Denkmälern aus Naturstern. In *Denkmalpflege und Naturwissenschaft, Natursteinkonservierung*. Edited by R. Snethalage. Berlin: n.p. 127-46.
- STEIGER, M., and A. ZEUNERT. 1996. Crystallizations Properties of Salt Mixtures: Comparison of Experimental Results and Model Calculations. In *Proceedings of the Eighth International Congress on Deterioration and Conservation of Stone, 30 September – 4 October 1996, Berlin*. Edited by J. Riederer. Berlin: Möller Druck und Verlag. 535-544.
- TANIMOTO, C., S. YOSHIMURA, and J. KONDO. 1993. Long-term Stability of the Underground Cavern for the Pharaoh and the Deterioration of the Great Sphinx. *International Journal of Rock Mechanics Mining Sciences & Geomechanic Abstracts* 30 (7): 1545-1551.
- VAN OLPHEN, H. 1977. *An introduction to clay colloid chemistry*. 2nd ed. New York: John Wiley & Sons.
- VELDE, B. 1995. *Origin and Mineralogy of Clays: Clays and the Environment*. Berlin: Springer.
- VENKATARAMAN, A. 1992. The Conservation of Salt-Contaminated Stone. Master of Science in Historic Preservation Thesis, University of Pennsylvania.
- WELLS, A. F. 1946. Crystal Habit and Internal Structure. Parts 1 and 2. *Philosophical Magazine Serie 7*, vol. 37, no. 266 (March): 184-199, no. 267 (April): 217-235.

- WENDLER E., A. E. CHAROLA, and B. FITZNER. 1996. Eastern Island Tuff: Laboratories Studies for its Consolidation. In *Proceedings of the Eighth International Congress on Deterioration and Conservation of Stone, 30 September – 4 October 1996, Berlin*. Vol. 2. Edited by J. Riederer. Berlin: Möller Druck und Verlag. 1159-70.
- WENDLER E., D. D. KLEMM, and R. SNETHLAGE. 1991. Consolidation and Hydrophobic Treatment of Natural Stone. In *Proceedings of the Fifth International Conference on Durability of Building Materials and Components, 7-9 November 1990, Brighton*. Edited by J. M. Baker, P. J. Nixon, A. J. Majumdar and H. Davies. London: Chapman & Hall. 203-212.
- WENDLER, E. and R. RÜCKERT-THÜMLING. (1993). Gefügezerstörendes Verformungsverhalten bei salzbefrachteten Sanstein unter hygrischer Wechselbeanspruchung. In *Werstoffwissenschaften und Bausanierung*. Edited by F. H. Wittman. Vol. 3. Kontakt und Studium 420. Ehningen bei Böblingen: Expert Verlag. 1818-1830.
- WENDLER E., and L. SATTLER. 1990. Modifizierung von siliziumorganischen Steinschuttmitteln. In *Denkmalpflege und Naturwissenschaft im Gespräch*. Workshop Fulda 3/1990. Sonderheft aus des Publikationsreihe des Verbundforschungsprojekts Steinzerfall und Steinkonservierung. 135-137.
- WHEELER, G. E., J. K. DINSMORE, L. J. RANSICK, A. E. CHAROLA, and R. J. KOESTLER. 1984. Treatment of the Abydos Reliefs: Consolidation and Cleaning. *Studies in Conservation* 29, no. 1 (February): 42-48.
- WINKLER, E. M. 1975. *Stone: Properties, Durability in Man's Environment*. 2nd, revised ed. New York: Springer-Verlag.
- ZAJAC J., and S. PARTYKA. 1996. Recent Progress in the Studies of Adsorption of Ionic Surfactants from Aqueous Solutions on Mineral Substrates: Adsorption on New and Modified Inorganic Sorbents. *Studies in Surface Science and Catalysis* 99: 797-828.
- ZEHNDER K., and A. ARNOLD. 1989. Crystal-Growth in Salt Efflorescence. *Journal of Crystal Growth* 97, no. 2 (September): 513-521.

INDEX

A

- Abd el-Hady, M. M., 19
- Abydos
geological formation, 22, 23, 24, 38, 85 (*see also* Egyptian limestone)
reliefs
composition, 20, 21
deterioration, 48-49, 53-54
environmental control, 59
treatment, 48-49, 53-54, 57
- acid-insoluble residue, content. *See also* clay minerals
in Egyptian limestone (*see* composition)
in limestone, city wall, 80, 82, 105, 109
- Aga Kahn Trust for Culture, 1, 3, 11, 12
- Agnew, N. H., 25, 35, 60
- alkyl- α - ω -di-ammonium-chloride, 73
See also surfactant; butyl- α - ω -di-ammonium-chloride
- Amaravati, limestone sculptures from,
treatment, 59
- Amenophis II, limestone head of,
composition, 20
- Amenophis III, royal head of, deterioration, 24
- ammonium
chloride, city wall limestone, 110
content, city wall limestone, 107-108
sulfate, city wall limestone, 110
- amphiphilic, surfactant, 64, 68
- amphoteric, surfactant, 65
- arid climate
of Cairo, 34-35
salt behavior in, 35-36
- Arnold, A., 27, 28, 29, 30, 32, 33, 42, 95
- ASTM
use of length comparator (ASTM C490-97),
127
- Ayyubid
city wall (*see* city wall)
dynasty, 4
limestone (*see* limestone, city wall)
- al-Azhar
park project, 1-3, 9, 11, 12, 56
street, 9, 12

B

- Bab Zwela temple, Egyptian limestone
composition, 19
- Badr al-Gamālī, Emīr al-Guyūsh, Cairo
fortification, 4
- Baker, S., 48, 52, 54, 56, 111, 112
- balance, manufacturer, 119
- barium
ethyl sulfate, conservation treatment, 48
hydroxide, consolidant, 47
- Barton, N. G., 22, 54
- Basma, A. A., 62
- BDAC. *See* butyl- α - ω -di-ammonium-chloride
- beeswax, consolidant, 48
- bioclast. *See* limestone city wall, fossil
- Blackshaw, S. M., 22, 54
- Böke, H., 76
- Bonnet, S., 30
- Borrelli, E., 100
- Boryk-Józefowicz, K., 19, 27, 51
- Bradley, S. M., 18, 21, 22, 23, 29, 47, 50, 51,
53, 55, 56, 58, 83, 111, 112
- Brimblecombe, P., 30, 34, 42, 59
- British Museum, 20, 22, 24, 48, 52, 56, 58, 59
- brushing surfactant, experiment, 124
salt-impregnated samples, 125
- burial
of the city wall, 6, 8, 11, 89
mounds (*see* Darassa hills)
- butyl- α - ω -di-ammonium-chloride. *See also*
surfactant
characteristics, 118
chemical formula, 117
manufacturer, 118
use on clay-rich sandstone, 74
use on Eastern Island tuff, 63, 118

C

- Caen stone, desalination after consolidation. 55
- Cairo
citadel of, 6, 19
climate, 34-35
geological formation, 24, 85
Governorate, 1
fortification
city wall (*see* city wall)

- first, 4
 - second, 4
 - third, 4, 6
 - map, 5, 11
 - soil, salt content, 20, 100
 - University (*see* Rock Engineering Laboratory)
- calcite. *See* calcium carbonate
- calcium
 - carbonate
 - content in city wall limestone, 110
 - content in Egyptian limestone, 19, 21, 23
 - hydroxide, consolidant, 47
 - magnesium carbonate (*see* dolomite)
 - nitrate content in Egyptian limestone, 21
 - sulfate dihydrate (*see* gypsum)
 - sulfite hemi-hydrate
- calibration, length comparator, 129
- caliper, 130
- Camuffo, D., 25, 26
- Caner, E. N., 36
- Caner-Saltik, E. N., 36
- Caneva, G., 112
- capillary absorption
 - discussion, 146-148
 - experimental procedure, 121-122
 - parameters, 119
 - results
 - capillary absorption coefficient, 131-132
 - capillary absorption rate, 130-131
 - graph, 131
 - total immersion, 132
 - sample preparation, 119, 121
 - of surfactant for salt-impregnated samples, 125
- capillary
 - absorption coefficient
 - definition, 119
 - result, 131-132
 - rise, 28, 89, 92, 100
 - preferential paths, 121
 - water absorption rate
 - definition, 119
 - result, 130-131
- carbonates
 - content, city wall limestone, 101
 - origin, 101
- Casanova, P., 6
- cement. *See* Portland cement
- change in weight
- Charola, A. E., 15, 21, 27, 47, 48, 54, 58, 61, 63, 118
- Chatterji, S., 43, 61, 62
- chloride
 - content
 - after desalination, 55
 - in city wall limestone, 100, 107-108
 - in Egyptian limestone, 20, 22
 - in London tap water, 52
 - requiring desalination, 24, 112
 - source, 28, 100
- Christensen, P., 43, 61, 62
- citadel of Cairo, 6, 19
- city wall, Cairo. *See also* limestone, city wall;
 - coring, city wall
 - burial, 6, 8, 89
 - conservation, 3
 - construction
 - material, 4, 9, 12, 13, 79
 - technique, 4, 7, 12, 13
 - coring
 - discussion, 110-113
 - methodology, 101-103
 - results, 103-110
 - dimensions, 12, 56
 - excavation, 9, 11, 89, 91
 - history, 3-9
 - first fortification, 4
 - second fortification, 4
 - third fortification, 4, 6
 - map, 5, 11
 - photo, 2, 7, 10, 91
 - previous intervention
 - by Comité, 9, 10, 27
 - by French, 8
 - use of Portland cement, 9, 27-28
 - salt
 - content, 28
 - deterioration pattern, 14, 89-92
 - distribution, 101-113
 - survey
 - condition assessment, 13, 14, 90
 - historic, 8
 - treatment, surfactant, 77-78, 156, 159
 - weathering, stone, 14
- clay minerals
 - content
 - in city wall, 80, 82
 - in Egyptian limestone, 19, 20
 - in limestone, 36-37
 - in marble, 36
 - in sandstone, 42, 73-74
 - influence on consolidant, 49
 - interlayer cations, 38-41, 73-74
 - ion-exchange of, 43, 61-62, 74
 - poultice, use in, 55
 - spatial distribution in stone, 36, 38-39, 43
 - stone deterioration, 36-39

- factor in, 24, 37, 38, 54-55, 111
- synergy with salts deterioration, 41-45
- swelling, 39-41
 - decrease of, by lime wash, 62
 - expansion, 37, 41, 43
 - inner-crystalline, 39-40, 44, 61-62
 - osmotic, 40-41
 - of salt-contaminated stones, 44-45
 - surfactant, influence of, 62-63, 73-75
- type
 - illite, 39
 - montmorillonite, 39-40
 - palygorskite, 40
 - sepiolite, 21, 40, 56
 - smectite, 42-43
- Clegg, computer model, 59
- climate
 - Cairo, 34-35
 - salt behavior in arid, 35-36
- CMC. *See* critical micelle concentration
- columnar crystal, photos, 92-94
- Comité de Conservation des Monuments de l'Art Arabe
 - creation, 8
 - limestone, 9, 79 (*see also* limestone, city wall)
 - procès-verbaux, 8
 - restoration campaign, 9, 10, 27
- comparator. *See* length comparator
- composition
 - case studies
 - Abydos reliefs, 20, 21
 - Amenophis II, limestone head of, 20
 - Bab Zwela temple, 19
 - Great Sphinx, 25-26
 - Harthur temples, 19
 - Ptolemy IV, limestone figure of, 21
 - Zoser's pyramid, 19
 - Egyptian limestone, 19-21
 - acid-insoluble residue, 21, 23
 - clay minerals content, 19
 - deterioration in function of, 22, 24, 37, 111, 112
 - salt content, 19, 21
 - and water sensitivity, 37, 53, 112
 - geographic provenance, in function of, 18
 - limestone, city wall, 80, 82
 - replacement limestone, 116
- compressive strength
 - limestone city wall, 88, 115
 - replacement limestone, 115
- Conseil Supérieur du Service de Conservation des Monuments Arabes. *See* Comité de Conservation des Monuments de l'Art Arabe
- Arabe
- consolidation
 - case studies
 - Abydos reliefs, 48
 - British Museum, 48
 - Coptic limestone reliefs, 49
 - Great Sphinx, 51
 - Ptolemaic period, limestone figure, 51, 56
 - tomb of Sri at Saqqara, limestone panel, 51
 - followed by desalination, 47, 55, 56
 - influence of
 - on clay minerals on, 50
 - on salts on, 49-50
 - products
 - barium hydroxide, 47
 - calcium hydroxide, 47
 - epoxies, 47, 48
 - methacrylates, 48
 - methyl trimethoxysilane, 48, 51, 56
 - oil, 47, 48
 - paraffin, 47, 48, 50
 - polyurethane, 49
 - silanes, 50
 - vinylite, 48
 - waxes, 47, 48
 - salt encapsulation by, 50-51
 - salt extraction by, 51
 - of stone
 - Egyptian limestone sandstone, 49
- construction, city wall. *See also* limestone, city wall
 - material, 4, 9, 12, 13
 - technique, 4, 12, 13
- Cooke, R. U., 35, 41
- Coptic limestone reliefs, deterioration and treatment, 49
- Coremans, P., 20, 50, 53
- coring, city wall
 - analysis, 103-110
 - acid insoluble residue content, 105, 109
 - salt content, 103-108
 - XRD, 109-110
 - discussion, 110-113
 - methodology, 101-103
- Creswell, K. A. C., 4, 5, 6
- critical moisture content, definition, 149n
- critical micelle concentration
 - change in presence of electrolytes, 69-70
 - definition, 67
 - and surface tension, 68
- crust, salt
 - on the city wall, 14, 89-92, 95-96
 - habit, 32, 52, 95

crystal, columnar. *See* columnar crystal
crystallization/dissolution cycling, salt, 19,
28-29, 29-32
in arid climate, 35-36
equilibrium relative humidity, 30
of salt mixtures, 33-34
cubes, Egyptian limestone. *See* experimental
samples
cycling. *See* wet-dry cycling

D

al-Darb al-Ahmar, district, 1, 3, 11, 12
Darassa Hills, 1, 3, 6, 12
formation, 6, 8
view of, 2, 7
Delagado-Rodrigues, J., 36
density,
BDAC, 118
city wall limestone, 82
replacement limestone, 115
sodium chloride solution, 117
desalination, 52-57
after consolidation, 47, 55, 56
maximum chloride content acceptable
without, 24
technique
alcohol immersion, 53
electro-osmosis, 57
mechanical removal, 52
poulticing, 55-57
water immersion, 52-55
deterioration, stone
in arid climate, 35-36
case studies
Abydos reliefs, 21, 48-49, 53-54
Amenophis III, royal head of, 24
Coptic limestone reliefs, 49
Great Sphinx, 25-26, 27
Hati, block Statute of, 23
Ptolemaic period, limestone figure, 51
Scribe Iahmose and family, limestone
relief panel of, 22
tomb of Sri at Saqqara, limestone panel, 51
by clay minerals, 36-39
of Egyptian limestone, 19, 20, 21-26
factors in, 23-25, 37, 54-55, 112
in function of the composition, 22, 24, 37
in museum environment, 21-25, 47, 50, 58
in outdoor environment, 25-26
Orthoceras limestone, 43
porosity, factor in, 24, 26, 32, 42, 83
by salts, 26-36

field observations, 27, 29
location, 30-31, 32, 95
mechanisms, 29-33, 96
theories of, 26-27, 29
surfactant, influence on, 62-63, 71-75
synergy between salts and clay minerals,
41-45
Dewey, C., 15, 79, 81, 82-87, 99, 101
dimensions
Cairo city wall, 12, 56
experimental samples, 116
discussion, experiment, 143-155
capillary rise, 146-148
cycling, 150-155
drying, 149-150
length changes, 153-155
weight changes, 150-153
sample preparation, 143-146
Doehne, E., 26, 27, 31, 32, 33, 36, 72
dolomite content
in city wall limestone, 110
in Egyptian limestone, 21
drying, experiment
discussion, 149-150
experimental procedure, 123-124
parameters, 122-123
result, 133-137
drying index, 136-137
graphs, 134-135
residual water content, 133-135
sample preparation, 122-124
drying index
definition, 122-123
results, 136-137
dumping ground near city wall, 6, 28, 100-101
Dunn, J. R., 36, 38
dynasty
Ayyubid, 4
Fatimid, 4

E

Easter Island, tuff, 63, 118
efflorescence, salt, 31-32, 47, 50-51, 57, 75, 95
Egypt
climate, 34-35
geology, 17, 18
Abydos formation, 22, 23, 24, 38, 85
Cairo formation, 24, 85
El Bersha formation, 24, 85
Muquattam Hill, 114,
Thebes formation, 22, 23, 24, 38, 85

- Egyptian limestone (*see also* limestone, city wall)
- composition (*see also* composition, Egyptian limestone), 19-21
 - acid-insoluble residue, 21, 23
 - clay minerals content, 19, 20
 - fossil, 17
 - salts, 19, 20, 23, 27-28
 - and water sensitivity, 37, 53
 - deterioration, 19, 20, 21-26
 - factors in, 23-25, 37, 54-55, 112
 - in function of the composition, 22, 24, 37, 54-55, 111
 - in museum environment, 21-25, 47, 50, 58
 - in outdoor environment, 25-26
 - determination of the geographic provenance, 18
 - expansion, hygric, 37, 43-44
 - geology, 17, 18, 19
 - Abydos formation, 22, 23, 24, 38, 85
 - Cairo formation, 24, 85
 - El Bersha formation, 24, 85
 - Muquattam Hill, 114,
 - quarries, 17, 18
 - Thebes formation, 22, 23, 24, 38, 85
 - treatment, 46-63
 - absence of, 58
 - consolidation, 47-51
 - desalination, 52-57
 - environmental control, 57-61
 - ion-exchange resins, 61-62
 - shelter, 60
 - surfactant application, 62-63, 71-76
 - surfactant treatment experiment (*see also* experiment, Egyptian limestone surfactant treatment), 114-155
 - discussion, 142-155
 - materials, 114-118
 - methodology, 118-129
 - results, 130-142
 - El Bersha, formation, 24, 85
 - See also* Egyptian limestone, geology
 - electro-osmosis, desalination method, 57
 - encapsulation, salt, 50-51
 - Engström, L., 61, 72, 73, 75
 - environmental
 - conditions
 - Cairo, 15, 34-35
 - experimental, 126-127
 - control, treatment, 57-61
 - examples, 59, 60
 - parameters, 58-59
 - monitoring, Great Sphinx, 25, 35
 - Scanning Electron Microscopy (ESEM), 42
 - epoxies, consolidant, 47, 48
 - equilibrium relative humidity
 - and salt crystallization, 30
 - of salt mixtures, 33-34
 - of sodium chloride, 30
 - excavation, city wall, 9, 11, 89, 91
 - experiment, Egyptian limestone surfactant treatment, 114-155
 - discussion, 142-155
 - capillary rise, 146-148
 - cycling, wet-dry, 150-155
 - drying, 149-150
 - sample preparation, 142-146
 - materials, 114-118
 - sodium chloride, 117
 - stone sample, 114-117
 - surfactant, 117-118
 - methodology, 118-129
 - capillary absorption, 119-122
 - cycling, wet-dry, 126-129
 - drying, 122-124
 - surfactant application to salt-impregnated samples, 125-126
 - surfactant brushing, 124
 - total immersion, 122
 - treatment procedures, 118-120
 - results, 130-142
 - capillary rise, 130-132
 - cycling, wet-dry, 137-142
 - drying, 133-137
 - total immersion, 132
 - experimental samples. *See also* replacement stone
 - chemical composition, 116
 - dimensions, 116
 - mechanical properties, 115
 - numbering system, 116-117
 - physical properties, 115
 - quarry, 114-115
 - extension, length comparator, 128
 - extraction, salt
 - by consolidant, 51
 - by surfactant, 75-76
- ## F
- Fatimid
 - fortification, Cairo, 4
 - period, 4
 - fire, stone microcracking, 85
 - Fitzner, B., 15, 61, 63, 118
 - Fong, K., 9, 12, 14

foraminifera. *See* limestone city wall, fossil
fortifications, Cairo. *See also* city wall
Ayyubid, 4
Fatimid, 4
first, 4
map of, 5, 11
second, 4
third, 4, 6
fossil, limestone, 17
city wall, 79-80, 81, 83, 86, 99
Fox, J. C., 49, 51
French occupation of Cairo, 8
Furlan, V., 28, 29, 31

G

Gauri, K. L., 19, 25, 26, 27, 35, 46, 53
geology, Egypt, 17, 18
Abydos formation, 22, 23, 24, 38, 85
Cairo formation, 24, 85
El Bersha formation, 24, 85
Muquattam Hill, formation, 114
Thebes formation, 22, 23, 24, 38, 85
Giza plateau, 25, 27, 35, 51, 60
See also Great Sphinx
glass beads, experimental use, 121
Göktürk, H., 76
Governorate of Cairo, 1
Great Sphinx
composition, 25
deterioration, 25-26, 27
environmental monitoring, 25, 34
shelter for, 60
treatment, 46, 51
gypsum (calcium sulfate dihydrate), content in
Egyptian limestone, 19, 26

H

halite (sodium chloride)
and clays swelling, 42-43
content
in city wall limestone, 110
in Egyptian limestone, 19, 20, 21, 26
consolidation treatment, 49
equilibrium relative humidity, 30, 42
experimental material, 117
main characteristics, 117
Hanna, S. B., 20, 21, 22, 24, 29, 31, 37, 47, 48,
50, 51, 53, 55, 56, 58, 111, 112
Harrell, J. A., 17, 18
Harthur temples, Egyptian limestone

composition, 19
Harvard University Art Museums, Kervorkian
collection, 49
Harvey, R. D., 41
Hati, block Statute of, deterioration, 23
Helmi, F. M., 19, 20, 25, 27
Helms, G. M., 47, 48
Heywood, A., 21, 48, 57
Holdren, G. C., 19, 26, 27, 35, 53
Houst, Y., 28, 29, 31
Hudec, P. P., 36, 38
Hughes, R., 48, 52, 54, 56, 111, 112
hydration/dehydration cycling, salt, 33

I

illite
content, Egyptian limestone, 21
as expandable clay, 39
industrial applications, surfactant, 71, 72
interfaces, surfactant
concentration at, 66, 68-69
spatial orientation at, 66-67
interfacial tension, 69
See also surface tension
inter-layer distance, clay minerals, 40
See also clay minerals
Invar, definition, 129n
ion exchange
of inter-layer cations, clay minerals, 39-41,
43, 61-62, 74
resins, treatment, 61-62
surfactant adsorption by, 70
iron
content, Egyptian limestone, 19
inclusions, limestone city wall, 80, 81, 82, 84
reinforcement, 48
Ivanova, N. I., 71

J

Japanese paper, poulticing, 55
Jarmontowicz, A., 19, 47
Jedrzejska, H.

K

kaolinite, Egyptian limestone composition, 19
Kevorkian collection, Harvard University Art
Museums, 49
Klemm, D. D., 15, 36, 50, 73, 74, 118
Koestler, R. J., 21, 47, 48, 54, 58

Kondo, J., 17, 25, 60
Kueng, A., 27, 29, 32, 33, 95

L

Lagaly, G., 73, 118
length comparator
 ASTM standard C490-97 for the use of, 127
 calibration, 129
 extensions built for, 128
 manufacturer, 128
 measurements, 129
Lewin, S. Z., 29, 30, 31
limestone
 city wall (*see* limestone, city wall)
 clay content in, 36-37
 Egyptian (*see* Egyptian limestone)
 Orthoceras
 deterioration, 43
 ion-exchange resin treatment, 61
 limestone, city wall. *See also* city wall, Cairo;
 coring, city wall
 composition
 acid-insoluble residue, 80, 82, 105, 109
 clay minerals
 fossil, 79-80, 81, 83, 86, 99
 iron inclusions, 80, 81, 82, 84
 micro-chemical spot test, 99-101
 salts, 99-101, 103-108
 deterioration pattern, 14, 89-92, 96
 mechanical properties, 87-88
 mineralogical and petrographic analysis,
 79-82
 color, 79, 82
 texture, 79-80, 81, 85
 origin of, 9
 physical properties, 82-87
 density, 82
 microcracking, 80, 81, 84, 85-87, 96-99
 porosity, 80, 81, 82-83, 84, 85, 86
 surface densification, 85, 87
 salt
 characterization, 99-101, 103-108
 crust and veil, 14, 89-92, 95-96
 deterioration pattern, 89-92
 distribution, 101-113
 growth conditions, 89, 92-94, 96
 stone type, 9, 79
 treatment, surfactant, 77-78, 156, 159
 weathering, 14
lime wash to decrease clay swelling, 62
London tap water, for desalination, 52
Lucas, A., 20, 100

lyophilic, surfactant, 64
lyophobic, surfactant, 64

M

Madsen, F. T., 38, 39, 40, 41
Maekawa, S., 25, 35, 60
Mannhardt, K., 71
manufacturer
 balance, 119
 BDAC, 118
 caliper, 130
 length comparator, 127
 oven, 119
 sodium chloride, 117
map
 city wall, site, 11
 historic fortifications, Cairo, 5
marble, clay minerals content, 36
mascagnite. *See* ammonium sulfate
materials, experiment
 Egyptian stone samples, 114-117
 chemical composition, 116
 dimensions, 116
 mechanical properties, 115
 numbering system, 116-117
 physical properties, 115
 quarry, 114-115
 sodium chloride, 117
 surfactant, 117-118
 characteristics, 118
 chemical formula, 117
 manufacturer, 118
McGreevy, J. P., 36, 42
mechanical
 properties
 limestone city wall, 87-88
 replacement limestone, 115
 removal, salts, 52
methacrylates, consolidant, 48
methodology, experimental
 capillary absorption, 119-122
 experimental procedure, 121-122
 parameters, 119
 sample preparation, 119, 121
 cycling
 conditions, 126-127
 measurement procedure, 127-129
 drying, 122-124
 experimental procedure, 123-124
 parameters, 122-123
 sample preparation,
 total immersion, 122

treatment procedures, 118-120
 matrix of treatment, 120
 surfactant application to salt-impregnated samples, 125-126
 surfactant brushing, 124
 methyl trimethoxysilane, consolidant, 48, 51, 56
 Metropolitan Museum of Art, New York, 20, 48
 micelle, 66, 70
See also Critical Micelle Concentration
 micro-chemical spot test, city wall limestone, 99-101, 112
 microcracking, city wall limestone, 80, 81, 85-87, 96-99
 Middleton, A. P., 18, 21, 22, 23, 58, 83, 111, 112
 Miller, E., 24, 48, 51, 57, 58, 59, 83, 111
 modulus of elasticity
 city wall limestone, 88, 115
 replacement limestone, 115
 molecular weight
 BDAC, 118
 sodium chloride, 117
 montmorillonites, clay minerals, 39-40
 Moore, D. M., 39
 Müller-Vonmoos, M., 38, 39, 40, 42
 Muquattam Hill, Egyptian limestone formation, 114
 museum. *See also under specific name*
 Egyptian limestone deterioration in, 21-25, 47, 50, 58
 Muslim calendar, definition, 4n
 Myers, D., 64, 65, 66, 68, 69, 70, 71

N

Naguib Bros. Co. quarry, 114
 Napoleonic campaign. *See* French occupation of Cairo
 Near East foundation, 1
 Nile valley, 17
 nitrate
 content, Egyptian limestone, 20, 22, 23, 100
 as adeterioration factor, 112
 micro-chemical spot test, 112
 origin, city wall, 28, 100-101
 nitrite
 content, city wall limestone, 100-101
 micro-chemical spot test, 112
 origin, 100-101
 Normal (Normativa Manufatti Lapidei)
 capillary water absorption and capillary absorption coefficient (Normal 11/85), 119
 measurement of the drying index (Normal

29/88), 123
 Novosad, J., 71
 Nugari, M. P., 112
 numbering system, experimental samples, 116
 nummulitic, definition, 115n
 Nunberg, S., 21, 48, 57

O

Oddy, W. A., 48, 52, 54, 56, 111, 1112
 oil
 conservation treatment, use in, 47, 48
 recovery, surfactant use in, 71
 osmosis, clay minerals swelling, 41
 outdoor environment, Egyptian limestone deterioration, 25-26
 oven
 drying, 119, 124
 manufacturer, 119
 Overgaard, G., 43, 61, 62

P

palygorskite, as a non-expandable clay, 40
 paraffin, consolidant, 47, 48, 50
 parameters, experimental
 capillary absorption, 119
 drying, 122-123
 Perrin, B., 30
 phosphate content, city wall limestone, 101
 physical properties
 limestone city wall, 82-87
 replacement limestone, 115
 polysiloxane, water-repellent, 74-75
 Polysupra Kregersol Blue, thin section preparation, 80, 99
 polyurethane, consolidant, 49
 porosity
 city wall limestone, 80, 81, 82-83, 85, 86, 115
 Egyptian limestone, 24, 26
 factor in stone deterioration, 24, 26, 32, 42
 replacement limestone, 115
 Porter, M. R., 64, 67, 68, 69
 Portland cement, city wall repair, 9, 27-28
 poulticing
 clay minerals, use in, 55
 desalination technique, 55-57
 effectiveness/limitations, 56
 Japanese paper, use in, 55
 Terylene, fine mesh of, use in, 56

preparation, experimental samples
 brushing, 124-125
 capillary absorption, 119-122
 discussion, 143-146
 drying, 122-124
 photo, 126
 second impregnation, 125
 total immersion, 122
 Price, C., 30, 34, 42, 59
 procedure, experimental
 capillary absorption, 121-122
 cycling, 127-129
 drying, 123-124
 protective treatments. *See* ion-exchange resin,
 treatment and surfactant, treatment.
 Ptolemaic period, limestone figure of the,
 deterioration and consolidation, 51, 56
 Ptolemy IV, limestone figure of, composition,
 21
 Pühringer, J., 30, 34, 42, 59

Q

quarry
 Egyptian limestone, 17, 18
 replacement limestone, 114-115
 quartz content
 city wall limestone, 110
 Egyptian limestone, 19

R

Renolds, R. C., 39
 replacement limestone
 chemical composition, 116
 mechanical properties, 115
 physical properties, 115
 quarry, 114-115
 resin, ion-exchange, 61-62
 results, experimental
 capillary rise, 130-132
 capillary absorption coefficient, 131-132
 capillary absorption rate, 130-131
 graph, 131
 total immersion, 132
 cycling, 137-142
 graphs, 138-139, 141-142
 drying, 133-137
 drying index, 136-137
 graphs, 134-135
 residual water content, 133-135
 Riecken, B., 49

rising damp. *See* capillary rise
 Rock Engineering Laboratory
 city wall limestone
 coring, 101-110
 mechanical properties, 85-87
 physical properties, 82-87
 replacement limestone
 chemical composition, 116
 physical properties, 115
 mechanical properties, 115
 Rodriguez-Navarro, C., 21, 26, 27, 31, 32, 33,
 36, 37, 41, 42, 43, 44, 58, 61, 62, 63, 72
 Roznerska, M., 19, 27, 51, 72
 rubble core, city wall construction technique,
 12, 13

S

Said, R., 18
 Salāh ad-Dīn. *See also* Ayyubid, dynasty
 citadel, Cairo, 6
 fortification, Cairo, 4
 Saleh, S. A., 51
 salt. *See also under specific name. See also* city
 wall, Cairo
 content
 Cairo's soil, 20, 100
 city wall limestone, 28
 Egyptian limestone, 20, 21, 23,
 Portland cement, 28
 replacement limestone, 116
 crystallization / dissolution cycling, 19,
 28-29, 29-32
 in arid climate, 35-36
 equilibrium relative humidity, 30
 of mixtures, 33-34
 deterioration caused by, 26-36
 in arid climate, 34-35
 field observations, 27, 29
 location, 30-31, 32, 95
 mechanisms, 29-33
 maximum content to avoid, 54-55
 surfactant effect on, 71-73
 synergy with clay minerals deterioration,
 41-45
 theories of, 26-27, 29
 habits, 31-32
 crust, 32, 52, 95
 cryptoflorescence, 31
 efflorescence, 31-32, 47, 50-51, 57, 75, 95
 subflorescence, 31
 whisker, 75
 hydration / dehydration cycling, 33

- influence on consolidant, 49-50
- limestone, city wall
 - characterization, 99-101
 - crust and veil, 14, 89-92, 95-96
 - deterioration pattern, 89-92, 96
 - growth conditions, 89, 92-94, 96
- movement, 28-29
- origins of, 27-28, 100-101
- removal
 - alcohol immersion, 53
 - electro-osmosis, 57
 - mechanical, 52
 - poulticing, 55-57
 - water immersion, 52-55
- salt deterioration. *See* salt, deterioration
- salt encapsulation, treatment, 50-51
- salt extraction
 - by consolidant, 51
 - by surfactant, 75-76
- salt removal. *See* desalination
- Salvadori, O., 112
- sandstone
 - consolidation of, 49
 - deterioration of clay-rich, 42
 - Nubian, 17
 - surfactant treatment, 73-74
- Saqqara, tomb of Sri, limestone panel
 - deterioration and consolidation, 51
- Sasse, H. R., 49
- Scanning Electron Microscopy (SEM), 96-98
 - See also* Environmental Scanning Electron Microscopy (ESEM)
- Schaffer, R. J., 29
- Schramm, L., 71
- scribe Iahmose and family, limestone relief
 - panel of, deterioration, 22
- second impregnation, salt-impregnated samples, 125-126
- Section française de l'IIC, 47
- Seeley, N. J., 36
- Seljūq, attacks on Cairo, 4
- Selwitz, C., 26
- SEM. *See* Scanning Electron Microscopy
- sepiolite
 - content, Egyptian limestone, 21
 - as a non-expandable clay, 40
 - for poulticing, 56
- shear strength, city wall limestone, 88
- shelter, 60
- Shoeib, A. S. A., 19, 27, 51
- silanes, consolidant, 50
- silicium oxide. *See* quartz
- smectite, clay minerals, 42-43
- Smith, B. J., 36, 42
- Snethlage, R., 15, 36, 44, 45, 50, 73, 74, 118
- sodium
 - carbonate, content in Egyptian limestone, 20
- chloride
 - and clays swelling, 42-43
 - and consolidation treatment, 49
 - content in city wall limestone, 110
 - content in Egyptian limestone, 19, 20, 21, 26
 - equilibrium relative humidity, 30, 42
 - experimental material, 117
 - main characteristics, 117
- nitrate
 - content in Egyptian limestone, 20
 - equilibrium relative humidity, 42
- sulfate
 - and clays swelling, 43
 - content in Egyptian limestone, 20
 - content in city wall limestone, 110
 - hydration/dehydration cycling, 33
- Sphinx. *See* Great Sphinx
- Steiger, M., 34
- sulphatation reaction, influence of surfactant, 76
- sulphate
 - content
 - in city wall limestone, 107-108
 - in Egyptian limestone, 20
 - in Portland cement, 28
 - origin, 28
- surface
 - activity, surfactant, 64
 - densification, city wall limestone, 85, 87
 - tension (*see also* surfactant)
 - definition, 67-68
 - of saturated solution of sodium chloride, 117
 - variation, use of a surfactant, 68, 72
 - variation, presence of electrolytes, 69
 - of water, 68
- surface-active agent. *See* surfactant
- surfactant
 - adsorption
 - by ion-exchange, 70
 - on solid surfaces, 70-71
 - behavior, 66-71
 - brushing, experiment, 124
 - classes of, 64-65
 - concentration and color change, 74
 - definition, 63-64
 - effect on clay minerals deterioration, 63, 73-75
 - Egyptian limestone treatment experiment (*see also* experiment, Egyptian limestone), 114-155

- discussion, 142-155
- materials, 114-118
- methodology, 118-129
- results, 130-142
- industrial applications, 71, 72
- interfaces
 - concentration at, 66, 68-69
 - spatial orientation at, 66-67
- salts
 - behavior in presence of, 69-70
 - deterioration, effect on, 71-73
 - extraction with, 75-76
- sulphatation reaction, influence on, 76
- surface activity, requirements for, 64
- surface tension, variations with addition of a, 68-69, 72
- treatment
 - city wall, Cairo, 77-78, 156, 156
 - conservation
 - with water-repellent treatment, 74-75
- survey, city wall
 - condition assessment, 13, 14, 90
 - historic, 8
- swelling, clay minerals, 39-41
 - expansion, 37, 41, 43
 - inner-crystalline, 39-40, 44, 61-62
 - lime wash to decrease, 62
 - osmotic, 40-41
 - of salt-contaminated stones, 44-45
 - surfactant, influence on, 62-63, 73-75
- synergy, salts and clay minerals deterioration, 41-45

T

- Tanimoto, C., 17, 25, 60
- tensile strength
 - city wall limestone, 88, 115
 - replacement limestone, 115
- Terylene, fine mesh of, poulticing, 56
- Thebes formation, 22, 23, 24, 38, 85
 - See also* Egyptian limestone
- Thenardite. *See* sodium sulfate
- thin section of city wall limestone, 80, 83, 85
 - photos, 81, 84, 86, 87, 99
 - preparation, 80
- tomb of Sri at Saqqara, limestone panel
 - deterioration and consolidation, 51
- total immersion
 - experiment
 - results, 132
 - sample preparation, 122
 - porosity measurement by, 83

- treatment,
 - absence of, 58
 - case studies
 - Abydos reliefs, 48-49, 53-54, 57, 59
 - Coptic limestone reliefs, 49
 - Great Sphinx, 46, 51, 60
 - limestone sculptures from Amaravati, 59
 - of the city wall, Cairo, 77-78, 156, 159
 - consolidation, 47-51
 - desalination, 52-57
 - alcohol immersion, 53
 - electro-osmosis, 57
 - in situ, 60
 - mechanical removal, 52
 - poulticing, 55-57
 - water immersion, 52-55
 - environmental control, 57-61
 - ion-exchange resins, 61-62
 - shelter, 60
 - surfactant application, 62-63, 71-76
 - surfactant treatment experiment (*see also* experiment, Egyptian limestone surfactant treatment), 114-155
 - discussion, 142-155
 - materials, 114-118
 - methodology, 118-129
 - results, 130-142
 - tuff, surfactant treatment, 63, 118
 - Tuncer, E. R., 62

U-V

- Vaughan, W. C., 19, 26, 27, 35, 53
- veil, salt, 89-92
- Velde, B., 39
- vener stone, city wall, 7, 12, 13, 14, 79, 115
 - See also* limestone, city wall
- Victoria and Albert Museum, 20
- vinilyte, treatment, 48

W

- water absorption
 - of city wall limestone, 115
 - of replacement limestone, 115
- water immersion
 - desalination treatment, 52-56
 - Egyptian limestone suitability for, 54-55
 - under vacuum, 53
 - porosity measurement by, 83
- water repellent, use with a surfactant, 74-75
- waxes, consolidant, 47, 48

Weber, J., 61, 75
Weiss, A., 73, 118
Wendler, E., 15, 36, 44, 45, 50, 61, 63, 73, 74,
118
wet-dry cycling
deterioration of Egyptian limestone, 37
experimental
conditions, 126-127
discussion, 150-155
measurement procedure, 127-129
results, 137-142
Wheeler, G. E., 21, 47, 48, 54, 57, 58
whisker, salt habit, 75
Winkler, E. M., 88

X

X-Ray Diffraction analysis (XRD), core
samples, 109-110, 112

Y

Yoshimura, S., 17, 25, 60

Z

Zehnder, K., 27, 30, 32
Zeunert, A., 34
Zoser's pyramid, Egyptian limestone
composition, 19
zwitterionic, surfactant, 65